



HAL
open science

**Metabolic programming of zebra fish, *Danio rerio*,
uncovered; physiological performance as explained by
Dynamic Energy Budget theory and life cycle
consequences of uranium induced perturbations.**

Starrlight Augustine

► **To cite this version:**

Starrlight Augustine. Metabolic programming of zebra fish, *Danio rerio*, uncovered; physiological performance as explained by Dynamic Energy Budget theory and life cycle consequences of uranium induced perturbations.. Environmental Sciences. Aix-Marseille Université; Vrije Universiteit, 2012. English. NNT: 2012AIXM4708 . tel-00761088

HAL Id: tel-00761088

<https://theses.hal.science/tel-00761088>

Submitted on 4 Dec 2012

HAL is a multi-disciplinary open access archive for the deposit and dissemination of scientific research documents, whether they are published or not. The documents may come from teaching and research institutions in France or abroad, or from public or private research centers.

L'archive ouverte pluridisciplinaire **HAL**, est destinée au dépôt et à la diffusion de documents scientifiques de niveau recherche, publiés ou non, émanant des établissements d'enseignement et de recherche français ou étrangers, des laboratoires publics ou privés.

Metabolic programming of zebrafish, *Danio rerio* uncovered

Physiological performance as explained by Dynamic
Energy Budget Theory and life-cycle consequences
of uranium induced perturbations



Starrlight Augustine



The research carried out in this thesis was supported by the IRSN research program ENVIRHOM and the Provence Alpes Côtes d'Azur region.

The animal on the cover is *Orsima ichneumon*. Photo courtesy of Bas Kooijman.

ISRN/IRSN-2012/154

© Copyright 2012 by Starrlight Augustine

VRIJE UNIVERSITEIT

METABOLIC PROGRAMMING OF
ZEBRAFISH, *Danio rerio* UNCOVERED.

PHYSIOLOGICAL PERFORMANCE AS EXPLAINED BY DYNAMIC
ENERGY BUDGET THEORY AND LIFE-CYCLE CONSEQUENCES
OF URANIUM INDUCED PERTURBATIONS.

ACADEMISCH PROEFSCHRIFT

ter verkrijging van de graad van Doctor aan
de Vrije Universiteit Amsterdam,
op gezag van de rector magnificus
prof.dr. L.M. Bouter,
in het openbaar te verdedigen
ten overstaan van de promotiecommissie
van de faculteit der Aard- en Levenswetenschappen
op maandag 23 april 2012 om 13.45 uur
in de aula van de universiteit,
De Boelelaan 1105

door

Starrlight Augustine

geboren te Texas, Verenigde Staten van Amerika

promotoren: prof.dr. S.A.L.M. Kooijman
 prof.dr. C. Adam-Guillermin
copromotor: dr. B. Gagnaire

UNIVERSITE DE PROVENCE - AIX-MARSEILLE I

METABOLIC PROGRAMMING OF
ZEBRAFISH, *Danio rerio* UNCOVERED.

PHYSIOLOGICAL PERFORMANCE AS EXPLAINED BY DYNAMIC
ENERGY BUDGET THEORY AND LIFE-CYCLE CONSEQUENCES
OF URANIUM INDUCED PERTURBATIONS.

ECOLE DOCTORALE
SCIENCE DE L'ENVIRONNEMENT ED 251

pour l'obtention du diplôme de Docteur de
l'Université de Provence Mention Sciences,
spécialité Environnement et Santé
par Starrlight Augustine
la soutenance a eu lieu au Pays Bas le
lundi 23 avril 2012 à 13:45 à la Vrije Universiteit
devant le jury composé de:

Dr. Marianne ALUNNIO-BRUSCIA	Chercheur IFREMER	Examinatrice
Dr. Herman SPAINK	Professeur Université Leiden	Examinateur
Dr. Jean-Christophe POGGIALE	Professeur Université Aix Marseille	Examinateur
Dr. Tjalling JAGER	Chercheur Université Libre d'Amsterdam	Rapporteur
Dr. Jaap van der MEER	Professeur Université Libre d'Amsterdam	Rapporteur
Dr. Sebastiaan A. L. M. KOOIJMAN	Professeur Université Libre d'Amsterdam	Directeur
Dr. Christelle ADAM-GUILLERMIN	Chercheur IRSN	Co-directrice
Dr. Béatrice GAGNAIRE	Chercheur IRSN	Tutrice

Contents

Preface	ix
Acknowledgements	ix
1 General Introduction	1
1.1 General background	1
1.2 Project outline	4
2 Developmental energetics of zebrafish, <i>Danio rerio</i>	7
2.1 Introduction	9
2.2 DEB model	10
2.3 Materials and methods	13
2.3.1 Caloric restriction experiment	13
2.3.2 Data and parameter estimation	14
2.4 Results	15
2.5 Discussion	19
3 Metabolic Handling of Starvation	25
3.1 Introduction	27
3.2 Model and methods	28
3.2.1 Formulation of starvation rules	28
3.2.2 Linking state variables to measurements	31
3.2.3 Stochastic feeding module	33
3.3 Results and Discussion	33
3.3.1 Constant food	33
3.3.2 Stochastic searching	36
3.4 Concluding remarks	40
4 Differential acceleration of development in Australian Myobatrachid frogs, captured by DEB theory	43
4.1 Introduction	45
4.2 Methods	46
4.2.1 Egg collection and incubation	46
4.2.2 Mass and energy density	47
4.2.3 O ₂ consumption	48

4.2.4	DEB Model	48
4.3	Results	49
4.3.1	Empirical results	49
4.3.2	DEB model	50
4.4	Discussion	58
5	Effects of uranium on the metabolism of zebrafish, <i>Danio rerio</i>	65
5.1	Introduction	67
5.2	DEB model	68
5.2.1	Temperature affects metabolic rates	73
5.2.2	Buffer handling rules	73
5.2.3	Starvation	74
5.2.4	Toxico-kinetics	74
5.2.5	Toxic effects	75
5.3	Materials and Methods	76
5.3.1	Animal maintenance	76
5.3.2	Experimental conditions	77
5.3.3	Water sample analysis	77
5.3.4	Biometry	78
5.3.5	Other data and parameter estimation	78
Fitting the model to individual data for each female	79	
15 day embryo and early juvenile experiments	81	
20 d adult accumulation experiments	81	
Estimation procedures	82	
5.4	Results	82
5.4.1	Control Reproduction trials	83
5.4.2	Fitting the control model to exposed females	87
5.4.3	Mode of action of uranium on females in reproduction trials	87
5.4.4	Adult whole body residues	92
5.4.5	Embryo and early juvenile	95
5.5	Discussion	98
5.5.1	Insights on reproductive physiology	98
5.5.2	Reproductive toxicology	99
5.5.3	Effects on growth	100
5.5.4	Elimination and uptake	101
5.5.5	On the origin of variability in bioaccumulation measurements	102
5.5.6	Deviations from the extended one compartment toxicokinetic model	102
5.5.7	Perspectives	103
5.6	Concluding remarks	104

6	Uranium induces ultra structural damage to gut wall of zebrafish, <i>Danio rerio</i>	107
6.1	Introduction	109
6.2	Material and Methods	111
6.2.1	Experimental conditions and tissue sampling	111
6.2.2	Light and transmission electron microscopy	111
	Light microscopy	111
	TEM	111
6.2.3	Fluorescent <i>in situ</i> hybridization	112
6.3	Results	112
6.3.1	Uranium induces damage to gut wall	112
6.3.2	Subcellular effects of uranium	114
6.3.3	Effects of U on bacterial colonization of intestinal lumen	114
6.4	Discussion	114
6.4.1	Histopathology of gut wall	114
6.4.2	Alterations of mitochondrial metabolism	118
6.4.3	Bacterial colonization of intestinal lumen	118
6.5	Conclusion	119
7	General Conclusion	121
7.1	Organism physiology	121
7.2	Organism stress responses	123
7.3	From individuals to molecules...	124
7.4	From individuals to populations...	125
7.5	Applications of this work to environmental risk assessment	126
	Bibliography	140
A	Standard DEB model with V1-morphic extension	141
A.1	Growth at constant food density	141
A.2	Dynamic formulation of the model	143
A.3	Survival probability	143
B	Experimental design for observing zebrafish growth and reproduction under controlled feeding conditions	145
C	Mineral fluxes	147
D	Parameter Estimation for <i>C. georgiana</i> and <i>P. bibronii</i>	149
E	Additional model predictions for <i>C. georgiana</i> and <i>P. bibronii</i>	153
F	Physical and chemical composition of exposure media for uranium toxicity experiments	159
G	Equations for modelling uranium toxicity experiments	161

H Additional model simulations for evaluating toxic mode of action on zebrafish metabolism	163
H.1 Control model fit to U-84 female reproductive data	163
H.2 Initial amount of reserve in two females	165
H.3 Simulating an increase in costs for synthesizing structure	166
I Model fits for individual females in the 15 day reproduction trial by Bourrachot 2009	167
Summary	171
Resumé	175
Samenvatting	179

Preface

On the cover, what at first glance appears to be an ichneumon wasp (or alternatively an ant) is actually a jumping spider *Orsima ichneumon*. This reflects the outlook I have developed over the last three years when interpreting biological data: things may not be as they seem at first glance. And I have always found it worthwhile to persist in looking for coherence between different observations.

I tried to remain fully consistent with the notation of DEB theory. A comprehensive list of all symbols and their meaning used in the context of DEB theory can be downloaded at http://www.bio.vu.nl/thb/research/bib/Kooy2010_n.pdf. I would recommend downloading the document as a companion to critically reading this thesis, if one is not familiar with the notation. While I tried very hard to minimize errors, there are most likely still a few. Please do not hesitate to tell me if you spot one.

Acknowledgements

First, I must extend my thanks to Bas Kooijman for accepting to supervise this thesis. You have been a source of inspiration and model of scientific rigour. I am very grateful for your patience in teaching me DEB theory and for dynamically illustrating what an enriching, exciting and stimulating arena science can be. Thank you for the extraordinary quality of your guidance; I hope I can also contribute in some small part to future developments. It has been a real pleasure to work with you and this thesis has been full of really exciting discoveries on the mysteries of life.

I am forever indebted to the kindness and hospitality of Truus Meijer. Thank you for receiving me in your home and sharing with me the many unique beauties of Holland. Thank you for your support, good humour and great conversations. And finally, thank you for your excellent and original cuisine, which was the source of energy fuelling my DEB adventures at the Free University and beyond.

I am grateful to Christelle Adam-Guillermin for the quiet encouragement and supervision, always present when needed and who gave me the freedom and flexibility to walk the road of my choice. Thank you for being so positive.

None of this work could have taken place without the unyielding support of Béatrice Gagnaire, who gracefully mentored my experimental work here at the IRSN. Thank you Béatrice.

Deep heartfelt thanks are attributed to Rodophe Gilbin for your support and critical interest in my work. I am grateful to all the help you have offered in technically difficult moments. I really appreciate the interest you have in all the students working in your laboratory, and the effort you invest so that we all carry out in the best possible conditions our respective projects.

I further extend my thanks to Jacqueline Garnier-Laplace for entrusting this exciting subject to me in July 2008 and allowing me to finish by extending my thesis contract.

I also sincerely thank Marianne Alunnio-Bruscia, Herman Spaink, Jaap van der Meer and Jean-Christoph Poggiale who honour me for accepting to judge this work and for accepting the jury role for this PhD defence in the Netherlands.

I am indebted to Claudine for always making me feel welcome, helping in the face of bureaucratic adversity; your patience, care and cheer are the beating heart and

soul of this laboratory. Merci Claudine pour tout.

Thanks are also due to Mme. Hamad Nobili for efficient organization of administrative matters relative to my doctoral school.

I am deeply grateful to the LRE laboratory and all of its members for receiving me. I have immensely enjoyed working with all of you. Thank you. Special thanks are due to Viginie Camilleri and Magali Floriani for a fruitful collaboration on the histological analysis of effects of uranium on the digestive tube, as well as gonad histology in response to food limitation. I further thank Virginie and Sylvie Pierrisnard for cation and anion analysis for both of my experiments.

Those experiments are coloured with a great many unique moments. In particular I will miss the warm atmosphere created by all the students within. Thank you, Morgan, Antoine, Benoit, Delphine and Adeline for all the support you have given me and the great lunches amongst the wild boars, great oaks and pines of Cadarache. Thank you Adelaide, for all the help and guidance you provided in the first months of my thesis. I have had many enjoyable moments sharing this office with you and now after all these years I also 'am on the road again'.

One of the greatest pleasures was crossing the road of so many 'master's of the art' who have patiently taught some of their skills. Fred Coppin, master of the art of chemistry. Thank you for your patience and time investment in sharing some skills with me. It has been a real pleasure to learn about UV and spectrometer dosing, preparation of calibration solutions for Uranium, nitrate, ammonium. I also enjoyed our heroic tentative to absorb all of the uranium in the waste water with calcite filters... I learned an important lesson: up-scaling from one to several hundred litres should not be done in a single step :-)

Sandrine Pereira, master in the art of cellular biology. Thank you for initiating me to the art of FISH, Immunohistology and cryo-sectioning. I am indebted to your time and energy investment and have learned a great deal working with you.

I can never thank the department of theoretical biology enough for receiving me in their midst. Thank you for the stimulating coffee breaks where theory and biology intermingle in the great story of life. Thank you Bob and Tjalling for the passion and strength of your persona. Thank you also for sharing your wisdom in the many discussions over sweet dark coffee, overlooking the vast expanse of the city, warmed by slanting rays of gold sunlight refracting off Free University glass.

And of course, where would I be without Elke? Thank you Elke for the wisdom without boundaries which floats so effortlessly across the time/ space spectra of your being. I have immensely enjoyed all of our scientific discussions and DEB adventures; but this inspiration was only strengthened through roving betwixt the streets of A'dam. And finally, thank you for the great company as we quietly tracked down, as silent detectives, deviating metabolic hints in our respective pets.

The work carried out in this thesis is the fruit of scientific exchange and collaboration with many authors of published papers on zebrafish physiology. I would like to thank C. Lawrence and G. Gerhard for their stimulating responses to my queries. I further thank Matt Litvak for a very fruitful collaboration on metabolic handling of starvation and the fun Skype conversations.

My first steps in the wild venture of science took place during my Masters thesis under the supervision of Jean-Christophe Poggiale. So I must also extend my thanks to this great master of the art- without whom I would not be where I am today. You are an excellent and passionate professor and I am honoured and richer for having been one of your students.

Life is a series of crossroads. And now comes the next one in my life. But I would like to reflect a little on the past and in particular on the important role my time working with Planetary Coral Reef Foundation played in where I am today. Gaie, Laser, Orla and Michel, thank you for receiving aboard your ship and teaching me reef ecology and seamanship. The two years spent aboard strengthened my person and expanded my cultural and moral horizons. A thesis is a long and exacting apprenticeship and a natural extension to the one I performed under your supervision. Thank you.

Nathalie, it has been extraordinary fun to cross the bridge at your side as it were, even if an ocean stood between the physical locations where we stand. We had a dream long ago in the corridors of Luminy and this dream came to life. It has truly been a pleasure. Thank you, and I look forward to perhaps collaborating in future projects.

Casey, thank you for the great and exciting times we had with the frogs :-), the insight we gained from the project was key to my scientific development. I enjoyed all the great virtual discussions we have had.

I would like to thank all the friends who accompanied me from afar on this adventure: Kakada, Naima, Yosmina, Rebecca, Fleure, Marjorie, Ratédé, Stephan, Kitty and many more.

And now, a very special and deep thanks to my entire family for their encouragement and love. For my grandparents, who have always remained present in the years I have grown even though I was always very far away. Cyclone and Cesco, Firefly, Cosmea, Menelik and Esperance: thank you for everything. If I am here today, it is thanks to you all. Your love and support is valued beyond the ken of words. Special thanks are due to Esperance and Manu for helping me design the cover of this thesis.

And last, but not least, thank you to Manu, my sweet love who stood by my side through it all. Your critical outlook on the societal significance of my type of work has been most stimulating :-). I particularly enjoyed our collaboration for designing the special aquaria for my experiments. Thank you for this valuable contribution and your enthusiasm.

“Every time man makes a new experiment he always learns more. He cannot learn less. He may learn that what he thought was true was not true. By the elimination of a false premise, his basic capital wealth which in his given lifetime is disembarrassed of further preoccupation with considerations of how to employ a worthless time-consuming hypothesis. Freeing his time for its more effective exploratory investment is to give man increased wealth.”

Buckminster Fuller, Operating Manual for Spaceship earth.

To my family

1

General Introduction

1.1 General background

Aquatic ecosystems are the recipient of toxic by-products of industrial activities linked to the nuclear fuel cycle (uranium ore leaching, storing of mine tailings, nuclear fuel enrichment processes, transport, industrial accidents etc.) and as such are submitted to chronic rejections of radionuclides which can directly interact with aquatic organisms. In 2009, 28.4% of primary energy production in Europe was of nuclear origin. France is particularly prominent in the field of civil nuclear use with 78% of its energy being of nuclear origin (Bosch et al., 2009).

At present, there is a heightened public awareness that long term effects of pollution linked to the nuclear industry on the environment may have negative human health and economic repercussions. According to the Institute of Radioprotection and Nuclear Safety's (IRSN) 2010 public barometer (IRSN, 2010), over 80% of the population demand increasing transparency and information concerning potential human health and environmental hazard concomitant with industrial activity. In 2010, detrimental effects of environmental pollution was ranked the third major concern of the French population. There is a real societal need to scientifically address these questions with less than half of the French population agreeing that scientific developments to date generate more benefits than prejudice to society. When faced with the question of who should be responsible for evaluating the risk associated with industrial pollution, most were in favour of a designated scientific committee over government, industrial representatives or non profit organisations. This type of study shows that ecologists and ecotoxicologists have an important responsibility to impartially evaluate and publicly communicate risks and impacts of industrial activities on the environment.

In 2002, the IRSN launched the ENVIRHOM project with the goal to evaluate the long term effects on the environment and human health of chronic exposure to low levels of radionuclides. Uranium is a heavy metal with dual

chemical and radiological toxicity depending on the isotopic composition (Barillet et al., 2007) and is generally the main component of the fuel for nuclear power plants. While it is a naturally occurring element, its concentrations in natural bodies of water are increased due to surrounding human activities (Fernandes et al., 1995; Jurgens et al., 2010; Uralbekov et al., 2011; Villa et al., 2011).

A body of literature results from this project and focusses on toxic effects of uranium at different levels of biological organization (molecular, cellular, tissular, organism and population). The research integrating effects and uptake was conducted on a wide variety of model organisms representative of different trophic levels in ecosystems: green algae *Chlamydomonas reinhardtii* (Fortin et al., 2004), asiatic clam *Corbicula fulminea* (e.g. Fournier et al., 2004; Simon and Garnier-Laplace, 2004; Simon et al., 2011a), crayfish *Procambarus clarkii* (Al Kaddissi et al., 2011), water flea *Daphnia magna* (Zeman et al., 2008; Massarin et al., 2010, 2011) and zebrafish *Danio rerio*. The focus of my thesis is toxic effects of uranium on this last species.

The short generation (around three months), ease of husbandry, small size (3-5 cm) and transparent eggs make zebrafish a popular model organism in ecotoxicology (Hill et al., 2005), developmental biology (Laale, 1977; Kimmel et al., 1995) and gerontology (Gerhard and Cheng, 2002). The full life-cycle of zebrafish is presented in fig. 1.1. Zebrafish are vertebrates and present many similarities with e.g. humans in terms of organization of development. It further plays an important role in present day medical and cancer research.

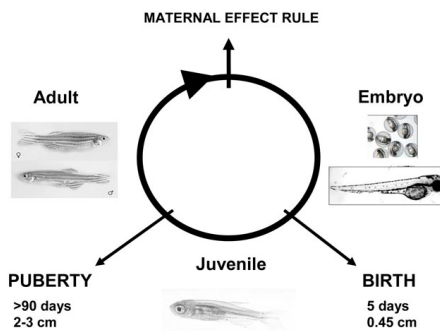


Figure 1.1: Life-cycle of zebrafish *Danio rerio*. Sizes and ages are qualitative. Embryo: no external feeding; juvenile: external feeding; adult: allocation to reproduction, but not to maturation. Initial reserve in an egg is specified in DEB theory using the maternal effect rule where the reserve density of the mother at spawning is equal to the reserve density of the offspring at birth (Kooijman, 2009b).

Extensive prior doctoral work already demonstrates genetic, molecular and individual level effects of exposure to water-borne uranium on zebrafish (Barillet, 2007; Bourrachot, 2009; Lerebours, 2009). Uranium impacts enzymatic

activity linked to cellular anti-oxidative stress defence systems (Barillet et al., 2005, 2007) and modifies the expression of genes involved in anti-oxidative stress (Lerebours et al., 2009, 2010b). Studies conducted at the individual level show that uranium reduces larval growth and survival (Bourrachot et al., 2008) as well as adult reproductive output (Bourrachot, 2009). In addition tissular damage to muscles, gills, gonads (Lerebours et al., 2009; Barillet et al., 2010) and the olfactory bulb (Lerebours et al., 2010b) have been reported.

Using data collected in the aforementioned studies as well as new additional experimental data, this fourth project seeks to understand how early responses of the immune and the oxidative stress systems (measured at molecular and cellular levels) are coupled to responses measured at the level of the individual (mortality, reproduction) or even the population. The main focus of this work is on linking these different levels of biological organisation through DEB theory.

DEB theory is a formal biological theory on the quantitative organisation of metabolism. The theory describes the uptake of substrate and its use to fuel metabolic processes (e.g. growth or reproduction) for all living organisms. The standard DEB model specifies all mass and energy fluxes for animals (Kooijman, 2010). Each one of the model parameters quantifies a single metabolic process. Compounds are assumed to be present in three concentration ranges within an organism: too little, enough and too much. Effects on the physiological performance of an organism commence below and above the too little and too much range (Kooijman, 2010, Chap.6). For a non-essential compound such as uranium there is no too little range. It is possible to capture distinct patterns of effects on development, growth and/or reproduction by modifying a single model parameter (Jager et al., 2010).

In general there is not enough information in toxicity data alone to estimate DEB parameters for the control. It is recommended to estimate control parameters separately including data on as many facets of metabolism as possible. The general method for parameter estimation is described in Lika et al. (2011a,b). There is a growing library of parameter values for many animals (one reserve and one structure): the Add_my_Pet library. The standard DEB model manages to capture in a simple way the interaction between physiological processes (growth, development, maintenance and reproduction) in a number of organisms rather accurately. This supports the idea that there is a baseline pattern for metabolism which allows the detection of physiological performance which deviates from it. Comparing organisms on the basis of differences in parameters values for a same model which applies to the entire life-cycle means that there are strong foundations for extrapolating between organisms. Major deviations of observations from model predictions give insight into species specific properties and continue to test the foundations of the theory. And more specifically deviations which are induced by the toxic compound of interest give insight into the mode of action onto the metabolism.

A very fruitful consequence of working within the framework of DEB theory is that insight on zebrafish is a small stepping stone to insight on what makes zebrafish special relative to other animal species and alternatively what aspects

of its metabolism are shared by other animal species. This strengthens the possibility to extrapolate the present findings to other species using body size scaling relationships (Kooijman, 1986) as well as reinforces extrapolations of effects of life stages where only sparse data is available within the species.

1.2 Project outline

The general philosophy of my project is that effects of uranium on individual fish appear as deviations from the unperturbed (blanc) situation. So I first paid due attention to quantify this blanc situation in some detail. Application of any model starts with the estimation of the parameter values. Hence, in chapter 2 parameter values for the standard DEB model for zebrafish are determined by fitting the model to observations published in the literature and an experiment performed in the laboratory where growth and reproduction at three food levels were measured simultaneously. The goal was to characterize the metabolism of zebrafish in the absence of perturbations such as extreme temperatures, absence of food and the presence (or absence) of toxic compounds.

DEB theory is useful for performing theory guided experiments and allows for detailed simulation of experimental design and optimization of type of measurements (e.g. length, mass), number of replicates etc. By playing with the notion of stochastic food input in a deterministic biochemical machine (the DEB organism) we simulated growth and reproduction of zebrafish before the experiment to decide on feeding protocols.

Constant food is in most cases a laboratory artefact and not a reflection of realistic environmental conditions. Food availability in the environment is fluctuating and organisms are subject to intermittent (or prolonged) periods of starvation. Further findings show that organism may even be food limited during part of their life-cycle in laboratory (toxicity) experiments (Jager et al., 2005; Zimmer et al., 2012).

During the course of my project it became clear that I must pay due attention to blanc physiological responses to starvation. Therefore, in chapter 3 the standard DEB model is extended in a simple way to deal with starvation. Monte Carlo simulation studies are performed to understand how environmental factors such as food availability can potentially override maternal effects (initial energy in the egg) and impact survival probability in early juveniles. While we simulated early juvenile zebrafish, the extension of the standard model is not species specific and brings up the notion of rejuvenation; a process where metabolic learning is not maintained. Shrinking can occur when energy from structure is taken to cover somatic maintenance. Death is instantaneous when structure reaches a specific fraction of the maximum one at the onset of shrinking.

At the start of the project we expected that uranium might impact development, because it might increase the need for (metabolic) defence and so reduce the maturation rate. During the project we learned that acceleration

and retardation of maturation comes naturally in some frogs for clear ecological reasons. We used the case to see if DEB theory can capture these processes accurately.

For this reason, the standard DEB model is applied to two species of Australian Myobatrachid frogs in chapter 4. Mass, age and dioxygen consumption are recorded for each stage of development as defined by Gosner (1960). The analysis of the data using the standard DEB model allows for the quantification of cumulated energy invested in maturation to reach each stage of development and number of mols of dioxygen consumed for each physiological process: assimilation, growth, maturation, somatic and maturity maintenance. Can the maturation concept of DEB theory give insight into how the development of one species of frog is accelerated relative to the other?

In chapters 2 to 4 the baseline metabolism of zebrafish is characterized. Effects of temperature and food on metabolism were studied using data and Monte Carlo simulation studies. The DEB model was also applied to other organisms illustrating the generality of the model to characterize the metabolism of diverse forms of life using a same set of assumptions on metabolic organisation (Kooijman, 2010, Chap.2).

A number of detailed studies from the Laboratory of Radioecology and Ecotoxicology shed light on effects of uranium on the life history of zebrafish. The objective is to analyse the data within the framework of DEB theory and determine if effects are explained by the modification of a single model parameter. If such is the case, the parameter which is modified represents the predominant mode of action of uranium. In chapter 5 the totality of zebrafish uranium toxicity data is compiled and analysed using the zebrafish DEB model. Reproduction buffer handling and Toxicokinetics modules are developed and incorporated into the study. Can the perturbation of a single process (as defined by DEB theory) explain the different observations? As we build the case that the life history of an individual zebrafish can be described by a single set of DEB parameters and that embryo metabolism gives insight into adult metabolism, we use simulation studies to imagine (through scenario analysis) how the mode of action translates to effects on observable (measurable) quantities such mass, length or number of eggs spawned.

Water-borne uranium may come into contact with the organism through cutaneous exchange, uptake by gills and absorption by the digestive tract. The morphology of gills and its role in uranium uptake has been previously studied (Barillet et al., 2010). I took an interest in the function of the digestive tract in nutrient assimilation, cellular defence and communication with microbiota. The processing of food requires symbiosis. In chapter 6 samples of the digestive tract of individuals exposed to water-borne uranium were compared histologically with the digestive tract of controls using fluorescent *in situ* hybridization, light microscopy and transmission electron microscopy to understand if tissue was impacted.

The final chapter presents concluding remarks and synthesis of insights and new research venues opened up through this study.

2

Developmental energetics of zebrafish, *Danio rerio*

Augustine, S., Gagnaire, B., Adam-Guillermin, C. and Kooijman, S. A. L. M. (2011). Developmental energetics of zebrafish, *Danio rerio*. *Comp Biochem Physiol A*, 159:275-283.

Abstract

Using zebrafish (*Danio rerio*) as a case study, we show that the maturity concept of Dynamic Energy Budget (DEB) theory is a useful metric for developmental state. Maturity does not depend on food or temperature contrary to age and to some extent length. We compile the maturity levels for each developmental milestone recorded in staging atlases. The analysis of feeding, growth, reproduction and ageing patterns throughout the embryo, juvenile and adult life stages are well-captured by a simple extension of the standard DEB model and reveals that embryo development is slow relative to adults. A threefold acceleration of development occurs during the larval period. Moreover we demonstrate that growth and reproduction depend on food in predictable ways and their simultaneous observation is necessary to estimate parameters. We used data on diverse aspects of the energy budget simultaneously for parameter estimation using the covariation method. The lowest mean food intake level to initiate reproduction was found to be as high as 0.6 times the maximum level. The digestion efficiency for TetraminTM was around 0.5, growth efficiency was just 0.7 and the value for the allocation fraction to soma (0.44) was close to the one that maximizes ultimate reproduction.

Key words: ageing, *Danio rerio*, development, Dynamic Energy Budget theory, feeding, growth, reproduction

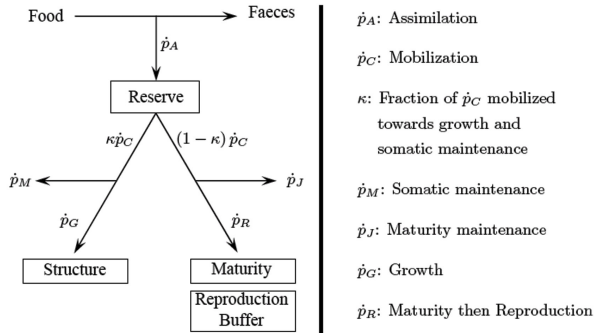


Figure 2.1: Conceptual organisation of animal metabolism as defined by DEB theory (Kooijman, 2010). Arrows: energy fluxes (J d^{-1}); boxes: state variables of the system. Embryo: $\dot{p}_A = 0$; birth: assimilation is switched on; puberty: allocation to maturity stops and allocation to reproduction starts. Energy allocated to reproduction accumulates in the reproduction buffer and is emptied at spawning.

2.1 Introduction

Experimental evidence points to developmental processes being heterochronic and they play an important role in evolutionary theory (McKinney and McNamara, 1991). Spicer and Burggren (2003) propose the concept of heterokairy to study how changes in the sequence of developmental events relate to changes in the timing of physiological regulatory systems and/or its components. Theoretical progress in the analysis of these processes lags behind experimental work for lack of a quantifier for internal time which does not necessarily correlate with morphological (e.g. length) or chronological (e.g. age) criteria (Reiss, 1989). The objective of the present study is to provide a such a quantifier for the rate of development of the individual. We focus on zebrafish *Danio rerio* since it is widely used to study development (Kimmel et al., 1995; Parichy et al., 2009). A growing number of disciplines use zebrafish as a model with the consequence that numerous observations on life history traits, under laboratory controlled conditions, are available (Laale, 1977; Gerhard and Cheng, 2002; Lawrence, 2007; Spence et al., 2008).

We undertake a theoretical analysis of zebrafish development over its entire life cycle using Dynamic Energy Budget (DEB) theory (Kooijman, 2001, 2010), see Sousa et al. (2010) for an introduction to the theory. The theory quantifies the uptake and use of substrates (food) by organisms, see figure 2.1. Stage transitions, such as from embryo to juvenile (defined as the initiation of feeding) and from juvenile to adult (defined as the ceasing of further maturation and the initiation of allocation to reproduction) are linked to the level of maturity. Maturity is quantified as the cumulated energy invested in development. Although the standard DEB model has been applied to a wide variety of animals

(Zonneveld and Kooijman, 1993; van der Veer et al., 2010; Bodiguel et al., 2009; Flye-Sainte-Marie et al., 2009; Pecquerie et al., 2009; Rico-Villa et al., 2010), tests that the parameters for the embryo, juvenile and adult are all the same are relatively rare (Kooijman et al., 2011; Lika et al., 2011a). We collected a number of detailed studies on the growth, reproduction and ageing of zebrafish, and we also did a growth-and-reproduction experiment at three feeding levels, to estimate the parameters of the standard DEB model and judge if the full life cycle could be captured with a single set of parameter values. We discuss the coupling of developmental milestone to age and size at stage transitions (e.g. birth and puberty) and give a mechanistic underpinning of effects of food and temperature.

2.2 DEB model

The conceptual organisation of metabolism, described in the DEB model, is presented in figure 2.1. The mobilisation of reserve \dot{p}_C is such that weak homeostasis is respected, i.e. the ratio of the amounts of reserve E (J) and structure V (cm), called the reserve density $[E]$, is constant at constant food densities in juveniles and adults. The increase in the maturity level E_H (J), called maturation, is by allocating a fixed fraction of mobilised reserve $(1 - \kappa)\dot{p}_C$ after subtraction of maturity maintenance costs \dot{p}_J (e.g. immune system, hormonal regulation, anti-oxidative stress system). $\dot{p}_J = k_J E_H$, with k_J (d^{-1}) the maturity maintenance rate coefficient. Positive maturity maintenance implies that reproduction is absent at low food levels. There is no assimilation during the embryonic period, i.e. when $E_H < E_H^b$, with E_H^b the cumulated amount of energy invested in maturity at birth.

From birth onwards reserve is replenished by assimilation, \dot{p}_A (J d^{-1}). We now explain how assimilation is linked to actual ingestion. Ingestion rate, \dot{p}_X (J d^{-1}), is a function of food density and is taken proportional to surface area L^2 , with $L = V^{1/3}$ the (volumetric) structural length of an organism. \dot{p}_X is quantified by the scaled functional response (ingestion level) f , defined as the ratio of actual ingestion rate and the maximum possible one for an individual of that size. This makes $\dot{p}_X = f\{\dot{p}_{Xm}\} L^2$, where $\{\dot{p}_{Xm}\}$ ($\text{J d}^{-1} \text{cm}^{-2}$) is the maximum surface area specific ingestion rate. The conversion efficiency of food to reserve (digestion efficiency), κ_X , is specific to each type of food. Finally, $\dot{p}_A = \kappa_X \dot{p}_X$. Digestion efficiency is calculated using the following relationship:

$$\kappa_X = \{\dot{p}_{Am}\} / \{\dot{p}_{Xm}\} \quad (2.1)$$

where $\{\dot{p}_{Am}\}$ ($\text{J d}^{-1} \text{cm}^{-2}$) is the maximum surface-area specific assimilation rate and a model parameter (see table 2.1).

Growth is defined as the increase of structure. Energy allocated to growth \dot{p}_G is a fixed fraction of mobilised reserve $\kappa\dot{p}_C$ after subtraction of somatic maintenance costs $\dot{p}_M = [\dot{p}_M] V$ (e.g. maintaining intra-cellular concentration,

protein turnover, movement), with $[\dot{p}_M]$ ($\text{J d}^{-1} \text{cm}^{-3}$) the volume-specific maintenance costs. The cost of the synthesis of a unit of structure is called $[E_G]$ (J cm^{-3}) which indirectly defines growth efficiency κ_G being the ratio of energy fixed and invested in new structure (see table A.3, online appendix A).

Allocation to maturation in juveniles is redirected to reproduction in adults (\dot{p}_R) at puberty which occurs at $E_H = E_H^p$. Reserve allocated to reproduction is first accumulated in a buffer which is emptied at spawning. The conversion of reserve to egg (embryo reserve) occurs with efficiency κ_R . The value of 0.95 in table 2.1 has been chosen in view of the absence of substantial chemical work. Allocation to growth and somatic maintenance occurs in parallel to allocation to maturation and reproduction (see figure 2.1). The embryo starts its development with zero structure and maturity, and an amount of reserve such that the reserve density at birth equals that of the mother at egg formation. The latter condition is a maternal effect Kooijman (2009b).

The standard DEB model assumes that the individual is isomorphic, i.e. it does not change in shape during growth, which makes that surface area is proportional to volume to the power 2/3. Motivated by studies on Anchovy, *Engraulis encrasicolus*, and Bluefin Tuna, *Thunnus orientalis*, (Pecquerie, 2007; Jusup et al., 2010), we implemented the possibility that development accelerates after birth ($E_H = E_H^b$) by including a V1-morphic stage (surface area grows proportional to volume) for the larva (early juvenile) till maturity reaches a threshold level for metamorphosis ($E_H = E_H^j$), after which growth resumes in an isomorphic fashion (Kooijman et al., 2011). If $E_H^j = E_H^b$ there is no acceleration, but if $E_H^j > E_H^b$ both $\{\dot{p}_{Am}\}$ and energy conductance \dot{v} (cm d^{-1}) increase with length. \dot{v} controls reserve mobilization.

Auxiliary theory assumes that the shape coefficient δ , i.e. the ratio of structural length (L) and physical observed length L_{obs} , is constant for isomorphs. Shape changes during the early juvenile (V1-morphic) period are described by the empirical function $\delta(L) = \delta_{\mathcal{M}} + (\delta_{\mathcal{Y}} - \delta_{\mathcal{M}}) \frac{L_j - L}{L_j - L_b}$ for $L \in [L_b, L_j]$ with $\delta_{\mathcal{Y}}$ and $\delta_{\mathcal{M}}$ shape coefficients for embryos and adults respectively, L_b structural length at birth and L_j structural length at metamorphosis.

The effect of temperature on all biological rates is well captured by the Arrhenius relationship (Kooijman, 2010), quantified by the Arrhenius temperature T_A . This relationship only holds within a particular temperature tolerance range.

DEB theory considers development and senescence to be parallel processes. The ageing module of DEB theory (Kooijman, 2010; van Leeuwen et al., 2010) specifies that the induction of damage inducing compounds (e.g. modified mitochondrial DNA) is proportional to the mobilisation rate of reserve, which is (about) proportional to the use of dioxygen (linking to free radicals) that is not associated with assimilation. Damage inducing compounds can also induce themselves at a rate that is proportional to their concentration and, again, to the mobilisation rate of reserve as quantifier for metabolic activity. Damage inducing compounds induce damage compounds (e.g. modified proteins) which

Table 2.1: State variables and primary parameters (affecting changes of state variables at 20°C of the zebrafish DEB model, and other parameters (see text)).

Sym- bol	Value	Unit	Name
<i>State Variables</i>			
E	-	J	Reserve
V	-	cm^3	Structure
L	-	cm	Structural length $V^{1/3}$
E_H	-	J	Cumulated energy invested in maturity uptill puberty and reproduction after puberty
<i>Primary Energy Parameters</i>			
$\{\dot{p}_{Am}\}$	246.3	$J \text{d}^{-1} \text{cm}^{-2}$	Embryo Maximum surface area specific assimilation rate
\dot{v}	0.0278	cm d^{-1}	Embryo Energy conductance
κ	0.437	-	A specific fraction of energy mobilized from reserve allocated to growth and somatic maintenance
κ_X	0.5	-	Digestion efficiency for Tetramin TM
κ_R	0.95	-	Reproduction efficiency
$[\dot{p}_M]$	500.9	$J \text{d}^{-1} \text{cm}^{-3}$	Volume specific somatic maintenance costs
\dot{k}_J	0.0166	d^{-1}	Maturity maintenance rate
$[E_G]$	4652	$J \text{cm}^{-3}$	Cost of synthesis of a unit of structure
E_H^b	0.54	J	Cumulated energy invested in maturity at birth
E_H^j	19.66	J	Cumulated energy invested in maturity at metamorphosis
E_H^p	2062	J	Cumulated energy invested in maturity at puberty
<i>Other parameters</i>			
T_A	3000	K	Arrhenius Temperature
\ddot{h}_a	$1.96 \cdot 10^{-9}$	d^{-2}	Weibull aging acceleration
s_G	0.0405	-	Gombertz stress coefficient
δ_Y	0.1325	-	Shape coefficient for embryos
δ_M	0.1054	-	Shape coefficient juveniles and adults for total length

accumulate in the body. The hazard rate due to ageing is taken proportional to the density of damage compounds. This specifies the ageing module, and how ageing depends on energetics, and so on the nutritional status of the organism.

2.3 Materials and methods

2.3.1 Caloric restriction experiment

We designed a caloric restriction experiment to obtain quantitative data on growth in combination with reproduction at 3 ingestion levels for individual fish.

2 cm (SL) fish were acquired from a commercial fish breeder (Elevage de la grande rivière, Lyon, France) and were 116 days post-fertilization (dpf) upon arrival. Based on this size and age we estimated the mean intake level f_{cult} . Animals were kept in soft water: $T = 26^\circ\text{C}$, $\text{pH} = 6.5 \pm 0.4$, electrical conductivity $200 \mu\text{S cm}^{-1}$. Food given was TetraminTM (proteins, 46%, lipids 7.0%, ash 10.0% cellulose 2.0% and moisture 8.0%). We calculated the energetic content of Tetramin as 19.1 kJ g^{-1} with 17.2 and 38.9 kJ g^{-1} for lipids and proteins respectively (Kooijman, 2010, table 4.2). This result is used to obtain κ_X (see equation 2.1) for individuals during acclimatization (116 and 132 dpf), where they were fed *ad libitum* f_{pretreat} . Caloric restriction took place between 132 and 214 dpf. We started with 6, 4.5 and 3 mg Tetramin per day per individual fish for the first (f_1), second (f_2) and third (f_3) ingestion level respectively. f_1 and f_2 were gradually raised to 10 mg d^{-1} while f_3 remained constant during the caloric restriction phase, in accordance with the expectation that feeding rate is proportional to squared length. The daily ration was hand weighed in aluminium micro weighing dishes (VWR) with an SE2 ultra-microbalance (Sartorius AG, Göttingen, Germany) and dispensed 2 to 3 times throughout the day. Individuals fasted one day per week. The experimental system is fully characterized in Appendix B. We kept 20 individuals per condition. Reproduction was assessed by forming couples (1:1 male to female ratio) in the evening and counting the number of eggs spawned the following morning. We followed the daily egg output of individual females over two successive breeding trials which lasted 22 and 15 days respectively.

To check the condition of the gonads three males and three females in each condition were sacrificed at the end of the experiment. Gonads were removed and immersed in 2.5% glutaraldehyde sodium cacodylate buffer (0.1 M, pH 7.4) for 24h at 4°C then post fixed with 1% osmium tetroxyde for 1h. The samples were dehydrated through a graded ethanol series and finally embedded in monomeric resin Epon 812. Semi-thin sections for light microscopy analysis (500 nm) were obtained with an ultramicrotome UCT (Leica Microsystems GmbH, Wetzlar, Germany). Plastic sections were stained with aqueous blue toluidine and gonad structure was examined under a light microscope (Leica, DM750) equipped with a Leica camera ICC50 and LAS EZ Software. For

each replicate, at least 20 micrographs of local detailed structures were taken, analysed and compared.

2.3.2 Data and parameter estimation

We incorporated real and pseudo data into the parameter estimation routine. Real data, compiled from the literature and the caloric restriction experiment, include observed lengths, weights, reproduction, and survival at single (0-variate) or multiple (1-variate) time and/or temperatures points. Pseudo data represent the more conserved aspects of animal metabolism; large deviations from these data are considered to be less likely. The pseudo data concern: $\dot{v} = 0.02 \text{ cm d}^{-1}$, $[\dot{p}_M] = 18 \text{ J d}^{-1} \text{ cm}^{-3}$, $\kappa = 0.8$, $\kappa_G = 0.8$ and $\dot{k}_J = 0.002 \text{ d}^{-1}$ (see Kooijman, 2010, pp.300). The chemical indices (c-mol per c-mol), molar weights (g mol^{-1}), and chemical potentials (J mol^{-1}) and are as given in Lika et al. (2011a) (table A.1, Appendix A). The densities d_{Vd} and d_{Ed} (g cm^{-3}) for structure and reserve were derived from Craig and Fletcher (1984) (table A.1, Appendix A).

Table 2.2: Model predictions for 0-variate data are compared with observations.

Data	Observations	Predictions	Unit	Reference
size at birth	0.39	0.40	cm	Schilling (2002)
maximum length (TL)	5.00	5.10	cm	Spence et al. (2008); Schilling (2002)
maximum reproduction rate	60 - 240	113.6	# eggs d^{-1}	Eaton and Farley (1974a) and Geffroy (Unpublished 2009)
egg dry mass	30 - 106	73	μg	Augustine (Unpublished 2010)
egg diameter	0.08 - 0.09	0.10	cm	Uusi-Heikkilä et al. (2010)
maximum wet weight	1	0.99	g	Pers. Obs

We allowed expectations to deviate from these values by giving them less weight relative to real data. We converted all rates and ages to a reference temperature of 20°C . We measured the ratio of standard length SL (tip of snout till base of caudal fin) and total length TL (tip of snout to end of caudal fin) of 70 adult zebrafish (Adam-Guillermin unpublished 2009) and found an average ratio of 0.8. DEB model predictions are given in TL so when necessary the predictions are corrected to standard length SL. We treated forked length FL (tip of snout till fork in the caudal fin) equal to TL.

We applied the method of covariation for parameter estimation (Lika et al., 2011a) using the freely downloadable software DEBtool (Kooijman et al., 2008). This software uses the simplex (Nelder-Mead) method to simultaneously minimise the weighted sum of squared deviations between model predictions and

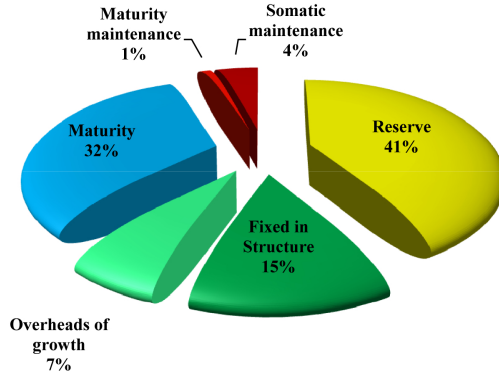


Figure 2.2: Energy budget at birth when the mother was at abundant food. Initial reserve in an egg (E_0) is 1.670 J while structure and maturity are zero. Slices represent the cumulated energy investments at birth relative to E_0 . Maturity (cumulated energy invested in maturity) as well as maturity and somatic maintenance are dissipated in the environment as minerals (e.g. CO_2). A fraction $1 - \kappa_G$ of energy invested in structure is lost as overheads of growth. The reserve and structure contribute to the actual mass of the organism at birth.

observations for a considerable number of data sets. Computations were performed with Matlab[®] (version 7.9.0.529). DEBtool routines and formula for calculating predictions for data in table 2.2 be found in table A.3 (Appendix A). Without information on mass and caloric content of food ingested per day we could not calculate the digestion efficiency each food type described in the data from the literature. We make the assumption that while diets differ between experiments they are similar enough for us to apply a scaled functional response $0 \leq f \leq 1$ for all data. f is a free parameter and is estimated for each data set. Although we could suppose constant food density and temperature for most data (Appendix A.1), a dynamic formulation of the model was needed to predict growth and reproduction in the caloric restriction experiment (Appendix A.2).

2.4 Results

The conversion efficiency of TetraminTM to reserve was found to be $\kappa_X = 0.5$. Parameter estimates (table 2.1) show a factor 40 difference between maturity level at metamorphosis and at birth (E_H^j and E_H^b) which translates into a factor 3 difference in structural lengths (L_j and L_b) at abundant food. So specific assimilation and energy conductance also increase by a factor 3 during the early juvenile period. Drain to maturity maintenance amounts to 34.27 J d^{-1} in adults and only a fraction $1 - \kappa = 0.56$ of mobilized reserve is allocated to maturity maintenance plus reproduction. This implies that puberty is not

reached for ingestion levels lower than $f = 0.6$. We were surprised that the lowest intake level for reproduction is that high. The value for κ is very close to the one which maximizes the ultimate reproduction rate (0.48) given the values of the other parameters. The Add_My_Pet collection typically shows values around 0.8 for which reproduction is far below the maximum possible one (Lika et al., 2011a). Some 44% of the initial energy in an egg is lost by the end of the embryonic period (birth), see figure 2.3, by mineralization of reserve. Although maintenance is relatively high (see the Add_My_Pet collection the cumulative amount spent at birth is small due to high costs for growth and maturation. Energy conductance is typical for embryos and relatively high for adults due to the acceleration during the early juvenile period.

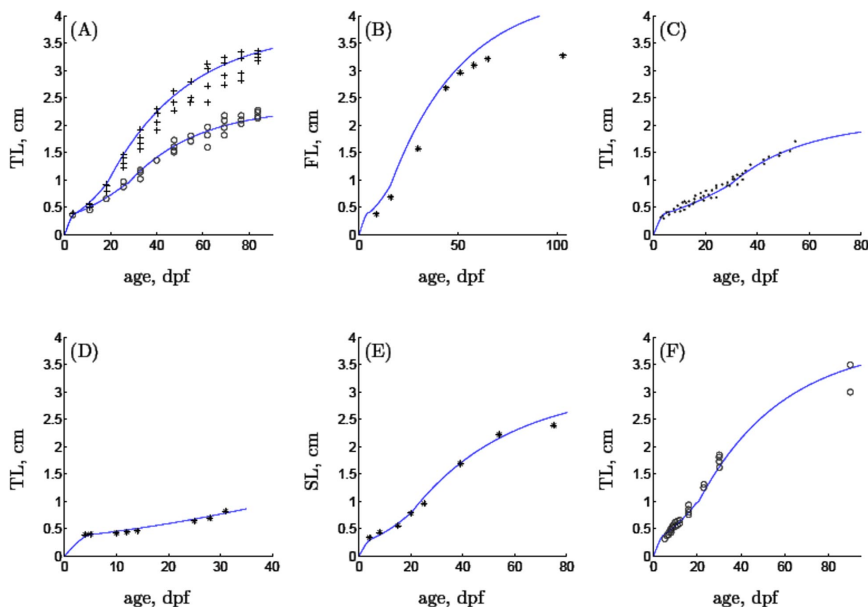


Figure 2.3: Synthesis of model predictions against observed lengths of fish from different published studies. Crosses or circles: observations; full lines: model predictions; TL: Total Length (snout till end of caudal fin); FL: Forked Length (snout till fork in caudal fin); SL: Standard Length (snout till base of caudal fin). For each data set we specify temperature and estimated ingestion level f ($0 \leq f \leq 1$). (A) Data from Lawrence et al. (2008) and pers. comm.. $T = 28.5^\circ\text{C}$; (+) individuals fed approximately twice as much as (o). $f_1 = 0.75$ for high ingestion level and $f_2 = 0.65 f_1$ for the lower ingestion level. (B) Data from Gómez-Requeni et al. (2010). $T = 28^\circ\text{C}$; $f = 0.88$. (C) Data from Schilling (2002); $T = 28.5^\circ\text{C}$; $f = 0.44$. (D) Data from Bagatto et al. (2001). $T = 25^\circ\text{C}$; $f = 0.4$. The type of length measurement is unknown but model predictions are in TL. (E) Data from (Eaton and Farley, 1974a). $T = 25.5^\circ\text{C}$; $f = 0.77$. (F) Data from Best et al. (2010) but we present the full growth curve provided through pers. comm. with C. Lawrence. $T = 25^\circ\text{C}$; $f = 0.78$.

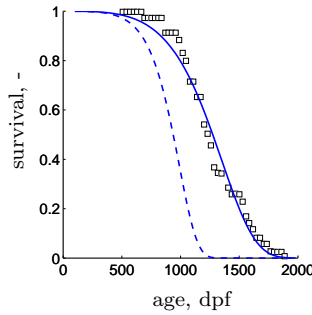


Figure 2.4: Survival probability in relation to nutritional status as predicted by the DEB ageing module. (□) data from [Gerhard et al. \(2002\)](#) outbred tank 2; solid line: model prediction for $f = 0.8$. Dashed line: predicted survival for $f = 1$. $T = 26^\circ\text{C}$.

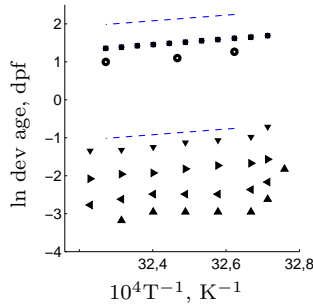


Figure 2.5: Ln developmental (dev) age as a function of inverse temperature (T). Model predictions for birth (■) and data: protruding mouth stage (○, from [Kimmel et al. \(1995\)](#)), 8 cell stage (▲), late cleavage (▼), very late blastula (▶), and blastoderme 3/4 yolk sphere (▼), all from [Shirone and Gross \(1968\)](#). The slope of the dashed lines gives an Arrhenius temperature of 3000 K.

Compiled growth curves (figure 2.3) are confronted with DEB predictions and we conclude that general growth patterns are accurately predicted by DEB theory for ingestion levels ranging from 0.4 in [Bagatto et al. \(2001\)](#) to 0.88 in [Gómez-Requeni et al. \(2010\)](#). Predicted egg dry mass ranges from 58 to 73 μg ($f = 0.5$ to $f = 1$). Maximum predicted wet weight for a fish is 0.99 g.

Age dependent survival was correctly predicted (see figure 2.4 and section A.3, online appendix A for equations). Lifespan is expected to decrease for increasing food. The ultimate size of the fish of around 3.5 cm SL ([Gerhard et al., 2002](#), pers. comm.) suggests that $f \approx 0.8$. figure 2.4 also presents model predictions for abundant food.

Predicted length at birth (4 mm at abundant food table 2.2) is not very sensitive to the nutritional status of the mother which is in line with both [Parichy](#)

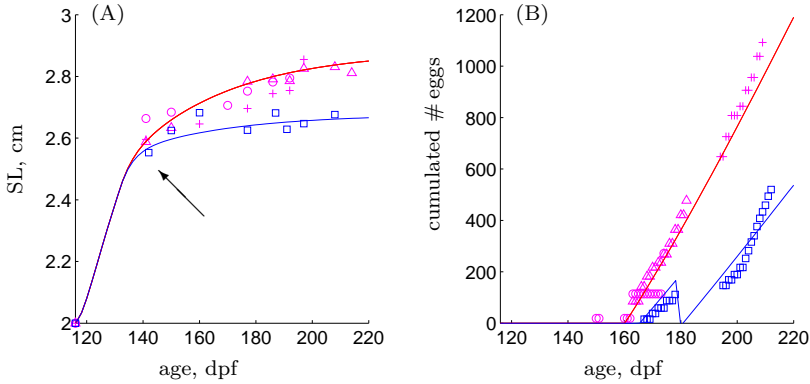


Figure 2.6: Observations, the symbols refer to the different individuals, and model predictions, solid lines, for growth (A) and reproduction (B) during 82 days of caloric restriction at two feeding levels which are estimated at $f_1 = 0.74$ and $f_2 = 0.69$. Animals are 116 days post-fertilization (dpf) and 2 cm standard length SL (tip of snout till base of caudal fin) at arrival. They are acclimated to laboratory conditions for two weeks. Caloric restriction is initiated at 132 dpf (arrow).

et al. (2009) (developmental milestone pSB+: inflation of posterior swim bladder, head showing anterior mouth position) and Schilling (2002) (length at first feeding). DEB theory predicts that age at birth also depends on ingestion level of the mother (maternal effect). However the effect is minimal. According to Kimmel et al. (1995) ‘birth’ (active feeding behaviour) is around 5 dpf at 28.5°C. DEB theory predicts birth in the range of 4.3 to 4.7 dpf ($f = 1$ to $f = 0.5$) at 28.5°C and in the range of 4.8 to 5.3 dpf ($f = 1$ to $f = 0.5$) at 25°C.

The Arrhenius relationship for the log of developmental age against inverse temperature should be linear. Figure 2.5 confirms this for different developmental milestones and also presents model predictions for age at birth. We see (a) that the estimated Arrhenius temperature of 3000 K (which corresponds graphically to the regression slope) is coherent with observations and (b) that birth occurs just after the protruding mouth stage described by Kimmel et al. (1995). Typical Arrhenius temperatures revolve around 8000 K (Add_My_Pet) making zebrafish less sensitive to temperature variations.

For $f = 0.77$ (figure 2.3, E) first spawns occurred at 71-75 dpf for females between 2.4 and 2.6 cm SL at 25.5°C (Eaton and Farley, 1974b). Predicted age and length at puberty for this data set is 88 dpf and 2.7 cm SL. Not only these data but also the complete growth curve is in remarkable agreement.

This agreement also applies to the growth and reproduction in our caloric restriction experiment (figure 2.6) ($f_{\text{cult}} = 0.55$, $f_{\text{pretreat}} = 0.9$, $f_1 = 0.74$ and $f_2 = 0.69$). Predicted ages at puberty are 160 dpf and 165.5 dpf and predicted reproduction rates are 19.84 and 13.01 eggs per day for f_1 and f_2 respectively at 26°C. Maximum predicted reproduction rate (table 2.2) at 26°C at abundant food is 113.6 eggs per day. This value represents the maximum daily energy

invested in reproduction by the largest possible individual ($L = L_m$) at highest ingestion level ($f = 1$).

Length at puberty ranges from 2.9 ($f = 0.6$) to 3.8 ($f = 1$) cm TL (2.3–3 cm SL) and age at puberty ranges from 178.8 – 59.18 dpf at 28°C. Contrary to age and length maturity levels at various developmental milestones are independent of temperature and nutritional status, see tables 2.3 and 2.4. Maturity levels are computed using parameters values in table 2.1. Standardized Standard Lengths (SSL) as given by Parichy et al. (2009) are converted to total lengths using their photographs for each milestone. The contribution of the caudal fin changes during development from 0.06 at birth to 0.2 at puberty. The estimated ingestion level is based on length at puberty in their staging atlas. We assume abundant food (of mother) for embryonic development in table 2.3.

Microscopic analysis of gonads revealed a remarkable effect of ingestion level on male gonads (figure 2.7): f_3 gonads were small empty shrivelled versions of healthy male testes such as those observed in f_1 and f_2 . The analysis of female gonads was not conclusive.

2.5 Discussion

Reports of deviating growth patterns can be found in the literature which we briefly discuss here. Gómez-Requeni et al. (2010) observed growth arrest after 65 dpf, an age at puberty of around 50 dpf and suggest that growth ceases during reproduction. This interpretation is at odds with other data (Barrionuevo and Burggren, 1999; Lawrence et al., 2008; Barrionuevo et al., 2010; Best et al., 2010) and our own experimental results; growth continues during reproduction at rates increasing with food level. Based on their growth data we estimate $f = 0.88$ with an ultimate length of 4 cm TL and an age at puberty of 67 dpf. Zebrafish growth was found to be indeterminate Gerhard et al. (2002). Accordingly, we found that length still increased by a factor 1.3 after puberty at abundant food.

Eaton and Farley (1974a); Schilling (2002); Best et al. (2010); Gómez-Requeni et al. (2010) observe juvenile growth that is consistent with our model predictions. Barrionuevo and Burggren (1999); Barrionuevo et al. (2010) however, observed growth arrest for about a month after birth (≈ 4 mm). They only started to feed the larvae when the yolk sac is completely absorbed, when zebrafish can begin actively feeding as soon the oesophagus opens and some of the yolk sac still remains (Lawrence, 2007; Best et al., 2010). Delaying initial feeding beyond this point impacts subsequent growth and survival (Guillaume et al., 1999). Except for a slow start, lengths and wet weight curves of Barrionuevo and Burggren (1999); Barrionuevo et al. (2010) are in agreement with our model predictions. During parameter estimation we assumed that all food types were equivalent. Practice teaches that food quality is an important parameter (Gergs and Rothhaupt, 2008) and it might contribute to deviation from general patterns. Moreover the model does not take digestion into ac-

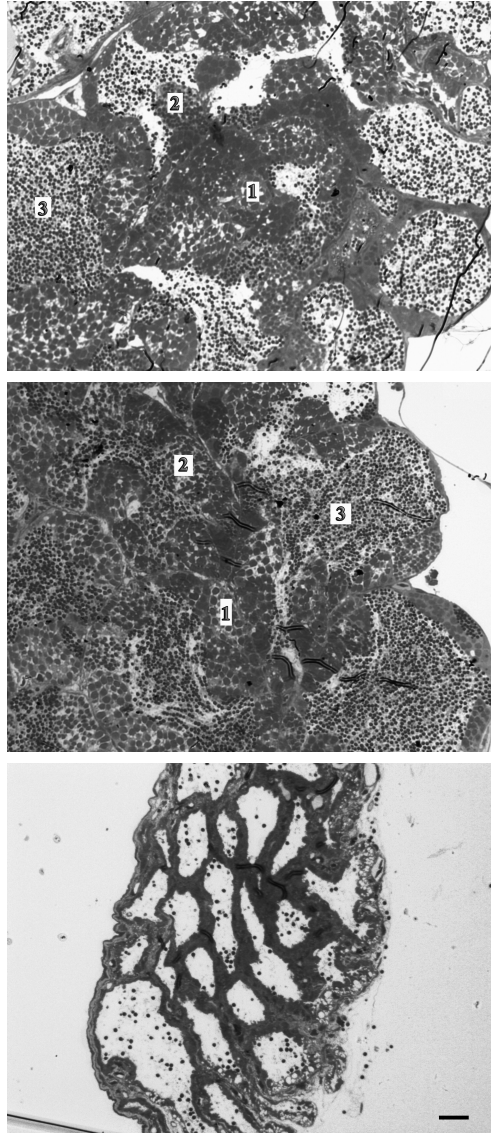


Figure 2.7: Microphotographs of male gonads after 82 days of caloric restriction for the ingestions levels f_1 (top), f_2 (middle) and f_3 (bottom). Scale bar: 20 μm ; 1: cysts with secondary spermatogonia; 2: cysts with spermatocytes; 3: cysts with spermatids or spermatozoa. At f_3 structures are shrivelled.

count (i.e. gut residence time). The model can be extended to capture this aspect of physiology for certain applications (e.g. Evers and Kooijman, 1989).

If well fed individuals of sufficient size are exposed to $f = 0.44$ computer simulations suggest that they should reproduce while growth is slightly negative. Pecquerie et al. (2009) consider that starved female Anchovy pay for somatic maintenance ($[\dot{p}_M]$) by reabsorbing energy from the reproduction buffer. This is confirmed by our observations of male gonads. We implemented this behaviour in our simulation studies and growth will not become negative in the case of mild starvation.

Reproductive patterns are found highly variable compared to growth. Eaton and Farley (1974b) report a maximum of 60.4 eggs per day (25.5°C, 497 dpf) over a period of 105 days, Hisaoka and Firlit (1962) observe 37.9 eggs per day over a period of 146 days (26°C) and Geffroy (unpublished data 2009) found 240 eggs per day over a 10 day period trial for zebrafish fed 5% their body weight (25°C). Our study shows that the simultaneous observation of food intake, body size and reproductive output provides insight into the degree/nature of this variability. We present such information for individual zebrafish taken from the caloric restriction experiment (figure 2.6) and find results consistent with growth and first spawnings in Eaton and Farley (1974a). The detailed rules for spawning are part of the behavioural repertoire that can be rather stochastic and differ between individuals (Eaton and Farley, 1974b; Gerlach, 2006; Spence and Smith, 2006) calling for advanced statistical methods to detect metabolic perturbations (Paull et al., 2008). The reproduction buffer can contribute up to 15% of adult weight (Forbes et al., 2010). Reproduction increases with size, consistent with the finding of Uusi-Heikkila et al. (2010), and food availability. Our results show that that a large variability of the reproduction buffer handling rules can combine with a low variability of the reproduction rate.


































Our assumption of a maternal effect is consistent with Brown (1958); Guillaume et al. (1999). It is not sure that this applies equally well to zebrafish. Forbes et al. (2010) suggest that egg size is decided during oocyte maturation and observe that higher food intake comes with the production of smaller eggs of poorer quality.

We measured egg dry mass of mature females (> 364 dpf, 26°C, *ad libitum* feeding) for each spawning event during a 2 month reproduction trial and found values ranging from 30 to 105 μg (Augustine unpublished 2010). This large variation makes it difficult to judge the model assumption on the maternal effect. Future extensions of the model might include this variation.

The data did not allow us to study the effect of temperature outside the tolerance range as has been done for marine fish species (Freitas et al., 2010). We suggest that for ecological purposes such a study should be considered. Although our model correctly predicts survival patterns at a single ingestion level, predictions at other levels need confirmation. Reproduction might be impacted by age (Tsai et al., 2007), but more quantitative data is needed for modelling. Gold fish, *Carassius auratus*, for example have maximum fertility

at 3 years, become sterile by 7 and can live as long as 40 (Brown, 1958, pp.370). Effects of toxicants can be captured by linking parameter values to internal concentrations. This can also be done for density of damage compounds to model post reproductive periods (Jager and Klok, 2010; Kooijman, 2010).


















Table 2.3: Cumulated energy invested in maturation, E_H (mJ) for the embryonic developmental milestones. Developmental stages and ages (28.5°C) are as defined by Kimmel et al. (1995). Ages are presented in hours post-fertilization, hpf.

	Stage	Age, hpf	E_H , (mJ)		Stage	Age, hpf	E_H , (mJ)
	2-cell	0.75	0.01		Shield	6	0.38
	4-cell	1	0.02		75%-epiboly	8	0.71
	8-cell	1.25	0.02		90%-epiboly	9	0.96
	16-cell	1.5	0.02		Bud	10	1.3
	32-cell	1.75	0.02		3-somite	11	1.7
	64-cell	2	0.03		6-somite	12	2.1
	128-cell	2.25	0.03		14-somite	16	4.6
	256-cell	2.5	0.04		21-somite	19.5	8.0
	512-cell	2.75	0.05		26-somite	22	11.2
	1k-cell	3	0.07		Prim-6	25	16.0
	High	3.33	0.088		Prim-16	31	29.5
	Oblong	3.66	0.11		Prim-22	35	41.4
	Sphere	4	0.14		High-pec	42	68.9
	Dome	4.33	0.171		Long-pec	48	99.6
	30%-epiboly	4.66	0.20		Pec-fin	60	180
	50%-epiboly	5.25	0.27		Protruding-mouth	72	280
	Germ-ring	5.66	0.33				

We found that puberty, defined as the onset of allocation to reproduction, occurs above $f = 0.6$. Lawrence et al. (2008) reported the appearance of secondary sexual characteristics after 4 months while we estimate an ingestion level of $f = 0.49$ for some of the fish. Additionally, Schilling (2002) reported such characteristics at TL = 2-3 cm which is 20% lower than predicted. Secondary sexual characteristics might occur at a lower maturity level than for puberty; first spawning events (Eaton and Farley, 1974b) must occur later. The various events might be difficult to recognize accurately which can contribute to the discrepancies.

Even after correcting for effects of temperature, we demonstrated that developmental state at a particular age depends on feeding history. To a lesser extent developmental state at a particular size also depends on feeding history: better fed individuals reach puberty faster and at a larger size. This is in agree-

Table 2.4: Maturity levels E_H for post embryonic developmental milestones. Standard length SL (tip of snout till base of caudal fin), developmental stages and names as given in Parichy et al. (2009). Ages, in days post-fertilization (dpf), at $f = 0.63$ and $f = 1$ as well as SL at $f = 1$ are model predictions at 28.5°C

STAGE		age, SL ^a ,		age, SL,		E_H (J)
		dpf	cm	dpf	cm	
		$f = 0.63$		$f = 1$		
	pSB+ swim bladder inflation ^b	4.5	3.8	4.0	3.7	0.5
	Fle early flexion	7.2	4.5	6.3	4.6	1.1
	CR caudal fin ray	8.9	4.9	7.4	5.1	1.6
	AC anal fin condensation	10.5	5.4	8.5	5.9	2.3
	DC dorsal fin condensation	12.3	5.7	9.6	5.8	3.3
	MMA metamorphic melanophore appearance	12.9	5.9	10.0	6.0	3.8
	AR anal fin ray appearance	14.2	6.2	10.9	6.3	5
	DR dorsal fin ray appearance	15.0	6.4	11.4	6.5	5.9
	PB+ following pelvic fin bud appearance	18.7	7.6	13.8	7.7	12.7
	PR pelvic fin ray appearance ^c	21.3	8.5	15.5	8.5	21.9
	PR+ following pelvic fin ray appearance	22.5	9.2	16.3	9.3	27.9
	SP onset of posterior squamation	23.8	9.8	17.2	9.8	34.9
	SA onset of anterior squamation	25.0	10.4	17.9	10.5	42.3
	J juvenile	26.2	11.0	18.7	11.0	50.9
	J+ following juvenile	30.8	13.0	21.6	13.2	91.7
	J++ following juvenile	40.7	16.0	27.5	16.4	221.6
	A adults ^d	218	26.0	59.9	30.6	2061

^aStandardized Standard Lengths as given in Parichy et al. (2009)

^bbirth are defined by the DEB model

^cmaturity level just above metamorphosis as defined by the DEB model

^dpuberty as defined in the DEB model

ment with the observations of Parichy et al. (2009). The impact of food history accumulates over time (see table 2.4) and can become irreversible (Kooijman et al., 2011).

Variations in development play an important role in evolutionary theory (McKinney and McNamara, 1991). To study heterochrony it is necessary to distinguish between the "time" spent in a particular stage of development and the rate of growth within it. For instance, embryonic growth between 0.6 and 1.3 dpf (13% of the embryonic period) is in the order of 3 mm d^{-1} (Kimmel et al., 1995) whereas growth rate between 18 and 40 dpf in a high and low food regime is roughly 0.6 and 0.35 mm d^{-1} (Lawrence et al., 2008) and in all cases growth rate continues to decrease with age (under constant ingestion level). The lower area-specific maximum assimilation and reserve mobilization rates in an embryo can combine with the higher growth rate because volume linked somatic maintenance, which always takes precedence over growth in DEB theory, are very small for embryos relative to juveniles and adults (Kooijman et al., 2011). DEB theory offers the framework for changes in maturity throughout the life cycle that is consistent with observations. The use of reserve, being a good quantifier for metabolic activity, not directly translates in changes in maturity and/or size.

Reiss (1989) proposed 7 criteria which should be respected by a metric for developmental time: (1) independent of morphology, (2) independent of body size, (3) depend on one a priori homologous event, (4) unaffected by changes in temperature, (5) similar between closely related species, (6) increase with clock time, and (7) physically quantifiable. The maturity concept of DEB theory complies to all criteria. Parameter values are individual specific. Intra-species variations are small relative to inter-species variations and parameter values of similar species are similar (Kooijman, 2010). In the particular case that maturity maintenance $k_J E_H$ is no longer be paid (starvation) rejuvenation can occur as has been observed in krill *Euphausia superba* (Thomas and Ikeda, 1987).

We show in this study that maturity is indirectly physically quantifiable see table 2.3 and 2.4. "Without a metric for developmental time the extent and meaning of evolutionary change in developmental timing simply cannot be assessed" (Reiss, 1989). We cannot agree more and suggest that maturity is a good candidate for such a metric.

Acknowledgements

This work is part of the ENVIRHOM research program supported by the Institute for Radioprotection and Nuclear Safety and the Provence Alpes Côte d'Azur region. We would like to thank N. Mente for contributing to the experimental design and the many authors who contributed their insights on zebrafish physiology in communications. We also thank two anonymous reviewers for their comments on an earlier version of the manuscript.

3

Metabolic Handling of Starvation

Augustine, S., Litvak, M. K., and Kooijman, S. A. L. M. (2011). Stochastic feeding of teleost fish and their metabolic handling of starvation. *J Sea Res.* 66:411-418.

Abstract

Developmental patterns of yolk-sac larvae are well captured by the standard DEB model: (i) when feeding is delayed post birth the size at which post-feeding growth begins is reduced but the rate of growth post-feeding is unaffected and (ii) maternal effects (initial energy in egg) show up as differences in condition at birth and maximum length of non fed individuals. We extended the standard DEB model in two ways to account for starvation. (I): if somatic maintenance can no longer be paid structure is also mobilized to cover the costs, but at an extra cost- conversion efficiency of structure to energy. Death occurs if structure reaches a fraction of the maximum at the onset of shrinking. (II): if maturity maintenance can no longer be paid then maturity level decays exponentially (rejuvenation). Hazard due to rejuvenation is proportional to the difference between maturity and the maximum maturity at the onset of rejuvenation.

We performed Monte Carlo simulation studies which treat feeding as a random process to evaluate the contribution of the metabolic handling of starvation to early teleost life history. The simulations suggest that food density strongly impacts growth, energy reserves, mineral fluxes, hazard and mortality from shrinking. Environmental factors can soon override maternal induced differences between individuals. Moreover in the low food density, simulated individuals from eggs of lower caloric content experience mortality from shrinking earlier than their counterparts issued from higher energy eggs. Empirically observed patterns of real data, i.e. high scatter in respiration in combination with low scatter in lengths, can be expected when the metabolism is treated as a deterministic system while behaviourally controlled input is stochastic. At low food densities where mortality from shrinking reaches 10% almost all individuals experience hazard due to rejuvenation. This hazard is difficult to access experimentally but represents moments of heightened susceptibility to pathogens and toxicants and could be ecologically significant.

Key words: DEB, starvation, stochastic feeding, rejuvenation, respiration, fish

3.1 Introduction

The ecology of teleost larvae has generated much interest in marine fisheries research. Survival through the early life history stages is thought to regulate recruitment and subsequent year-class strength (Hjort, 1914; May, 1974; Cushing, 1975; Bailey and Houde, 1989, among others). Starvation (Hjort, 1914) and predation (Bailey and Houde, 1989) have been hypothesized as major factors controlling survival. Predation has been considered to be the primary agent of mortality during the yolk-sac stage (Blaxter and Fuiman, 1990; Paradis et al., 1996) while starvation may only become important after the transition to exogenous feeding (Leggett and Deblois, 1994) as there are potential interactions of larval size (Miller et al., 1988), developmental rate (Houde, 1987), environmental effects (Shepherd et al., 2000), predation and starvation. To date, with much of the emphasis focused on how growth and survival relate to environmental conditions, few studies consider how larval metabolism handles starvation.

The focus of our paper is (i) to formalise starvation rules which operate at the individual level and (ii) further investigate the importance of metabolism on starvation during teleost early life history stages. The study is conducted within the conceptual framework of Dynamic Energy Budget (DEB) theory (Sousa et al., 2008; Kooijman, 2010; Sousa et al., 2010): a well-tested theory on the uptake and use of substrate by all organisms. Parameters for the standard DEB model (see Kooijman, 2010, Chap.2) have been estimated for a number of animal species and can be found in the Add_My_Pet collection http://www.bio.vu.nl/thb/deb/deblab/add_my_pet/ (Lika et al., 2011a, this special issue). The standard DEB model is extended in this paper to deal with starvation in more detail. The question we ask is how does the metabolic handling of starvation contribute to growth, survival, dioxygen consumption, and carbon dioxide, water and ammonia production (hereafter referred to as mineral fluxes) during the early life history of the individual when resources are fluctuating. It is practical to conduct this study using a DEB model where the parameters of a teleost have already been estimated as well as with data which relate egg size to growth and survival. A full life cycle model for zebrafish, *Danio rerio* was previously developed (Augustine et al., 2011a) and Jardine and Litvak (2003) have unique results where initial egg size was controlled by microinjection technique and lengths, yolk volumes and survival were observed for each individual. This makes zebrafish an ideal candidate for conducting theoretical studies on starvation.

Within the context of DEB theory the life cycle is divided in three stages: embryo (no assimilation), juvenile (assimilation) and adult (allocation to reproduction but no longer to maturation). Two important events bound the embryonic stage: (i) age zero where reserve is maximal and starts to reduce and structure and maturity are close to zero and start to increase and (ii) age at birth where external feeding is initiated and the embryo switches to a juvenile. Hatch precedes birth for many teleost species since the mouth is not yet

formed and the individual is still reabsorbing the yolk sac inherited from the mother. Birth is initiated the moment the oesophagus opens and the digestive tract is open to the environment. Birth corresponds to a specific developmental milestone and so it makes sense to compare ages and lengths at this point in development between different individuals to understand maternal effects. Age and length at hatch is a more commonly found endpoint, but has the drawback of preceding birth and not occurring at strictly the same stage of development for all individuals (e.g. [Kimmel et al., 1995](#), for zebrafish). Furthermore, age at hatch can be influenced by rearing protocol: sterilisation procedures such as bleaching can delay hatching by hardening the chorion (e.g. [Zhang et al., 2009](#)). Yolk consists of lipo-proteins, and during embryonic development it is rapidly converted into proteins, lipids and carbohydrates while hardly losing energy or building blocks. These three products are stored in different places in the body, a process known as internalisation of yolk. These 'details' are not included in the standard model explicitly, and the yolk-sac is treated as a temporary organ with specialised functions, similar to adipose tissue of juveniles and adults in many taxa.

We first examine to what extent the DEB model is representative of impacts of maternal effects (initial egg caloric content) and delays in initial feeding on early juvenile development. Predictions are compared to actual observations of length against age of individuals born of eggs with initial yolk volumes ranging from 126 to 628 nl (see [Jardine and Litvak, 2003](#), for detailed protocol).

It has already been shown that stochastic food availability can explain the large variance in size of individuals in a same aquarium from a same brood due to amplification of difference by social interaction ([Kooijman, 2009a](#)). Large variation in larval zebrafish lengths (and high mortalities) were demonstrated to be a consequence of low food density, which was amplified by changes in food types, from small to larger food particles ([Eaton and Farley, 1974a](#)). To emulate a random encounter rate between food items and juveniles we consider a natural stochastic version of the feeding module and perform Monte Carlo simulation studies to generate lengths, mass, reserve, mineral fluxes and survival for 5000 individuals. We perform the studies at low and high food densities and with populations born of different initial egg energy content. The importance of including the metabolic handling of starvation when studying the ecology of juvenile teleosts is discussed.

3.2 Model and methods

3.2.1 Formulation of starvation rules

We use embryo parameter values for zebrafish provided in [Augustine et al. \(2011a\)](#) while simplifying their model by neglecting deviations from isomorphy and effects of ageing. We also ignore any surface-area linked maintenance costs. As mentioned before, we focus on the early juvenile that follow the standard DEB model ([Kooijman, 2010](#)) and have two life stages (embryo and juvenile)

using 3 state variables: energy in reserve E (J), structural length L (cm) and maturity E_H (quantified in J) (see table 3.1) and 7 parameters (see table 3.2). $L = V^{1/3}$ where V (cm³) is the structural biovolume.

The assimilation flux \dot{p}_A (J day⁻¹) is

$$\dot{p}_A = 0 \quad \text{for embryos} \quad \text{and} \quad \dot{p}_A = f\{\dot{p}_{Am}\}L^2 \quad \text{for juveniles}$$

with $\{\dot{p}_{Am}\}$ the maximum (surface-area) specific assimilation rate, and f the scaled functional response, defined as the feeding rate on a particular food type as a fraction of the maximum possible one for an individual of that size. It can be specific for a particular diet. The standard model uses the Holling type II function response, $f = x/(1+x)$, with x the scaled food density.

A fraction κ of the flux \dot{p}_C (J d⁻¹) that is mobilized from reserve is invested in somatic maintenance $\dot{p}_M = [\dot{p}_M]V$ and growth $\dot{p}_G = \kappa\dot{p}_C - \dot{p}_M$. A fraction κ_G (the conversion efficiency) of the flux allocated to growth is fixed in new structure. $\kappa_G = \bar{\mu}_V d_V ([E_G]w_V)^{-1}$ (Lika et al., 2011a, this special issue), with $[E_G]$ the cost per unit of structure and $\bar{\mu}_V$, d_V , w_V the chemical potential, density and molar weight of structure (see table 3.2).

A fraction $(1-\kappa)\dot{p}_C$ is invested in maturity maintenance $\dot{p}_J = \dot{k}_J E_H$ and maturation $\dot{p}_R = (1-\kappa)\dot{p}_C - \dot{p}_J$. Maturity does not have mass or energy itself, but is quantified as the cumulative energy investment in maturation. Maturity maintenance can be conceived as all processes responsible for maintaining the current state of maturity, i.e. immune, hormonal and cellular defence systems. An analogy would be that considerable energy is invested in learning and if the knowledge level is not maintained it is forgotten.

The mobilization flux is given by $\dot{p}_C = E(\dot{v}/L - \dot{r})$, with \dot{v} (cm d⁻¹) the energy conductance and \dot{r} (d⁻¹) the specific growth rate. Reserve dynamics are specified as follows: $\frac{d}{dt}E = \dot{p}_A - \dot{p}_C$.

Maintenance always has priority over investment in growth or maturation. Starvation occurs when energy mobilised no longer suffices to cover (I) the somatic maintenance cost, i.e. $\kappa\dot{p}_C < [\dot{p}_M]V$, with shrinking as result and (II) the maturity maintenance costs, i.e. $(1-\kappa)\dot{p}_C < \dot{k}_J E_H$, with rejuvenation as result. It seems reasonable to assume that shrinking has a maximum and death occurs instantaneously when it exceeds a fixed fraction δ_X . This construct comes with the need to introduce a new state variable $\max L$, i.e. the maximum length the individual once had. It seems likely that maturity maintenance is more optional than somatic maintenance in the sense that paying for the immune or the cellular defence systems might not be obligatory. Yet there is a penalty in the form of an increased hazard proportional to the fraction of maturity maintenance that is not paid (assuming implicitly that there is a constant need for defence). Also this construct comes with a need to introduce a new state variable $\max E_H$, i.e. the maximum maturity level the individual once had.

Both shrinking and rejuvenation have an extra parameter in the specification of their dynamics. On the assumption that the somatic maintenance costs

expressed as energy flux is the same for growth and shrinking, the change in structural length is $\frac{d}{dt}L = L\dot{r}/3$ with specific growth rate

$$\dot{r} = \dot{k}_M g \frac{e/l - 1}{e + g} \quad \text{if positive, else } \dot{r} = \dot{k}_M g \frac{e/l - 1}{e + \kappa_G g}$$

where $l = L/L_m$ is scaled length and $e = \frac{E\dot{v}}{L^3\{\dot{p}_{Am}\}}$ is scaled reserve density. The somatic maintenance rate coefficient $\dot{k}_M = [\dot{p}_M]/[E_G]$, the ultimate structural length $L_m = \kappa \frac{\{\dot{p}_{Am}\}}{[\dot{p}_M]}$ and the energy investment ratio $g = \frac{[E_G]\dot{v}}{\kappa\{\dot{p}_{Am}\}}$ are compound parameters of the standard DEB model. Somatic maintenance might have a ‘building block’ aspect that might cause growth efficiency κ_G to deviate from the value mentioned above.

Following the previous analogy we can imagine that forgetting follows a first order process with rate parameter \dot{k}'_J , say:

$$\begin{aligned} \frac{dE_H}{dt} &= (1 - \kappa)\dot{p}_C - \dot{k}_J E_H \quad \text{if positive, else} \\ \frac{dE_H}{dt} &= -\dot{k}'_J \left(E_H - \frac{(1 - \kappa)\dot{p}_C}{\dot{k}_J} \right) \end{aligned}$$

Hazard due to rejuvenation \dot{h}_J is considered proportional to the difference between actual maturity level and maximum maturity level at the onset of rejuvenation $\max E_H$:

$$\dot{h}_J = \dot{k}_M \frac{\max E_H - E_H}{E_H^h}$$

and

$$E_H^h = \frac{(1 - \kappa)[E_G]L_m^3}{\kappa s_H}$$

where s_H is the rejuvenation stress coefficient. The result is that \dot{h}_J contributes to survival as:

$$\frac{dS}{dt} = -S(\dot{h}_J + \dot{h}_a + \dot{h}_{acc} + \dot{h}_{sh})$$

In this study we consider that hazard from ageing \dot{h}_a and from accidents \dot{h}_{acc} is negligible. We consider that hazard from shrinking of structure \dot{h}_{sh} is infinite with instantaneous death as a result when the shrinking threshold is passed.

The starvation module has, in summary, two new state variables, $\max L$ and $\max E_H$, and four new parameters κ_G , δ_X , \dot{k}'_J and s_H . Growth efficiency also occurs under non-starvation conditions, but there it does not play a role in the dynamics of the state variables.

Embryo and juvenile mineral fluxes are specified in [Appendix C](#). For a full discussion we refer to [Kooijman \(2010, Chap.4\)](#).

Table 3.1: State variables of the DEB model.

Variable	Unit	Name
<i>standard DEB model</i>		
E	J	reserve
L	cm	structural length
E_H	J	cumulated energy invested in maturity
<i>forcing variables</i>		
x	-	scaled food density
<i>Additional state variables</i>		
max L	cm	maximum structural length before shrinking
max E_H	J	maximum E_H before rejuvenation

3.2.2 Linking state variables to measurements

Structural length L is taken proportional to some well-chosen physical (observed) length L_f : $L = \delta_M L_f$, with δ_M the (constant) shape correction factor. [Augustine et al. \(2011a\)](#) show that the shape of early juvenile zebrafish changes during the first month of development. This is most likely the case for many teleost species who undergo metamorphosis after early juvenile development. We exclude this detail from our study by considering that δ_M is constant.

Freshly spawned eggs are taken to be composed uniquely of reserve inherited from the mother. Maternal effects are expressed as differences in the initial energy content of the egg E_0 (J). We relate observed egg volume to initial energy content as follows:

$$V_f^Y = \frac{E_0}{\delta_Y^3} \frac{w_E}{\bar{\mu}_E d_E}$$

δ_Y is an empirical shape correction factor. w_E , d_E and $\bar{\mu}_E$ are the molar weight, density and chemical potential of reserve (table 3.2). We assume an Arrhenius relationship between metabolic rates and temperature (Eqn. 1.2 [Kooijman, 2010](#)). Computations are made at reference temperature of 20°C. Predictions which are compared to observations by [Jardine and Litvak \(2003\)](#) are temperature corrected to 28°C.

Dry biomass W_d has contributions from both reserve and structure and is expressed as:

$$W_d = d_V L^3 + \frac{w_E}{\bar{\mu}_E} E$$

with d_V the density of structure (table 3.2). We make the simplified assumption that wet biomass W_w is equal to 6 W_d on the basis of observations by [Craig and Fletcher \(1984\)](#); [Bagatto et al. \(2001\)](#).

Table 3.2: Model parameters (affecting state variables at 20°C)

Parameter	Value	Unit	Name
<i>DEB model parameters (Augustine et al., 2011a)</i>			
$\{\dot{p}_{Am}\}$	246.3	J day ⁻¹ cm ⁻²	maximum surface-area assimilation
\dot{v}	0.0287	cm day ⁻¹	energy conductance
$[\dot{p}_M]$	500.9	J day ⁻¹ cm ⁻³	volume-linked somatic maintenance costs
$[E_G]$	4652	J cm ⁻³	cost of a unit of structure
k_J	0.0166	day ⁻¹	maturity maintenance rate
κ	0.44	-	allocation fraction to soma
E_H^b	0.54	J	cumulated energy invested in maturity at birth
<i>temperature correction module (Augustine et al., 2011a)</i>			
T_A	3000	K	Arrhenius temperature
<i>auxiliary parameters (Lika et al., 2011a)</i>			
w_E	23.9	g C-mol ⁻¹	molar weight of reserve
w_V	23.9	g C-mol ⁻¹	molar weight of structure
d_E	0.15	g cm ⁻³	density of reserve
d_V	0.15	g cm ⁻³	density of structure
$\bar{\mu}_E$	555	kJ c-mol ⁻¹	chemical potential of reserve
$\bar{\mu}_V$	500	kJ c-mol ⁻¹	chemical potential of structure
<i>parameters linked to starvation (this study)</i>			
k'_J	depends on study	day ⁻¹	specific maturity decay
s_H	depends on study	-	rejuvenation stress coefficient
δ_X	0.75	-	maximum shrinking fraction
<i>parameters linked to respiration (this study)</i>			
y_{XE}	1.25	c-mol X/ c-mol E	yield of food on reserve
y_{PX}	0.1	c-mol P/ c-mol X	yield of faeces on food
<i>shape coefficients</i>			
δ_Y	1.2521	-	yolk shape coefficient
δ_M	0.1245	-	shape coefficient
<i>stochastic feeding module</i>			
M_X	0.06	μmol	Mass of food particle

3.2.3 Stochastic feeding module

Suppose that food density, in terms of particles per volume, is constant, such as in a polyculture (e.g. Best et al., 2010). We simplify the system by considering all food items to be of constant chemical composition with mass M_X (μmol). Each fish is either searching for food (i.e. $f = 0$) or handling food (i.e. $f = 1$). Time interval spent handling food t_h is inversely proportional to squared length (of the individual), so larger individuals take less time to handle a food item. $\{\dot{J}_{XAm}\}$ is the surface-area specific maximum intake rate (in C-mol food per day per surface area) and relates to surface-area maximum assimilation rate $\{\dot{p}_{Am}\}$ as: $\{\dot{J}_{XAm}\} = \{\dot{p}_{Am}\}y_{XE}/\bar{\mu}_E$. y_{XE} is the yield of food on reserve (see table 3.2).

$$t_h = \frac{M_X}{\{\dot{J}_{XAm}\} L^2}$$

Food searching intervals t_s are considered as an exponentially distributed random variable with mean t_h/x . Mean feeding rate is defined as $\dot{h}_X = (t_s + t_h)^{-1} = f/t_h$. This natural introduction of stochasticity does not come with any new parameters.

Two populations are created from two pools of initial energy contents: $E_0^1 = 1.18$ J and $E_0^2 = 1.68$ J. Populations E_0^1 and E_0^2 both develop in two different environments: $x_1 = 0.3$ and $x_2 = 0.75$. This makes 4 experimental conditions: (i) E_0^1, x_1 , (ii) E_0^1, x_2 , (iii) E_0^2, x_1 , and (iv) E_0^2, x_2 . We run 5000 Monte Carlo simulation for each condition and represent results as the distributions of lengths, mass, scaled reserve density e , and respiration at 30 days since birth. In addition, we look at the distribution of age at death from shrinking for the entire study and the number of live individuals at 30 days since birth who have experienced rejuvenation hazard. Stochastic simulation routines (traject.m and traject.m.m) are part of the DEBtool software (Kooijman et al., 2008) and are freely downloadable at <http://www.bio.vu.nl/thb/research/>.

3.3 Results and Discussion

3.3.1 Constant food

Model simulations show that when initial feeding is delayed post birth, size at which post-feeding growth begins is reduced but the rate of growth post-feeding is unaffected (figure 3.2A). This is in line with general observations by Guillaume et al. (1999). Individuals from the lower E_0 die from shrinking if feeding is delayed beyond 4 days. The initial caloric content of the egg influences post-birth lifespan when feeding is never initiated which is again in agreement with general patterns noted by Kamler (2005). Rejuvenation hazard contributes to reducing survival probability (figure 3.2B and C). The time an individual can handle delays in initial feeding before rejuvenation hazard starts contributing to survival relates to initial energy in the egg.

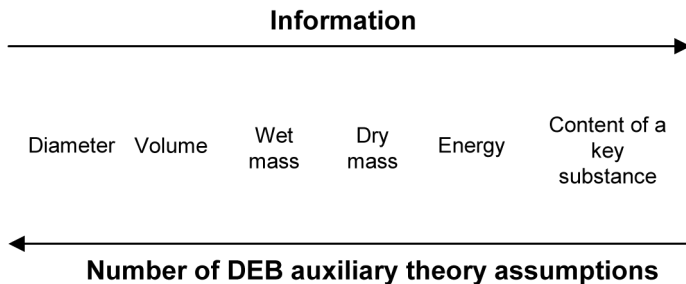


Figure 3.1: Modified from Kamler (2005). Egg size is measured in many different ways. Assumptions of auxiliary theory link these measurements to amounts of reserve and structure (egg size to initial amount of energy in reserve), which comes with some parameters (see table 3.2, auxiliary parameters).

The model predicts that maternal effects (initial energy in egg) influence condition at birth in terms of amount of reserve per unit structure and maximum length of non fed individuals. Birth does not occur if $E_0 < 1.1$ J because the cumulated energy invested in maturity never attains the threshold value E_H^b (see table 3.2). Hence eggs are considered non viable when $E_0 < 1.1$ J. It would be interesting to verify experimentally the realism of this lower boundary value of E_0 for which an egg is viable. Should such a lower boundary exist then maternal effects can also contribute to embryonic survival.

The maternal effect rule (Kooijman, 2009b), implemented by default into the standard DEB model, stipulates that the reserve density of the mother equals the reserve density of her offspring at birth. $E_0 = 1.67$ J for mothers at $f = 1$ (for this parameter combination). Between the narrow caloric range of $E_0 = 1.1$ to 1.67 J, the maximum structure for a non fed juvenile increases by 10%, and the maximum maturity attained increases by 40%. This explains the increased hazard experienced by lower E_0 individuals during starvation (figure 3.2C). Caloric values of egg dry mass for teleost species are generally very conserved ranging from 20 – 30 J mg⁻¹ (Kamler, 2005). If we consider the dry mass of an egg as $W_0 = E_0 w_E / \bar{\mu}_E$, then the caloric value of $E_0 = 1.6$ J is 22.9 J mg⁻¹ which falls within the boundaries suggested by Kamler (2005).

We do not propose a maximum egg size in this study. Links between egg size and the mother's condition might be more complex and depending on the applications deviations from the maternal effect rule should be considered. The maximum surface-area specific assimilation rate $\{\dot{p}_{Am}\}$ is sensitive to the type of food. Consequently, maximum assimilation rate which corresponds to $f = 1$ for one type of food might correspond to $f < 1$ for another. Since the maternal effect rule implies that the e of the embryo at birth equals the value of f of the mother at spawning and that diets differ between individuals, using $E_0 > 1.67$ J as starting values to calculate life history traits is coherent with

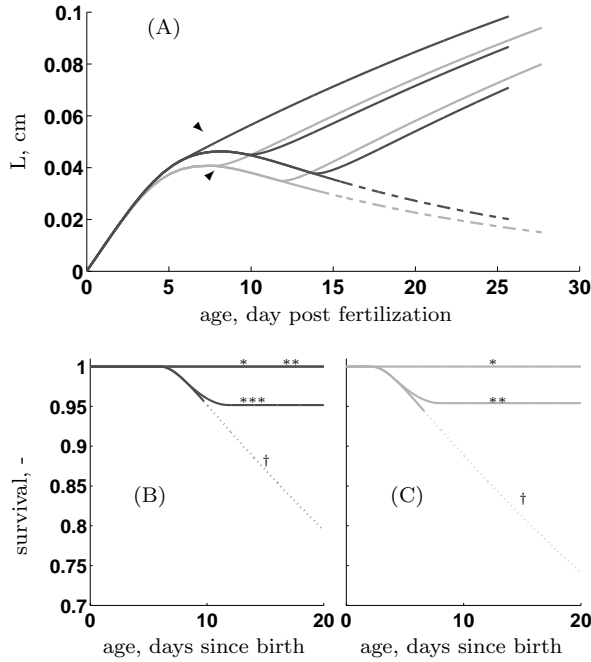


Figure 3.2: Impact of delays in first feeding on growth at reference temperature (20°C). $s_H = 2$; $k'_J = 2.4$; $f = 1$ (see table 3.2). (A) structural length (L) against age for $E_0 = 1.7$ (black lines) and $E_0 = 1.1$ (grey lines); arrowheads: birth; dashed lines: instantaneous death by shrinking. $E_0 = 1.7$: feeding is never initiated (negative growth till death by shrinking) and feeding is delayed 0, 4 and 8 days after birth. $E_0 = 1.1$: feeding is never initiated and feeding is delayed 0 and 4 days after birth. Survival probability for $E_0 = 1.67$ (B) and $E_0 = 1.1$ (C). Survival for delays in initial feeding of 0 days after birth (*), 4 days after birth (**), 8 days after birth (***) and feeding is never initiated (†). Dotted line: all organisms have died from shrinking.

model assumptions.

In figure 3.3A we computed lengths of non fed juvenile zebrafish for $1.1 \leq E_0 \leq 2.5$ J as suggested by the large range of observed yolk volumes V_f^Y . Predicted maximum length as a function of V_f^Y is compared with the actual observations from Jardine and Litvak (2003). Maximum size attained seems to saturate for initial yolk volumes above 314 nl. This points to an uneasy relationship between yolk volume and water content. Large eggs tend to have higher caloric value than small eggs, but this is not always the case (Kamler, 2005). For *Sardina pilchardus*, Riveiro et al. (2000) found that time to yolk absorption was not a function of egg size but a function of egg biochemical composition (protein content) which illustrates the point we make in figure 3.1. We converted E_0 to V_f^Y with the implicit assumption that the fraction of water per volume is constant. There is no solid evidence that this is the case. Still, the data are overall supportive of a positive relationship between E_0 and maximum length of a non fed individual.

We further compare predicted lengths of individuals issued from eggs with energy content $1.1 \leq E_0 \leq 2.5$ J to observed lengths against age for each V_f^Y (figure 3.3B). We show two cases: (i) paying maintenance from structure increases somatic maintenance costs by a factor κ_G^{-1} and (ii) there is no extra cost involved ($\kappa_G = 1$) which is not thermodynamically coherent. In both cases predicted negative growth rate at the onset of maximum structure is overestimated. The discrepancy might be explained by parameter values. On the other hand, does an organism shrink isomorphically? Yin and Blaxter (1986) found that it was the ratios of morphometric measurements which were sensitive to the state of starvation for larval *Gadus morhua* L. and *Platichthys flesus* L.. A length measurement following the spinal cord, as is the case here, might be relatively insensitive to shrinking. Nonetheless, the model reflects the observed relationships between V_f^Y and maximum lengths while lengths at starvation are underestimated.

The predicted effects of initial energy in egg on growth and metabolic handling of starvation lends support to current views where maternal effects contribute to resistance to starvation. Yet it remains difficult to assess the importance of this maternal effect in real life situations. We tackle the question theoretically using Monte Carlo simulations with stochastic food input in the following section.

3.3.2 Stochastic searching

All stochasticity that we propose is in food searching, not in food handling. This is natural because we assume a fixed particle size for simplicity's reasons, consistent with the idea that the standard DEB model pushes simplicity into the extreme. In many natural situations, food particles will show a particle-size distribution, which introduces stochasticity in handling as well, but also comes with new parameters and the results become dependent on the particle size distribution, which itself will be affected by many factors.

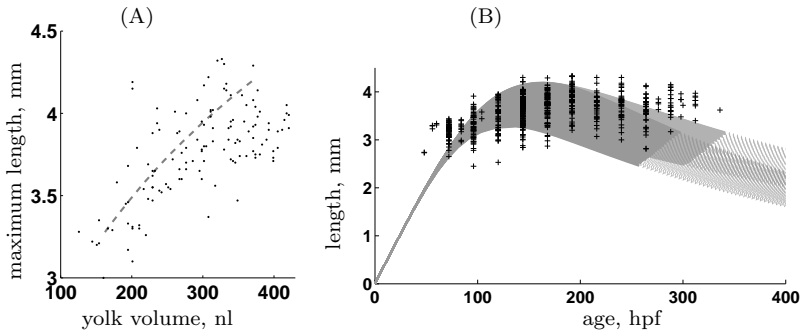


Figure 3.3: Points: data from [Jardine and Litvak \(2003\)](#) (28°C). (A) maximum observed length attained during development in the absence of feeding against yolk volume expressed in nanolitres (nl). Dashed line: model predictions of this maximum length for $1.1 \leq E_0 \leq 2.5$ J. (B) observed length against age (hours post fertilization hpf) for eggs with all yolk volumes shown on left. Solid dark grey: model predictions supposing $\kappa_G = 0.67$, solid light grey: model predictions supposing $\kappa_G = 1$, dashed grey: death from shrinking in both cases, i.e. the length reached a fraction $\delta_X = 0.75$ of the maximum at the onset of negative growth.

The values of e , L_f , Ww , \dot{h}_J and mineral fluxes against age since birth of an individual experiencing a stochastic encounter with food particles in environment E_0^1 , x_1 is compared to deterministic predictions for an individual at $f = x_1/(1 + x_1)$ (expected mean) and a starved individual ($f = 0$). See figure 3.4, first and second row.

Stochastic mineral fluxes show rapid small scale variation since f is fluctuating continuously between 0 and 1. The distribution of daily mineral production (CO_2 , H_2O , NH_3 figure 3.4I, J and L) or consumption (O_2 figure 3.4K) of 5000 individuals at the end of the simulation time shows considerable deviation from the mean. Future research however could include digestion (see e.g. [Kooijman, 2010](#), Chap.7) which would make assimilation a smoother process at small time scales. Differences in prior food history will still accumulate however and contribute to inter-individual differences in lengths, mass, reserve and mineral production and consumption. The mineral flux curves all show the same morphology, but this is a result of choice of parameter values and not a model property. The mineral fluxes are closely tied to energetics and go to zero when the individual is starved. No individuals in the $x = 0.75$, E_0^1 environment experience rejuvenation hazard. Figure 3.4D shows rejuvenation hazard when $f = 0$ and the organism is shrinking.

The Monte Carlo simulation studies reveal the predicted scatter in lengths, weights, survival and respiration at different time points when food availability fluctuates. Monte Carlo results of simulations for each of the 500 individuals at day 30 since birth are presented in figure 3.5. Interestingly the largest scatter is observed in the predicted mass and respiration data and the lowest

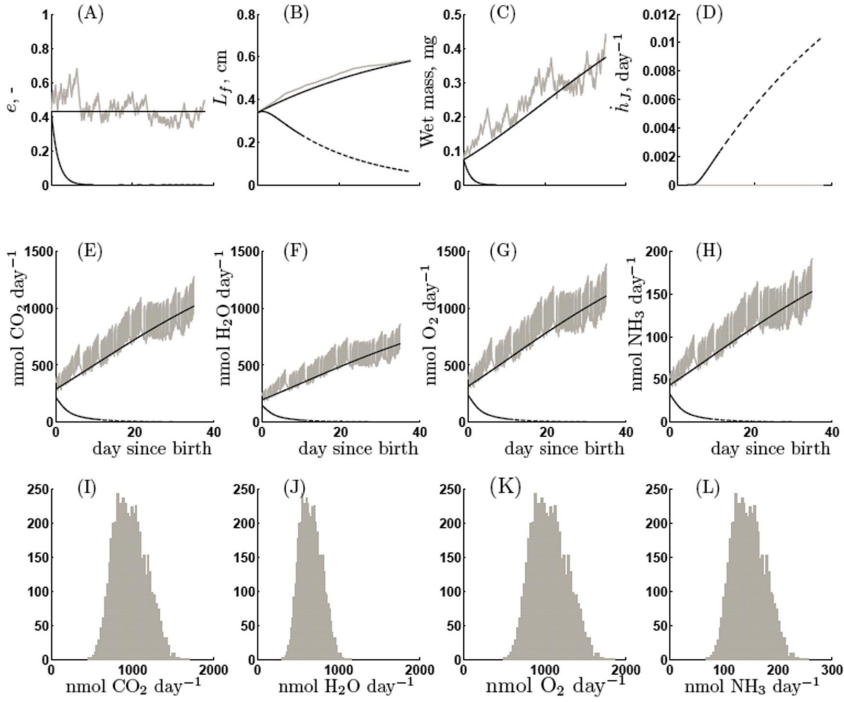


Figure 3.4: Model outputs computed at 20°C . $s_H = 2$ and $\dot{k}'_J = 0.024 \text{ day}^{-1}$. First row: an example of scaled reserve density (e_i), observed length (L_f), wet mass, rejuvenation hazard (\hat{h}_J) for an individual sampled randomly from the Monte Carlo simulation study. Second row: an example of fluxes of CO_2 , H_2O , O_2 and NH_3 against age since birth from the same individual sampled randomly from the Monte Carlo simulation study. Black: stochastic mineral fluxes for that individual ($x = 0.75$, $E_0 = 1.67 \text{ J}$, f alternates between 0 and 1) are compared to deterministic predictions (smooth lines) for $f = x/(1+x)$ and $f = 0$ ($E_0 = 1.67 \text{ J}$). When $f = 0$ the deterministic mineral fluxes go to 0 and the dotted line is when structure reaches a fraction $\delta_X = 0.75$ of the maximum structure (instantaneous death is assumed at this point). Bottom row: distribution of each mineral flux at age 30 since birth for 5000 Monte Carlo trials ($x = 0.75$, $E_0 = 1.67 \text{ J}$, f alternates between 0 and 1). Please note that the x and y axis of fluxes of NH_3 differ.

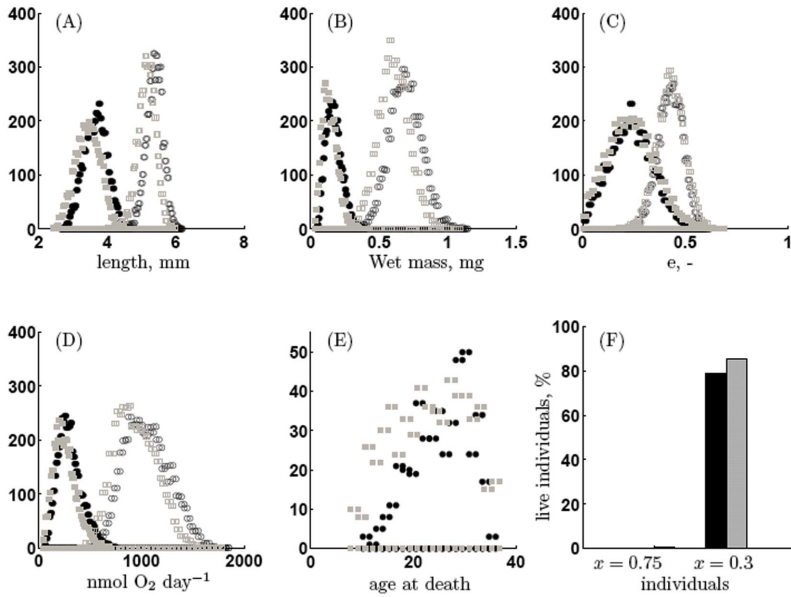


Figure 3.5: Output of 5000 Monte Carlo simulation studies at reference temperature (20°C). $s_H = 2$ and $k'_J = 0.024 \text{ day}^{-1}$. Open symbols: $x = 0.75$, closed symbols $x = 0.3$, circles: $E_0 = 1.8 \text{ J}$, squares: $E_0 = 1.2 \text{ J}$. (A) Distribution of lengths of live individuals after 30 days. (B) Distribution of wet mass of live individuals after 30 days. (C) Distribution of scaled reserve density (e) of live individuals after 30 days. (D) Distribution of respiration (nmol O₂ day⁻¹) for live individuals at day 30. (E) Age at death by shrinking for each individual. Black: E_0^1 , grey: E_0^2 . Note that no deaths occurred for $x = 0.75$. (F) Percentage of live individuals who experience hazard due to rejuvenation during the simulation interval. Black: E_0^1 , grey: E_0^2 . No hazard is experienced for individuals in E_0^1 , $x = 0.75$. Percentage of population in E_0^2 , $x = 0.75$ is barely perceptible on the graph.

in the predicted length data: the coefficient of variation (CV) of mass and O_2 consumption is almost four times the CV of length in all cases. In the x_2 , E_0^1 environment for example the CV is 9% for L_f , 34 % for Ww and 38% for O_2 consumption. Monte Carlo simulations of DEB models with stochastic food input seem to inherently capture patterns of scatter observed in real data sets where high scatter in measured mass or respiration combines with much lower scatter in observed lengths.

The CV increases twofold between the high and the low food density environments for all predicted observations regardless of the initial energy content of the egg. For example, the CV of the L_f distribution for x_1 , E_0^1 is 4% whereas it is 9% for x_2 , E_0^1 (figure 3.5A). This links up beautifully with the results of Eaton and Farley (1974a) where lengths of individuals sampled after 16 days of development in containers with 2 free-swimming prey per mL had a CV of 16.8% and lengths of individuals sampled after 15 days of development in containers holding 200-300 free-swimming prey per mL had a CV of 3.8%.

Populations E_0^1 and E_0^2 evolve in a very similar manner in terms of lengths, weights, respiration and survival at both food densities ($x = 0.3$ and $x = 0.75$). Thus the present simulations hint at a negligible contribution of maternal effects to measurable endpoints after a month of development regardless of the food density. Maternal effects can be diluted by the individuals (chance) encounter rate with food items.

The most sensitive difference between E_0^1 and E_0^2 at $x = 0.3$ is in the distribution of age at death (figure 3.5E). Population E_0^2 shows higher mortalities from age 8 to 20 since birth than the population E_0^1 . After 20 days, age at death distributions are quasi identical between both populations. At $x = 0.3$ about 10% of both populations die from structure shrinking. At $x = 0.2$ about 50% of both populations die from shrinking (not shown).

Almost all individuals in both populations in the low food density environment ($x = 0.3$) experience hazard due to rejuvenation. This is shown in figure 3.5F where 79% of live individuals experienced hazard in E_0^1 , $x = 0.3$ and 85% of live individuals experienced hazard in E_0^2 , $x = 0.3$. Rejuvenation hazard hardly occurred for individuals in x_1 , E_0^1 and x_2 , E_0^1 . This hazard (\dot{h}_J) can be translated biologically as moments of increased susceptibility to pathogens and stressors and contributes to survival probability. It is difficult to evaluate \dot{h}_J experimentally, but the present simulations suggest that it could be a relevant factor regulating survival should additional environmental stressors and small periods of starvation occur simultaneously.

3.4 Concluding remarks

There exists strong empirical support for maternal effects as a general pattern but our simulations show how environmental conditions soon override such effects. Inter-individual differences in prior food history accumulate and can be responsible for the observed scatter in the data.

The problem of inherent variability in biological data must be addressed in all fields of biology. The present study shows that empirically observed patterns of real data, i.e. high scatter in respiration in combination with low scatter in lengths, can be expected when the metabolism is treated as a deterministic system while behaviourally controlled input is stochastic. This is consistent with general patterns in observations.

Monte Carlo simulation studies are powerful tools to understand how stochasticity of food searching translates into variability in measured endpoints such as respiration, growth or reproductive output. This insight can be useful for designing experiments: e.g. feeding protocols, types and frequencies of measurements and sampling.

The concept of rejuvenation and rejuvenation hazard follows directly from the structure of the DEB model but further theoretical work needs to be done to understand how to estimate it from data. The concept links up neatly with empirical support that starved organisms show a heightened susceptibility to disease and environmental stressors such as toxicants (Rougier et al., 1996).

The extension we propose of the standard DEB model specifying shrinking and rejuvenation is not species-specific and applies to the entire life-cycle. Further dedicated research will test to what degree these rules are inherent to the functioning of all organisms and further our understanding of which adaptations are species specific and/ or specific to a particular life stage of the organism.

Acknowledgements

This work is part of the ENVIRHOM research program supported by the Institute for Radioprotection and Nuclear Safety and the Provence Alpes Côte d'Azur region. Béatrice Gagnaire and Christelle Adam-Guillermin are gratefully acknowledged for the stimulating discussions and useful comments. We would like to thank two anonymous referees for their constructive comments on the manuscript

4

Differential acceleration of development in Australian Myobatrachid frogs, captured by DEB theory

Mueller, C. A., Augustine, S., Kearney, M. R., Kooijman, S. A. L. M. and Seymour, R. S. (2012). The trade-off between maturation and growth during accelerated development in frogs. In prep.

Abstract

Dynamic energy budget (DEB) theory was used to model energy use and partitioning of two Myobatrachid frogs, *Crinia georgiana* and *Pseudophryne bibronii*. Energy use until metamorphosis at 12°C was measured by respirometry and bomb calorimetry. Dry mass was also measured intermittently until metamorphosis. Mass and energy content of fresh ova were comparable between the species, indicating they had the same initial energy available for development. Development to metamorphosis was 1.7 times faster in *C. georgiana*, yet *P. bibronii* produced nine times the dry biomass at metamorphosis. The overall mass-specific oxygen (O₂) cost of development, the O₂ required to build 1 mg of dry gut-free mass, was 101 μmol mg⁻¹ in *P. bibronii* compared to 156 μmol mg⁻¹ in *C. georgiana*. Between hatching and birth *C. georgiana* increased allocation of energy to maturation over growth. In comparison, *P. bibronii* juveniles partitioned energy in the same way as the embryos, therefore, juvenile growth was greater, but maturation slower than *C. georgiana*. The fast, but costly, development and facultative feeding of *C. georgiana* allows the species to escape the ephemeral pools in which it develops. A change in water level may act as an environmental trigger which alters the allocation of energy to favour maturation over growth. The DEB model was also applied to two additional species, *Crinia nimbus* and *Geocrinia vitellina*, which sport direct development. Only *C. nimbus* increases allocation to maturation, suggesting that a change in energy allocation during development may result from a selective pressure to increase development rate and not as a result of developmental mode

Key words: DEB theory, energy partitioning, maturation, growth, Myobatrachid frogs

4.1 Introduction

Amphibian development is controlled by a number of intrinsic factors, such as egg size and initial energy content, and extrinsic factors, such as temperature and oxygen (O_2) availability. These factors are largely determined by an individual species' mode of development, of which amphibians have evolved a variety (Duellman and Trueb, 1986). Developmental modes include purely aquatic to terrestrial eggs with aquatic larvae to direct development, in which fully-formed metamorphs emerge directly from eggs. The generally high O_2 availability in air allows for an increase in egg size (Packard and Seymour, 1997), which matches the decreasing reliance on water during development so that terrestrial and direct developers have the largest eggs (Salthe and Duellman, 1973).

Across species studies indicate larger egg size slows the rate of embryonic development (Bradford, 1984, 1990; Pauly and Pullin, 1988). However, one Australian Myobatrachid frog appears to be an exception to this rule. The aquatic breeding *Crinia georgiana* produces relatively large eggs that are comparable in size to those of the closely related terrestrial breeder, *Pseudophryne bibronii*. The two species also have similar adult size, produce loose egg clutches of similar egg number and breed under comparable temperatures (Seymour and Roberts, 1995). Despite these parallels in egg characteristics and reproductive traits, studies have shown that *C. georgiana* embryos develop almost two times faster than *P. bibronii* (Seymour and Roberts, 1995; Seymour, 1999).

The ephemeral pools in which *C. georgiana* embryos develop are likely to exert a selective pressure on development rate. Rapid development is considered an advantage in species that oviposit in temporary pools or puddles, as short development times ensure that metamorphosis occurs before the water body dries and may also decrease exposure to aquatic predators. As a consequence, species that breed in ephemeral water bodies are likely to exhibit relatively high rates of development for both their ovum size and incubation temperature (Bradford 1990). However, the physiology behind this faster development is still unexplained. This study examines development, growth and O_2 consumption of *C. georgiana* and *P. bibronii* under an identical incubation temperature until metamorphosis. The partitioning of energy for growth, maturation and maintenance is examined to elucidate how energy use is related to growth and development rate using the Dynamic Energy Budget (DEB) theory (Kooijman, 2010), which can successfully describe embryonic energetics (Zonneveld and Kooijman, 1993). DEB theory describes an organism's energy assimilation and use as a function of its state (age, size, etc.) and the state of the environment (temperature, food, etc.) (Nisbet et al., 2000). We here focus on early developmental physiology.

DEB theory describes developmental transitions, such as from embryo to juvenile (equivalent to amphibian larva), as being linked to the level of maturity, which is quantified as the cumulative energy used for development, E_H . The other two state variables are structure, which can be quantified as volume,

length or mass, and reserve, quantified as energy content or mass (Kooijman, 2010). In DEB theory all energy acquired by an organism goes into reserve before it is allocated to different processes (fig.4.1). The κ -rule for allocation states that a fixed portion, κ , of mobilised reserve is used for somatic growth and maintenance and the remaining, $1 - \kappa$, is used for maturation and/or reproduction (Kooijman, 2010). In embryos and juveniles, in which reproduction does not yet occur, $1 - \kappa$ quantifies energy used for maturation and maturity maintenance (fig. 4.1). We apply this theoretical framework to empirical data collected for *P. bibronii* and *C. georgiana* in order to understand the relationship between energy allocation and developmental trajectories.

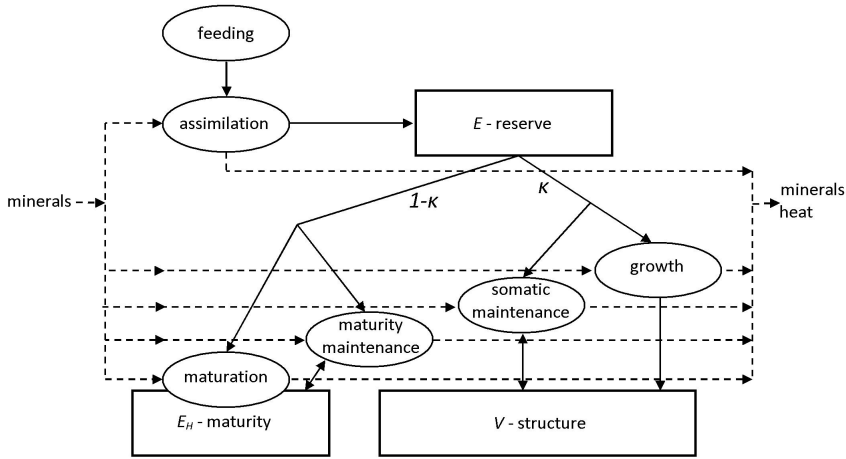


Figure 4.1: Metabolism in a juvenile DEB organism. Rectangles represent state variables, ovals are processes, solid lines are flows from state variables to processes and vice versa and dashed lines are flows of minerals (O_2 , CO_2 , nitrogenous wastes and H_2O) to and from processes. The processes of feeding and assimilation are absent in embryos.

4.2 Methods

4.2.1 Egg collection and incubation

Embryos and juveniles were staged throughout experiments according to Gosner (1960). Developmental stages were related to maturity level E_H^1 , where i represents Gosner stages 1 (oviposition) - 46 (metamorphosis). Clutches of terrestrial *P. bibronii* eggs were collected by marking the sites of calling males at Watt's Gully Native Forest Reserve, 50 km from Adelaide, South Australia. Three clutches (E_H^{21} , approximately 22 days old) were collected on the 28th May 2008 and another clutch (E_H^9 , approximately 3 days old) on the 11th

June 2008.

The clutches were taken to the laboratory and cleaned by gently rolling them on moist towelling. The eggs were incubated in air in covered containers on 20 Whatman No. 1 filter papers saturated with reverse osmosis water in a dark constant temperature room set at 12°C. The filter papers were maintained at saturation by ensuring that free water contacted them. Eggs were not touching each other and any that died or failed to develop were discarded. When the embryos reached E_H^2 7 they were flooded in water until they hatched.

One clutch of aquatic *C. georgiana* eggs (laid the previous night) were collected from the field, near Brookton Highway, 35 km southeast of Perth, Western Australia, on the 22nd August 2008. Another four clutches (laid the previous night) were collected from captive adults at the University of Western Australia on the 9th August 2009. Clutches were held at the University of Western Australia and transported by air to the University of Adelaide. The eggs were incubated in enough filtered rainwater to completely cover them at 12°C in a dark constant temperature room. Any eggs that died or failed to develop were discarded.

Upon hatching in both species, juveniles were placed in individual containers with approximately 250 mL of filtered rainwater with aquarium sand as a substrate and incubated under a 10:14 h light: dark regime to replicate winter conditions. Every two months throughout juvenile development, 50% of the water was replaced with fresh water. The juveniles were fed boiled lettuce and then a mix of boiled lettuce and fish flakes *ad libitum* until metamorphosis. When the forelimbs emerged, small rocks were placed in the containers so that the juveniles could climb out of the water. This incubation method was highly successful, with metamorph survival around 90%.

4.2.2 Mass and energy density

Ova were dissected from fresh eggs, dried to constant mass over silica gel and weighed to 0.01 mg on an electronic balance (Mettler AE183, Greifensee, Switzerland). Embryos and juveniles were selected at random throughout development, killed by freezing and placed in Tyler's preservative (Tyler, 1962). They were then dissected into body and gut, dried over silica gel and weighed. Dried samples of fresh ova, hatching gut-free body and gut and metamorph gut-free body were homogenized using a mortar and pestle to make a pellet of at least 25 mg. The energy density of the pellets was measured with an 1107 semi-micro bomb of a 1261 bomb calorimeter (Parr, Moline, U.S.A.) after calibration with dry benzoic acid. Statistical analyses to test differences between masses and energy density of the two species were performed in JMP IN (Version 4.0.4, SAS Institute). Data did not meet the parametric assumption of normality as tested by the Shapiro-Wilk test, so a nonparametric Kruskal-Wallis test with a chi-square approximation was used. A significance value of 0.05 was set for all statistical analyses.

4.2.3 O₂ consumption

O₂ consumption rates ($\dot{M}O_2$) of embryos and juveniles, until E_H^{35} (hindlimb toe maturation), were determined from the decrease in PO₂ within sealed water-filled respiratory chambers (0.67 mL, model 1271, Diamond General, Ann Arbor, MI) fitted with Clark-type O₂ electrodes (model 730, Microelectrodes Inc., Bedford, NH). The chambers were thermostated at 12 C using a thermocirculator (Julabo HC, Seelbach, Germany). The chamber water was mixed by a miniature magnetic stirring bar controlled by a revolving magnet behind the chamber.

After E_H^{35} , when juveniles outgrew the chambers, custom-made syringe respirometers were used. The chambers consisted of four, 5 mL glass syringes, each with a 5 mm hole in the side into which an O₂ electrode (model 730) was inserted and sealed with silastic tubing. The syringe barrels were suspended horizontally across plastic water baths and the spouts closed by three way valves. The baths were perfused from a thermocirculator (Thermomix 1442D, B.Braun, Melsungen, Germany). Current from the electrodes was measured via an O₂ analyzer (ReadOx-4H, Sable Systems, Las Vegas, NV). The electrodes were calibrated each day with a fresh zero solution of 20 mg sodium sulphite in 1 mL of 0.01 M sodium tetraborate and with air-equilibrated water (Tucker, 1967). An individual embryo or juvenile was sealed inside each chamber and left to stabilise before readings of PO₂ were taken every 1 - 20 min, depending upon the stage of the embryo or juvenile. Measurements were taken for a minimum of 3 h. Air-equilibrated water was measured after each run and $\dot{M}O_2$ corrected for electrode drift, which was assumed to be linear. Embryos were run in reverse osmosis water while juveniles were run in filtered rainwater. To account for this difference, $\dot{M}O_2$ of water-filled chambers was also measured to control for microorganism O₂ consumption in the water. These values averaged 6 ± 3 nmol h⁻¹ for reverse osmosis water and 12 ± 2 nmol h⁻¹ for filtered rainwater and were subtracted from the embryonic or juvenile $\dot{M}O_2$ readings of relevant experiments. Juveniles were starved for 48 h prior to $\dot{M}O_2$ measurement to reduce the effect of digestion on $\dot{M}O_2$. After forelimb emergence (E_H^{42}) $\dot{M}O_2$ was measured in air at 100% humidity. Total O₂ consumed was calculated for the entire development period and also to E_H^{22} , between E_H^{22} and E_H^{27} and between E_H^{27} and E_H^{46} . A polynomial equation was fitted to the data for $\dot{M}O_2$ against the age corresponding to each maturity level and the equation integrated to calculate the area under the curve. The O₂ cost of development was calculated from the total O₂ consumed divided by dry gut-free mass produced for each interval.

4.2.4 DEB Model

We applied the standard DEB model (Kooijman, 2010, Chap.2) to the data we collected in order to estimate energy parameters for *C. georgiana* and *P. bibronii*. Parameter estimation was performed simultaneously on all datasets

(Lika et al., 2011a,b). Data included lengths (snout to vent), dry mass, energy and respiration against age in combination with several key adult life history traits (ultimate dry mass, ultimate reproduction rate, age, mass and length at puberty). Specification of the model and computation of model $\dot{M}O_2$ are detailed in [Appendix D](#). The amount of data used was too extensive to present in the main text of this study but is summed up in [Appendix E](#).

The method of parameter estimation, using the downloadable software DEBtool (Kooijman et al., 2008) run in Matlab (MathWorks, MA, U.S.A.), is detailed in [Appendix E](#). We used a constant cost of an egg, E_0 , to equate the initial amount of reserve energy to the observed value of each species. This removed the maternal effect rule, where the reserve density of the mother is equal to the reserve density of the offspring, which is built into the standard DEB model (Kooijman, 2010). The effect of temperature on biological rates was described by the Arrhenius relationship ([Appendix E](#), fig. E.1C), determined from rate data from Seymour et al. (1991).

We assumed constant food and excluded water dynamics from the analysis by using dry mass. Each stage is quantified by the cumulated energy invested to reach that stage, known as maturity level, E_H^i . The cumulated energy invested to reach each stage is dissipated in the form of minerals and contributes to O_2 consumption. The transition from embryo to juvenile, called birth, and from juvenile to metamorph are represented by E_H^{27} and E_H^{46} , respectively. Birth is used to describe the onset of feeding. This corresponds with hatching in *P. bibronii* as the species fed immediately, but as *C. georgiana* did not feed immediately upon hatching an additional life parameter, E_H^{22} , was added to represent maturity level at hatching.

The standard DEB model was also applied to data for two additional Australian Myobatrachid amphibians, *C. nimbus* and *G. vitellina*. Data for *C. nimbus* was taken from Mitchell and Seymour (2000) and data for *G. vitellina* from Mitchell (2001).

4.3 Results

4.3.1 Empirical results

Fresh ova of *C. georgiana* had a similar dry mass to *P. bibronii* ($\chi_2 = 0.64$, $P = 0.42$, table 4.1). Likewise, energy density of fresh ova was not significantly different between the two species ($\chi_2 = 2.23$, $P = 0.14$), and therefore energy content was similar.

Development was faster in *C. georgiana* than *P. bibronii* (fig. 4.2). Metamorphosis was completed by 108 days in *C. georgiana* compared to 185 days for *P. bibronii*. Hatching also occurred earlier in *C. georgiana* (19 ± 2 days) compared to *P. bibronii* (39 ± 2 days). However, *C. georgiana* hatched at E_H^{22} compared to E_H^{27} in *P. bibronii*. Dry gut-free body mass at EH 22 was similar between the species ($\chi_2 = 3.11$, $P = 0.08$, table 4.1), as was dry gut

mass ($\chi_2 = 3.20$, $P = 0.07$). At E_H^{27} dry gut-free body mass was comparable ($\chi_2 = 0.008$, $P = 0.98$), but dry gut mass was greater in *C. georgiana* ($\chi_2 = 9.66$, $P = 0.002$). Energy content was measured at hatch in each species (table 4.1), so a direct comparison cannot be made due to the different hatching stage. Mass increased quite rapidly during *P. bibronii* juvenile development (fig. 4.3b), but this did not occur in *C. georgiana* (fig. 4.3a). Upon completion of metamorphosis (E_H^{46}) the dry gut-free body mass of *P. bibronii* was much larger than *C. georgiana* ($\chi_2 = 16.29$, $P = 0.0001$). Energy density of the gut-free body was similar, but due to the much larger mass, *P. bibronii* metamorphs had higher energy content (table 4.1).

During the majority of embryonic development, $\dot{M}O_2$ was higher in *C. georgiana*, especially after E_H^{22} at 19 days when *C. georgiana* hatched but *P. bibronii* was still confined in the egg capsule (fig. 4.3c, d). However, juvenile *P. bibronii* increased $\dot{M}O_2$ quite rapidly beyond birth to reach a much greater maximum of approximately 1350 nmol h^{-1} at the onset of metamorphosis compared to 230 nmol h^{-1} in *C. georgiana* (fig. 4.3e, f).

Integration of $\dot{M}O_2$ data indicated that embryos of *C. georgiana* consumed more total O_2 , but produced a similar dry gut-free body mass at E_H^{22} , which resulted in a slightly higher mass-specific O_2 cost of development compared to *P. bibronii* (table 4.1). Between E_H^{22} and E_H^{27} the O_2 cost of development switched to being higher in *P. bibronii*, due to a lower mass produced in relation to O_2 consumed. However, juvenile O_2 cost of development, from E_H^{27} to E_H^{46} , was over three and a half times higher in *C. georgiana*, due to a combination of less O_2 consumed and reduced mass production. Overall mass-specific O_2 cost of development was 1.5 times higher in *C. georgiana* compared to *P. bibronii* (table 4.1).

4.3.2 DEB model

We successfully determined a set of DEB parameters (table 4.2) that quantified the development times, dry biomass and $\dot{M}O_2$ patterns measured throughout *C. georgiana* and *P. bibronii* development. The chemical potential of reserve in the DEB model was held constant between the two species (table 4.2), which together with the similar initial dry mass of the ova, indicates that *C. georgiana* and *P. bibronii* had near-identical initial biochemical conditions in the model.

DEB predictions for dry biomass and $\dot{M}O_2$ against age are well matched to empirical results (fig. 4.1). The model captured the abrupt increase in $\dot{M}O_2$ at birth in both species: the onset of assimilation involves a conversion of food into reserve, which comes with overhead costs. This is likely the case for *C. georgiana*, but *P. bibronii* was not fed prior to the first $\dot{M}O_2$ measurement after birth (which corresponds to hatching), and the increase in $\dot{M}O_2$ is attributed to the removal of the diffusive barrier of the egg capsule (Mueller and Seymour, 2011).

Model $\dot{M}O_2$ was partitioned into contributions from somatic maintenance, growth, maturation (and maturity maintenance) and assimilation (for juve-

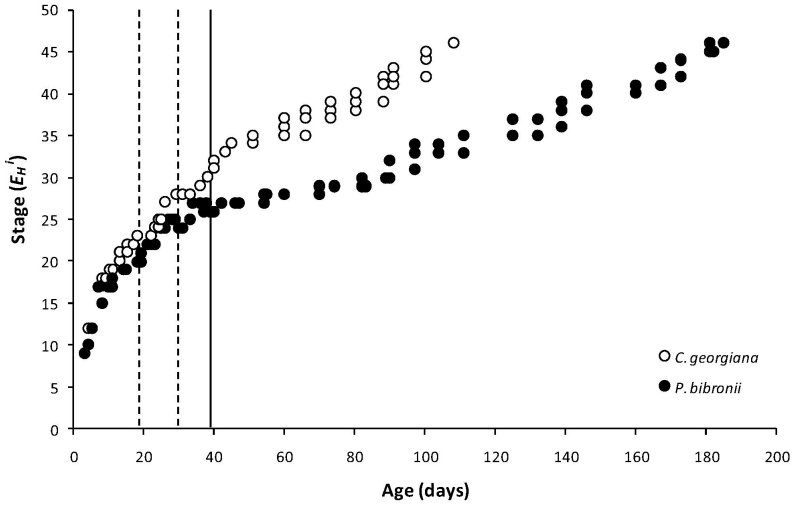


Figure 4.2: Stage of development as a function of age in *Crinia georgiana* and *Pseudophryne bibronii*. Each stage is represented by E_H^i where i refers to stage 1 - 46 (Gosner, 1960). The dashed lines indicate first hatch then birth in *C. georgiana* and the solid line represents both hatch and birth in *P. bibronii*, which occur at the same age and stage.

niles) (fig. 4.3c, d, e, f). Throughout embryonic development *C. georgiana* allocated more O_2 to growth than *P. bibronii* (fig. 4.1c, d). Between *C. georgiana* hatching and birth the fraction of mobilised reserve allocated to growth and somatic maintenance (κ) decreased from 0.86 at E_H^{22} to 0.61 at E_H^{27} (table 4.2); the complementary fraction ($1 - \kappa$) to maturation and maturity maintenance thus increased, meaning an acceleration of maturation. This resulted in κ being initially higher in *C. georgiana* during embryogenesis, before falling below the constant κ of *P. bibronii* by birth (table 4.2). This switch in κ matched well with the rapid increase in $\dot{M}O_2$ that occurred between hatch and birth in *C. georgiana* (fig. 4.1e), and changed the partitioning of $\dot{M}O_2$ during *C. georgiana* juvenile development. The contribution to maturation increased between E_H^{22} and E_H^{27} while the contribution to growth declined and continued to do so throughout juvenile development (fig. 4.1e). In comparison, *P. bibronii*, continued to partition energy by the same proportion after birth so that there was no rapid increase in contribution to maturation (fig. 4.1f).

Model predictions of the total O_2 consumed at three developmental intervals also matched closely with empirical results. To reach E_H^{22} the model predicted a total O_2 amount of 13.8 μmol and 9.3 μmol for *C. georgiana* and *P. bibronii*, respectively, which are very close to empirical values (table 4.1). Between E_H^{22} and E_H^{27} the model total O_2 was 37.1 μmol in *C. georgiana* and 34.1 μmol in *P. bibronii*, slightly higher than the empirical results. Likewise, the values for

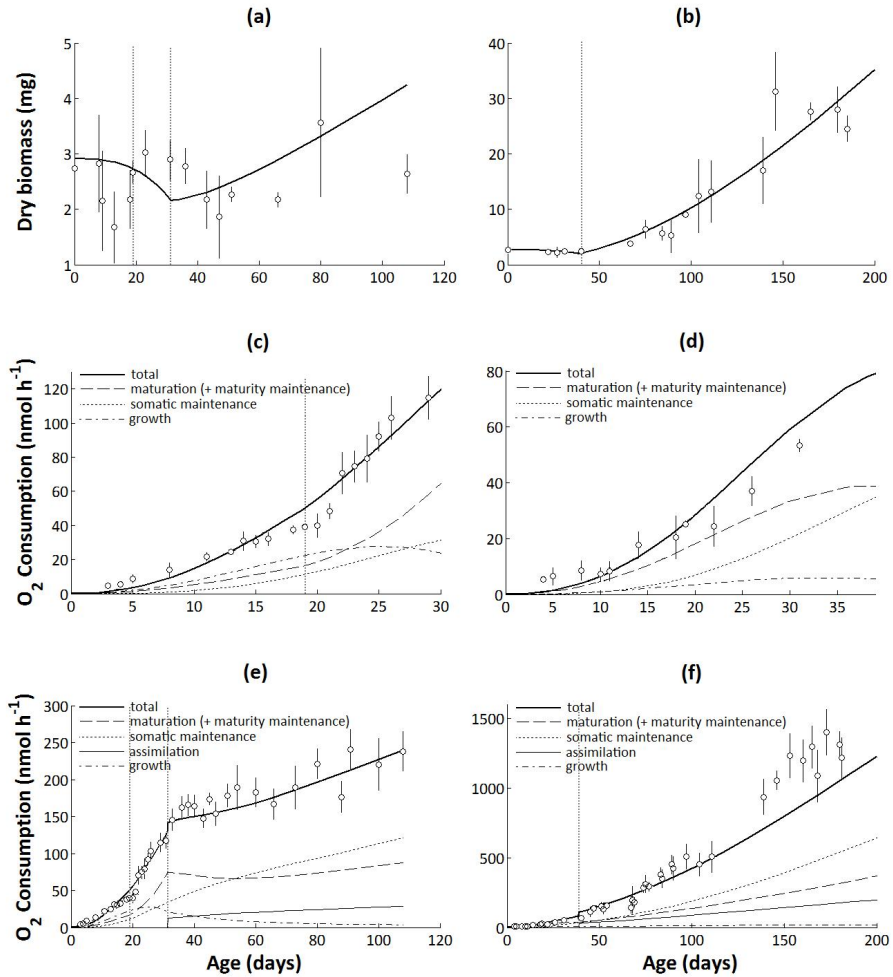


Figure 4.3: Experimental data (circles) compared to dynamic energy budget model results (lines) for *Crinia georgiana* (first column) and *Pseudophryne bibronii* (second column). Experimental data presented as means with 95% CI error bars. Vertical dotted lines indicate first hatching and then birth for *C. georgiana* and birth for *P. bibronii*. (a) and (b) show model output for dry biomass against age. (c) and (d) show model embryonic O₂ consumption partitioned into different energetic processes against age. (e) and (f) show model O₂ consumption until metamorphosis partitioned into different energetic processes against age. Note the different scales on the axes.

juvenile development, between E_H^{27} and E_H^{46} were 306.7 and 2095.1 μmol in *C. georgiana* and *P. bibronii*, respectively, slightly lower but still a good fit with empirical data.

The allocation of total O_2 clearly demonstrates how partitioning of energy changed throughout development (fig. 4.4). Until E_H^{22} , *C. georgiana* partitioned a greater percentage of total O_2 to growth and less to maturation than *P. bibronii* (fig. 4.4). The decrease in κ between E_H^{22} to E_H^{27} in *C. georgiana* resulted in an increase in the percentage of O_2 allocated to maturation, compared to the slight decrease in *P. bibronii* (fig. 4.4). From E_H^{27} to E_H^{46} the difference in partitioning between the two species was most pronounced, with *C. georgiana* partitioning 37% of its total O_2 to maturation while *P. bibronii* partitioned only 28%. Minimal feeding of *C. georgiana* juveniles was indicated by both a low functional response, (table 4.2), and a low (11%) contribution from assimilation compared to *P. bibronii* (17%) (fig. 4.4). The decrease in allocation to growth, and increase in somatic maintenance, as development progresses is also clear in both species. For the entire development period till metamorphosis, *C. georgiana* allocated 7% more of its total O_2 to maturation, 9% more oxygen to growth and 8% less to somatic maintenance than *P. bibronii* (fig. 4.4).

The cumulative energy invested in maturity to reach each developmental stage was quantified for both species. Cumulative energy for maturity in *C. georgiana* increased above *P. bibronii* during early embryonic development (fig. 4.5). However, by birth the cumulative energy was lower in *C. georgiana* than *P. bibronii*, a trend that increased during juvenile development (fig. 4.5). $\dot{M}\text{O}_2$ against maturity level using empirical data and model results were well matched for both species (fig. 4.6). The lower cumulated energy required for maturity in *C. georgiana* juveniles was matched by the much lower maximum $\dot{M}\text{O}_2$ compared to *P. bibronii* (fig. 4.6).

DEB parameters were also successfully estimated for *C. nimbus* and *G. vitellina* (table 4.2). Both *C. nimbus* and *G. vitellina* had lower embryo energy conductance (\dot{v}) values than the other two species, but \dot{v} was particularly low for *C. nimbus*. A decrease in κ described the increase in $\dot{M}\text{O}_2$ after hatch in *C. nimbus*, similar to *C. georgiana*, however κ was much lower in *C. nimbus*. The parameters of *G. vitellina* were similar to *P. bibronii*, with no change in κ . Further details of parameter estimation can found in the Add_My_Pet collection (http://www.bio.vu.nl/thb/deb/deblab/add_my_pet/).

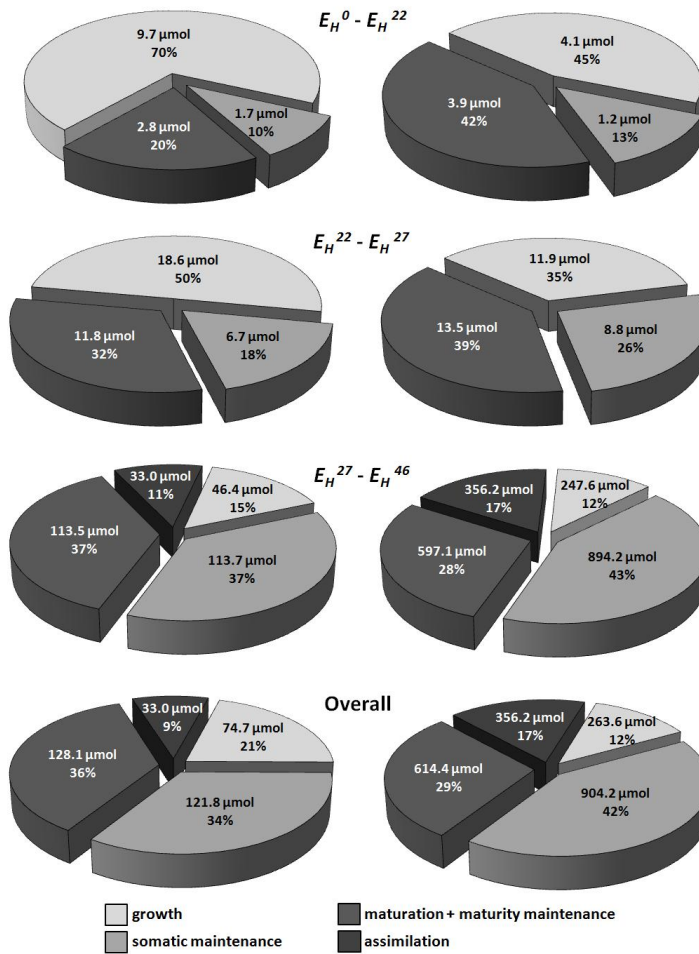


Figure 4.4: Total O₂ consumed during three developmental intervals and overall development partitioned into energetic processes (absolute amount and percentage of total) as predicted by a dynamic energy budget model for *Crinia georgiana* (first column) and *Pseudophryne bibronii* (second column). $E_H^0 - E_H^{22}$ represents embryonic development, $E_H^{22} - E_H^{27}$ represents from hatch to birth in *C. georgiana* and continued egg incubation until birth in *P. bibronii* and $E_H^{27} - E_H^{46}$ represents juvenile development until metamorphosis in both species.

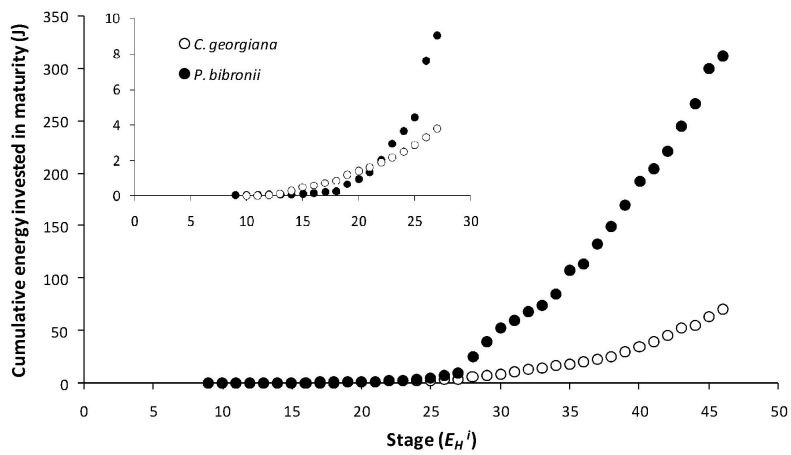


Figure 4.5: Cumulated energy invested in maturity against stage of development for *Crinia georgiana* and *Pseudophryne bibronii* until metamorphosis. Insert shows cumulated energy invested in maturity against stage until birth. Each stage is represented by E_H^i where i refers to stage 1 - 46 (Gosner, 1960). Hatch occurs at E_H^{27} and birth at E_H^{27} in *C. georgiana*. Hatch and birth both correspond with E_H^{27} in *P. bibronii*.

Table 4.1: Summary empirical data for *Crinia georgiana* and *Pseudophryne bibronii* development at four stages: fresh ovum, E_H^{22} (hatch in *C. georgiana*), E_H^{27} (birth in *Crinia georgiana*, hatch and birth in *Pseudophryne bibronii*) and E_H^{46} (completion of metamorphosis in both species). Data are presented as mean \pm 95% CI (n).

	Parameter	C. georgiana	P. bibronii
ovum	Dry mass (mg)	2.74 \pm 0.12(91)	2.68 \pm 0.11(69)
	Energy density (J mg ⁻¹)	25.64 \pm 1.18 (6)*	24.26 \pm 91 (4)*
	Energy content (J)	70.27	65.03
E_H^{22}	Dry gut-free body mass (mg)	0.68 \pm 0.06(56)	0.89 \pm 0.15(5)
	Energy density of body (J mg ⁻¹)	20.73	-
	Energy content of body (J)	14.10	-
	Dry gut mass (mg)	1.98 \pm 0.22(56)	1.40 \pm 0.27(5)
	Energy density of gut (J mg ⁻¹)	25.97 \pm 2.50(2)*	-
	Energy content of gut (J)	51.43	-
	Total energy content (J)	65.53	-
	Total O ₂ consumed ($E_H^0 - E_H^{22}$) (μ mol)	8.2	6.3
	O ₂ cost of development ($E_H^0 - E_H^{22}$) (μ mol mg ⁻¹)	12.1	7.1
E_H^{27}	Dry gut-free body mass (mg)	1.49 \pm 0.20(5)	1.48 \pm 0.06(167)
	Energy density of body (J mg ⁻¹)	-	21.41 \pm 69(4)*
	Energy content of body (J)	-	31.69
	Dry gut mass (mg)	1.53 \pm 0.30(5)	0.92 \pm 0.05(167)
	Energy density of gut (J mg ⁻¹)	-	23.06 \pm 0.48(4)*
	Energy content of gut (J)	-	21.22
	Total energy content (J)	-	52.82
	Total O ₂ consumed ($E_H^{22} - E_H^{27}$) (μ mol)	22.0	21.5
	O ₂ cost of development ($E_H^{22} - E_H^{27}$) (μ mol mg ⁻¹)	27.2	36.4
E_H^{46}	Dry gut-free body mass (mg)	2.52 \pm 0.35(8)	23.19 \pm 2.07(19)
	Energy density of body (J mg ⁻¹)	17.07	20.01 \pm 0.37 (6)*
	Energy content of body (J)	43.02	464.02
	Dry gut mass (mg)	0.13 \pm 0.03(8)	1.17 \pm 0.14(19)
	Total O ₂ consumed ($E_H^{27} - E_H^{46}$) (μ mol)	363.5	2310.2
	O ₂ cost of development ($E_H^{27} - E_H^{46}$) (μ mol mg ⁻¹)	352.9	106.4
overall	Total O ₂ consumed (μ mol)	393.7	2338.0
	O ₂ cost of development (μ mol mg ⁻¹)	156.2	100.8

*n refers to number of bomb calorimetry pellets

Table 4.2: State variables, primary parameters and other parameters (affecting changes of state variables at 20°C) for the standard DEB model (Kooijman, 2010) of *Crinia georgiana*, *Pseudophryne bibronii*, *Crinia nimbus* and *Geocrinia vitellina*.

Symbol	C. georgiana	P. bibr-onii	C. nimbus	G. vitellina	Unit	Name
<i>state variables</i>						
E					J	reserve energy
V					cm ³	structural volume
L					cm	structural length $V^{1/3}$
E_H					J	cumulated energy invested in maturity
<i>primary energy parameters</i>						
$\{p_{Am}\}$	546	565	263	565	J d ⁻¹ cm ⁻²	maximum surface area specific assimilation rate
\dot{v}	0.056	0.040	0.0085	0.017	cm d ⁻¹	Energy conductance
κ	0.86	0.69	0.50	0.69	-	fraction of energy allocated to growth and somatic maintenance
	0.61		0.30			
$[p_M]$	368	491	205	491	J d ⁻¹ cm ⁻³	volume specific somatic maintenance
k_J	0.002	0.002	0.002	0.002	d ⁻¹	maturity maintenance rate
$[E_G]$	6502	5397	5185	5397	J cm ⁻³	cost of synthesis of structure
<i>life stage parameters</i>						
E_{22}^{22}	1.5				J	cumulated energy invested in maturity at hatching
E_H^{27}	7.7	9.2	90.4	11.3	J	cumulated energy invested in maturity at birth
E_H^{46}	70.8	313.5	90.4	11.3	J	cumulated energy invested in maturity at metamorphosis
<i>other parameters</i>						
f	0.3	0.8	1	1	-	scaled functional response
T_A	12000	12000	10800	8000	K	Arrhenius temperature
δ_M	0.40	0.35	0.23	0.35	-	shape coefficient for snout to vent length
$\bar{\mu}_E$	577.5	577.5	550.0	577.0	kJ c-mol ⁻¹	chemical potential of reserve
$\bar{\mu}_V$	500.0	500.0	550.0	500.0	kJ c-mol ⁻¹	chemical potential of structure
d_V	0.2	0.2	0.2	0.2	g cm ⁻³	density of structure
y_{XE}	1.25	1.25	1.25	1.25	c-mol c-mol ⁻¹	yield of food on reserve
y_{PX}	0.1	0.1	0.1	0.1	c-mol c-mol ⁻¹	yield of faeces on food

4.4 Discussion

At fertilization the dry biomass and energy density of the eggs of *C. georgiana* and *P. bibronii* are highly comparable (table 4.2). Therefore, the species have the same amount of initial energy at their disposal for embryonic development. Despite these similarities, the time to reach hatching is much shorter in *C. georgiana* (fig. 4.2). However, in contrast to previous studies that reported hatching at E_H^{27} for both species (Seymour, 1999; Seymour and Roberts, 1995), this study found that *C. georgiana* hatches at E_H^{22} . The discrepancy in reported hatching stage in *C. georgiana* may be due to the rapid development of stages $E_H^{23} - E_H^{25}$ (fig. 4.2), which Seymour and Roberts (1995) reported as being difficult to recognise at 15°C. At hatching *C. georgiana* has yet to develop eyes, mouthparts and intestinal loops at 12°C, all of which usually occur at $E_H^{23} - E_H^{25}$, but they do have hindlimb buds, which normally form at E_H^{26} (Gosner, 1960). However, development of mouthparts and intestinal loops were used to assign stages, so hatching is considered to occur at E_H^{22} in *C. georgiana*. Hatchlings of *C. georgiana* are less developed than *P. bibronii*, in which hatching corresponds with birth at E_H^{27} , when the species has well development mouthparts and intestinal loops. Therefore, a comparison of time to hatching is less informative in terms of development rates, and time to reach E_H^{22} is only slightly faster in *C. georgiana* (fig. 4.2).

DEB modelling, used to describe energy use throughout development, is consistent with empirical data and indicates that the two species require vastly different amounts of energy to reach metamorphosis (fig. 4.3, 4.6). Embryonic $\dot{M}O_2$ does differ somewhat between the species (fig. 4.3c, d), but it is during juvenile development that $\dot{M}O_2$ greatly diverges, with a much higher maximum $\dot{M}O_2$ in *P. bibronii* compared to *C. georgiana* (fig. 4.3e, f). The substantial difference in $\dot{M}O_2$ and the cumulative energy required for maturity between the two species is directly related to their different development rates and energy partitioning.

Avian egg metabolism has been modelled, in which $\dot{M}O_2$ is partitioned into growth and maintenance. This has been useful in understanding different patterns of $\dot{M}O_2$, particularly between altricial and precocial birds (Hoyt, 1987; Vleck and Hoyt, 1991; Vleck and Vleck, 1987; Vleck et al., 1980). Unlike DEB theory, however, the model does not include the energy cost of maturation, nor of its maintenance, and is confined to embryo development only. The relationship between maturity level, a concept of DEB theory, and morphologically defined stage of development, allows us to think about development as an energy allocation strategy: age and body size at a particular developmental stage depend on environmental conditions, maturity levels do not. While *Crinia* shows a change in allocation to accelerate maturation before the onset of assimilation, quite a few other species, such as some fish (e.g. pleuronectiformes), some crustaceans (e.g. *Carcinas*) and bivalves, show an acceleration of metabolism as a whole after the onset of assimilation (Kooijman et al., 2011): the surface area-specific assimilation and searching rates, as well as the energy

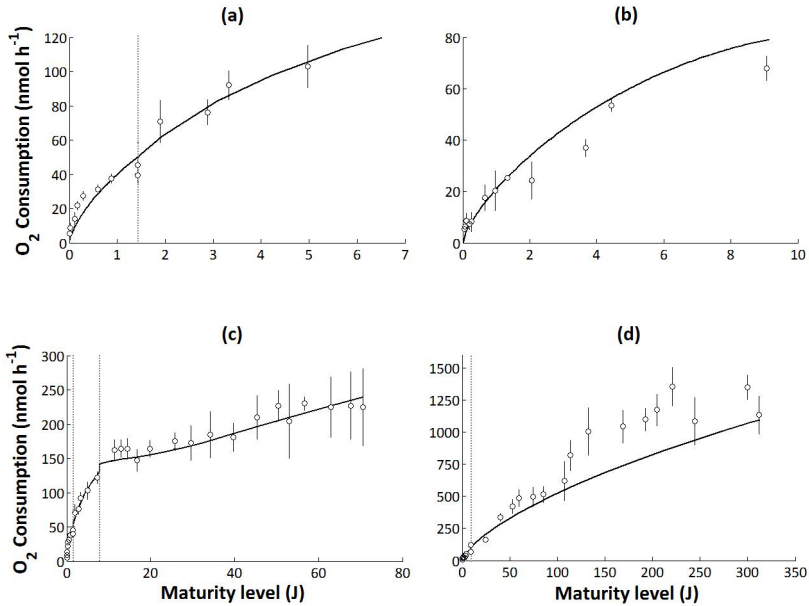


Figure 4.6: Experimental data (circles) compared to dynamic energy budget results (lines) for O₂ consumption against maturity level in *Crinia georgiana* (first column) and *Pseudophryne bibronii* (second column). (a) and (b) are during embryonic development and (c) and (d) are until metamorphosis. Experimental data presented as means with 95% CI error bars. Vertical dotted lines indicate first hatching and then birth for *C. georgiana* and birth for *P. bibronii*. Note the different scales on the axes.

conductance increase during a certain confined period, while allocation fraction κ and other parameters remain constant. This not only leads to an acceleration of development, but also of growth, unlike what we here see in *Crinia*. The developmental stages of the zebrafish (*Danio rerio*), a species that also sports metabolic acceleration, has also been linked to maturity levels as specified by DEB theory (Augustine et al., 2011a). DEB theory helped in recognising the fundamental difference in these acceleration strategies.

Despite the substantial morphological changes, the standard DEB model with constant parameters values, seems to apply to the full life cycle of *P. bibronii* and *G. vitellina* and a single, temporary change in one parameter suffices to capture the full life cycle of both *Crinia* species. It is the juvenile stages of *C. georgiana* and *P. bibronii* that provide the greatest insight into their different development times.

After hatching, *C. georgiana* begins to partition more energy into maturation (fig. 4.3, 4.4), so that the species completes metamorphosis 1.7 times faster than *P. bibronii* (fig. 4.2). In comparison, *P. bibronii* juveniles continue the same energy use strategy as the embryos (fig 4.3d, f) and, as a consequence,

the percentage of O_2 used for maturation decreases (fig. 4.4) and development is slower. The increase in energy allocation to maturation reduces energy contribution to growth, resulting in much smaller *C. georgiana* metamorphs than *P. bibronii* (table 4.1). This large difference in juvenile tissue contributes to the lower $\dot{M}O_2$ of *C. georgiana* (fig. 4.3, 4.6). Both species were fed ad libitum during juvenile stages but *P. bibronii* consumed noticeably more exogenous food than *C. georgiana*, allowing for a higher growth rate. This is reflected in the higher scaled functional response, f , which relates ingestion as a function of food availability in the model (Kooijman, 2010) (table 4.2). As food availability was the same for both species, the difference in f reflects differences in feeding.

The difference in energy partitioning between *C. georgiana* and *P. bibronii* influences the total O_2 required to complete metamorphosis. Total O_2 required during embryogenesis does not vary much between the species but the total O_2 required by *P. bibronii* juveniles is significantly higher than *C. georgiana* due to their greater mass (table 4.1, fig. 4.3a, b). The mass-specific O_2 cost of development for the three developmental intervals and overall development is determined using a method of previous studies, in which the total O_2 consumed, or energy used, is divided by gut-free mass produced (Booth and Astill, 2001; Mueller et al., 2011; Thompson and Russell, 1999; Vleck and Hoyt, 1991; Whitehead and Seymour, 1990). The O_2 cost of development to reach E_H^{22} and between E_H^{22} and E_H^{27} is not overly different between the species, but the O_2 cost of building 1 mg of juvenile gut-free dry mass is much higher in *C. georgiana*, which increases overall mass-specific O_2 cost (table 4.1). The higher mass-specific O_2 cost indicates that the low $\dot{M}O_2$ of *C. georgiana* juveniles is coupled by a disproportionately lower mass production.

The method of calculating mass-specific O_2 cost of development using dry gut-free body mass differs with DEB theory. The theory partitions biomass into structure and reserve which is different to the partitioning of gut-free body and gut mass. In reality, when the gut is dissected from the body it includes yolk and gut, and therefore contains reserve and some structure. Additionally, the body is likely to contain, apart from structure, also some reorganised reserve. The composition of reserve and yolk being essentially identical, yolk is transported to the body and partly used for metabolism. DEB theory assumes weak homeostasis, i.e. reserve density of the body remains constant during growth in constant environments. This assumption leads to good fits for both total biomass (fig. 4.3a, b) and gut-free body and gut masses during embryogenesis (Appendix E, fig. E.2B, fig. E.1B). See Eqn. E.1 and E.2 for output mapping of embryo reserve and structure to experimentally measured yolk dry mass and embryo dry mass.

Using either gut-free mass or dry biomass, it is quite clear that a discrepancy exists between the difference in mass of the two species at metamorphosis and the difference in total O_2 consumed. Dry biomass is nine times greater in *P. bibronii* compared to *C. georgiana*, yet total O_2 consumed for the entire developmental period is only six times greater (table 4.1). This indicates that

not only do differences in growth, and therefore mass, influence total O_2 used, but the species must have different energy requirements for other processes, such as maturation. The benefits of faster development must outweigh the higher mass-specific O_2 cost of development of *C. georgiana*.

The trade off between *C. georgiana* juvenile development rate and growth can be related to the species' reproductive mode. The earlier hatching stage in *C. georgiana*, together with its faster development to metamorphosis, is in accordance with the trend seen in other aquatic breeding species (Bradford, 1990), despite its comparable egg size with *P. bibronii*. The species lays its eggs in ephemeral pools so fast development is advantageous in escaping the pools before they dry. Aquatic predation may also promote fast development, however no aquatic predators have been observed in the pools in which *C. georgiana* develops (Doughty and Roberts, 2003). A deteriorating incubation environment may contribute to the ability to decrease energy allocated to growth after hatch. Upon hatching, *C. georgiana* apparently detects water level which acts as an environmental trigger for faster development. In shallow water the species metamorphoses faster than in deeper water, and only when resource availability is high under such conditions is the species able to increase growth and maturation concurrently (Doughty, 2002; Doughty and Roberts, 2003).

The model results for this study provide strong empirical support for the maturation concept and the κ -rule of allocation of DEB theory (Kooijman, 2010), in which mobilised reserve not used for growth (and somatic maintenance) is used for maturation (and maturity maintenance) (fig. 4.1). Juvenile *C. georgiana* convincingly demonstrate how energy used for maturation is dissipated as minerals (carbon dioxide, nitrogenous wastes, water) without contributing to biomass. Initially, the same standard DEB model was applied to *C. georgiana* and *P. bibronii*. The experimental data for *P. bibronii* fit this standard model rather well. However, *C. georgiana* deviates from the expected pattern with a rapid increase in $\dot{M}O_2$ between hatch and birth (fig 4.3, 4.6). This change in $\dot{M}O_2$ is best explained in the model by a changing κ value, supporting the notion that dissipation for maturity increases. Furthermore, the strong agreement between empirical and model results for the relationship between maturity level and $\dot{M}O_2$ (fig. 4.6) indicates that DEB theory can predict the interaction between growth, development rate and O_2 demand.

The ability of *C. georgiana* to switch energy partitioning to favour maturation over growth upon hatching raises the question as to why it does not do so throughout embryonic development as well, which would further shorten its development time. Firstly, as discussed, the shift in κ may have evolved in response to an environmental trigger. The environmental cue of water level takes effect upon hatching so this is when κ changes. Secondly, the species needs to produce a certain amount of tissue before it switches to the energy use strategy which disfavours growth. Juveniles of *C. georgiana* are able to complete metamorphosis without feeding and therefore without large increases in mass (Doughty, 2002; Doughty and Roberts, 2003) and this strategy would be difficult without an initial mass buffer. Facultative feeding is possible due to

the relative large eggs of *C. georgiana*, which provide more reserves for development (Doughty, 2002). The larger eggs and facultative feeding of *C. georgiana* may be hypothesised as representing a development mode that lies somewhere in between the ancestral amphibian development of aquatic obligate feeding juveniles and direct development, in which all nutrition is provided by the yolk and small metamorphs emerge directly from large eggs. The changing κ value and a reduction in feeding and growth may reflect a transition in developmental strategy.

Both *C. georgiana* and *P. bibronii* show divergences from the ancestral development mode of amphibians, which reduce the reliance on free water. The terrestrial oviposition of *P. bibronii* eggs eliminates the need for water during embryogenesis, while the rapid facultative feeding juvenile development of *C. georgiana* reduces the time water is required to reach metamorphosis. These different strategies are linked to the slightly different spawning times of the species. Autumn spawning in *P. bibronii* reduces water availability for eggs, but increases it for juvenile development which occurs throughout winter. The species lays eggs along drainage lines that, once winter rains set in, generally hold a large amount of water that would allow the species to complete its significantly long development. Spawning of *C. georgiana*, two to three months later in winter, ensures water is available for the eggs, but shortens water availability for the juveniles. The developmental strategy that contributes more to fitness of the species post-metamorphosis is unclear as the survival of the metamorphs is unknown. However, adult characteristics, such as ultimate length, mass and reproduction rate, are similar between the two species (Barker et al., 1995; Main, 1957; Smith and Roberts, 2003; Woodruff, 1976). Moreover, they are well matched by model predictions (Appendix E, tables E.2, E.1). This indicates that κ must switch back to the pre-hatch value after metamorphosis in *C. georgiana*, which would increase allocation to growth and result in comparable adult size and reproduction of the two species. Future experiments which include post-metamorphic growth (in terms of length and mass) would support (or infirm) this hypothesis.

To assess if the change in κ in *C. georgiana* but constant κ in *P. bibronii* is related to their different development modes, DEB theory was applied to two direct developing Myobatrachid frogs, *C. nimbus* and *G. vitellina*. Acceleration in $\dot{M}O_2$ after hatch in *C. nimbus* is described by a decrease in κ , much like *C. georgiana*, while *G. vitellina* does not accelerate $\dot{M}O_2$, much like *P. bibronii* (table 4.2). Such a difference between two species using a very similar mode of direct development suggests there may be no relationship between a direct development strategy and a change in κ . However, *C. nimbus* and *G. vitellina* have appreciably different incubation environments and egg sizes. The incubation of large *C. nimbus* eggs in subalpine conditions at 5 to 15 C takes a long time, due to a low value for the energy conductance, \dot{v} (even when temperature corrected). The low embryo energy conductance means a low reserve mobilisation rate, which increases the ability to survive a long incubation time. Metamorphs can emerge before winter or juveniles overwinter and emerge in

spring (Mitchell and Seymour, 2000). However, the cost of overwintering is greater (Mitchell and Seymour, 2000) and there is a risk that temperatures may drop so low that juveniles run out of reserves, yet temperatures are perhaps not low enough that the species undergoes torpor to conserve energy. In comparison, *G. vitellina* develops in a temperate environment over spring and summer when nest temperatures can reach 20°C (Mitchell, 2001). The decrease in κ in *C. nimbus* may reflect the greater instability in its environment and an increase in allocation to maturation increases the likelihood that development will be complete before winter. The smaller eggs of *G. vitellina*, in combination with a larger energy conductance, result in an already inherently faster development rate and so they, as in *P. bibronii*, are not under a selective pressure to increase energy allocation to maturation. Additional developmental data, and corresponding DEB parameter estimations, are required for future investigation of the selective pressures that result in a change in κ during development. However, in the case of *C. georgiana* and *C. nimbus*, time constraints placed upon their development by their incubation environments appear to act as triggers for a change in energy allocation.

Acknowledgements

We thank Nicola Mitchell and Sharron Perks from the University of Western Australia for provision of *C. georgiana* eggs. We acknowledge funding from the University of Adelaide. This work is also part of the ENVIRHOM research program supported by the Institute for Radioprotection and Nuclear Safety and the Provence Alpes Côte d'Azur region. Laure Pecquerie is gratefully acknowledged for critical feedback thus improving the the manuscript.

5

Effects of uranium on the metabolism of zebrafish, *Danio rerio*

Augustine, S., Gagnaire, B., Adam-Guillermin, and Kooijman, S. A. L. M.
(2012) Effects of uranium on the metabolism of zebrafish, *Danio rerio*. Aquatic
Toxicology. Accepted.

Abstract

The increasing demand for nuclear energy results in heightened levels of uranium (U) in aquatic systems which present a potential health hazard to resident organisms. The aim of this study was to mechanistically assess how chronic exposure to environmentally relevant concentrations of U perturbs the complex interplay between feeding, growth, maintenance, maturation and reproduction throughout the life-cycle of an individual. To this end we analysed literature-based and original zebrafish toxicity data within a same mass and energy balancing conceptual framework. U was found to increase somatic maintenance leading to inhibition of spawning as well as increase hazard rate and costs for growth during the early life stages. The fish's initial conditions and elimination through reproduction greatly affected toxico-kinetics and effects. We demonstrate that growth and reproduction should be measured on specific individuals since mean values were hardly interpretable. The mean food level differed between experiments, conditions and individuals. This last 'detail' contributed substantially to the observed variability by its combined effect on metabolism, toxic effects and toxico-kinetics. The significance of this work is that we address exactly how these issues are related and derive conclusions which are independent of experimental protocol and coherent with a very large body of literature on zebrafish eco-physiology.

Key words: DEB theory, growth, metabolism, reproduction, toxicity, uranium, zebrafish

5.1 Introduction

Uranium (U) is an ubiquitous element in the environment but natural concentrations in aquatic systems are increased in response to human activities linked to the nuclear fuel cycle (e.g. Fernandes et al., 1995; Jurgens et al., 2010; Uralbekov et al., 2011; Villa et al., 2011). A renewed international use of nuclear power as energy source (Nuclear Energy Agency, 2008) and increased public awareness of long term impacts of environmental pollution motivate the study of uranium's toxicity to living organisms. The objective of this study is to mechanistically assess how chronic exposure to environmentally relevant concentrations of U perturbs the complex interplay between feeding, growth, maintenance, maturation and reproduction throughout the life-cycle of an individual. Unfortunately, many toxicity tests concern organisms at particular life stages and experiment duration may be short relative to total lifespan meaning that our method must be able to extrapolate effects across life stages. An additional complex issue for extrapolation purposes is accounting for the relationship between U speciation and water hardness and pH in combination with toxic effects (Fortin et al., 2004, 2007).

We first compiled four literature-based studies where zebrafish, *Danio rerio* were chronically exposed to water-borne depleted U. Second, we designed an experiment to mechanistically assess toxicological effects of U on reproductive physiology of zebrafish. Behavioural effects might result from an impairment of sensory organs and inhibit spawning or even oocyte maturation but not the actual mass investment in reproduction. On the other hand allocation to reproduction might be modified in response to perturbations of energy allocation to physiological processes such as growth. The advantage of working with these particular studies is twofold. First, zebrafish are extremely well studied model organisms (Laale, 1977; Hill et al., 2005). Second, the chemical composition of U used for the exposure in combination with the pH, chemical composition and temperature of the medium were similar across all five experiments (table F.1, Online Appendix F).

Differences in effects and accumulation observed across all of the experiments may be (partially) explained by differences in size and growth rate. Therefore there is a need to specify energetics (growth and reproduction) in combination with toxico-kinetics (dynamics of internal concentration) in a unique theoretical framework (Jager et al., 2006b; Jager and Klok, 2010; Jager and Zimmer, 2012). A well worked out quantitative theory on metabolic organisation, Dynamic Energy Budget (DEB) theory, provides the toolkit necessary to address this problem (Kooijman, 2010). The theory provides a standard DEB model applicable to all animals (Kooijman, 2010, Chap.2); the model is mechanistic so each parameter quantifies a single metabolic process. The DEB model fully specifies all mass and energy fluxes (Sousa et al., 2010) over the entire life-cycle. 7 metabolic processes are defined: assimilation, mobilization, allocation, synthesis of structure, somatic maintenance, maturation, maturity maintenance (fig. 5.1A). For our specific purpose we needed to extend the stan-

standard model with a module for the preparation of batches of eggs from material in the reproduction buffer (fig. 5.1B).

A DEB model was previously fully parametrized to zebrafish; predicted development, growth and reproduction closely matched observations published in numerous studies ranging from the 1960's to the present day (Augustine et al., 2011a) and covering the full life-cycle. The zebrafish DEB model presents coherence between observations made with different individuals in combination with different temperature and feeding protocols and further provides estimates for all of the standard DEB model parameter values (table 5.1). We consider that this model provides a correct quantitative characterization of the baseline metabolism of (control) zebrafish. The model can be extended with a one compartment toxico-kinetics module (Kooijman and van Haren, 1990) which specifies the dynamics of the internal concentration, expressed in $[M_Q]$ (nmol U cm⁻³), which then gets treated as a state variable. In line with DEB theory we assume three ranges of $[M_Q]$ for all compounds: too little, enough and too much. Uranium is a non-essential element, and accordingly, our focus is on what happens in the neighbourhood of the too much range which occurs just above the no effect internal concentration $[M_{Q0}^*]$ (nmol U cm⁻³) for process *. Complex patterns of organism level effects which occur just above $[M_{Q0}^*]$ can be captured by the modification of a single parameter value; this modified parameter quantifies process *. If the (internal) concentration further increases, more and more parameters can become affected. From an environmental risk assessment perspective, the interest is on how organism level effects observed in the neighbourhood of $[M_{Q0}^*]$ translates into long term effects on populations and ecosystems. Thus the identification of the first process which is affected in the presence of uranium is the primary concern of this analysis (Kooijman and Bedaux, 1996; Kooijman, 2010; Jager et al., 2010).

We test the hypothesis that the results across studies are coherent when accounting for effects of energetics (differences in feeding, size, initial amount of reproductive material, elimination through reproduction) on toxico-kinetics. We first describe the zebrafish DEB model and specify the five modules needed to conduct this study. Second we compare model predictions with data. We finish with a discussion on insight gained through the comparative analysis of all data sets using the same coherent framework.

5.2 DEB model

Figure 5.1A specifies the conceptual organisation of metabolism as defined by DEB theory. We refer to Augustine et al. (2011a) for the full description of the zebrafish DEB model. Source code for the parameter estimates of the model are freely downloadable at http://www.bio.vu.nl/thb/deb/deblab/add_my_pet/.

Briefly, the assimilation energy flux $\dot{p}_A = f\{\dot{p}_{Am}\}L^2$ (J d⁻¹) quantifies energy from food assimilated into reserve E , with f the scaled functional response

and L the structural length and $\{\dot{p}_{Am}\}$ the maximum surface-area linked assimilation ($\text{J cm}^{-2} \text{d}^{-1}$). L is the cubic root of structural volume V (table 5.2). f is the ratio of actual ingestion over the maximum ingestion possible for an individual of size L , also called ingestion level. Differences in feeding across experiments and/ or individuals are quantified by differences in f . Dynamics of the four state variables (V , E , maturity E_H and cumulated energy invested in reproduction E_R) are specified in table G.1, Appendix G.

Reserve dynamics are such that weak homeostasis is respected (Kooijman, 2010, Chap.2), i.e. under constant feeding conditions reserve density $[E] = E/L$ remains constant and reserve energy $E(t)$ can be computed as:

$$E(t) = f[E_m]V(t) \quad (5.1)$$

with $[E_m] = \{\dot{p}_{Am}\}/\dot{v}$ (J cm^{-3}) maximum reserve density and \dot{v} (cm d^{-1}) reserve mobilisation (table 5.1).

A fraction κ of mobilised reserve is allocated to somatic maintenance and growth, the remaining fraction to maturity maintenance and maturation. Somatic maintenance, $\dot{p}_M = [\dot{p}_M]V$ (J d^{-1}), always takes priority over growth (dV/dt); as does maturity maintenance, $\dot{p}_J = \dot{k}_J E_H$ (J d^{-1}) over maturation dE_H/dt (J d^{-1}). The maturity maintenance coefficient \dot{k}_J and volume-linked somatic maintenance $[\dot{p}_M]$ are model parameters (table 5.1).

Transitions from one life-stage to another occur at fixed maturity levels. Four life stages are defined: embryo, juvenile (juv) I, juv II and adult. Embryo, juv II and adult all grow isomorphically (no change in shape, so surface area is proportional to volume^{2/3}), but juv I grows V1-morphically (surface area is proportional to volume). The latter gives metabolic acceleration. Birth ($E_H = E_H^b$) marks the end of the embryo phase and beginning of juv I; external assimilation is switched on and growth is V1-morphic. $f = 0$ during the embryonic stage. Implication of V1-morphy are that $\{\dot{p}_{Am}\}$ and \dot{v} increase proportional to L (see Kooijman et al., 2011, for full discussion of the concepts behind V1-morphic extensions of the model). In practice both $\{\dot{p}_{Am}\}$ and \dot{v} are multiplied by a shape correction function (Eq. (G.5), Appendix G). Metamorphosis ($E_H = E_H^j$) marks the end of juv I and beginning of juv II; adult values of $\{\dot{p}_{Am}\}$ and \dot{v} are reached and isomorphic growth ensues. Puberty ($E_H = E_H^p$) marks the onset of adulthood. E_H^b , E_H^j and E_H^p are three life stage parameters (table 5.1).

Several processes interact simultaneously in observable quantities such as growth, measured as incremental differences in physical length (L_f) and/or mass, or reproduction measured as number of eggs produced. Auxiliary theory (Kooijman et al., 2008; Lika et al., 2011a) relates observable quantities, L_f , W_d (dry mass), W_d^0 (egg dry mass), W_w (wet mass) and N (# eggs), to DEB model state variables (table 5.2). L is taken proportional to some well chosen physical length L_f such that: $L = \delta_M L_f$, with δ_M the shape coefficient.

We incorporate five modules into the zebrafish DEB model which further specify toxico-kinetics (Kooijman and van Haren, 1990) and how effects on metabolism relate to internal concentration (toxico-dynamics) (Kooijman and

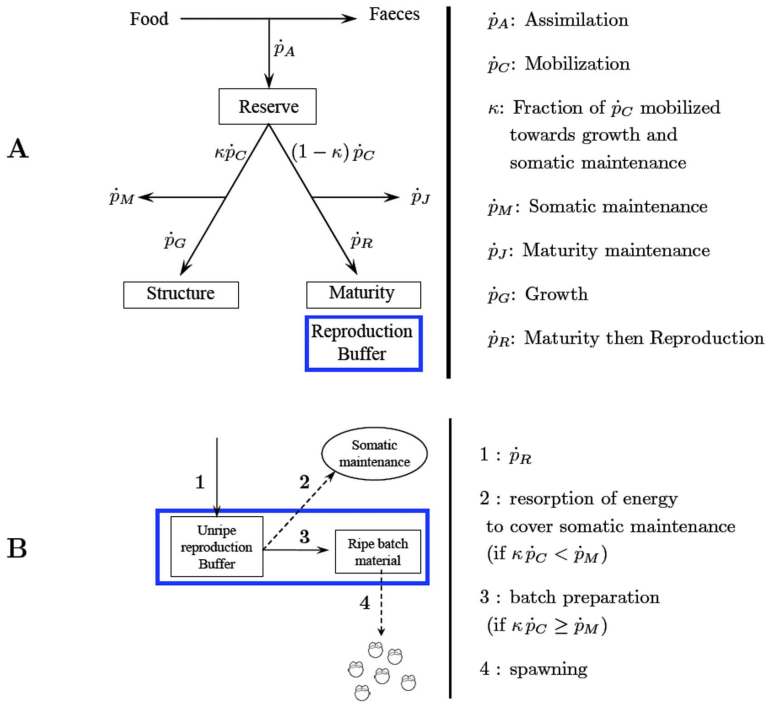


Figure 5.1: Conceptual organisation of animal metabolism as defined by DEB theory (Kooijman, 2010) and modified from Pecquerie et al. (2009). Full arrows: energy fluxes (J d^{-1}); dotted arrows: energy (J); boxes: state variables of the system; circle: energy sink. Embryo: $\dot{p}_A = 0$; birth: assimilation is switched on; puberty: allocation to maturity E_H stops and allocation to reproduction E_R starts. Energy allocated to reproduction accumulates in the reproduction buffer and is emptied at spawning. A: Overview of metabolic organisation. B: reproduction buffer handling rules.

Table 5.1: Parameters affecting state variables at reference temperature (20°C). When Adult values differ from that of embryos and early juveniles they are specified in parentheses. g: gram dry mass unless specified otherwise. See tables 5.4 and 5.3 for values of toxicity and buffer handling rule parameters used in this study.

sym- bol	definition	unit	value
<i>Toxicity parameters (this study)</i>			
k_e	elimination rate	d^{-1}	-
P_{Vd}	biomass/ environmental U partition coefficient	l cm^{-3}	-
P_{EV}	reserve/ structure partition coefficient	mol mol^{-1}	-
$[M_{Q0}^*]$	no effect internal concentration for processes *, with $* \in [G, M, A]$ (see text)	nmol cm^3	-
$[M_{QT}^*]$	tolerance concentration for processes *, with $* \in [G, M, A]$ (see text)	nmol cm^3	-
$[M_{Q0}^S]$	no effect internal concentration for survival	nmol cm^3	-
\dot{b}_\dagger	killing rate	$\text{cm}^3 \text{ nmol}^{-1} \text{ d}^{-1}$	-
\dot{h}_{acc}	hazard due to accidents	d^{-1}	-
<i>Reproduction buffer handling rules (this study)</i>			
$[E_B]$	energetic density of batch	J cm^{-3}	-
t_b	time of initiation of batch preparation	d	-
<i>Starvation</i>			
κ_G	growth conversion efficiency	-	$\frac{\bar{\mu}_V d_V}{[E_G] w_V}$
k'_J	specific maturity decay	d^{-1}	0
<i>DEB model parameters (Augustine et al., 2011a)</i>			
T_A	Arrhenius temperature	K	3000
$\{\dot{p}_{Am}\}$	maximum surface area-specific assimilation rate	$\text{J d}^{-1} \text{ cm}^{-2}$	246.3 (775.8) ^a
\dot{v}	energy conductance	cm d^{-1}	0.03 (0.09) ^a
κ	allocation fraction to soma	-	0.437
κ_R	reproduction efficiency	-	0.95
$[\dot{p}_M]$	volume-specific somatic maintenance costs	$\text{J d}^{-1} \text{ cm}^{-3}$	500.9
\dot{k}_J	maturity maintenance rate	d^{-1}	0.0166
$[E_G]$	cost of synthesis of a unit of structure	J cm^{-3}	4652
E_H^b	cum. energy invested in E_H at birth	J	0.54
E_H^j	cum. energy invested in E_H at metamorphosis	J	19.66
E_H^p	cum. energy invested in E_H at puberty	J	2062
d_V	density of structure	g cm^{-3}	0.2
$\bar{\mu}_E$	chemical potential of E	J mol^{-1}	$5.00 \cdot 10^5$
$\bar{\mu}_V$	chemical potential of V	J mol^{-1}	$5.00 \cdot 10^5$
w_E	molar weight of reserve	g mol^{-1}	23.9
w_V	molar weight of structure	g mol^{-1}	23.9
δ_M	shape coefficient	-	0.1128 (0.1325)

^a assuming $f = 1$.

Table 5.2: DEB model variables and observable quantities. Parameters used for linking observable quantities to state variables can be found in table 5.1, Appendix G. Dynamics of state variables are summed up in table G.1.

symbol	meaning	unit	equations
<i>State variables</i>			
c_d	environmental concentration of U	nM	
V	structure	cm^3	
L	structural length	cm	$V^{1/3}$
E	reserve	J	
$[E]$	reserve density	J cm^{-3}	$[E] = E/V$
E_R^0	unripe reproduction buffer	J	
E_R^1	ripe batch material	J	
E_R	reproduction buffer	J	$E_R = E_R^0 + E_R^1$
E_H	maturity	J	
$[M_Q]$	internal concentration of U	nmol cm^{-3}	
<i>How observable quantities relate to state variables</i>			
L_f	total length (snout to tip of caudal fin)	cm	$L_f = L/\delta_M$
W_d	dry mass	g	$W_d = d_V L^3 + w_E (E + E_R) / \bar{\mu}_E$
W_d^0	egg dry mass	g	$W_d^0 = w_E E_0 / \bar{\mu}_E$
W_w	wet mass	g	$W_w = 6 W_d$
$\langle M_Q \rangle_d$	concentration per unit dry mass	nmol U/g	$[M_Q]V/W_d$
$\langle M_Q \rangle_w$	concentration per unit wet mass	nmol U/g	$[M_Q]V/W_w$
N	number of eggs	#	$N = [E_B]V/E_0$

Bedaux, 1996), temperature effects on metabolic rates (Kooijman, 2010, Chap.1), the frequency of spawning events in combination with # of eggs per spawn as defined by Pecquerie et al. (2009) (reproduction buffer handling rules in fig. 5.1B) and starvation rules (Augustine et al., 2011b). The five modules are introduced in the following paragraphs. The modules do not modify the dynamics of state variables E , V , E_H or E_R (table G.1, Appendix G).

5.2.1 Temperature affects metabolic rates

Parameter values given in table 5.1 affect state variables at 20°C. We assume that the effect of temperature on all biological rates is well captured by the Arrhenius relationship (Kooijman, 2010, Eqn. 1.2 pp.17), quantified by the Arrhenius temperature T_A (table 5.1).

5.2.2 Buffer handling rules

Allocation to reproduction, \dot{p}_R is a continuous process whereby energy/mass cumulates in the reproduction buffer E_R . Spawning on the other hand, represents a discontinuous process whereby energy/mass (and U) is lost during each event. Reproduction buffer handling rules specify the dynamics of spawning and play an important role in the dynamics of total dry mass W_d . Buffer handling rules were previously specified for a multiple batch spawner of indeterminate fecundity, *Engraulis encrasicolus* (Pecquerie et al., 2009). The general idea is that E_R is partitioned into an unripe reproduction buffer E_R^0 and ripe batch material E_R^1 such that: $E_R = E_R^0 + E_R^1$ (fig. 5.1B).

We implement the same rules published in Pecquerie et al. (2009, table 1), with three subtle differences: (a) batch preparation is triggered at time $t = t_b$, (b) batch preparation stops when energy is taken from E_R^0 to cover somatic maintenance and (c) batch energetic density $[E_B]$ (J cm⁻³) remains constant. Spawning can only happen when lights go on (unique event in a day) and when $E_R^1 \geq [E_B]V$, with $[E_B]V$ the amount of energy in a spawned batch.

Allocation to reproduction cumulates in E_R^0 (fig. 5.1B). If batch preparation is initiated ($t > t_b$) energy is mobilized from E_R^0 at maximum mobilization rate for an individual of size L : \dot{p}_{Cm} (eq. (G.4), Appendix G). Energy is resorbed from the buffer to cover somatic maintenance if $\kappa\dot{p}_C < \dot{p}_M$ in which case batch preparation stops. We assumed that the reproduction overheads ($1 - \kappa_R$) are incurred during batch preparation. Dynamics of E_R^1 and E_R^0 are specified in Appendix G, table G.1. After a spawning event t_s (d) the amount of energy in the reproduction buffer is:

$$E_R(t_s + dt) = E_R(t_s) - [E_B]V(t_s) \quad (5.2)$$

The initial amount of energy in the egg E_0 (J) is calculated using the maternal effect rule: $[E]$ of the mother equals $[E]$ of the offspring (Kooijman, 2009b). Please see table 5.2 for equations linking state variables to values of observable quantities W_d , W_d^0 (egg dry mass), W_w and N .

5.2.3 Starvation

As stated previously, if the flux of mobilized reserve is too small (i.e. $\kappa\dot{p}_C < \dot{p}_M$), energy is first taken from E_R^0 to cover somatic maintenance. In this case specific growth rate \dot{r} (d^{-1}) is 0 (table G.1, Appendix G). When there is no energy left in the reproduction buffer then $\dot{r} < 0$ and energy is degraded from structure to cover \dot{p}_M with efficiency κ_G (table 5.1; Eq. (G.2), Appendix G).

Maturity maintenance \dot{p}_J also needs to be paid, and in the event that reserve mobilization is insufficient for maturity maintenance, i.e. $(1 - \kappa)\dot{p}_C < \dot{p}_J$, Augustine et al. (2011b) specified how maturity level might decay exponentially with specific decay rate \dot{k}'_J (d^{-1}). We set \dot{k}'_J to zero in this study, with the implication that no rejuvenation occurs. The penalty for not (or only partially) covering maturity maintenance comes theoretically with increased hazard (h_J d^{-1}) which would show up in the data as decreasing the survival probability because organisms become more susceptible to pathogens, bad water quality etc. We assume however that experimental conditions are favourable enough to health of individuals that such hazard is null.

5.2.4 One compartment toxico-kinetic module

We implement the simplest model formulation for specifying internal concentration: the one compartment toxico-kinetic module with time varying coefficients proposed by Kooijman and van Haren (1990); Kooijman (2010, Chap.6 pp.223-234) provides a more detailed discussion.

We make the simplified assumption that uptake is only from dissolved U in the water. In short, uptake is taken proportional to external concentration c_d (nM). Elimination \dot{k}_e (d^{-1}) is taken proportional to internal concentration $[M_Q]$ (nmol cm^{-3}) and inversely proportional to length.

Biomass is partitioned into V , E , and E_R (table 5.2). Partitioning of U in the organism is assumed to be instantaneous between reserve material ($E + E_R$) and structure V . Total mass of U in body, M_Q (nmol) has contributions from mass of U in V (M_{QV}), E (M_{QE}), and E_R (M_{QR}). Let's consider M_{ER} (mol) as the total mass of reserve material ($M_{ER} = (E + E_R)/\bar{\mu}_E$).

$$M_Q = M_{QV} \left(1 + P_{EV} \frac{M_{ER}}{M_V} \right) = M_{QV} P_{WV}$$

with $M_V = V \frac{dw_V}{w_V}$, mass of V (mol) and w_V the molar weight of V (g mol^{-1}). Kinetics of internal concentration amount to:

$$\frac{d}{dt}[M_Q] = \frac{\dot{k}_e}{l} (P_{Vd}c_d - [M_Q]P_{VW}) - [M_Q]\dot{r} \quad (5.3)$$

with P_{Vd} (1 cm^{-3}) the biomass/ environmental uranium partition coefficient, l a dimensionless scaled length measure $l = L/L_m$ ($L_m = \kappa\{\dot{p}_{Am}\}/\dot{p}_M$) and c_d the environmental concentration of U (nM). Density of U in reserve material

m_{QER} is given by

$$m_{QER} = \frac{M_Q - M_{QV}}{M_{ER}}$$

Total internalized U after a spawning event amounts to:

$$M_Q(t_S + dt) = M_Q(t_S) - \frac{m_{QER}(t_S)}{\bar{\mu}_E} [E_B] V(t_S) \quad (5.4)$$

5.2.5 Characterizing effects on survival or on metabolism

Survival probability ($S, -$) is modelled as a sum of contributing hazards:

$$\dot{h} = \dot{h}_{acc} + \dot{h}_a + \dot{h}_j + \dot{h}_q + \dot{h}_{sh}$$

and

$$\frac{dS}{dt} = -\dot{h}S \quad (5.5)$$

Contributions from ageing \dot{h}_a and from rejuvenation \dot{h}_j are neglected. As stated in [Augustine et al. \(2011b\)](#), hazard from shrinking \dot{h}_{sh} is infinite with instantaneous death when a certain shrinking threshold is crossed. This case is also not addressed in this study. Contributions from accidents \dot{h}_{acc} are estimated directly from control data ([Bourrachot et al., 2008](#)) and contributions from U \dot{h}_q are taken proportional to $[M_Q]$ such that:

$$\dot{h}_q = \dot{b}_\dagger ([M_Q] - [M_{Q0}^S])_+ \quad (5.6)$$

where \dot{b}_\dagger is the killing rate ($\text{cm}^3 \text{ nmol}^{-1} \text{ d}^{-1}$) and $[M_{Q0}^S]$ is the no effect internal concentration for survival.

Effects of uranium on measurable quantities such as growth and reproduction are assumed to occur when $[M_Q] > [M_{Q0}^*]$, with * the metabolic process targeted by uranium. As we saw previously, there are 7 metabolic processes defined in the model (fig. 5.1A). An effect on a metabolic process is captured by the modification of the model parameter associated with that process (table 5.1). In the neighbourhood of $[M_{Q0}^*]$ for process *, the intensity of effect is taken linear to $[M_Q]$ by multiplying the targeted parameter with the dimensionless stress function s :

$$s = \frac{([M_Q] - [M_{Q0}^*])_+}{[M_{QT}^*]} \quad (5.7)$$

with $[M_{QT}^*]$ the tolerance concentration for process *. In short two extra parameters are required for modelling effects on metabolism and two extra parameters for modelling effects on survival.

5.3 Materials and Methods

5.3.1 Animal maintenance

Adult fish were acquired from a commercial fish breeder (Elevage de la grande rivière, Lyon, France) and were almost a year old upon arrival.

We used the same custom made experimental system as [Augustine et al. \(2011a\)](#). Briefly, an experimental condition consists of one holding tank containing 5 aquaria. The aquaria are permeable to holding tank water (fig. [B.1](#)). There are 4 fish per aquaria (2 female and 2 male) and 20 fish (forming 10 couples) per experimental condition. There are three experimental conditions.

Each of the five aquaria in a holding tank is equipped with a water distributor. Each distributor occupies a central position above an aquaria.

We incorporated an internal recirculating pump (Hydor) inside the holding tank. Eheim hose connectors are used to link the pump to plastic hosing ensuring water arrival to each water distributor. The pump is equipped with a foam filter and continuously runs holding tank water through each individual water distributor ensuring homogeneous mixing of the holding tank water throughout each of the permeable aquaria between daily water renewal events. About 25% of holding tank water is removed daily (care is taken to remove all feces and debris at this stage) and fresh water is brought to the system. Air stones linked to air pumps and immersed thermostat resistances were used to maintain temperature and oxygen levels. Fresh water is kept in 100 or 300L reservoirs and drawn to the holding tank with an immersible pump (Hydor).

At arrival fish are acclimated to the experimental system for 28 d. During this time small groups in each aquaria are gradually thinned to 4 fish per aquaria (2 male and 2 female) in each of the 3 experimental conditions. Then follows 35 d acclimation to individual feeding and reproduction protocol which is identical to that described in [Augustine et al. \(2011a\)](#). Individuals are sometimes switched places to promote forming successful couples. After exposure, each fish remains in its position until the end of the experiment. Exposure duration is 37 d.

Animals were kept in synthetic water (see table [F.1](#), Appendix [F](#) for composition). $T = 26.2^{\circ}\text{C} \pm 0.7$, $26.3^{\circ}\text{C} \pm 0.6$ and $26.4^{\circ}\text{C} \pm 0.7$ (mean \pm sd) in each respective condition over the entire acclimation and exposure duration; $\text{pH} = 6.5 \pm 0.1$ (mean \pm sd) in all three conditions over the entire acclimation and exposure duration; electrical conductivity was 191 ± 8 , 192 ± 8 and $193 \pm 8 \mu\text{S cm}^{-1}$ (mean \pm sd) in U-0, U-84 and U-420 respectively over the entire acclimation period and was not measured during exposure.

NO_2^- was monitored daily for the first 18d of acclimation and was subsequently monitored about thrice weekly. NO_2^- concentration, 0.08 ± 0.05 (mean \pm sd), never exceeded 0.2 mg l^{-1} ; this is acceptable with regards to zebrafish health ([Lawrence, 2007](#)).

Fish were individually fed *Ad libitum* Tetramin™ granules (see Appendix [B](#) for details). Granules were dispensed in small amounts to each individual

2-3 times daily. Granules were dispensed slowly to limit contact of food with (contaminated) water. Water renewal always took place after morning feeding. Weekly supplements of spirulina and/or live *Daphnia magna* were given.

5.3.2 Experimental conditions

Fish were exposed to three different concentrations of depleted uranium: 0, 84 and 420 nM. Each exposure condition which hereafter will be referred to as U-0, U-84 and U-420. Water in reservoirs for daily water renewal for each respective condition were maintained at nominal c_d .

To compensate for daily absorption of U (by experimental system, biofilms, algae or faeces) exposure media was continuously adjusted with uranium from a concentrated stock solution prepared in 1L glass bottles. The solution was released drop by drop into exposure media close to the internal recirculating pump (and away from individual aquaria) via capillaries and debit was regulated to approximately 0.04 l h^{-1} . The stock solution was prepared on the onset of each day according to U absorption by the experimental system assessed the previous day. Thus after a week the exposure concentration was stabilized to nominal concentration of 84 and 420 nM U (fig. F.1, Appendix F) in each respective condition.

During acclimation the pH remained stable. During exposure pH was monitored continuously by pH regulators (Consort R301, Illkirch, Belgium) linked to a pH electrode and a peristaltic pump. This was carried out to avoid variations in pH in response to addition of U to water. The regulator switched on the peristaltic pump in the event the electrode recorded a pH below 6.4. The peristaltic pump transported NaOH 10^{-1}M to exposure media several cm away from the pH electrode and away from aquaria. Electrodes were verified once daily by immersion into 2 buffer solutions (pH = 4, pH = 7, VWR). pH was further measured on separate electrodes (VWR) which were calibrated every 3 days to test for consistency of measurements between both types of electrodes. After the first few days of exposure the regulator was rarely used and pH was stable even considering the continuous addition of U to the system via the capillaries.

5.3.3 Water sample analysis

Water samples were collected 2-3 times daily during the acclimation and exposure periods. Major anion concentrations were analysed by ionic chromatography (Dionex DX- 120, Sunnyvale, CA, USA). Major cation and uranium concentrations were measured after 2% (v/v) HNO_3 acidification by means of inductively coupled plasma-atomic emission spectrometry (ICP-AES; Optima 4300DV, Perkin-Elmer, Wellesley, MA, USA). Uranium detection limit is 42 nM.

5.3.4 Biometry

Dorsal and lateral portraits of each individual were taken weekly (Nikon D3000) to assess visible signs of strain. Furthermore, each individual has a distinct pattern of stripes used to confirm individual identity of each female at the end of the experiment.

Reproduction was assessed by forming couples (1:1 male to female ratio) in the evening and counting the number of eggs spawned the following morning. The same couples were maintained during the 37d exposure. Egg output N of each individual was assessed on a daily basis.

At the end of the experiment fish were sacrificed, weighed and measured with a ruler from tip of to snout to base of caudal fin (standard length). Two females in the control condition were not weighed (females 3 and 4 in fig. 5.3). We provide estimates for their final wet mass as: $W_w \approx W_1(L_{f1}/L_f)^3$, with L_f observed final length of female 3 or 4 and W_1 and L_{f1} the observed wet mass and final length of female 1.

Final $\langle M_Q \rangle_d$ was determined for a random sub sample of 10 individuals in the 84 and 420 nM conditions in addition to 5 random control individuals.

After each spawn, eggs were rinsed in clean medium and placed in petri dishes and photographed (Nikon D3000) from above on a macro bench (VWR). Eggs were subsequently counted manually on photos (using Adobe® Photoshop® CS4 11.0 and ImageJ 1.43u). Live and dead eggs were recorded.

3 samples of 10 live eggs were placed in 3 (pre-weighed) aluminium capsules (VWR 13 x 5 mm width x height). Capsules were dried at 60°C for a minimum of 48 h then weighed on an ultra micro balance (Sartorius SE2, Göttingen, Germany). The samples were kept in an airtight plastic chamber over desiccated silica crystals after removal from 60°C oven and before weighing.

Adult fish were dried for 6 d at 60°C. Whole body dry tissue was placed in a small glass beaker and digested in 8 ml of 65% HNO₃ (Sigma Aldrich). Samples were evaporated to incipient dryness on a sand tray at 120-150°C. The digestion process was followed by a 2 ml H₂O₂ attack and evaporation to incipient dryness followed by a 2 ml 65% HNO₃ digestion and evaporation to incipient dryness. These last two steps were repeated three times. Digested mineral residues were suspended in 5 ml of 2% HNO₃ (v/v) acidified ultrapure water for ICP-AES analyses.

5.3.5 Other data and parameter estimation

In addition to the 37 d exposure described above, data from 4 additional studies were also analysed with the DEB model. Exposure conditions were similar across all experiments (table F.1, Appendix F).

DEB model parameters for zebrafish were already obtained in Augustine et al. (2011a) (table 5.1) using the covariation method (Lika et al., 2011a,b). We made two minor adjustments to parameter values: the specific density of structure $d_V = 0.2$ instead of 0.15 g cm⁻³ and reserve's chemical potential $\bar{\mu}_E =$

$5.00 \cdot 10^5 \text{ J mol}^{-1}$ instead of $5.55 \cdot 10^5$. We updated the parameter estimation files provided in [Augustine et al. \(2011a\)](#) with these values and the overall fit is slightly better with a growth conversion efficiency $\kappa_G = 0.9$ (table 5.1) instead of 0.7. Primary energy parameters and parameters linking energy to volume or mass are herein treated as given.

For simplicities sake, concentration of U in the water $c_d(t)$ is taken constant and equal to nominal exposure concentration for each experiment.

Fitting the model to individual data for each female

We perform the comparative analysis of data from [Bourrachot \(2009\)](#) and from our 37 d reproduction trial.

The three exposure conditions in [Bourrachot \(2009\)](#) will hereafter be referred to as: 15d-U0 for controls ($n = 7$), 15d-U84 for individuals exposed to 84 nM ($n=8$) and 15d-U1054 for individuals exposed to 1054 nM ($n=7$). Each individual was first exposed to 0, 84 or 1054 nM U for 20 d and then placed in clean water for 15 d. During exposure both sexes were separated. During depuration individuals were set up as triplets (1:2 female:male sex ratio), allowed to reproduce and daily N was recorded for each individual female.

Alternatively, the three exposure conditions in the reproduction trials presented in this study will hereafter be referred to as: 37d-U0 for controls ($n = 10$), 37d-U84 for individuals exposed to 84 nM U ($n=10$) and 37d-U420 for individuals exposed to 420 nM U ($n=10$).

The DEB model is fit to observed N (sum of live and dead eggs) and final W_w for each female in both experiments by adjusting f and initial conditions only (table 5.3).

We also fit predicted W_d^0 to that observed for each individual female in the 37d trial using the maternal effect rule.

In the 15d experiment we found that t_b was a free parameter, while in the 37d experiment we assumed that $t > t_b$ on the basis that couples were already formed during 35 d preceding exposure. For the 15 d trial we assumed that energy cumulated in E_R during the first 20d and spawning was only allowed to be triggered during depuration.

Batch energetic density $[E_B]$ was found to vary between females and consequently was estimated for each one. To remove a parameter we computed initial amount of structure as 0.94 the final amount of structure, assuming negligible growth during each experiments. Thus $L(0) = 0.94 \delta_M L_f$. For comparison purposes between experiments we assumed 20% difference between standard and total length and expressed all lengths as total length (fig. 5.2).

Toxicity parameters P_{Vd} , P_{EV} and \dot{k}_e are estimated for all of the females in both experiments. W_w was computed for each female with and without the buffer handling rules. With buffer handling rules wet mass after spawning amounts to:

$$W_w(t_S + dt) = W_w(t_S) - 6 \frac{w_E}{\mu_E} [E_B] V(t_S) \quad (5.8)$$

Table 5.3: Initial conditions for each female in the 37d (this study) and in the 15d (Bourrachot, 2009) reproduction trials. $L(0)$: Initial structure (cm); $[E_B]$ (J cm^{-3}): batch energy density; $E_R(0)$ (J): initial amount of reproduction buffer material; t_b day of experiment batch preparation is triggered during the 20d accumulation phase which preceded the 15d reproduction trial. We assume that $E_R(0)$ comprises only unripe buffer material. n.a.: not applicable.

Repli- cate	This study (37 d trial)			Bourrachot (2009) (14 d trial)			
	f (-)	$[E_B]$ (J cm^{-3})	$E_R(0)$ (J)	f (-)	$[E_B]$ (J cm^{-3})	$E_R(0)$ (J)	t_b (d)
Control:							
1	0.76	3000	450	0.65	1200	0	13
2	0.60	3000	718	0.72	1000	0	20
3	0.75	3000	700	0.70	1000	0	15
4	0.80	3000	700	0.66	1400	0	20
5	0.94	8000	300	0.78	1500	100	0
6	0.60	3000	745	0.73	1580	0	19
7	0.66	3000	744	0.67	1800	400	0
8	0.54	3000	734	n.a.	n.a.	n.a.	n.a.
9	0.54	3000	736	n.a.	n.a.	n.a.	n.a.
10	0.64	3000	713	n.a.	n.a.	n.a.	n.a.
84 nM:							
1	0.77	7000	350	0.71	2000	413	0
2	0.82	1734	1000	0.63	1000	0	20
3	0.82	1734	200	0.78	1000	50	0
4	0.75	7000	350	0.70	1000	0	20
5	0.77	3000	80	0.68	1000	0	20
6	0.82	2200	100	0.67	1000	0	20
7	0.82	2000	500	0.73	1446	0	7
8	0.69	3000	50	0.72	1446	0	20
9	0.80	3000	200	n.a.	n.a.	n.a.	n.a.
10	0.88	2000	600	n.a.	n.a.	n.a.	n.a.
420 (37d) and 1054 (15d) nM:							
1	0.85	3000	1000	0.75	1000	0	20
2	0.79	3000	350	0.76	1000	450	0
3	0.85	1000	1800	0.76	1000	150	0
4	0.84	1200	900	0.75	1000	150	20
5	0.82	3000	350	0.74	1000	450	0
6	0.73	3000	350	0.76	1000	0	20
7	0.82	1000	350	0.73	1000	0	20
8	0.81	3000	350	n.a.	n.a.	n.a.	n.a.
9	0.76	3000	350	n.a.	n.a.	n.a.	n.a.
10	0.81	3000	350	n.a.	n.a.	n.a.	n.a.

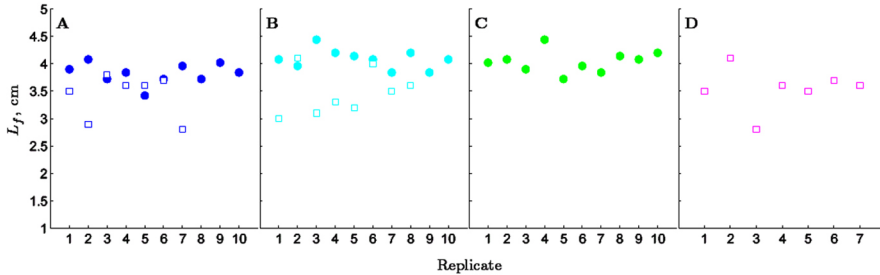


Figure 5.2: Final observed length for each female in 37d (full circles) and 15d (square) reproduction trials. A: control; B: $c_d = 84$ nM; C: $c_d = 420$ nM; D: $c_d = 1054$ nM, with c_d the nominal concentration of depleted uranium in holding tank water (nM); see fig. F.1, Appendix F for measured values. x-axis: replicate number with e.g. 1 designating female 1. y-axis: total length L_f (snout to end of caudal fin) cm. The initial amount of structure for each replicate was computed as: $L(0) = 0.94 \delta_M L_f$ (see text). Please note, females in the 15d trial were on average smaller.

and without the buffer handling rules, considering the observed amount of eggs spawned N_{obs} :

$$W_w(t_S + dt) = W_w(t_S) - 6 N_{\text{obs}} W_d^0 \quad (5.9)$$

The computation of wet mass in Eq. (5.9) serves as a constraint for value of initial amount of reserve material for a given combination of f and $L(0)$.

15 day embryo and early juvenile experiments

We assume $E_0 = 1.7\text{J}$ (calculated with maternal effect rule taking $f = 1$ for the mother). Bourrachot et al. (2008) presents data from 0 to 15 d and the authors started feeding early juveniles on day 9; control mortality also increases after 9 d. The increase in control mortality in combination with low control W_d indicate that food is hardly eaten and suggests a water quality problem. For this reason we restrict analysis to the first 9 d where no extra organic material (liquid food) was added to the system. Nonetheless, f is freely estimated after birth; the slight increase in mean control W_d suggest some assimilation took place. δ_M was shown to increase during the early juvenile period with ontogeny of caudal fin (Augustine et al., 2011a), but such 'details' are here neglected. We calibrate an overall embryo δ_M to L_f at 9 d (table 5.1).

20 d adult accumulation experiments

We calibrated initial conditions to initial observed mean W_w in each condition in Barillet et al. (2005) and to initial observed mean W_w and L_f in Barillet

et al. (2011). Assuming $E_R^1(0) = 0$, then there are three free parameters for each condition in Barillet et al. (2005): f , $E_R^0(0)$ and $L(0)$ and only two free parameters for the condition in Barillet et al. (2011): f and $E_R^0(0)$. Nominal c_d for each condition in both studies are provided in table F.1, Appendix F. At each sampling time 10 random individuals were sampled and biometry and $\langle M_Q \rangle_w$ was recorded. In the study by Barillet et al. (2005) fish of both sexes were sampled, while in the study by Barillet et al. (2011) only males were sampled. We consider that males and females both possess the same model parameters (table 5.1).

Estimation procedures

The general strategy was to first fit the control model to all of the data sets to first determine that controls were correctly described and second confirm that the control model could not adequately describe the toxicity data. The second phase was to determine toxico-kinetic parameters and test which metabolic process (*) was most likely impacted.

We performed a sensitivity analysis (not shown) on the control model to ascertain what combination of effects on measurable quantities are obtained through which parameter modification. Thus we qualitatively assessed the three most likely metabolic processes (*) targeted by uranium: (G) uranium may be increasing cost of synthesis of a unit of structure: $[E_G^s] = [E_G](1 + s)$, (M) uranium might be increasing volume-linked somatic maintenance $[p_M^s] = [p_M](1 + s)$ and (A) uranium may be decreasing surface-area linked assimilation $\{p_{Am}^s\} = \{p_{Am}\}(1 - s)$.

We fit the model three times to toxicity data; first assuming mode of action G , then mode of action M and finally mode of action A .

All computations were performed with Matlab (R2010b, Mathworks®). Parameters for modelling survival were estimated using the regression method (Kooijman, 1981). The simplex (Nelder-Mead) method was used to simultaneously minimise the weighted sum of squared deviations between model predictions and observations for all of the other data sets (Lika et al., 2011a). Parameter estimates were performed using freely downloadable software DEBtool (<http://www.bio.vu.nl/thb/deb/>). E_0 was computed using DEBtool routine `initial_scaled_reserve` (for details on computation see Kooijman, 2010, pp.54-66).

5.4 Results

A rapid synthesis of the five studies teaches that effects are (somehow) related to internalized U and two different types of organism level effects were observed when comparing the early life stages to adults: an effect on growth and survival for the first and an effect on reproduction attributed to modified behaviour for the latter. Parameters provided in Augustine et al. (2011a) are in line with all

of the control data of the 5 studies when (i) taking differences in feeding into account and (ii) using appropriate initial conditions.

Bourrachot (2009) concluded that the decrease in N stemmed from a reduction in number of spawning events per female and suggested that this may be a consequence of U induced impairment of sensory organs. Ovulation is in fact stimulated in female zebrafish though pheromones liberated by the partner and may be further influenced through female dominance structures, mate preference and spawning substrate (Gerlach, 2006; Spence et al., 2008). The purpose of our 37 d exposure experiment where daily N was measured was to test this particular hypothesis. Surprisingly, we obtained conflicting results with the previous reproduction experiment. Whereas 20 d accumulation (without reproduction) to 84 nM followed by 15 d depuration with reproduction showed strong impacts on mean cumulated N (Bourrachot, 2009), our 37 d accumulation to 84 nM U with reproduction did not. However, the same decrease in N stemming from drastic reduction in inter-spawning events was observed at 420 nM U as for the 1054 nM U condition in Bourrachot (2009). Absence of effects on adult growth and inexplicable variability in bioaccumulation in all of the experiments were also observed.

In the following sections we present results of fitting the control model to controls from both reproduction trials (15 d and 37 d). We then present results of fitting the control model to exposed females from both trials. We continue by explaining how effects on exposed females are captured by the perturbation of a specific physiological process. The last two sections compare model predictions with observations of adult whole body residues and embryo and early juvenile growth, bioaccumulation and survival.

5.4.1 Control Reproduction trials

At first, we assumed that even if some energy is taken from E_R to cover somatic maintenance, batch preparation continues until E_R is emptied. This does not fit the observations from both reproduction trials. The control data empirically support that batch preparation stops when not enough energy is mobilized from reserve to cover somatic maintenance. Predicted cumulated number of eggs and final wet mass for control females are presented in fig. 5.3. We plot predicted wet mass with and without buffer handling rules (Eq. (5.8) and (5.9)). We consider that fits are good when absence or presence of spawning is accurately depicted and predicted values of eggs per spawn is close to that observed. Predicted cumulated number of eggs is in line with observations for females 1,3, 4, 5, 8, 9 and 10 respectively. The spawning behaviour of females 2, 6 and 7 seems to escape buffer handling rules, but predicted final mass without buffer rules is in line with that observed.

The mean of each prediction for cumulated number of eggs spawned is compared with the mean of that observed for 15d-U0, 15d-U84 and 15d-U1054 (fig. 5.4A). Final predicted wet mass is compared with that observed for all three conditions (fig. 5.4B). Predictions for each replicate in all three conditions

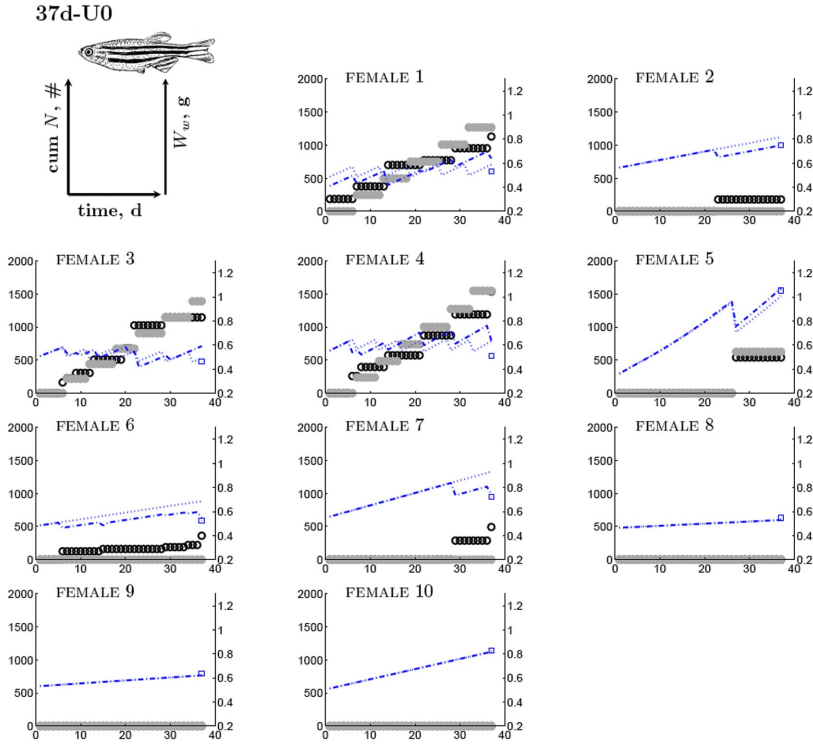


Figure 5.3: DEB Model predictions and observations for each control females in the 37d reproduction trial. Left y-axis: empty circles (black) represent observed cumulated (cum) number N of eggs spawned ($\#$) and full circles (grey) represent model predictions. Right y-axis: dotted (blue) line: predicted wet mass W_w (mg) computed with buffer handling rules, Eq. (5.8). Dot-dashed (blue) line: predicted W_w computed without buffer handling rules, Eq. (5.9). Square symbol (blue): final observed W_w . Final observed W_w was not measured for females 3 and 4. We provide estimates for their final wet mass as: $W_w \approx W_1(L_{f1}/L_f)^3$, with L_f observe final length of female 3 (or 4) and W_1 and L_{f1} the observed final wet mass and final length of female 1.

can be found in fig. I.1, I.2 and I.3, Appendix I.

f , $[E_B]$ and initial E_R were found to differ between females (table 5.3). $[E_B]$ seemed to be in the range of $1000 - 3000 \text{ J cm}^{-3}$ with some exceptions (e.g. female 5 in 37d-U0). All of the control females spawned in 15d-U0, whereas 3 did not in 37d-U0. Furthermore females 2, 6 and 7 (37d-U0) kept most of the cumulated energy invested in reproduction inside the body.

Total wet mass is partitioned into three types of material: E , E_R and V (table 5.2). The observed length gives an estimate for mass of V , but the assumption of constant food and an estimate of ingestion level f are needed to quantify relative contributions of E and E_R to total biomass. Without observed initial W_w the values of f and $E_R(0)$ are not accurately fixed, especially if there is no spawning, since there is no handle on f . In this case several local minimums may exist in the parameter space comprising initial conditions and $[E_B]$. However, by computing W_w without buffer handling rules we introduce a constraint on the lower boundary of initial E_R for a given value of f . In the event the individual spawned, then f also conditions the slope of cumulated N in the 37d trial. On the contrary, f hardly conditions the slope of N in the 15d trial. Indeed, the slope of cumulated N in the 15d trial is conditioned by how much energy is in E_R at the onset of the trial and more specifically how much of that energy is ripe batch material.

At first, we assumed $t > t_b$ at the onset of both reproduction trials, on the basis that the presence of a male stimulates ovulation in females. This assumption does not hold for the 15d trial. Actually, considering a batch energy density of about $1000\text{-}2000 \text{ J cm}^{-3}$, 5 females out of 7 must already have had ripe batch material at the onset of the 15d trial (table 5.3). Predicted mean dry mass of an egg in each spawn, for each female in 37d-U0, are compared with the observed values (fig. 5.5). The results cannot prove that the maternal effect is accurate, but do strongly support linking zebrafish egg mass to maternal condition quantified by $[E]$. Assuming the maternal effect, then $[E]$ of female 4 seems to be underestimated. We estimated an f of 0.94 for female 5, but observed W_d^0 was still higher than predicted.

Three (37d trial) or four parameters (15d trial) are needed to specify initial conditions and buffer handling for a female (table 5.3). This makes one parameter per curve for the 37d trial considering the three types of observations N , W_w and W_d^0 and 2 parameters per curve for the 15d trial considering the two observations N and W_w . Lastly, predicted reproductive output in the 37d experiment is less sensitive to initial value of E_R than the 15d trial. In the latter case the entire curve is conditioned by the amount ripe batch material available the first day of the trial.

Females in the 37d trial were on average longer than females in the 15d trial (fig. 5.2). The implication is that females in the 37d trial have on average higher V than in the 15d trial. The DEB model takes somatic maintenance proportional to V , so the average minimum ingestion level for which somatic maintenance is covered is higher in the 37d trial relative to the 15d trial.

We assumed a constant $[E_B]$ for each female, but in practice $[E_B]$ might be

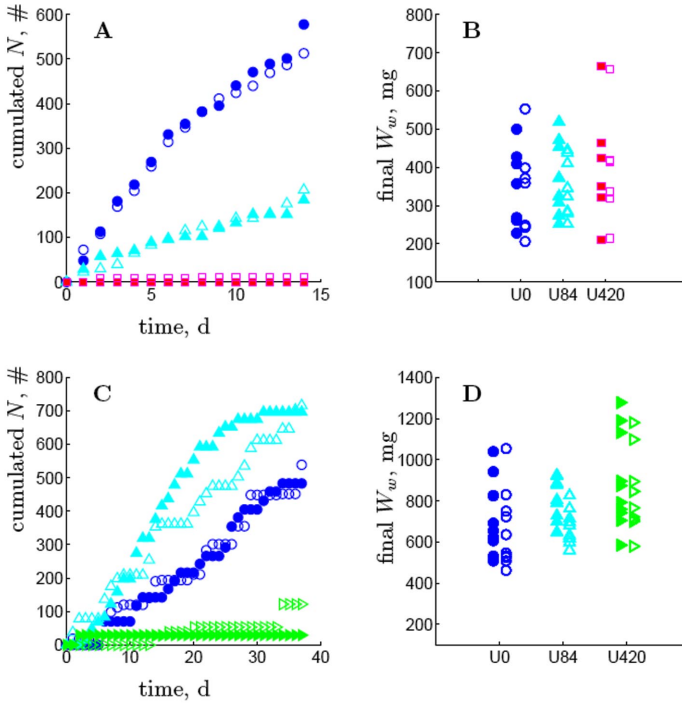


Figure 5.4: Full symbols: model predictions; empty symbols: observations; circles: controls; upwards triangles: exposed to 84 nM; sideways triangles: exposed to 420 nM; squares: exposed to 1054 nM. (A) mean cumulated number of eggs (N) spawned for 15d trial. (B) Final observed and predicted wet mass W_w , mg for each individual in the 15d trial. Model fits for each individual in the 15d trial can be found in Appendix I. (C) mean cumulated N spawned during the 37d trial. (D) Final observed and predicted wet mass W_w , mg for each individual in the 37d trial. Model fits for each individual in the 37d trial can be found in fig. 5.3, 5.6 and 5.7.

variable. Both reproduction trials sported very different protocols for evaluating reproductive output. The 15d trial maintained both sexes in separate tanks for 20d before placing each individual female with two male partners in small spawning chambers and in the 37d trial couples were already formed 35d before the onset of the experiment. By incorporating experiment design, the model captures the pattern where cumulated number of eggs spawned rises steeply then saturates in the 15d trial (fig. 5.4A) and alternatively where it rises with an approximately constant slope for females in the 37d trial (fig. 5.4C).

5.4.2 Fitting the control model to exposed females

The control model was fit to each exposed female in order to detect if the model for baseline metabolism could explain the observations simply on the basis of physiological differences in initial E_R and/or feeding.

The result is, certain exposed females indeed present quantitative energetic differences from predictions for baseline metabolism. There is a discrepancy between model predictions for cumulative reproductive investment relative to actual (indirectly) observed cumulative reproductive investment. This was clearly the case for three females in the 15d-U84 condition (not shown) and in all but one reproducing female in the 37d-U84 condition (fig. H.1, Appendix H). Incidentally, degrees of freedom for parameter estimation are higher in the 15d experiment than in the 37d experiment.

Initial slope of cumulated number of eggs spawned for females 2,3,6,7 and 10 in 37d-U84 are suggestive of an f of at least 0.8 (see estimated values in table H.1). The observed dry mass of an egg for females 2,3, 6 and 7 (fig. 5.5) are also supportive of a high $[E]$. When fitting the control model to 37d-U84 data we found that the wet mass computed with buffer handling rules Eq. (5.8) and predicted cumulated number of eggs spawned matched observations for the above mentioned females (fig. H.1, Appendix H). Predictions deviated from observations around 20d for e.g. females 2, 3, 6 and 7 as does the wet mass computed without the buffer handling rules Eq. (5.9). This illustrates that less material is actually in the reproduction buffer than predicted for these females. The control model predictions are in harmony with observations for female 10.

The absence of spawning in the 37d-U420 and 15d-U1054 conditions could be explained by a reduced f in most instances (not shown).

The 37d-U84 data sets provided the most convincing evidence of uranium-induced metabolic deviations, because of the varying degrees of deviations between real and predicted wet mass and cumulated number of eggs spawned for a large number of females.

5.4.3 Mode of action of uranium on females in reproduction trials

The three modes of action (G), (M) and (A) were tested to determine which one best captures uranium induced effects on female cumulated reproductive

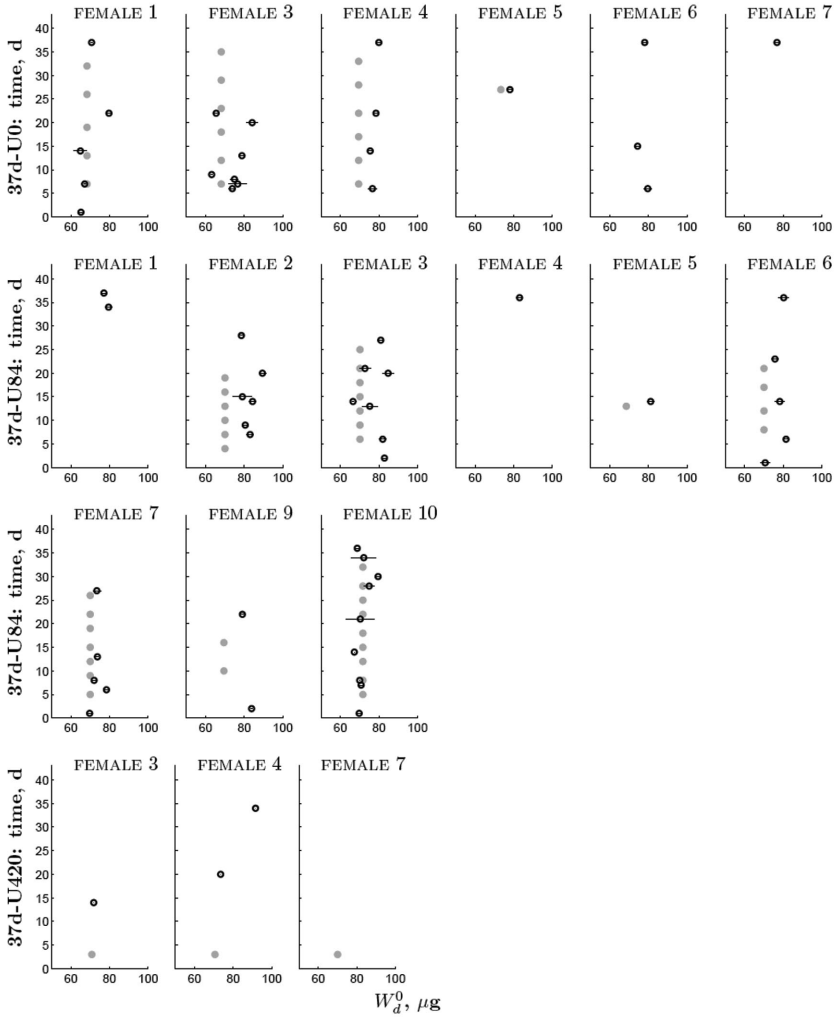


Figure 5.5: Egg dry mass W_d^0 (μg) of a live egg for each spawn of various females in the 37 d reproduction trial. First row: controls; second and third row: U-84; fourth row: U-420. Empty (black) circles: observed mean W_d^0 ; bars: standard deviation (n=3, see text for protocol). Full (grey) circles: predicted W_d^0 considering the maternal effect rule. Predicted W_d^0 is constant because f is constant and thus $[E]$ is constant (weak homeostasis see text).

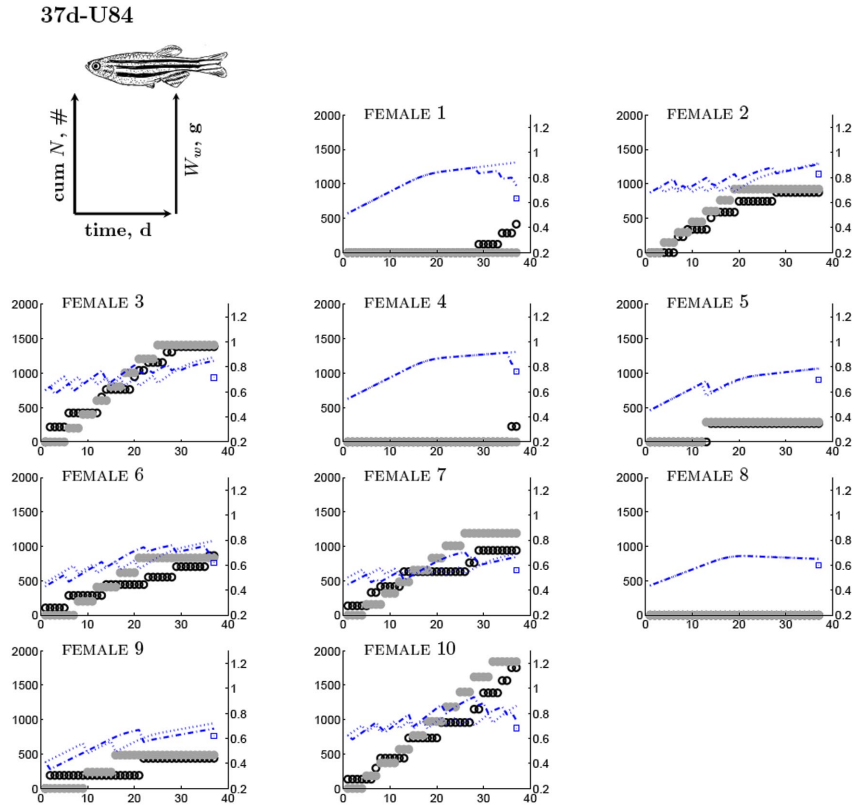


Figure 5.6: DEB Model predictions and observations for each female exposed to 84 nM for 37d assuming that uranium increases volume-linked somatic maintenance. Left y-axis: empty circles (black) represent observed cumulated (cum) number N of eggs spawned (#) and full circles (grey) represent model predictions. Right y-axis: dotted (blue) line: predicted wet mass W_w (mg) computed with buffer handling rules, Eq. (5.8). Dot-dashed (blue) line: predicted W_w computed without buffer handling rules, Eq. (5.9). Square symbol (blue): final observed W_w .

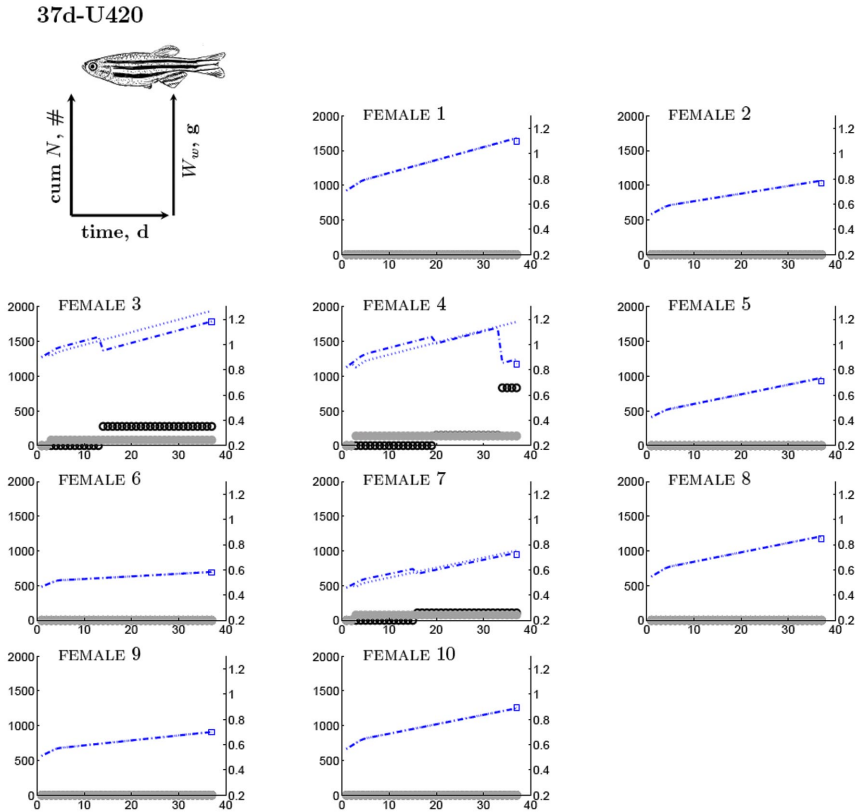


Figure 5.7: DEB Model predictions and observations for each female exposed to 420 nM for 37d assuming that uranium increases volume-linked somatic maintenance.. Left y-axis: empty circles (black) represent observed cumulated (cum) number N of eggs spawned (#) and full circles (grey) represent model predictions. Right y-axis: dotted (blue) line: predicted wet mass W_w (mg) computed with buffer handling rules, Eq. (5.8). Dot-dashed (blue) line: predicted W_w computed without buffer handling rules, Eq. (5.9). Square symbol (blue): final observed W_w .

investment at low concentrations.

As stated before, growth is negligible for females in the 37d trial and most likely negligible for a number of females in the 15d trial. We simulated effects of increasing $[E_G]$ considering experimental conditions of both reproduction trials and found that cumulated reproductive investment would hardly be impacted considering individuals of the size used and experiment duration (fig. H.3, Appendix H). Thus, mode of action (G) cannot explain the observations.

Since, decreasing f seemed to increase goodness of fit for all exposure conditions (when using only the control model), then mode of action (A) is a likely candidate to explain effects. Ingestion level can be high, but by decreasing surface area-linked assimilation it is possible to emulate a decline in the slope of reproductive output due to reduced reserve mobilization. Finally, energy assimilated in reserve would no longer suffice to cover somatic maintenance and reproduction would be inhibited. We fit the model considering mode of action (A) to the various females. In doing so, the decrease in N was captured but final predicted W_w still overshoot observed W_w for the females in the 37d-U84 condition.

Mode of action (M) assumes an increase in volume-linked somatic maintenance costs. In this scenario, ingestion level can remain high as does reserve mobilisation. Spawning is brusquely inhibited when somatic maintenance is so high that $\kappa\dot{p}_C$ no longer suffices to pay it and energy is resorbed from the reproduction buffer. Since the amount of metabolic work associated with somatic maintenance is so high, a large amount of reproduction buffer material is burned to cover it. Mode of action (M) most satisfactorily captured final mass and observed cumulated N for females in the 37d-U84 condition (fig. 5.6).

In the absence of further information we assumed mode of action (M). Individual model predictions for cumulated number of eggs spawned and final wet mass for 37d-U84 and 37d-U420 are presented in fig. 5.6-5.7. The mean of all the model predictions for the 15d trial are compared to mean observed cumulated number of eggs spawned in fig. 5.4A.

We further plot mean observed cumulated number of eggs against the mean of the predictions for 37d-U0, 37d-U84 and 37d-U420 respectively (fig. 5.4C). The individual model fits (fig. 5.6) look better graphically than the mean of the predictions for 37d-U84 because the model assumes batch preparation stops immediately when energy is resorbed from E_R to cover $[\dot{p}_M]V$ and that $[E_B]$ remains constant.

If we had plotted observed mean cumulated number of eggs spawned with say standard deviations, the plot would be unreadable. We displayed both representations: individual females and means to illustrate that we are not comparing number of eggs produced, but indirectly quantifying cumulative energy investment in reproduction for each individual female. The latter depends on surface area (length) and feeding (f) and is much less variable between females than spawning behaviour.

Finally, we draw attention to the higher mean reproductive output in the 37d-U84 condition relative to controls (fig. 5.4C). This is explained by the

higher ingestion levels in the 37d-U84 (mean $f = 0.79 \pm 0.05$ sd) condition relative to controls (mean $f = 0.68 \pm 0.13$ sd). The mean ingestion level in 37d-U420 was 0.81 ± 0.04 sd.

The value of the partition coefficient P_{EV} in combination with $[E_B]$ regulates how much and at what frequency U is eliminated through reproduction. As such, both parameters modulate dynamics of $[M_Q]$ relative to spawning behaviour. Within this modelling framework, spawning patterns manifested by the 10 females in 37d-U84 are captured by different kinetics of effects with female 8 and female 10 at two extremities of the effect spectrum. The more the female spawns, the more she eliminates and so the longer she stays beneath the no effect internal concentration. Female 10 for example spawned regularly all the way to the end while females 1,4 and 8 did not. In the first three cases the longer the inter-spawning interval the more intense is the increase in somatic maintenance. Females 1 and 4 did spawn towards the end of exposure, hampering firm conclusions.

Predictions using the control model match model predictions considering mode of action (M) for female 10 for (a) certain value(s) of P_{EV} . This is the reason why the simultaneous analysis of all the females in the 37d-U84 condition also allows us to fix the value of P_{EV} for a certain combination of $[M_{Q0}^*]$, $[M_{QT}^*]$, $[E_B]$.

The values of toxicity parameters used to obtain the fits provided for each of the exposed females in this study can be found in table 5.4.

The broad patterns in toxicity were captured assuming a no internal effect concentration for $[\dot{p}_M]$ $[M_{Q0}^M]$ of 32 nmol cm^{-3} and a tolerance concentration $[M_{QT}^M]$ of $28.9 \text{ nmol cm}^{-3}$. P_{EV} is $13.1 \text{ mol mol}^{-1}$. The biomass/ water partition coefficient for uranium was determined to be 19.1 l cm^{-3} and elimination rate k_e to be 0.003 d^{-1} (table 5.4). This entails that the No Effect Concentration (NEC) of uranium in the exposure media is $[M_{Q0}^M]/P_{Vd} \approx 1.7 \text{ nmol l}^{-1}$.

If $[\dot{p}_M]$ continues to increase linearly to internal concentration even beyond $[M_{Q0}^M]$, then the individuals in the 37d-U420 and 15d-1054 as well as in the higher exposure conditions by Barillet et al. (2005, 2011) would have shrunk to death during the experiment. This is manifestly not the case. Portraits of all of the individuals at the end of the experiment (not shown) corroborate this. In the absence of further information (and to avoid numerical errors) we set a maximum value to $[\dot{p}_M]$ equal to $1000 \text{ J cm}^{-3} \text{ d}^{-1}$.

5.4.4 Adult whole body residues

Of the 10 random individuals sampled for measuring final $\langle M_Q \rangle_d$ in each conditions, only four were females. Predicted $\langle M_Q \rangle_d$ are compared to that observed for four individual females in conditions 37d-U84 and 37d-U420 (fig. 5.8).

Bourrachot (2009) presents mean $\langle M_Q \rangle_d$ at onset and end of the 15d trial. There is some uncertainty in the interpretation of these $\langle M_Q \rangle_d$ measurements. The data are presented as concentrations in gonad and whole body excluding

Table 5.4: Toxicity parameters and initial conditions used for modelling all of the data sets in this study. For the reproduction trials initial structural length $L(0)$ was computed for each female according to her final observe length; initial amount of energy in the reproduction buffer $E_R(0)$ was also estimated for each female. In this case we set '-' in the fields of $E_R(0)$ and $L(0)$ and refer the reader to table 5.3 for the values for each individual. $E(0)$ is computed according to Eq. (5.1). U-84, U-420 and U-2100 refer to three exposure conditions in Barillet et al. (2005). Survival parameters are non applicable (n.a.) to adult data sets. Parameter definition and units are specified in table 5.1.

parameter	this study	Bourrachot (2009)	Barillet et al. (2005)			Barillet et al. (2011)	Bourrachot et al. (2008)
			U-84	U-420	U-2100		
k_e	0.003	0.003	0.003	0.003	0.003	0.003	0.003
P_{Vd}	19.1	19.1	19.1	19.1	19.1	19.1	0.005
P_{EV}	13.1	13.1	13.1	13.1	13.1	13.1	13.1
P_{EV}	13.1	13.1	13.1	13.1	13.1	13.1	13.1
$[M_{Q0}^M]$	32	32	32	32	32	32	32
$[M_{QT}^M]$	28.9	28.9	28.9	28.9	28.9	28.9	28.9
$[M_{Q0}^G]$	0	0	0	0	0	0	0
$[M_{QT}^G]$	0.211	0.211	0.211	0.211	0.211	0.211	0.211
$[M_{Q0}^S]$	n.a.	n.a.	n.a.	n.a.	n.a.	n.a.	0
b_{\dagger}	n.a.	n.a.	n.a.	n.a.	n.a.	n.a.	0.375
h_{acc}	n.a.	n.a.	n.a.	n.a.	n.a.	n.a.	0.02
f	-	-	0.7	0.85	0.85	0.7	0.3
$L(0)$	-	-	0.383	0.383	0.383	0.451	0
$E_R(0)$	-	-	250	250	250	250	0
$E_H(0)$	E_H^p	E_H^p	E_H^p	E_H^p	E_H^p	E_H^p	0

gonad respectively. The two concentrations cannot be added in a meaningful way to obtain whole body residues.

Bourrachot (2009) also measured $\langle M_Q \rangle_d$ in the eggs of several females at the onset and the end of the 15d trial in both exposure conditions. The author found mean values of 540 and 35 nmol U per g dry egg mass (n=3) for the first day of the reproduction trial in both 15d-U84 and 15d-U1054, and a mean value of 26 nmol U per g dry egg mass (n=3) the final day of 15d-U84. The model predictions deviate from these observations. For the 15d-U84 condition, predicted $\langle M_Q \rangle_d$ in eggs on the first day of the 15d trial is around 200-300 nmol g⁻¹ and ranges from 11 to 52 nmol g⁻¹ on the last day (depending on the replicate). The module assumes uptake is proportional to environmental concentration. But when we adjust the DEB model with the one compartment toxico-kinetic module to whole body residues provided in Barillet et al. (2005) and Barillet et al. (2011), we see that at 2100 nM U, uptake should be very important but it hardly is compared to predictions (fig. 5.9C).

When looking at the scatter in the data then only some individuals actually have really high $\langle M_Q \rangle_w$ (maybe even one replicate out of 10), while values in

other replicates are comparable across conditions. This can be seen by the factor 5 difference in final $\langle M_Q \rangle_d$ between female 8 and female 10 in 37d-U420 (fig. 5.8) bearing in mind that their final W_w and L_f are quasi-identical: 845.5 mg/ 41.4 cm and 894.5 mg/ 42.0 cm for female 8 and 10 respectively. We further illustrate this point by representing final $\langle M_Q \rangle_w$ of the ten individuals in the U-420 condition in Barillet et al. (2011) (fig. 5.10A). $\langle M_Q \rangle_w$ seems inversely related to condition (W_w/L_f^3). We are able to explain part of this observed variability in bioaccumulation by differences in feeding (fig. 5.10B). Differences in initial L_f and initial contribution of E_R to total W_w further exacerbate the variability in the signal (not shown).

Predicted bioaccumulation is sensitive to the incorporation of metabolic handling of starvation into the core DEB model. The starvation rules (resorption of E_R and degradation of V) are responsible for the (predicted) extreme concentrations of non fed individuals (triangle symbol fig. 5.10B).

If we wanted predictions more in the neighbourhood of observed final $\langle M_Q \rangle_d$ for the four females in 37d-U84, predicted values would be far too high in the 37d-U420. We chose values of P_{Vd} and \dot{k}_e which were also in line with the U84 and U420 conditions in Barillet et al. (2005) and Barillet et al. (2011) (fig. 5.9A,B,D and E). And are left with the discrepancies seen for females in 37d-U84 (fig. 5.8, first row) and for the U-2100 condition in Barillet et al. (2005) (fig. 5.9C,F). The factor two difference in final $\langle M_Q \rangle_w$ for both conditions exposed to 420 nmol U l⁻¹ was nicely explained by dilution by growth, i.e. last term in eq. 5.3 (fig. 5.9B,E). But we assumed that average length of fish in U420 conditions by Barillet et al. (2005) was smaller than for Barillet et al. (2011) (table 5.4). In the 2011 study mean wet mass increase over 20 d is in the order of 30 mg, while in the 2005 study it is in the order of 100 mg.

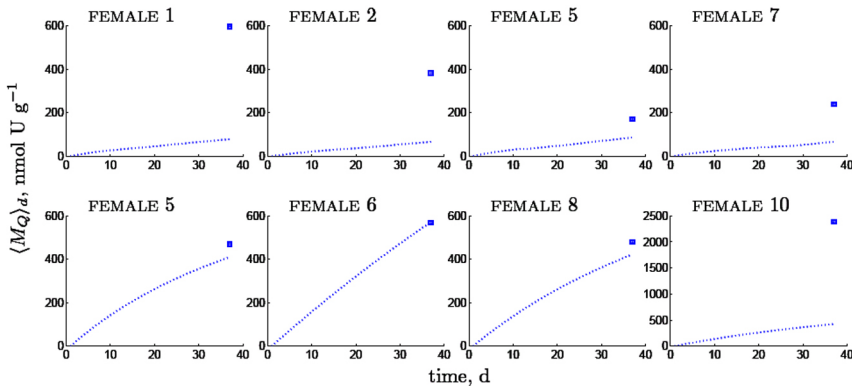


Figure 5.8: First row: U-87; second row: U-420. Square: final measured internal concentration $\langle M_Q \rangle_d$ (nmol g⁻¹ dry mass); dotted line: predicted $\langle M_Q \rangle_d$.

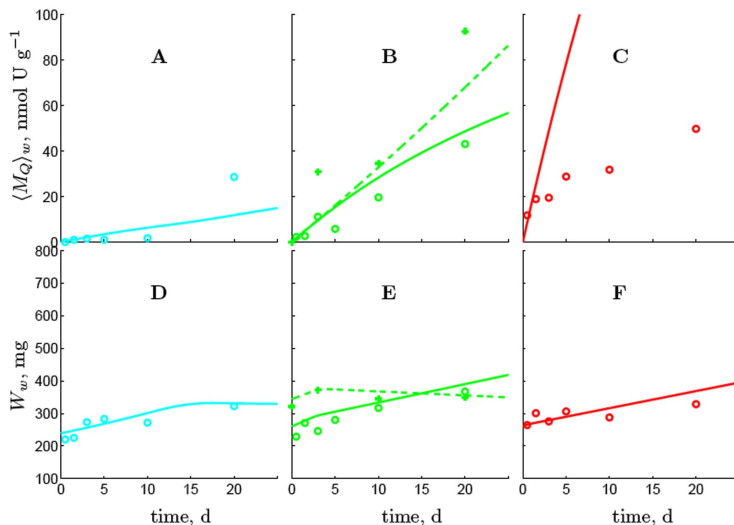


Figure 5.9: DEB model fits to adult bioaccumulation data. Circles: data published in Barillet et al. (2005); crosses: data published in Barillet et al. (2011). Solid lines: DEB model predictions for Barillet et al. (2005); dotted lines: DEB model predictions for Barillet et al. (2011). Parameters for each data set are in table 5.4. (A), (B) and (C): mean internal concentration $\langle M_Q \rangle_w$, nmol U g⁻¹ fresh mass (W_w) for exposure conditions 84, 420 and 2100 nmol/l respectively. (D), (E) and (F): mean W_w , mg for exposure conditions 84 and 420 nmol/l and 2100 nmol/l respectively.

5.4.5 Embryo and early juvenile

A value of $f = 0.3$ was estimated for embryos and early juveniles; initial energy in the egg was set to 1.7J (table 5.4). Model predictions are compared with data from Bourrachot et al. (2008) (fig. 5.11).

Uranium bioaccumulation could not be captured using the same set of toxico-kinetic parameters as for adults (table 5.4). Embryo U biomass/water partition coefficient was estimated to be almost a factor 4000 lower than for adults. Predicted $\langle M_Q \rangle_d$ is in line with that observed (fig. 5.11A).

The best fit for W_d and final L_f of embryos and early juveniles exposed to 84 and 1054 nM U was obtained assuming mode of action (G) with $[M_{Q0}^G] = 0$ nmol cm⁻³ and $[M_{QT}^G] = 0.211$ nmol cm⁻³ (table 5.4, fig. 5.11B,C). Thus the NEC for effects on growth in the exposure media is 0 nmol U l⁻¹.

Mode of action (M) and (A) could not capture the importance of effects on growth in the embryo period. As hardly any feeding occurred, mode of action (A) would hardly impact early juvenile growth. As structure is small during embryo and post embryo development, mode of action (M) entails small devia-

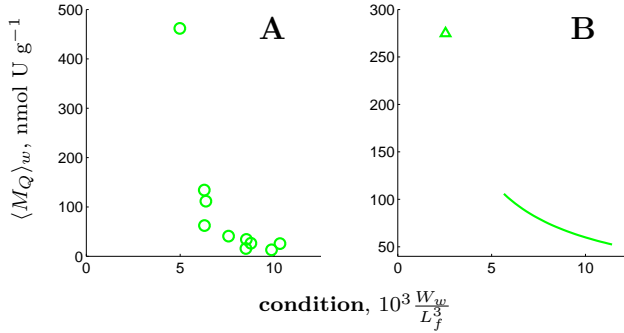


Figure 5.10: $T = 25^\circ\text{C}$. (A) Circles: data published in Barillet et al. (2011): internal concentration $\langle M_Q \rangle_w$, nmol U g⁻¹ fresh mass (W_w) of the 10 individuals after 20d of exposure to 420 nmol U/ l. The extreme $\langle M_Q \rangle_w$ belongs to an individual with $L_f = 2.9$ cm and $W_w = 121.5$ mg. It is most likely a starving individual who has already started degrading structure to cover maintenance. (B) Solid line: DEB model predictions for internal concentration $\langle M_Q \rangle_w$, nmol U g⁻¹ W_w of individuals after 20d of exposure to 420 nM U. $L_f = 3.6$ cm, negligible initial energy in reproduction buffer and no batch preparation. Computations are performed for values of f ranging from 0.5 to 0.7. If we compute ultimate $\langle M_Q \rangle_w$ for a starved individual over the 20d period we obtain an extreme concentration (green triangle) right.

tions of cumulative energy investment in growth. As starvation is included, an increase in somatic maintenance would increase shrinking from starvation but a more detailed data set (mass against time for several individuals) would be needed to detect this type of effect.

Effects on survival are modelled assuming that survival is the sum of contributing hazards, Eq. (5.5): we assume a hazard due to accidents of $\dot{h}_{\text{acc}} = 0.02$ d⁻¹ which explains background control mortality and a killing rate of $b_{\dagger} = 0.375$ cm³ nmol⁻¹ d⁻¹ which quantifies hazard induced by uranium on organism survival, Eq. (5.6). The NEC for survival is estimated to be 0 nmol U l⁻¹ with with $[M_{Q0}^s] = 0$ nmol cm⁻³ (table 5.4). Predictions are in harmony with observed survival (fig. 5.11D).

These results answer our first question: effects of uranium on embryo and early juveniles differs from that of adults. Furthermore, the same set of toxicokinetic parameters cannot describe the dynamics of $[M_Q]$ in both the early and late life stages.

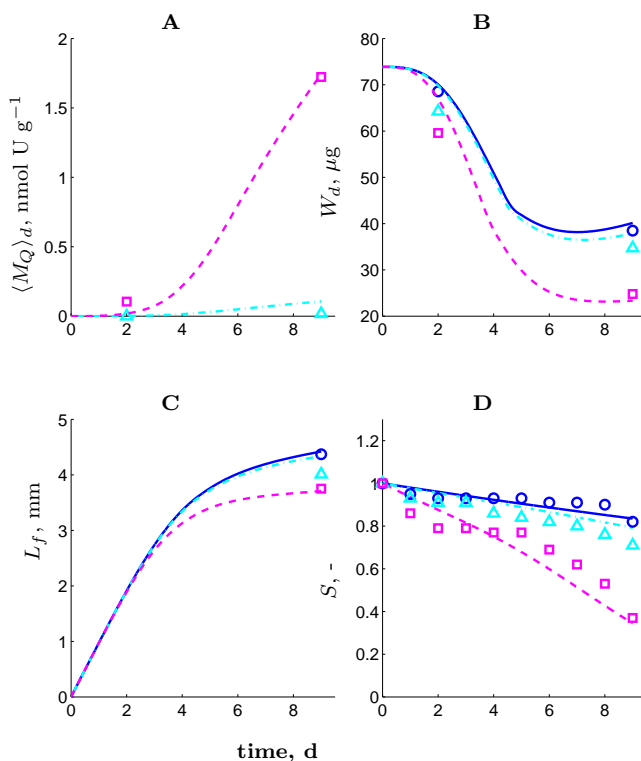


Figure 5.11: Symbols: data published in Bourrachot et al. (2008). $T = 25^\circ\text{C}$, $f = 0.3$. Lines DEB model predictions. Circles: control; triangles: exposed to 84 nM U; squares: exposed to 1054 nM U; solid lines: predictions for control; dot-dashed lines: predictions for 84 nM U; dashed line: predictions for 1054 nM U. A: Internal concentration: $\langle M_Q \rangle_d$, nmol U g⁻¹ dry mass, B: Dry mass (W_d), μg, C: physical length L_f and D: survival fraction S . Parameter values and initial conditions are in table 5.4.

5.5 Discussion

5.5.1 Insights on reproductive physiology

We show that cumulated energy investment in reproduction can be quantified separately from behavioural effects on reproductive output in a bioenergetic context. Toxicants can modify energetics (modification of a DEB model parameter), but can also modify behaviour. We offer the methodology to analyse both types of effects within a same DEB modelling framework.

This study further provides new scientific insight into reproductive physiology of zebrafish. Buffer handling rules turn out to be similar to multiple batch spawners such as Anchovy (Pecquerie et al., 2009). However, contrary to Anchovy batch preparation seems mainly food driven. We were surprised to see that in 15d-U0 batch preparation was either initiated at the onset of the 20d accumulation, or during the 20d accumulation and sometimes at the beginning of the reproduction trial (table 5.3). Perhaps in the first case batch preparation was already triggered before the experiment. In the second case, maybe visual contact with males who were kept in neighbouring plexiglass aquaria sufficed. Further research is needed to understand the exact nature of the batch preparation trigger. Model fits to 15d-U0 (table 5.3 and fig. I.1, Appendix I) show that there may indeed be an important behavioural component to triggering batch preparation. A physiological interpretation of t_b (time at which batch preparation is triggered) could be the onset of ovulation.

In line with Pecquerie et al. (2009), inhibition of batch preparation seems to be triggered internally and we found the internal trigger to be when energy is taken from the buffer to cover somatic maintenance. This study shows that this is most likely the mechanism through which uranium inhibits spawning.

Effects of sensory organs and/ or behaviour should be quantifiable via effects on $[E_B]$ or t_b . We found that $[E_B]$ comports a lot of inherent scatter already in controls. In addition $[E_B]$ cannot be estimated when females do not spawn as is the case in 15d-U1054 and 37d-U420. Thus we are unable to conclude on absence or presence of an effect on $[E_B]$.

With more detailed mass measurements in combination with N , then contributions of E_R to total biomass can be quite accurately quantified; assuming of course that a robust set of DEB parameters for the species is available. Performing mass and energy balancing on ripe and unripe buffer is a bit trickier, but after this first study, it also seems possible if well thought out experiments are performed. The 15d trial protocol (Bourrachot, 2009) is actually a good basis for designing such a study. Perhaps a clearer physiological link between ripe batch material and histological tissue analysis could be made in the future (e.g. linking batch preparation to oocyte maturation).

In this study, the total (live + dead) observed number of eggs N was used to compare model predictions to observations. Observed dead eggs in this study comprise three types: (i) non fertilized but otherwise healthy, (ii) coagulated, and (iii) small totally opaque white spheres. We are not sure about the phys-

iological nature of the latter two categories of dead eggs and understanding its dynamics was beyond the scope of this study. However we would like to highlight an interesting possibility for future research venues wishing to link sub-organismal to organismal responses: the proportion of dead eggs of type (ii) and (iii) in a batch may be related to residence time of ripe/ripening batch material inside the body.

Our results lend support to the role of maintenance as a demand system. The results empirically support an underlying assumption of DEB theory: that supply is surface area controlled and demand is volume linked (Kooijman, 2010). The theory would predict that fish close to ultimate size (as in the 37 d experiment) would need higher f to cover somatic maintenance than individuals of smaller size. The sensitivity of fish to value of initial structure and f in the 37d experiment relative to the 15 d experiment with the smaller size class is indeed remarkable. Basically, fish in the 37 d experiment need at least $f = 0.75$ to spawn and sometimes need $f \geq 0.8$, whereas in the 15 d experiment some fish can spawn with less than $f = 0.7$.

5.5.2 Reproductive toxicology

When looking at mean cumulated N in 37d-U84 (fig. 5.4C) relative to control, a first interpretation would be a hormesis phenomenon. Accounting for physiological differences between females and ingestion levels f , then no hormesis is observed. Secondary stress induced through uranium might have increased ingestion for individuals in 37d-U84 and 37d-U420 who manifestly have much higher values of f than controls. This was observed for *Daphnia magna* (Kooijman, 2010, Chap.6). In fact we even visually observed the much higher appetite in conditions 37d-U84 and 37d-U420 during the 37d exposure. Food availability is a major factor regulating effects (Kooijman, 1991; Jager et al., 2004; Zimmer et al., 2012)

On the basis of the 37d-U84 data, we explained effects on reproductive output as an increase in buffer material being burned to fuel maintenance processes. The increase in demand driven metabolic work must have an upper limit in the concentration ranges where survival is not impacted. We propose an upper limit to the increase in the neighbourhood of $1000 \text{ J d}^{-1} \text{ cm}^{-3}$, but further research is needed to test this.

Although we assumed the mode of action is an increase in the value of $[\dot{p}_M]$, more detailed physiological studies might better distinguish between an eventual effect on assimilation. An implied model property is that if O_2 consumption were measured, then decreasing $\{\dot{p}_{Am}\}$ would decrease O_2 consumption while increasing $[\dot{p}_M]$ would increase it.

If the targeted metabolic process is assimilation, it would not modify the conclusion that the mechanism behind inhibiting spawning is the process where energy is taken from the buffer to cover somatic maintenance. Analysis of uranium toxicity data on *Daphnia magna* using DEB theory concluded that assimilation decreased in response to water-borne exposure to U (Massarin et al.,

2010, 2011). Their study showed that effects of uranium on growth and reproduction were captured equally well when assuming a decrease in assimilation or an increase in somatic maintenance in the first two generations, but that effects on the third generation were better characterized by a decrease in assimilation. The authors used this last piece of evidence in combination with histological analysis of uranium induced damage to the gut wall to favour mode of action (A). A complementary study also reveals uranium induced damage to the gut wall in zebrafish (Augustine et al., 2012b). More specifically there was an increase in damaged mitochondria, loss of gut wall architecture, presence of large necrotic zones and an overall decreases in gut bacteria.

It would be possible to obtain adequate fits for modes of actions (M) and (A) for the 15d reproduction trials by Bourrachot (2009) as well as for all the females in 37d-U420. And it is indeed tempting to use histological analysis to tip the balance in favour of a decrease in assimilation. The deciding factor lies in the reproductive output of the females in the 37d-U84 condition. A decrease in assimilation cannot satisfactorily match the data. Somehow too much material in the reproduction buffer in being burned. An increase in $[\dot{p}_M]$ does however explain the phenomena. Uranium not only induces damage to the digestive tract, but also to the gills, liver, muscle, brain and gonads (Lerebours et al., 2010a,b; Barillet et al., 2010). Each organ comprises both reserve and structure. While it is tempting to at least delimit the reproduction buffer reserve material to the gonad, there is no satisfactory proof that even this is an accurate approximation.

5.5.3 Effects on growth

This study also shows that uranium can target two separate metabolic processes in zebrafish, but further research is needed to understand how the two modes of action act together upon the organism. The contribution of initial amount of reproductive material to total biomass at the onset of adult exposure experiments in combination with negligible growth hampers firm conclusions about effects on growth when analysing adult data sets. However, uranium clearly impacts embryo and early juvenile growth (Bourrachot et al., 2008), fig. 5.11.

Exposure to uranium contaminated lake effluent also negatively impacted growth of early juvenile green frogs *Rana perezi* (Marques et al., 2008). During the early life stages, growth may be a more sensitive endpoint than survival for evaluating uranium induced effects, although few toxicity studies address this problem. Since our results suggest a no effect concentration of 0 for effects on growth, this should be corrected for in future risk assessment studies.

Absence of observed effects on growth in adult fish (Cooley et al., 2000; Barillet et al., 2011) can be explained by the capacity of adults to resorb material in the reproduction buffer to cover somatic maintenance. Independent empirical support for this assertion is that no significant mortality was observed when adult zebrafish were starved for 70 d (pers. comm. X. Cousin). The

analysis of adult data sets alone, would have been quite misleading since we would have concluded that there are no effects on growth.

The model predicts that combining increasing $[E_G]$ and $[p_M]$ would lead to severe effects on both growth and reproduction if young juveniles were exposed all the way to puberty. Survival of juveniles should also be more impacted relative to adults because the latter have the possibility to draw on reproductive material to cover somatic maintenance; juveniles do not. Dual modes of action have also been observed for *Folsomia candida* exposed to chlorpyrifos (Jager et al., 2006a).

5.5.4 Elimination and uptake

This study also shows that elimination through reproduction explains why reproductive output was severely impacted in the study by Bourrachot (2009) but not in the 37d trial. Empirical support for the detoxifying role of reproduction is in the sensitivity of effects relative to value of batch energy density. Female 10 was not impacted but females 2 and 3 were in 37d-U84. We were surprised to see that effects on metabolism were so sensitive to batch energy density and wonder again at what factors play an important role in the value of $[E_B]$.

By accounting for elimination through reproduction, qualitative trends in accumulation and depuration are captured (Bourrachot, 2009). Nonetheless, the overall capacity of zebrafish to (totally) eliminate uranium still remains an open question. Uranium was not entirely eliminated in muscle, liver, gills or brain after a week (Lerebours et al., 2009) nor in whole body residues after 30 days (Labrot et al., 1999). However, uranium was eliminated from muscle tissue of goldfish *Carassius auratus* previously exposed for 4 days (Lourenço et al., 2010). After 6 months of depuration, humans previously exposed to mean values of 2.6 mM U in their drinking water still had high levels of U in their urine (Orloff et al., 2004). However, U was efficiently eliminated in the annelid *Eisenia fetida* (Labrot et al., 1999) and the arthropod *Hyalella azteca* (Alves et al., 2009).

We made the simplifying assumption that the only uptake route is through the water. Uptake can also occur through food and also be transferred maternally to offspring (Simon et al., 2011b). In experimental settings, as analysed here, food (TetraminTM) is not spiked but may contain background levels of U (≈ 2.6 nmol U g⁻¹ TetraminTM, K. Faucher pers. comm.) as well as may contain uranium adsorbed from the water column between reaching the water and being eaten. Care was always taken to reduce that time interval, but control $\langle M_Q \rangle_d$ presents background levels of uranium (not shown).

5.5.5 On the origin of variability in bioaccumulation measurements

Using DEB theory, internalized PCB was correlated to prior feeding history for many individuals in a study involving the common sole, *Solea solea* (Eichinger et al., 2012). Growth trajectories of each individual were found to differ considerably; differences in feeding history were quantified by estimating individual values of f . Very importantly, the authors demonstrate that using the mean f value from all the sampled individuals does not always provide accurate predictions for data expressed as the average observed values. Our study is fully in line with that result. We further contribute to this insight by showing that not only does feeding history contribute to the variability, but so does initial amount of reproduction buffer material. In some instances, such as the 15d reproduction trial, even the initial amount of ripe batch material relative to total available reproduction buffer material matters for interpreting results.

A high percentage of variability in accumulation can be explained by energetics, but not all. Uranium showed the same propensity to accumulate in an extreme manner in certain but not all replicates of *Corbicula fluminea*. The inter-individual variability in bioaccumulation was very much reduced for *Corbicula fluminea* exposed to selenium (Adam, 2006, pp.40). A prior study on uranium bioaccumulation in zebrafish brain and muscle tissue also recorded the same high inter-individual variability (Lerebours et al., 2010a). This pattern holds for actinide uptake in general for the mussel *Mytilus edulis* (Lobel et al., 1991). Future studies might remove variability in initial conditions of fish in each exposure condition and compare bioaccumulation across groups of adults of different classes of initial conditions to a same exposure condition to more accurately determine dynamics of uptake and elimination.

5.5.6 Deviations from the extended one compartment toxic-kinetic model

In this study effects were taken proportional to total density of U in the body expressed as nmol U cm^{-3} structure. As suggested by Muller and Nisbet (1997), it may be relevant to take effects proportional to density of U in structure only: M_{QV}/V . This may help explain how growth of F1 embryos and early juveniles, who inherited U from the mother and were raised in clean water, was hardly impacted (Bourrachot, 2009).

A very enigmatic aspect is the systematic presence of individuals with extreme $\langle M_Q \rangle_d$ relative to other replicates (fig. 5.10A and 5.8). What could be the energetic difference between female 8 and 10 in the U-420 condition that could promote a factor 5 difference in accumulation (fig. 5.8)? We compared acclimation history of both females and found that in the 35 d acclimation to individual feeding and reproduction, female 8 never reproduced while female 10 reproduced once; 574 eggs were spawned the day before exposure. We further compared lateral and dorsal portraits of both individuals at exposure day

3 (fig. H.2, Appendix H). Both fish look quasi-identical, however the 574 eggs spawned by female 10 represents a loss of approximately 280 mg, W_w (assuming $E_0 = 1.7J$). If we assume W_w is similar at time of portrait then the difference between female 8 and 10 is in reserve density. In this case $[E]$ for female 8 must have been less important than for female 10 at the onset of exposure. This is suggestive of a link between between reserve density and bioaccumulation. A possible hypothesis is that U binds (maybe even irreversibly) with receptors in E . Such receptors could represent a constant fraction of E . When comparing between individuals, higher $[E]$ would entail more fixation sites. A process potentially involving precipitating uranium in specialized vacuoles (Pereira et al., 2012) might also be involved in detoxification bringing up internal concentrations but lowering the internal fraction of active compound which induces effects.

Embryo and adult toxico-kinetic parameters seem to differ. This may be due to the very sparse data sets but may also be linked to different surface area volume relationships in the early juvenile and the adult. Take for instance ratio of gill surface to total surface: adults have more gill surface per total surface than juveniles. We aimed for maximum simplicity: leading to the simplest formulation possible of toxico-kinetics (eqn. 6.3, 6.31 Kooijman, 2010). The chorion is assumed to be part of the overheads of growth (quantified by κ_R) and Bourrachot (2009) has demonstrated that a small part of uranium ends up in the chorion in the case of maternal transfer to offspring. We also did not account for adsorption to the chorion during direct exposure to offspring which was also demonstrated to occur (Bourrachot et al., 2008). It is capital to link any toxico-kinetic module with the energetics of the organism (e.g. van Haren et al., 1994; Bodiguel et al., 2009; Ng and Gray, 2009; Eichinger et al., 2010). However the details around how water chemistry (e.g. pH) affects ionisation which in turn modulates the amount of uranyl ion (thought to be the most bioavailable (Fortin et al., 2007)) has not been addressed in this study. Natural extensions can be built to deal with water chemistry for operational purposes (Kooijman, 2010, Chap.6).

5.5.7 Perspectives

Future studies might consider presenting data as individual mass and reproductive output. Monte Carlo simulation methods where uncertainty is placed on behaviourally controlled parameters (f , t_b , $[E_B]$) might be developed to estimate toxicity parameters for each individual separately. Perhaps taking differences in initials conditions and buffer handling rules in combination with perfecting experimental protocols to reduce inter-individual variability in ingestion might allow for even more accurate quantification of very subtle sublethal effects on metabolism. In future experiments smaller adults should be preferred to individuals who are close to ultimate size to reduce inter spawn interval and sensitivity of spawning to small behavioural differences in ingestion. The biggest weakness in all the data sets is absence of initial measurements of

mass and length. This happily can very easily be corrected in future experiment protocols. It would be possible to extend the same modelling framework to understand effects of ionizing radiation relative to depleted uranium. For instance, Bourrachot et al. (2008) show that ionizing radiation are seemingly on development in combination with survival, but not on growth which is in stark contrast to effects of depleted uranium alone. Effects on maturation (quantified by the life stage parameters) would emulate this type of effect.

5.6 Concluding remarks

We show here that it is possible to analyse toxicity data from a number of separate experiments using DEB model parameters previously estimated using independent eco-physiological data on the species. Zebrafish is an OECD test species and so there is now a unifying framework for analysing effects of any number of chemicals considering a same DEB parameter set for the control. This will allow impartial evaluation of effects of feeding on results and reinforce robustness for each of the studies. This study further provides a handle for analysing behavioural data (spawning and/or feeding) using an individual based bio-energetic model. Behavioural response to toxicants are a very ecologically relevant response.

Finally, the random sampling strategy seems really counter-productive in a laboratory setting. A lot of the differences between individuals seems to be in size, mass, relative contributions of reserve and reproductive material to total wet mass and maybe even how much of the reproductive material is ripe batch material at the time of sampling. These types of differences are not important and are simply random chance events (artefacts). Comparing mean values of measurable quantities at each sampling time amounts to assuming that the distribution of each one of the parameters which quantifies each one of these differences is identical and has same parameters (e.g. same mean and standard deviation assuming normal distribution) at each time point. What we hoped to have illustrated through this study is that while size, mass, relative contributions of reserve and reproductive material to total wet mass, spawning behaviour etc. may be (very) different in each of the replicates in a condition, the cumulated reproductive investment and cumulative mass investment in growth during the experiment is quantifiable for each individual. Whatever scientific philosophy is adopted, we will all agree that it is the quantification of these last two physiological processes which are of primary concern in ecotoxicology.

Acknowledgements

This work is part of the ENVIRHOM research program supported by the Institute for Radioprotection and Nuclear Safety and the Provence Alpes Côte d'Azur region. We are grateful to Stephanie Bourrachot for providing raw data

from her thesis, to Virginie Camilleri for ICP-AES analysis and technical insight into how to maintain a constant exposure level of U over 37 days, to Sylvie Pierrisnard for ionic chromatography analysis, to Alban Carlat for assisting in data collection and to François Brion and Alexandre Péry for helpful comments during experimental design phase.

6

Uranium induces ultra structural damage to gut wall of zebrafish, *Danio rerio*

Augustine, S., Pereira, S., Floriani, M., Camilleri, V., Gagnaire, B., Kooijman, S. A. L. M., and Adam-Guillermin, C. (2012). Uranium induces ultra structural damage to gut wall and potentially impacts residing gut microflora of zebrafish, *Danio rerio*. In prep.

Abstract

Uranium is a naturally occurring element, but activities linked to the nuclear fuel cycle can increase background levels in the surrounding waters. Sublethal effects of water-borne uranium (U) on cumulative energy investment in growth and reproduction of zebrafish, *Danio rerio* have already been demonstrated. Since the intestine is an exchange surface across which energy is assimilated to fuel all of metabolism, we examined the histology of intestines of zebrafish exposed to 84 and 420 nM water-borne uranium for over a month.

Light microscopy shows a loss of architectural fold in gut wall in both treatments. Furthermore, the mucosa was degraded in numerous regions. Using transmission electron microscopy (TEM) we evaluated the number of electron dense mitochondrial matrix granules per mitochondria in two random cross sections of intestine using an image sampling strategy. We found a decrease in granules per mitochondria. This is suggestive of perturbations to cellular metabolism and more specifically to cellular calcium homeostasis. TEM coupled to energy-dispersive X-ray spectroscopy microanalysis of gut wall tissue shows that some uranium was internalized in the nucleus of epithelial cells in the 420 nM treatment.

Fluorescent *in situ* hybridization using specific probes to detect all eubacteria was performed on frozen sections of 6 individual fish in the 87 nM and 420 nM treatments. We observed hardly or no fluorescence in 2 out of 6 replicates whereas all controls and 84 nM individuals fluoresced. This indicates that host-microbiota interactions are potentially disturbed in response to uranium induced stress.

Key words: Zebrafish, uranium, gut, histopathology

6.1 Introduction

There is an international increase in demand for primary energy production of nuclear origin. Uranium (U) is the main component of nuclear fuel. Activities such as U ore extraction (e.g. leaching) and storing of mine dam tailings are among the activities which can contribute to increasing background levels of U in surrounding waters (e.g. [Fernandes et al., 1995](#)). Radioactive elements such as U can exert a dual radiological and chemical toxicity depending on the isotopic composition ([Domingo, 2001](#)). Depleted U however has low specific activity and its toxicity is mainly chemical. Consequently, environmental risk associated with uranium are considered to be mainly of chemical origin ([Mathews et al., 2009](#)). International drinking water guidelines for U is 84 nM ([WHO, 2001](#); [HC, 2008](#)). This is a protective measure for human health, but what are long term effects on resident aquatic fauna who are chronically exposed to increased levels of U in the water column?

Histological analysis of tissues of organisms exposed *in situ* to uranium mine effluent or soil can be sensitive indicators of perturbations to overall organism health and survival ([Marques et al., 2009](#); [Lourenço et al., 2011](#)). The simultaneous exposure to a mixture of compounds, unknown prior history of specimens and perhaps limited literature on the histology of the organism can make some results difficult to interpret (e.g. [Kelly and Janz, 2009](#)).

Characterizing sublethal histological alterations induced by U, under carefully controlled laboratory conditions, on well characterized model organisms is an important complementary approach to *in situ* observations of histopathology. Moreover, for extrapolation purposes mechanisms underlying the observed effects must be determined.

Zebrafish, *Danio rerio* are a small (3-5 cm) teleost species with a long history as model organism in the fields of ecotoxicology and development ([Laale, 1977](#)). Consequently, the histology and development of zebrafish have been extensively studied in the literature and so form the basis for characterizing physiological alterations induced by uranium. Similarities between zebrafish and mammalian development, immune and neuronal systems further justify the use of zebrafish as a model for quantifying physiological consequence of U toxicity.

The (blank) metabolism of zebrafish was previously quantified ([Augustine et al., 2011a](#)) in detail. U toxicity studies on growth, reproduction, and bioaccumulation were analysed with the model for blank zebrafish metabolism in order to quantify uranium induced deviations in metabolic functioning ([Augustine et al., 2012a](#)). The main results of their study are that uranium first targets the overall cost for growth and second targets either assimilation or somatic maintenance. However an increase in somatic maintenance was suspected over a decrease in assimilation, because this better described some of their observations.

The two above mentioned studies are carried out using the conceptual framework of Dynamic Energy Budget (DEB) theory ([Kooijman, 2010](#)). In this

framework growth, assimilation or somatic maintenance represent integrated energy fluxes (processes) and are each considered as motors who use and transform mass for (metabolic) work and synthesis of new materials. The work performed by each process can be indirectly quantified (in mass or joules per time) on the basis of dynamic observations on e.g. development, length measurements, recorded egg output or respiration (Lika et al., 2011a,b). Although all of the studies analysed by Augustine et al. (2012a) assumed that uptake was through water, (contaminated) water and food must enter the digestive tract at each feeding event.

Zebrafish is a stomachless teleost. The digestive tract consists of two main layers: muscularis and mucosa (Wallace et al., 2005). The latter is organized in broad irregular folds. The outer layer of the mucosa (epithelium) is in direct contact with the environment. Thus, the intestine represents an interface with a large surface area (epithelium) where material is exchanged between the environment and the organism. The intestinal lumen is a veritable miniature ecosystem with complex interactions between bacteria and the organism. Host-microbe interactions are important players in terms of energetics (food assimilation) and innate immunity (Bates et al., 2006; Kanther and Raws, 2010).

Assimilation may be directly linked to epithelium surface area and overhead costs of assimilation may somehow be linked to host-microbe interactions and correct functioning of epithelium cells. This is why histological analysis of gut wall may help explain some of the results obtained using bio-energetic modelling. Moreover, effects of U on growth and reproduction of *Daphnia magna* was also characterized using DEB theory (Massarin et al., 2010, 2011). It was demonstrated that a decrease in assimilation can explain the observed decrease in growth and reproduction (Massarin et al., 2011). The authors suggest that the decrease in assimilation is concomitant to the observed degradation of gut wall, i.e. increase of missing intestinal cells and vacuolization. Intriguingly, observed damage to gut occurred after several weeks of exposure to 210-420 nM U, whereas observed organism levels responses such as growth or reproduction started to occur above 2-42 nM U.

A contrario, effects of U on the metabolism of zebrafish are shown to occur around exposure media concentrations of 0-2 nM U (Augustine et al., 2012a). The authors performed a 37d zebrafish exposure experiment to 84 and 420 nM of water-borne depleted U. At the end of the 37d exposure 9 individuals from both the 84 and 420 nM treatments were removed and sacrificed. The intestine from each individual was dissected and histology of the mucosa is examined in the present study. The objective of this study was to determine if U induced ultra-structural perturbations to the gut wall. We wish to further understand if alterations to tissue and cell organisation in the gut wall corroborate organism level responses on growth and reproduction observed on those same individuals (Augustine et al., 2012a). Finally, we looked for an eventual perturbation to host-microbe interactions by qualitatively assessing total bacterial colonization in the intestinal lumen.

6.2 Material and Methods

6.2.1 Experimental conditions and tissue sampling

Wild type zebrafish were obtained from a commercial fish supplier (Elevage de la grande rivière, Lyon). Zebrafish were housed in synthetic water as in (Augustine et al., 2012a) at 26°C, pH = 6.5 (12:12 light: dark cycle). Fish were fed commercial fish feed (TetraminTM, Germany) 2-3 times a day. Water was renewed manually on a daily basis. There were three conditions: control, 84 nM U in water and 420 nM U in water. Exposed fish were sampled after 37 d exposure to 84 and to 420 nM U respectively. Exposure protocol and water sample analysis can be found in Augustine et al. (2012a). Control fish were from the same supplier. They were kept in the same synthetic water and fed the same food as exposed individuals. Controls were maintained at a density of less than 5 fish per litre in well oxygenated plexiglass aquaria. We examined the gut wall of individuals from the 3 treatment conditions: 0 nM, 84 nM and 420 nM depleted U in the media. The three conditions will hereafter be referred to as the U0, U84 and U420 treatments. Fish were sacrificed in melting ice and intestines was subsequently dissected. No food was introduced into the system 24H prior to sacrifice for all treatments.

6.2.2 Light and transmission electron microscopy

The intestines of 3 fish per condition were prepared for light microscopy, transmission electron microscopy (TEM) and high-energy dispersive X-ray spectrometry analysis. The exact same protocol and same equipment (unless specified otherwise in the text) were used as in Barillet et al. (2010).

Light microscopy

For each of the three replicates, 6 cross sections (3 in the anterior part and 3 in the posterior part) were observed under a light microscope (Leica Microsystems GmbH, Wetzlar, Germany) and subsequently photographed (Leica camera ICC50; LAS EZ Software) at magnifications x40, x100 and x400 respectively. Alterations of histology of gut wall were examined.

TEM

For each of the 3 replicates, two random cross sections were observed using TEM. 10 regions between base and tip of the intestinal folds and comprising the epithelium were photographed at magnification x6000 (fig. 6.1C-D). at least 10 regions were randomly chosen and photographed at magnification x43000 in each of the x6000 regions (fig. 6.1F-H). In each of the x43000 magnification photographs, number of mitochondria and number of electron dense mitochondrial matrix granules, MMG, (fig. 6.1D) were scored. The total of each of the

above elements were summed for each replicate. Results are presented as total observed MMG/ mitochondria for each section of all replicates (fig. 6.1B).

6.2.3 Fluorescent *in situ* hybridization

The intestines of 6 fish per condition were prepared for fluorescent *in situ* hybridization (FISH). Each intestine was dissected and fixed with paraformaldehyde 4%, sucrose in phosphate buffered saline solution (overnight at 4°C). The following day, intestines were cut in 2-3 sections and embedded in OCT Tissue Tek freezing medium before storing at -80°C. 12µm transversal sections of the intestine were obtained with a cryostat (Leica CM 3050) and placed on superfrost slides (Superfrost Plus; Menzel). Slides were dried on a 42°C hotplate for several hours before storage at -80°C.

FISH was performed according to a protocol very slightly modified from Bates et al. (2006). Detection of general bacterial colonization of the digestive tract was performed using a mixture of oligonucleotide probes Eub338-I (GCTGCCTCCCGTAGGAGT), Eub338-II (GCTGCCACCCGTAGGTGT) and Eub338-III (GCTGCCACCCGTAGGTGT) modified with Cy3 fluorecein at 5' extremity (Eurogentec). Modifications of protocol were as follows: slides were incubated in a dark incubation chamber at 42°C and sections were post washed in SSC 1x. Slides were then mounted in 4',6' Diamidino-2-Phenylindole stained Vecashield (Abcys) and examined with a Nikon fluorescence microscope (Nikon Eclipse E600). FISH was performed on at least two transversal sections spanning the entire lumen for each embedded section of intestine. Presence or absence of colonization was visually recorded. Intense and less intense colonization was qualitatively specified depending on the amount of observed fluorescence.

6.3 Results

6.3.1 Uranium induces damage to gut wall

The mucosa layer is directly in contact with the environment via the intestinal lumen. The epithelium comprises the outermost layer of the muscosa and is organised in broad irregular folds (fig.6.2A-D). The epithelium consists of a regular row of columnar shaped enterocytes (brush border cells) and mucus secreting goblet cells (Wallace et al., 2005). Increased vacuolization of epithelium cells at tips of intestinal folds was observed in controls (fig. 6.2C). Based on the study by Wallace et al. (2005), we interpret this is as the physical manifestation of apoptotic cells at the tips of the folds. The authors demonstrate that epithelial cells exit the base of the folds and migrate lumenally ensuring cell renewal and that tips of folds are apoptotic. Vacuolization of apical end of folds increased between anterior and posterior regions of the digestive tract in all conditions (controls and exposed). We found that vacuolization of epithelial cells is not a sensitive endpoint for assessing U induced perturbations

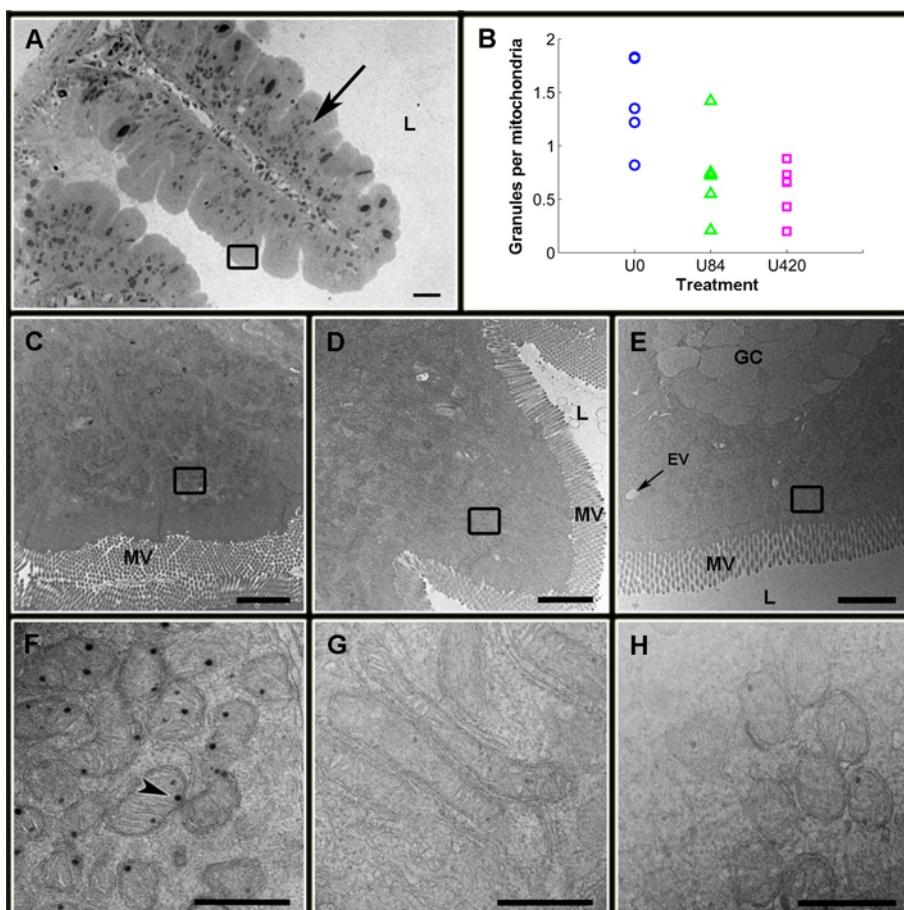


Figure 6.1: The number of mitochondrial matrix granules (MMG) per mitochondria decreases in epithelial cells of individuals chronically exposed to 84 and 420 nM of uranium. L indicates lumen of intestine. (A) $\times 400$ toluidine blue plastic section of an intestinal fold. Black arrow designates the epithelium. The black box indicates typical region which is enlarged in (C-E). Scale bar: $20 \mu\text{m}$. (B) Results of image analysis. Number of MMG per mitochondria observed in each cross section. There are two cross sections per replicate and three replicates per treatment. U0: controls; U84 and U420: individuals exposed to 84 and 420 nM U respectively for 37 days. (C-E) Example of Transmission electron microscopy (TEM) micro photographs ($\times 6000$) for the U0, U84 and U420 treatments respectively. Each image is representative of an enlargement of region in black box shown in (A). MV shows the microvillus brush border of the epithelium; GB is a goblet cell; EV is an endocytosis vesicle. Scale bars: $2 \mu\text{m}$. The black boxes indicate typical regions which are enlarged in order to count MMG/ mitochondria. (F-G) TEM photograph ($\times 43000$) U0, U84 and U420 treatments respectively. Each photo represents enlargements of regions in black boxes in (C-E) respectively. The number MMG (arrowhead) and total number of mitochondria are scored in each $\times 43000$ photo. Scale bars: 500 nm .

to zebrafish gut wall. However after 37 d exposure to 84 nM and to 420 nM water-borne uranium, histological observations showed a loss of intestinal fold architecture (fig. 6.2E), large empty spaces at certain tips of intestinal folds (fig. 6.2F) and degenerating mucosa along the digestive tract, DT, (fig. 6.2G-I). There is not a clear dose dependant response between individuals exposed to 84 or to 420 nM U since the above mentioned histological effects were observed in both exposure conditions.

6.3.2 Subcellular effects of uranium

The amount of electron dense MMG decreased with exposure condition (fig. 6.1B). Energy-dispersive X-ray spectroscopy elemental analysis of electron dense granules in the mitochondria show that granules are mainly composed of calcium and phosphorus (not shown). There was no difference in total amount of mitochondria scored between conditions. Background levels of what appeared to be damaged mitochondria were similar between conditions. High-energy dispersive X-ray spectrometry analysis of gut wall tissue revealed U precipitates in the nucleus of an enterocyte cell (fig. 6.3C) in the U420 condition. Large amounts of phosphorus and to a lesser extent calcium were co-localized with uranium.

6.3.3 Effects of U on bacterial colonization of intestinal lumen

The qualitative scoring of bacterial colonization in intestines in each condition (n=6) revealed that each condition fluoresced differently (table 6.1). Lumen of control digestive tracts were generally colonized by thin clouds of bacteria. The fluorescence was rod shaped and in one instance appeared thinly spread out in the form of very intense specks. Lumen of DT in 84 nM condition seemed more densely colonized by eubacteria than control; lumen was occupied by dense clouds of eubacteria with rod shaped fluorescence. In one instance, part of the lumen was also intensely colonized by eubacteria with roundish fluorescence. Lumen of DT in the 420 nM condition were much less colonized by eubacteria than controls or 84 nM conditions. A third of the replicates showed negligible fluorescence. The second third was colonized by eubacteria with roundish fluorescence organized in roundish packets. However, one replicate was very intensely colonized with eubacteria with rod shaped fluorescence as in the 84 nM and control conditions.

6.4 Discussion

6.4.1 Histopathology of gut wall

Water-borne exposure to uranium also induced damage to gut wall of *Daphnia magna* exposed for 21d to 210 and 420 nM U respectively (Massarin et al.,

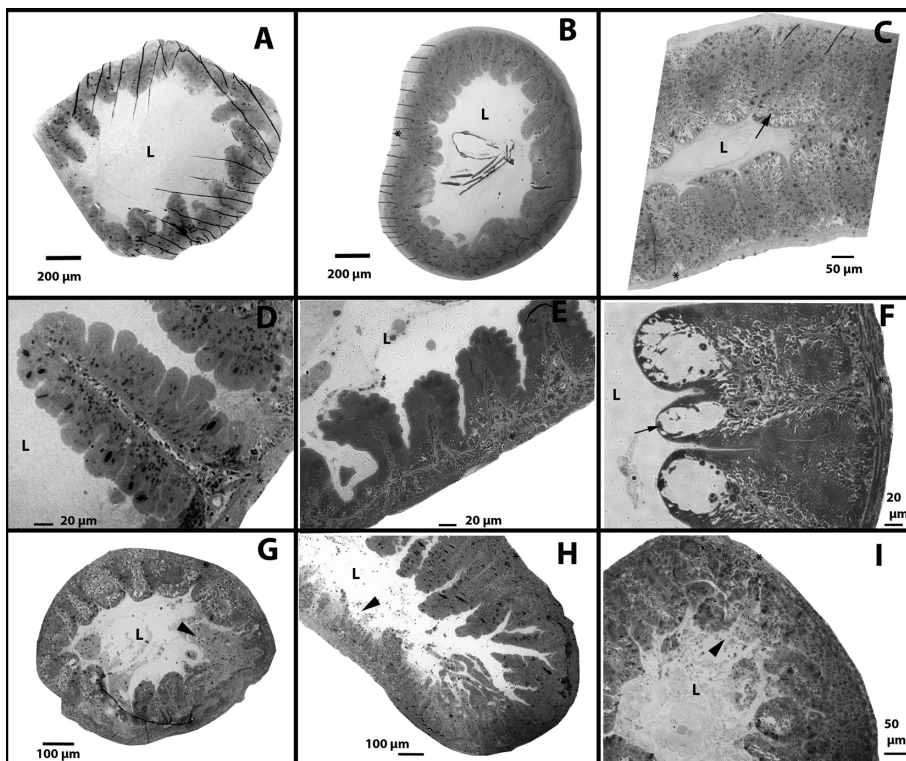


Figure 6.2: Tolidine blue plastic cross section of digestive tract (DT) of *Danio rerio*. * indicates muscularis and L shows the intestinal lumen. The mucosa comprises all of the cells layers between the muscularis and the lumen. Histology of control DT (A-D) shows that the mucosa is arranged in broad irregular folds. (A) cross section in anterior part of control intestine and (B) cross section in posterior part of control intestine; some debris is visible in lumen. (C) In many instances, vacuolization of cells increases at tips of intestinal folds as indicated by arrow. (D) Cross section of an anterior intestinal fold. The surface of the fold (epithelium) is organized as an irregular succession of hills and valleys. After 37 d of exposure to water-borne depleted uranium some histological changes to the gut wall can be observed (E-I). (E) The hill-valley configuration of the surface of intestinal folds in the anterior part of the intestine is mostly much smoother than control. (F) In some instances tips of intestinal folds are emptied of cell content (arrow). (G-I) entire portions of the mucosa degenerates (arrowhead) in some parts of the DT.

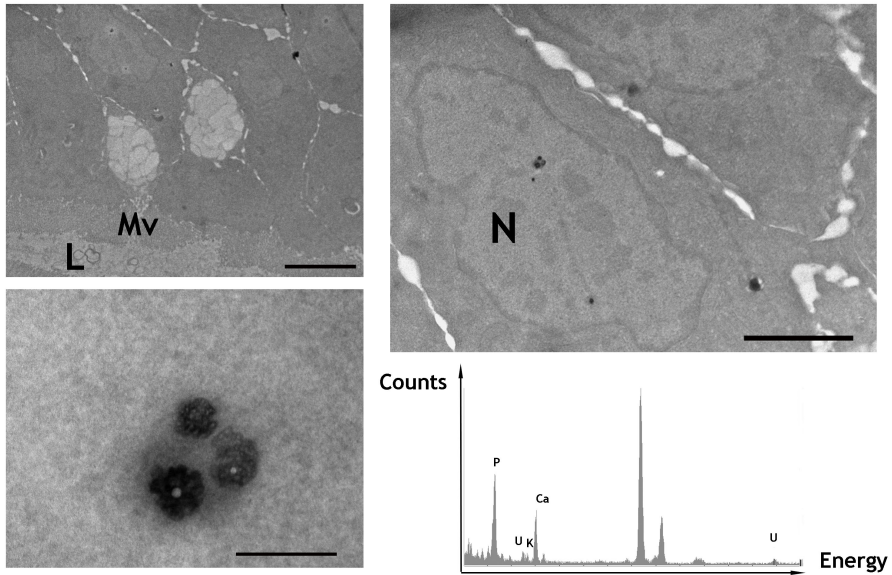
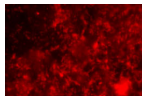
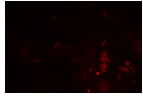
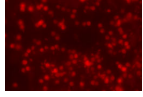
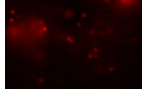
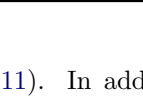


Figure 6.3: Histology and transmission electron microscopy (TEM) of uranium (U) precipitates in the nucleus of an epithelial cell. TEM images of an adult *Danio rerio* epithelium after 37d exposure to 420 nM water-borne depleted U. (A) TEM photo of epithelium,. Mv indicates microvillus brush border of enterocyte cells and L shows the intestinal lumen. (B) Enlargement of (A) with N indicating the nucleus. (C) Higher-power view of uranium precipitates in the nucleus. (D) Energy-dispersive X-ray spectroscopy microanalysis indicated the presence of U precipitates in the nucleus. Phosphorus (P), calcium (Ca) and to a lesser degree potassium (K) are co-localized. The two highest unlabelled peaks correspond to osmium and copper and are artefacts (see text). Scale bars: (A) 2 μm , (B) 5 μm and (C) 200 nm.

Table 6.1: Qualitative assessment of bacterial colonization of intestine of zebrafish, *Danio rerio* (n=6). (++) dense clouds of bacteria and (+) thinly dispersed bacteria across the lumen of the digestive tract with rod shaped fluorescence. (oo) dense packets of bacteria and (o) few packets of bacteria in lumen of the digestive tract with roundish shaped fluorescence. The images show representations of each type of scoring. (-) no or barely any fluorescence was observed. 0.5 is scored when both types of fluorescence is observed in lumen.

representative image	score	Control	U-84	U-420
	-	0	0	2
	++	2	4	1
	+	4	1.5	0
	oo	0	0.5	1
	o	0	0	2

2011). In addition, morphological changes in the gastrointestinal tract were observed for the earthworm *Eisenia andrei* (50d soil exposure) (Lourenço et al., 2011) and *Eisenia fetida* (28d soil exposure) (Giovanetti et al., 2010).

Histopathology of zebrafish tissue in response to similar exposure conditions reveal ultra-structural damage to gills, muscle and gonadal tissue after 20 d exposure to 420 nM U in the water (Barillet et al., 2010). Furthermore, at concentration ranges of 60-130 nM U in water, alterations to both muscle and olfactory bulb tissue were recorded in zebrafish after only 10 days (Lerebours et al., 2010b,a). This last observation constitutes the earliest histopathological response to water-borne U at such low concentrations.

In this study we are unable to evaluate how long before the mucosa began to degenerate and if in fact the phenomenon would intensify if we continued exposure. It is of interest to note that the link between alteration of structure is not so easily made with alteration of function. Most likely, the numerous tissue alterations which occur impact health on a much longer term than experiment duration. The loss of architectural folds of mucosa (fig. 6.2) and tissue degeneracy observed in some parts of the mucosa are suggestive of an

overall decrease in assimilation surface. But [Augustine et al. \(2012a\)](#) surmise that increases in costs for synthesis of structure and somatic maintenance best explain the phenomenon. Perhaps a whole mount histological study should be preferred over the study of each organ separately. In fact, somatic maintenance comprises protein turnover and maintaining cellular homeostasis. It is likely that detoxification pathways also contribute to somatic maintenance.

6.4.2 Alterations of mitochondrial metabolism

The physiological functions for which mitochondria sequester Ca^{2+} may be to induct mitochondria permeability transition and perhaps induce cell death ([Gunter et al., 2004](#); [Jiang et al., 2010](#)). The decrease in electron dense calcium containing MMG is suggestive of an onset of apoptosis in gut wall. This would explain how entire regions of the mucosa degenerate, although histological proof of apoptosis should be acquired in future experiments to confirm this.

A number of studies support toxicological action of U on mitochondrial metabolism. According to [Lerebours et al. \(2010a\)](#), U may increase permeability of the inner mitochondrial membrane to protons resulting in proton leakage through the inner mitochondrial membrane from the periplasmic space toward the matrix. U potentially targeted gill mitochondrial metabolism of *Procambarus clarkii* exposed to 126 nM U for 60d ([Al Kaddissi et al., 2011](#)).

This is in fact the first study where U was localized in the nucleus of zebrafish cells. It is assumed that uranium mainly enters the organism via the gills. ([Lerebours, 2009](#)) proposes that U may also enter via the olfactory rosettes since U accumulates in the olfactory bulb. Zebrafish, as fresh water organisms do not drink, and it is generally assumed that uptake via the gut wall must be negligible. Since U was found in epithelial cells, the importance of uptake through the gut wall and contributions of this uptake route to total internalized U remain an open question. [Pereira et al. \(2012\)](#) showed that uranium precipitates were internalized in zebrafish fibroblast cell vacuoles suggestive of a detoxification mechanism, although no U was found in muscles, gonad or brain tissue ([Barillet, 2007](#); [Bourrachot, 2009](#); [Lerebours, 2009](#)).

6.4.3 Bacterial colonization of intestinal lumen

The microbial community might be strongly shaped by deterministic forces inside the intestinal habitat. Bacteria are important partners for invertebrates and vertebrates. And it is only in the latter that symbiotic interactions with large diverse communities of bacteria are found. The host-microbe interaction is rarely studied in an ecotoxicity context, but the present study shows that bacterial colonization of the intestinal lumen may be sensitive to environmental stressors such as U. Parasites were observed in the lungs of frogs at the mine ([Marques et al., 2009](#)), but not in the lungs of frogs in the reference lake. This is further empirical support that host-microbe interaction may be modified when the organism is under stress.

6.5 Conclusion

We show in this study that chronic exposure to concentrations of uranium as low as 84 nM U already perturbs the homeostasis of the digestive system. Several alterations were observed. Entire regions of the mucosa were degenerating. Ultra structural TEM analysis show a decrease in electron dense mitochondrial matrix granules. We confirmed that the granules contain important amounts of calcium and suggest that they are involved in sequestering calcium and so important in the regulation of calcium homeostasis. The degradation of the mucosa may be a consequence of increased apoptosis, although future studies should include markers for apoptosis to confirm this. There is no clear dose-response for damage to gut wall. However at higher concentrations the lumen of some replicates were hardly colonized by bacteria. Furthermore the morphology of the fluorescence was different between both exposure conditions. All together these last results suggest that uranium may perturb host-microbe interaction.

Acknowledgements

This work is part of the ENVIRHOM research program supported by the Institute for Radioprotection and Nuclear Safety and the Provence Alpes Côte d'Azur region. We are grateful to Karine Faucher for helping with tissue preparation of controls.

General Conclusion

The objective of this thesis was first to understand effects of uranium at the organism level (growth and reproduction), second to link those effects to mechanisms operating at cellular and molecular levels and third to extrapolate to effects on population level dynamics. Deleterious effects on the organism are detected by comparing the performance of individuals who are exposed to the stressor (uranium) to the performance individuals who are not (blank). Therefore, to understand uranium induced deviations on physiological performance of zebrafish, I first needed to understand (and quantify) the physiological performance of the blank.

The results of this work gave rise to a state of the art in zebrafish, *Danio rerio* metabolism with a number of novel insights which are discussed in section 7.1. Section 7.2 further discusses the main findings in terms of organism level response to depleted uranium. Perspectives for integrating organism level physiology to sub(cellular) and population level responses are then presented in sections 7.3 and 7.4. Finally, section 7.5 is a general reflection on the role this work has to play in modern day environmental risk assessment and (eco)toxicological research.

7.1 Organism physiology

Since uranium was previously shown to impact the anti-oxidative stress system: upregulation of genes (Lerebours et al., 2009) and perturbation of enzyme levels (Barillet et al., 2007) and may be responsible for DNA strand breaks (Barillet et al., 2005), I postulated that effects on maturity maintenance or ageing (ROS production) were important physiological processes to quantify for this study. Consequently, experimental and theoretical effort was invested in quantifying maturity maintenance (growth and reproduction experiment at three food levels). Furthermore, I also parametrized the ageing module (Kooijman, 2010, Chap.6) to zebrafish ageing data (fig. 2.4).

However, the maturity concept of DEB theory, needed to quantify maturation rates, was a very abstract concept. In chapters 2 and 4 cumulated energy invested in maturation to reach each developmental milestone as defined in published staging atlases was determined for three species of animals: zebrafish, the quacking frog (*C. georgiana*) and Bibron's toadlet (*P. bibronii*). In chapter 2 data from a wide variety of data sets was integrated into a single estimation procedure from which we deduced the cumulative energetic investment in maturity for development. In chapters 4 the focus was more on empirical support for the concept using very careful data on developmental energetics acquired by C. Mueller in the context of her PhD research (Mueller, 2011).

The physiological insight is that the contribution of maturation to total O₂ consumption is not negligible for any of the species; the theoretical insight is that DEB theory can capture heterochrony (McKinney and McNamara, 1991) as has been experimentally measured when comparing the developmental timing of two separate species of frogs on the basis of a generic staging atlas for all frogs (Gosner, 1960); an ecological insight is that the maturity concept is very useful for understanding evolutionary flexibility in parameter values in response to environmental constraints; an ecotoxicological insight is that O₂ consumption in combination with developmental stage against age are data sets which can be included into the analysis of toxic effects on organisms.

Furthermore, additional measurements of O₂ consumption and developmental stage in combination with the more traditional measurements of growth and reproduction would help discriminate between different types stressor induced effects on the metabolism.

Fig. 1.1 represented the life-cycle of zebrafish as published in the literature. Based on the insight provided in chapter 2 the life-cycle scheme is updated with the cumulative energy invested to reach each life stage (J) and an additional life stage (metamorphosis) which marks the transition from the V1-morphic juvenile I stage to the isomorphic juvenile II (fig. 7.1).

The inclusion of a V1-morphic juvenile I stage to explain accelerated growth and differences in parameter values between juveniles and adults (Kooijman et al., 2011) still remains an open point of discussion. Nonetheless there exists a tantalizing piece of empirical evidence in support of changing surface area to volume relationships during the ontogeny of certain teleost species as briefly explained in the following paragraph.

Mineral fluxes relate to energetics using the mass balance equation (??) from Kooijman (2010). The morphology of O₂ consumption against volume (or mass) curve changes relative to surface-area to volume relationships (see White et al., 2011, for a concrete example), thus the inclusion of a V1-morphic juvenile I stage may represent a corollary for observed biphasic allometric relationships between O₂ consumption and body mass for certain teleost species (Post and Lee, 1996; Killen et al., 2007).

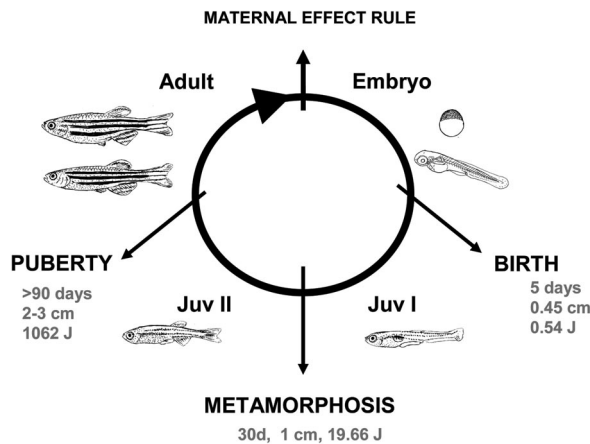


Figure 7.1: Life-cycle of zebrafish, *Danio rerio*. Sizes and ages are qualitative. Embryo: no external feeding; juvenile (juv) I: external feeding starts and surface area increases proportional to volume; juv II: isomorphic growth resumes; adult: energy allocation to maturity stops and allocation to reproduction starts. Initial energy in an egg is specified in DEB theory using the maternal effect rule where the reserve density of the mother at spawning is equal to the reserve density of the offspring at birth (Kooijman, 2009b). Length (cm), age (d) and cumulative investment in maturity (J) are specified for the three life stages: birth, metamorphosis and puberty.

7.2 Organism stress responses

DEBtox was originally the name of a software designed to analyse toxicity data issued from standardized OECD guideline assays (Kooijman and Bedaux, 1996). The term has been expanded (see e.g. Jager and Zimmer, 2012) to include the analysis of all types of toxicity data using a DEB model. In the case of the present thesis the standard DEB model with V1-morphic juvenile I phase extension (Kooijman et al., 2011) was applied to several data sets simultaneously. This study is original in four respects

- the non-scaled standard DEB model was used for a DEBtox analysis, as in Jager and Klok (2010)
- different toxicity experiments with different protocols were included in the same study
- DEB model parameter values were not estimated from the controls of the toxicity data but were obtained in a separate study (chapter 2)
- toxic effects on reproduction were further detailed with a buffer handling rules module

By integrating buffer handling rules, there is now a handle to analyse behavioural data using the DEB model. Certain parameters such as ingestion

level, triggering batch preparation or batch energy density quantify certain aspects of the individuals behaviour. If ranges of values are systematically observed for controls, then it is possible to evaluate effects on these parameters. This opens up a very exciting research venue where energetics and behavioural ecology link up quantitatively.

It turns out, that while a very useful tool for evaluating effects on maturation was developed, we did not actually detect effects on maturation in the concentration ranges of water-borne depleted uranium studied in our laboratory (84 - 1054 nmol U l⁻¹). A very promising research venue would be applying the maturity concept for quantifying effects of ionizing radiation. The general philosophy is that effects of irradiation on development could potentially be captured in this same modelling framework by assuming that ionizing radiation effects maturation by lowering the maturity thresholds to reach each developmental stage (tables 2.3 and 2.4). By lowering the maturity threshold to reach each stage of development, i.e. the amount of joules necessary to reach a particular stage, development is accelerated. But this may come with a penalty: certain regulatory or physiological systems may not be fully formed which may then impact survival and/ or be expressed in the form of developmental abnormalities. We suggest careful observations of stage of development against age in combination with growth and survival in future experiments to evaluate the potential of modifying energy invested in maturation and its consequences on development and survival.

Effects on the embryo and early juvenile stages are really suggestive of an increase in the cost of synthesis of a unit of structure, but this was not proven to be the case for adults. For the latter the data show either an increase in volume linked somatic maintenance costs or a decrease in assimilation.

DEB theory allows automatic generation of complexity via the environment and parameters Marques et al. (2011). The standard DEB model responds to forcing variables allowing individuals in different environments to behave differently (Kooijman et al., 2011). An important recurring theme in each of the studies in this thesis is that environmental conditions (such as food availability) contribute in an important manner to the scatter naturally inherent in biological data (e.g. Kooijman, 2010; Augustine et al., 2011b).

7.3 From individuals to molecules...

We are still far from quantifying which (sub)cellular processes interact in which process of the standard DEB model. A lot of work lies ahead to link organism level response to genetic and protein assays used to determine (sub)cellular responses to uranium toxicity.

The research line aiming to bridge the gap between individual and (sub)cellular responses should work stepwise (and in small increments) down the ladder of complexity with the individual as starting point. For this reason, I took an interest in possible alterations of the histology of the intestine in chapter 6.

While we found signs of damage to the gut wall and perhaps even a disturbance to host-microbe interactions, no quantitative mechanistic link can be made between results in chapters 6 and 5.

I argued in chapter 5 that depleted uranium increases somatic maintenance of exposed individuals. Somatic maintenance comprises a multitude of coordinated processes operating at sub-cellular levels: protein ubiquitylation, exocytosis, endocytosis, post-translational protein modification (N-glycosylation, acetylation, O-glycosylation), regulated forward membrane flux etc. Maturity maintenance is assumed to comprise processes linked to the hormonal and immune systems which also comprise very complex cellular mechanisms. The (subtle) assumed difference between both types of maintenance is that the first is compulsory and the second is perhaps optional. Some very interesting data can be acquired based on this type of discrimination which may help quantification of both types of processes. An example would be to compare the physiological performance of sick and healthy individuals exposed to a same toxicant who has already been shown to increase somatic maintenance costs.

A lot of insight would be gained if sub-organismal toxicity studies would include the quantification of energetics at the individual level as has been previously done in [Swain et al. \(2010\)](#); [Wren et al. \(2011\)](#). However we choose to broach to problem of how microscopic spatial and rapid temporal scales relate to the integrated physiology of an organism, I would always recommend maintaining controls and exposed at several different types of environments (e.g. different food levels). Future experimental design should further standardize and/ or quantify ingestion as in e.g. [Evers and Kooijman \(1989\)](#).

7.4 From individuals to populations...

The third overarching objective of this project was extrapolation of individual response to population dynamics. I am less convinced than at the onset of the project about the relevance of population growth rates since populations are not isolated groups but subject to input (prey) and predation and disease (output). [Muller et al. \(2009\)](#) conclude that identifying the correct toxicity sub-model is unimportant for population dynamics at constant food levels. I think a more useful formulation of this conclusion is: physiology of exposed organisms must be evaluated at several food levels in order to correctly identify the toxic mode of action of a compound on the metabolism. Constant food conditions are useful experimentally but not an environmentally relevant situation in itself. If the aim is to extrapolate effects to the field and so to ecosystem level effects, conclusions must be robust to varying food levels.

This robustness increases with increasing accuracy in quantification of physiological processes operating at the individual level (DEB model parameter values). This is in line with [Jager and Klok \(2010\)](#) who compare three different formulations of a DEB model, including the full standard model which is also more exacting in terms of required data. It was the full standard model which

was parametrized to zebrafish in this thesis.

The standard DEB model offers the best ratio of detail over (structural) simplicity for quantifying metabolic organisation in respect to stylized facts in biology (Sousa et al., 2008; Kooijman, 2010; Lika and Kooijman, 2011). Some concern has been expressed in the ecotoxicology community as to the difficulty in fully parametrizing a DEB model. I think the outcome of this thesis shows such an obstacle is surmountable, furthermore increasing time investment in clean water experiments (parametrizing the blank) relative to exposure experiments for increased extrapolation robustness is a very environmental friendly and cost efficient research perspective.

A promising research venue would be to integrate properties of individual zebrafish as quantified in this thesis to population models who explicitly treat the dynamics of prey and the substrate of the prey along the lines of Kooi et al. (2008); Bontje et al. (2009).

7.5 Applications of this work to environmental risk assessment

Data on physiological performance generally comprises one or more of the following types of measurements: ingestion rates, length, mass, age, developmental stage, number of eggs, O₂ consumption, bomb calorimetry, survival etc. DEB model parameters are estimated from the simultaneous observation of one or more of the above types of measurements preferably in dynamic or contrasting (controlled) environments. According to DEB theory, parameter values are individual specific meaning that genetic differences between individuals translates into (slight) differences in parameter values.

In practice the detail at which the measurements are acquired do not allow precise quantification of each parameter value such that we can discriminate between different values for members of a same species. At present, we do not even have an accurate idea about the natural distribution of values between similar individuals. However, for many applications that level of precision is not required and it is possible to obtain estimates for the mean value of the species; these may or may not differ between gender and/or life stages.

The mean parameter set concisely summarizes the state of the art of the eco-physiology for a given species. It can be referred to as the species baseline metabolism or metabolism of the blank. Ideally, this mean parameter set should be independent of experimental protocol and laboratory.

Parameter estimation for the species under consideration constitutes the groundwork for applying DEB theory to any concrete open problem in biology. From an ecological/ evolutionary perspective the aim is to quantify evolutionary/geographical trends via changes or patterns in parameter values (Alunno-Bruscia et al., 2009, 2011). In the field of ecotoxicology, the general aim is to quantify perturbations to metabolism as changes in specific parameter values (e.g. Kooijman and Bedaux, 1996; Muller et al., 2009; Jager and Zimmer,

2012). A natural habitat is inherently dynamic and (chemical) stressors are always naturally present so both ecology and ecotoxicology share a similar problem: DEB model parameter estimation.

Whether or not (i) the standard DEB model (Kooijman, 2010, Chap.2) is the reference for the metabolic organisation of animals and (ii) a single set of parameters quantifies energy fluxes throughout the life-cycle continuously needs to be verified. The work carried out in this thesis lends support to both (i) and (ii) for the following reasons.

The DEB model was applied to three separate species (chapters 2 and 4). Acceleration of growth in zebrafish and of development in the quacking frog were detected thanks to deviations of observations from the predictions of the standard DEB model. Alternatively the life history of Bibron's toadlet nicely matches that predicted by the standard DEB model. A critical reader might inspect the growing library of DEB parameter values, the Add_my_Pet library (<http://www.bio.vu.nl/thb/deblab>, (Lika et al., 2011a)), where the mean parameter values for more than a 100 animal species can be compared.

In chapter 2 (fig. 2.6) the simultaneous observation of growth and reproduction in four separate females was crucial for quantifying the allocation fraction to soma (κ) maturity maintenance (\dot{k}_J) and cumulative energy investment to reach puberty (E_H^p). What we see in chapter 5, is that cumulated reproductive output of the different individual females is remarkably well captured using the mean parameters values for zebrafish obtained in chapter 2 for two separate reproduction trials sporting two distinct experimental protocols (fig. 5.3 and fig. I.1). The DEB model was also fitted to published respiration data (not shown) and it was also consistent the observations when taking feeding (inferred from growth) into account.

In sum, what we show via this thesis is that a mean set of DEB parameter values really does concisely summarize the state of the art on zebrafish metabolism and that these values are independent of the study and experimental protocol.

Reproduction data are typically very difficult to analyse because the scatter is so high, however it is an extremely important endpoint from a population dynamics perspective. Embryo development is of particular interest in radiation ecology and is born of our direct concern with our own offsprings well fare. Effects of any type of (chemical) stressor on the growth, reproduction and development of zebrafish can now be assessed on the basis of deviations from the mean parameter values of the species.

The continuous standardization of toxicity experiments (e.g. OECD guideline) may not be promoting (scientific) progress because the protocol needs to be based on how long it takes for the internal concentration of compound Q to be in equilibrium with its surroundings and so depends on the species, the life-stage of the individual and the type of compound (Baas, 2010). Results need to be comparable across experiments and across species and yet the solution is not in standardization of experimental protocol. In light of the results obtained in this thesis, DEB theory is perfectly suited to solve this particular

conundrum.

The insight provided in chapter 5, where the intensity of the effect of uranium on reproduction depends on initial conditions of each individual and initial conditions vary too much across individuals to enable comparison of means, is a really typical illustration of why biology based modelling is important for understanding toxic effects.

The applications of this work for environmental risk assessment are thus very clear: the same parameters can be used to evaluate toxic effects of a library of chemicals/ environmental stressors and there is no need to use identical/ standard experimental protocols.

Bibliography

- Adam, C. (2006). Indicateurs de l'exposition et des effets des radionucléides dans les écosystèmes aquatiques continentaux. HDR, Université Aix-Marseille I.
- Al Kaddissi, S., Legeay, A., Gonzalez, P., Floriani, M., Camilleri, V., Gilbin, R., and Simon, O. (2011). Effects of uranium uptake on transcriptional responses, histological structures and survival rate of the crayfish *Procambarus clarkii*. *Ecotoxicol Environ Saf*, 74:1800–1807.
- Alunno-Bruscia, M., Veer, H. v. d., and Kooijman, S. A. L. M. (2009). The AquaDEB project (phase i): Analysing the physiological flexibility of aquatic species and connecting physiological diversity to ecological and evolutionary processes by using Dynamic Energy Budgets. *J Sea Res*, 62:43–48.
- Alunno-Bruscia, M., Veer, H. v. d., and Kooijman, S. A. L. M. (2011). The AquaDEB project: Physiological flexibility of aquatic animals analysed with a generic dynamic energy budget model (phase II). *J Sea Res*, 66:263–269.
- Alves, L., Borgmann, U., and Dixon, D. (2009). Kinetics of uranium uptake in soft water and the effect of body size, bioaccumulation and toxicity to *Hyalella azteca*. *Env Poll*, 157(8-9):2239–2247.
- Augustine, S., Gagnaire, B., Adam-Guillermin, and Kooijman, S. A. L. M. (2011a). Developmental energetics of zebrafish, *Danio rerio*. *Comp Biochem Physiol A*, 159:275–283.
- Augustine, S., Gagnaire, B., Adam-Guillermin, and Kooijman, S. A. L. M. (2012a). Effects of uranium on the metabolism of zebrafish, *Danio rerio*. *Aquat Toxicol*. accepted.
- Augustine, S., Litvak, M. K., and Kooijman, S. A. L. M. (2011b). Stochastic feeding of teleost fish and their metabolic handling of starvation. *J Sea Res*, 66:411–418.
- Augustine, S., Pereira, S., Gagnaire, B., Floriani, M., Camilleri, V., Adam-Guillermin, C., and Kooijman, S. A. L. M. (2012b). Uranium induced alteration of gut wall histology in zebrafish, *Danio rerio*. in prep.
- Baas, J. (2010). *Effects of mixtures explained: From laboratory tests to effects in the environment*. PhD thesis, Vrije Universiteit, Amsterdam.
- Bagatto, B., Pelster, B., and Burggren, W. W. (2001). Growth and metabolism of larval zebrafish: effects of swim training. *J Exp Biol*, 204:4335–4343.
- Bailey, K. M. and Houde, E. D. (1989). Predation on the eggs of larvae of marine fishes and the recruitment problem. *Adv Mar Biol*, 25:1–83.
- Barillet, S. (2007). *Toxicocinétique, Toxicité Chimique et Radiologique de l'Uranium chez le poisson zèbre, (Danio rerio)*. PhD thesis, Université Paul Verlaine de Metz.

- Barillet, S., Adam, C., Palluel, O., and Devaux, A. (2007). Bioaccumulation, oxidative stress, and neurotoxicity in *Danio rerio* exposed to different isotopic compositions of uranium. *Envir Toxicol Chem*, 3(3):497–505.
- Barillet, S., Adam, C., Palluel, O., M., P. J., and Devaux, A. (2011). Uranium bioaccumulation and biological disorders induced in zebrafish (*Danio rerio*) after a depleted uranium waterborne exposure. *Env Poll*, 159:495–502.
- Barillet, S., Buet, A., Adam, C., and Devaux, A. (2005). Does uranium exposure induce genotoxicity in the teleostean *Danio rerio*? First experimental results. *Radioprotection*, 40:S175–S181.
- Barillet, S., Larno, V., Floriani, M., Devaux, A., and Adam, C. (2010). Ultrastructural effects on gill, muscle, and gonadal tissues induced in zebrafish (*Danio rerio*) by a waterborne uranium exposure. *Aquat Toxicol*, 100:295–302.
- Barker, J., Grigg, G. C., and Tyler, M. J. (1995). *A field guide to Australian frogs*. Surrey Beatty and Sons, Chipping Norton NSW.
- Barrionuevo, W. R. and Burggren, W. W. (1999). O₂ consumption and heart rate in developing zebrafish (*Danio rerio*): Influence of temperature and ambient O₂. *Am J Physiol - Reg I*, 276:505–513.
- Barrionuevo, W. R., Fernandes, M. N., and Rocha, O. (2010). Aerobic and anaerobic metabolism for the zebrafish, *Danio rerio*, reared under normoxic and hypoxic conditions and exposed to acute hypoxia during development. *Braz J Biol*, 70:425–434.
- Bates, J. M., Mittige, E., Kuhlman, J., Baden, K. N., Cheesman, S. E., and Guillemain, K. (2006). Distinct signals from the microbiota promote different aspects of zebrafish gut differentiation. *Dev Biol*, 279:374–386.
- Best, J., Adatto, I., Cockington, J., James, A., and Lawrence, C. (2010). A novel method for rearing first-feeding larval zebrafish: polyculture with Type L saltwater rotifers (*Brachionus plicatilis*). *Zebrafish*, 7(3):89–295.
- Blaxter, J. and Fuiman, L. (1990). The role of sensory systems of herring larvae in evading predatory fishes. *J mar biol Ass UK*, 70:413–427.
- Bodiguel, X., Maury, O., Mellon-Duval, C., Rounsard, F., Le Guellec, A. M., and Loizeau, V. (2009). A dynamic and mechanistic model of PCB bioaccumulation in the European hake (*Merluccius merluccius*). *J Sea Res*, 62:124–134.
- Bontje, D., Kooi, B. W., Liebig, M., and Kooijman, S. A. L. M. (2009). Modelling long-term ecotoxicological effects on an algal population under dynamic nutrient stress. Water Research. *Wat Res*, 43:3292–3300.
- Booth, D. and Astill, K. (2001). Incubation temperature, energy expenditure and hatching size in the green turtle (*Chelonia mydas*), a species with temperature-sensitive sex determination. *Aust J Zool*, 49:389–396.
- Bosch, J., Johnson, F. X., Clément, E., Mertens, R., and Roubanis, N. (2009). Panorama of energy: energy statistics to support eu policies and solutions. Technical report, Eurostat.
- Bourrachot, S. (2009). *Etude des effets biologique de l'exposition à l'uranium chez le poisson zèbre (D. rerio). Impact sur les stades de vie*. PhD thesis, L'Université Aix-Marseille I - Université de Provence.
- Bourrachot, S., Simon, O., and Gilbin, R. (2008). The effects of waterborne uranium on the hatching success, development, and survival of early life stages of zebrafish (*Danio rerio*). *Aquat Toxicol*, 90:29–36.

- Bradford, D. (1984). Physiological features of embryonic development in terrestrially-breeding plethodontid salamanders. In Seymour, R., editor, *Respiration and Metabolism of Embryonic Vertebrates.*, pages 87–98. Dordrecht.
- Bradford, D. (1990). Incubation time and rate of embryonic development in amphibians: the influence of ovum size, temperature, and reproductive mode. *Physiol Zool*, 63:1157–1180.
- Brown, E. B. (1958). *The physiology of fish. Volume I. Metabolism.* Academic Press Inc., Publishers, New York.
- Cooley, H. M., Evans, R. E., and Klaverkamp, J. F. (2000). Toxicology of dietary uranium in lake whitefish (*Coregonus clupeaformis*). *Aquat Toxicol*, 48:495–515.
- Craig, J. F. and Fletcher, J. M. (1984). Growth and mortality of zebrafish, *Brachydanio rerio* (Hamilton Buchanan), maintained at two temperatures and on two diets. *J Fish Biol*, 25:43–55.
- Cushing, D. (1975). *Marine ecology and fisheries.* Cambridge.
- Domingo, J. L. (2001). Reproductive and developmental toxicity of natural and depleted uranium: a review. *Repro Toxicol*, 15:603–609.
- Doughty, P. (2002). Coevolution of developmental plasticity and large egg size in *Crinia georgiana* tadpoles. *Copeia*, 4:928–937.
- Doughty, P. and Roberts, J. (2003). Plasticity in age and size at metamorphosis of *Crinia georgiana* tadpoles: responses to variation in food levels and deteriorating conditions during development. *Aust J Zool*, 51:271–284.
- Duellman, W. and Trueb, L. (1986). *Biology of Amphibians.* McGraw-Hill, New York.
- Eaton, R. C. and Farley, R. D. (1974a). Growth and the reduction of depensation of zebrafish, *Brachydanio rerio*, reared in the laboratory. *Copeia*, 1:204–209.
- Eaton, R. C. and Farley, R. D. (1974b). Spawning cycle and egg production of zebrafish, *Brachydanio rerio* in the laboratory. *Copeia*, 1:195–204.
- Eichinger, M., Loizeau, V., Le Guellec, A. M., Gastineau, O., Rroupsard, F., and Bacher, C. (2012). An individual modelling approach to estimate polychlorinated biphenyl (PCB) bioaccumulation and their potential effects on common sole growth. in prep.
- Eichinger, M., Loizeau, V., Rroupsard, F., Le Guellec, A., and Bacher, C. (2010). Modelling growth and bioaccumulation of Polychlorinated biphenyls in common sole (*Solea solea*). *J Sea Res*, 64(3):373 – 385.
- Evers, A. G. and Kooijman, S. A. L. M. (1989). Feeding, digestion and oxygen consumption in *Daphnia magna* a study in energy budgets. *Neth J Zoo*, 39(1-2):56–78.
- Fernandes, H. M., Veiga, L. H. S., Franklin, M. R., Prado, V. C. S., and Taddei, J. F. (1995). Environmental impact assessment of uranium mining and milling facilities: A study case at the poços de caldas uranium mining and milling site, brazil. *J Geochem Explor*, 52:161–173.
- Flye-Sainte-Marie, J., Jean, F., Paillard, C., and Kooijman, S. A. L. M. (2009). A quantitative estimation of the energetic cost of brown ring disease in the Manila clam using Dynamic Energy Budget theory. *J Sea Res*, 62:114–123.
- Forbes, E. L., Preston, C. D., and Lokman, P. M. (2010). Zebrafish (*Danio rerio*) and the egg size versus egg number trade off: effects of ration size on fecundity are not mediated by orthologues of the Fec gene. *Reprod Fert Develop*, 22:1015–1021.

- Fortin, C., Denison, F. D., and Garnier-Laplace, J. (2007). Metal-Phytoplankton interactions: modeling the effect of competing ions (H^+ , Ca^{2+} , and Mg^{2+}) on uranium uptake. *Envir Toxicol Chem*, 26(2):242–248.
- Fortin, C., Dutel, L., and Garnier-Laplace, J. (2004). Uranium complexation and uptake by a green alga in relation to chemical speciation: the importance of the free uranyl ion. *Envir Toxicol Chem*, 23:974–981.
- Fournier, E., Tran, D., Denison, F., Massabuau, J.-C., and Garnier-Laplace, J. (2004). Valve closure response to uranium exposure for a freshwater bivalve (*Corbicula fluminea*): Quantification of the influence of pH. *Envir Toxicol Chem*, 23(5):1108–1114.
- Freitas, V., Cardosa, J. F. M. F., Lika, K., Peck, M. A., Campos, J., Kooijman, S. A. L. M., and van der Veer, H. W. (2010). Temperature tolerance and energetics: a dynamic energy-based comparison of North Atlantic marine species. *Philos Trans R Soc B*, 365:3553–3565.
- Gergs, R. and Rothhaupt, K. O. (2008). Feeding rates, assimilation efficiencies and growth of two amphipod species on biodeposited material from zebra mussels. *Freshwater Biol*, 53:2494–2503.
- Gerhard, G. S. and Cheng, K. C. (2002). A call to fins! Zebrafish as a gerontological model. *Aging Cell*, 1:104–111.
- Gerhard, G. S., Kauffman, E. J., Wang, X., Stewart, R., Moore, J. L., Kasales, C. J., Demidenko, E., and Cheng, K. C. (2002). Life spans and senescent phenotypes in two strains of Zebrafish (*Danio rerio*). *Exp Gerontol*, 37(8-9):1055–1068.
- Gerlach, G. (2006). Pheromonal regulation of reproductive success in female zebrafish: female suppression and male enhancement. *Anim Behav*, 72:1119–1124.
- Giovanetti, A., Fesenko, S., Cozzella, M., Asencio, L., and Sansone, U. (2010). Bioaccumulation and biological effects in the earthworm *Eisenia fetida* exposed to natural and depleted uranium. *J Environ Radioact*, 101(6):509–516.
- Gómez-Requeni, P., Conceição, L. E. C., Olderbakk Jordal, A. E., and Rønnestad, I. (2010). A reference growth curve for nutritional experiments in zebrafish (*Danio rerio*) and changes in whole body proteome during development. *Fish Physiol Biochem*, pages 1–17.
- Gosner, K. (1960). A simplified table for staging anuran embryos and larvae with notes on identification. *Herpetologica*, 16:183–190.
- Guillaume, J., Kaushik, S., Bergot, P., and Métailler, R. (1999). *Nutrition et alimentation des poissons et crustacés*. INRA.
- Gunter, T. E., Yule, D. I., Gunter, K. K., Eliseev, R. A., and Salter, J. D. (2004). Calcium and mitochondria. *FEBS letters*, 567:96–102.
- HC (2008). Guidelines for Canadian Drinking Water Quality Summary Table. Federal-Provincial-Territorial Committee on Drinking Water of the Federal-Provincial-Territorial Committee on Health and the Environment. Technical report, Health Canada.
- Hill, A. J., Teraoka, H., Heideman, W., and Peterson, R. E. (2005). Zebrafish as a model vertebrate for investigating chemical toxicity. *Toxicol Sci*, 86(1):6–19.
- Hisaoka, K. K. and Firlit, C. F. (1962). Ovarian cycle and egg production in the zebrafish, *Brachydanio rerio*. *Copeia*, 4:788–792.
- Hjort, J. (1914). Fluctuations in the great fisheries of Northern Europe viewed in the light of biological research. *Rapp P-V Reün Cons Int Explor Mer*, 20:1–228.

- Houde, E. D. (1987). Early life dynamics and recruitment variability. *Am Fish Soc Symp*, 2:17–29.
- Hoyt, D. (1987). A new model of avian embryonic metabolism. *J Exp Biol Supp*, 1:127–138.
- IRSN (2010). Baromètre IRSN 2010: perception des risques et de la sécurité. <http://www.irsn.fr>, IRSN: Publications et Baromètre IRSN.
- Jager, T., Alda Alvarez, O., Kammenga, J. E., and Kooijman, S. A. L. M. (2005). Modelling nematode life cycles using dynamic energy budgets. *Funct Ecol*, 19:136–144.
- Jager, T., Crommentuijn, T., Van Gestel, C. A. M., and Kooijman, S. A. L. M. (2004). Simultaneous modeling of multiple end points in life-cycle toxicity tests. *Environ Sci Technol*, 38:2894–2900.
- Jager, T., Crommentuijn, T., van Gestel, C. A. M., and Kooijman, S. A. L. M. (2006a). Chronic exposure to chlorpyrifos reveals two modes of action in the springtail *Folsomia candida*. *Env Poll*, 145:452–458.
- Jager, T., Heugens, E. H. W., and Kooijman, S. A. L. M. (2006b). Making sense of ecotoxicological test results: towards application of process-based models. *Ecotoxicology*, 15:305–314.
- Jager, T. and Klok, C. (2010). Extrapolating toxic effects on individuals to the population level: the role of dynamic energy budgets. *Philos Trans R Soc B*, 365:3531–3540.
- Jager, T., Vandenbrouck, T., Baas, J., De Coen, W. M., and Kooijman, S. A. L. M. (2010). A biology based approach for mixture toxicity of multiple endpoints over the life cycle. *Ecotoxicology*, 19:351–361.
- Jager, T. and Zimmer, E. I. (2012). Simplified dynamic energy budget model for analysing ecotoxicity data. *Ecol Model*, 225:74–81.
- Jardine, D. and Litvak, M. K. (2003). Direct yolk sac volume manipulation of zebrafish embryos and the relationship between offspring size and yolk sac volume. *J Fish Biol*, 63:388–397.
- Jiang, L., Allagnat, F., Nguidjoe, E., Kamagate, A., Pachera, A., Vanderwinden, J.-M., Bini, M., Carafoli, A., Eizirik, D. L., Cardozo, A. K., and Herchuelz, A. (2010). Plasma Membrane Ca^{2+} -ATPase overexpression depletes both mitochondrial and endoplasmic reticulum Ca^{2+} stores and triggers apoptosis in insulin-secreting BRIN-BD11 cells. *J Biol Chem*, 285(40):30634–30643.
- Jurgens, B. C., Fram, M. S., Belitz, K., Burow, K. R., and Landon, M. K. (2010). Effects of Groundwater Development on Uranium: Central Valley, California, USA. *Ground Water*, 48(6):913–928.
- Jusup, M., Klanjscek, T., Matsuda, H., and Kooijman, S. A. L. (2010). A full lifecycle bioenergetic model for bluefin tuna. *PLoS ONE*, 6(7):e21903.
- Kamler, E. (2005). Parent-egg-progeny relationships in teleost fishes: an energetics perspective. *Rev Fish Biol Fisher*, 15:399–421.
- Kanther, M. and Rawls, J. F. (2010). Host-Microbe interactions in the developing zebrafish. *Curr Opin Immunol*, 22:10–19.
- Kelly, J. and Janz, D. (2009). Assessment of oxidative stress and histopathology in juvenile northern pike (*Esox lucius*) inhabiting lakes downstream of a uranium mill. *Aquat Toxicol*, 92(4):240–249.

- Killen, S. S., Costa, I., Brown, J. A., and Gamperl, A. K. (2007). Little left in the tank: metabolic scaling in marine teleosts and its implications for aerobic scope. *Proc Royal Soc B*, 274:431–438.
- Kimmel, C. B., Ballard, W. W., Kimmel, S. R., Ullmann, B., and Schilling, T. F. (1995). Stages of embryonic development of the zebrafish. *Dev Dynam*, 203(3):253–310.
- Kooij, B. W., Bontje, D., Voorn, G. A. K. v., and Kooijman, S. A. L. M. (2008). Sublethal contaminants effects in a simple aquatic food chain. *Ecol Model*, 112:304–318.
- Kooijman, S. A. L. M. (1981). Parametric analysis of mortality rates in bioassays. *Wat Res*, 15:107–119.
- Kooijman, S. A. L. M. (1986). Energy budgets can explain body size relations. *J Theor Biol*, 131:269–282.
- Kooijman, S. A. L. M. (1991). Effects of feeding conditions on toxicity for the purpose of extrapolation. *Comp Biochem Physiol C*, 100C(1/2):305–310.
- Kooijman, S. A. L. M. (2001). Quantitative aspects of metabolic organization: A discussion of concepts. *Philos Trans R Soc B*, 356(1407):331–349.
- Kooijman, S. A. L. M. (2009a). Social interactions can affect feeding behaviour of fish in tanks. *J Sea Res*, 62:175–178.
- Kooijman, S. A. L. M. (2009b). What the egg can tell us about its hen: Embryonic development on the basis of dynamic energy budgets. *J Math Biol*, 58(3):377–394.
- Kooijman, S. A. L. M. (2010). *Dynamic Energy Budget Theory for metabolic organization*. Cambridge.
- Kooijman, S. A. L. M. and Bedaux, J. J. M. (1996). *The analysis of aquatic toxicity data*. VU University Press, Amsterdam. ISBN 90-5383-477-X.
- Kooijman, S. A. L. M., Pecquerie, L., Augustine, S., and Jusup, M. (2011). Scenarios for acceleration in fish development and the role of metamorphosis. *J Sea Res*, 66:419–423.
- Kooijman, S. A. L. M., Sousa, T., Pecquerie, L., Van der Meer, J., and Jager, T. (2008). From food-dependent statistics to metabolic parameters, a practical guide to the use of dynamic energy budget theory. *Biol Rev*, 83(4):533–552.
- Kooijman, S. A. L. M. and van Haren, R. J. F. (1990). Animal energy budgets affect the kinetics of xenobiotics. *Chemosphere*, 21(4–5):681–693.
- Laale, H. W. (1977). The biology and use of zebrafish, *Brachydanio rerio* in fisheries research. *J Fish Biol*, 10:121–173.
- Labrot, F., Narbonne, J. F., Ville, P., Saint Denis, M., and Ribera, D. (1999). Acute Toxicity, Toxicokinetics, and Tissue Target of Lead and Uranium in the Clam *Corbicula fluminea* and the Worm *Eisenia fetida*: Comparison with the Fish *Brachydanio rerio*. *Arch Environ Con Tox*, 36:167–178.
- Lawrence, C. (2007). The husbandry of zebrafish (*Danio rerio*) : a review. *Aquaculture*, 269:1–20.
- Lawrence, C., Ebersole, J. P., and Kesseli, R. V. (2008). Rapid growth and out-crossing promote female development in zebrafish (*Danio rerio*). *Environ Biol Fish*, 81:239–246.
- Leggett, W. C. and Deblois, E. (1994). Recruitment in marine fishes: is it regulated by starvation and predation in the egg and larval stages? *Neth J Sea Res*, 32(2):119–134.

- Lerebours, A. (2009). *Caractérisation des effets de l'uranium chez le poisson zèbre *Danio rerio*. Mécanismes de stress, neurotoxicité et métabolisme mitochondrial*. PhD thesis, Université de Provence.
- Lerebours, A., Adam-Guillermin, C., Brêthes, D., Frelon, S., Floriani, M., Camilleri, V., Garnier-Laplace, J., and Bourdineaud, J.-P. (2010a). Mitochondrial energetic metabolism perturbations in skeletal muscles and brain of zebrafish (*Danio rerio*) exposed to low concentrations of waterborne uranium. *Aquat Toxicol*, 100:66–74.
- Lerebours, A., Bourdineaud, J.-P., Van Der Ven, K., Vandenbrouck, T., Gonzalez, P., Camilleri, V., Floriani, M., Garnier-Laplace, J., and Adam-Guillermin, C. (2010b). Sublethal effects of waterborne uranium exposures on the zebrafish brain: Transcriptional responses and alterations of the olfactory bulb ultrastructure. *Environ Sci Technol*, 44(4):1438–1443.
- Lerebours, A., Gonzalez, P., Adam-Guillermin, C., Camilleri, V., Bourdineaud, J.-P., and Garnier-Laplace, J. (2009). Comparative analysis of gene expression in brain, liver, skeletal muscles, and gills of zebrafish (*Danio rerio*) exposed to environmentally relevant waterborne uranium concentrations. *Environ Toxicol Chem*, 28(6):1271–1278.
- Lika, K., Freitas, V., van der Veer, H. W., van der Meer, J., Wijsman, J. W. M., Pecquerie, L., Kearney, M. R., and Kooijman, S. A. L. M. (2011a). The "covariation method" for estimating the parameters of the standard Dynamic Energy Budget model I: philosophy and approach. *J Sea Res*, 66:270–277.
- Lika, K., Kearney, M. R., and Kooijman, S. A. L. M. (2011b). The "covariation method" for estimating the parameters of the standard Dynamic Energy Budget model II: properties and preliminary patterns. *J Sea Res*, 66:278–288.
- Lika, K. and Kooijman, S. A. L. M. (2011). The comparative topology of energy allocation in budget models. *J Sea Res*, 66:381–391.
- Lobel, P. P., Longuerich, H., Jackson, S. E., and Belkhode, S. (1991). A major factor contributing to the high degree of unexplained variability of some elements concentrations in biological tissue: 27 elements in 5 organs of the mussel *Mytilus* as a model. *Arch Environ Con Tox*, 21:118–125.
- Lourenço, J., Castro, B., Machado, R., Nunes, B., Mendo, S., Gonçalves, F., and Pereira, R. (2010). Genetic, biochemical, and individual responses of the teleost fish *Carassius auratus* to uranium. *Arch Environ Con Tox*, 58(4):1023–1031.
- Lourenço, J., Silva, A., Carvalho, F., Oliveira, J., Malta, M., Mendo, S., Gonçalves, F., and Pereira, R. (2011). Histopathological changes in the earthworm *Eisenia andrei* associated with the exposure to metals and radionuclides. *Chemosphere*, 85:1630–1634.
- Main, A. (1957). Studies in Australian amphibia I. The genus *Crinia Tschudi* in southwestern Australia and some species from south-eastern Australia. *Aust J Zool*, 5:30–55.
- Marques, G., Lorena, A., Magalhães, J., Sousa, T., Kooijman, S., and Domingos, T. (2011). Life Engine - Creating Artificial Life for Scientific and Entertainment Purposes. In Kampis, G., Karsai, I., and Szathmáry, E., editors, *Advances in Artificial Life. Darwin Meets von Neumann*, volume 5778 of *Lecture Notes in Computer Science*, pages 278–285. Springer Berlin / Heidelberg. 10.1007/978-3-642-21314-4_35.
- Marques, S., Antunes, S., Pissarra, H., Pereira, M., Gonçalves, F., and Pereira, R. (2009). Histopathological changes and erythrocytic nuclear abnormalities in Iberian green frogs (*Rana perezi* Seoane) from a uranium mine pond. *Aquat Toxicol*, 91(2):187–195.
- Marques, S., Gonçalves, F., and Pereira, R. (2008). Effects of a uranium mine effluent in the early-life stages of *Rana perezi* Seoane. *Sci Tot Environ*, 402(1):29–35.

- Massarin, S., Alonzo, F., Garcia-Sanchez, L., Gilbin, R., Garnier-Laplace, J., and Poggiale, J.-C. (2010). Effects of chronic uranium exposure on life history and physiology of *Daphnia magna* over three successive generations. *Aquat Toxicol*, 99(3):309–319.
- Massarin, S., Beaudouin, R., Zeman, F., Floriani, M., Gilbin, R., Alonzo, F., and Pery, A. R. R. (2011). Biology-based modeling to analyze uranium toxicity data on *Daphnia magna* in a multigeneration study. *Environ Sci Technol*, 45(9):4151–8.
- Mathews, T., Beaugelin-Seiller, K., Garnier-Laplace, J., Gilbin, R., Adam, C., and Della-Vedova, C. (2009). A probabilistic assessment of the chemical and radiological risks of chronic exposure to uranium in freshwater ecosystems. *Environ Sci Technol*, 43(17):6684–6690.
- May, R. (1974). Larval mortality marine fishes and the critical period concept. In Blaxter, J., editor, *The early life history of fish*, pages 3–19. Springer-Verlag, Berlin.
- McKinney, M. L. and McNamara, K. J. (1991). *Heterochrony : the evolution of ontogeny*. Plenum Press, New York.
- Miller, T., Crowder, L., Rice, J., and Marschall, E. (1988). Larval size and recruitment mechanisms in fishes: toward a conceptual framework. *Can J Fish Aquat Sci*, 45:1657–1670.
- Mitchell, N. (2001). The energetics of endotrophic development in the frog *Geocrinia vitellina* (Anura: myobatrachidae). *Physiol Biochem Zool*, 74:832–842.
- Mitchell, N. and Seymour, R. (2000). Effects of temperature on the energy cost and timing of embryonic and larval development of the terrestrially breeding moss frog, *Bryobatrachus nimbus*. . *Physiol Biochem Zool*, 73:829–840.
- Mueller, C. (2011). *Developmental energetics and gas exchange in amphibians and lungfish*. PhD thesis, The University of Adelaide.
- Mueller, C., Joss, J., and Seymour, R. (2011). The energy cost of embryonic development in fishes and amphibians, with emphasis on new data from the Australian lungfish, *Neoceratodus forsteri*. *J Comp Physiol B*, 181:43–52.
- Mueller, C. and Seymour, R. (2011). The regulation index: an new method for assessing the relationship between oxygen consumption and environmental oxygen. *Physiol Biochem Zool*, 84:522–532.
- Muller, E. and Nisbet, R. (1997). Modeling the effect of toxicants on the parameters of dynamic energy budget models. In Dwyer, F. J., Doane, T. R., and Hinman, M., editors, *Environmental toxicology and risk assessment: modeling the risk assessment (sixth volume)*, ASTM STP 1317. American society for testing and materials.
- Muller, E., Nisbet, R., and Berkley, H. A. (2009). Sublethal toxicant effects with dynamic energy budget theory: model formulation. *Ecotoxicology*.
- Ng, C. A. and Gray, K. A. (2009). Tracking bioaccumulation in aquatic organisms: A dynamic model integrating life history characteristics and environmental change. *Ecol Model*, 220(9–10):1266–1273.
- Nisbet, R., Muller, E., Lika, K., and Kooijman, S. (2000). From molecules to ecosystems through dynamic energy budget models. . *J Anim Ecol*, 69:913–926.
- Nuclear Energy Agency (2008). *Uranium 2007: Resources, Production and Demand*. OECD Publishing.

- Orloff, K. G., Mistry, K., Charp, P., Metcalf, S., Marino, R., Shelly, T., Melaro, E., Donohoe, A. M., and Jones, R. L. (2004). Human exposure to uranium in groundwater. *Env Res*, 94:319–326.
- Packard, M. and Seymour, R. (1997). Evolution of the amniote egg. In Sumida, S. and Martin, K., editors, *Amniote origins: completing the transition to land*, pages 265–290.
- Paradis, A. R., Pepin, P., and Brown, J. A. (1996). Vulnerability of fish eggs and larvae to predation: review of the influence of the relative size of prey and predator. *Can J Fish Aquat Sci*, 53:1226–1235.
- Parichy, D. M., Elizondo, M. R., Mills, M. G., Gordon, T. N., and Engeszer, R. E. (2009). Normal table of postembryonic zebrafish development: staging by externally visible anatomy of the living fish. *Dev Dynam*, 238:2975–3015.
- Paull, G. C., Van Look, K. J. W., Santos, E. M., Filby, A. L., Gray, D. M., Nasha, J. P., and Tyler, C. R. (2008). Variability in measures of reproductive success in laboratory-kept colonies of zebrafish and implications for studies addressing population-level effects of environmental chemicals. *Aquat Toxicol*, 87:115–126.
- Pauly, D. and Pullin, R. (1988). Hatching time in spherical, pelagic, marine fish eggs in response to temperature and egg size. *Environ Biol Fish*, 22:261–271.
- Pecquerie, L. (2007). *Bioenergetic modelling of growth, development and reproduction of a small pelagic fish: the Bay of Biscay anchovy*. PhD thesis, Agrocampus Rennes.
- Pecquerie, L., Petitgas, P., and Kooijman, S. A. L. M. (2009). Modeling fish growth and reproduction in the context of the dynamic energy budget theory to predict environmental impact on anchovy spawning duration. *J Sea Res*, 62:93–105.
- Pereira, S., Camilleri, V., Floriani, M., Cavalie, I., Garnier-Laplace, J., and Adam-Guillermin, C. (2012). Genotoxicity of uranium contamination in embryonic zebrafish cells. *Aquat Toxicol*, 109:11–16.
- Post, J. R. and Lee, J. A. (1996). Metabolic ontogeny of teleost fishes. *Can J Fish Aquat Sci*, 56:910–923.
- Reiss, J. O. (1989). The meaning of developmental time: a metric for comparative embryology. *Am Nat*, 134:170–189.
- Rico-Villa, B., Bernard, I., Robert, R., and Pouvreau, S. (2010). A Dynamic Energy Budget (DEB) growth model for Pacific oyster larvae, *Crassostrea gigas*. *Aquaculture*, 305:84–94.
- Riveiro, I., Guisande, C., Lloves, M., Maneiro, I., and Cabanas, J. M. (2000). Importance of parental effects on larval survival in *Sardina pilchardus*. *Mar Ecol Prog Ser*, 205:249–258.
- Rougier, F., Menudier, A., Bosgiraud, C., and Nicolas, J. A. (1996). Copper and zinc exposure to zebrafish, *Brachydanio rerio* (hamilton-buchaman): effects in experimental listeria infection. *Ecotoxicol Environ Saf*, 34:134–140.
- Salthe, S. and Duellman, W. (1973). Quantitative constraints associated with reproductive mode in anurans. In Vial, J., editor, *Evolutionary Biology of the Anurans*, pages 229–249. University of Missouri Press, Columbia, USA.
- Schilling, T. F. (2002). The morphology of larval and adult zebrafish. In Nüsslein-Volhard, C. and Dahm, R., editors, *Zebrafish: a practical guide.*, pages 59–83. Oxford University Press Inc., New York.
- Seymour, R. (1999). Respiration of aquatic and terrestrial amphibian embryos. *Am Zool*, 39:261–270.

- Seymour, R., Geiser, F., and Bradford, D. (1991). Metabolic cost of development in terrestrial frog eggs (*Pseudophryne bibronii*). *Physiol Zool*, 64:688–696.
- Seymour, R. and Roberts, J. (1995). Oxygen uptake by the aquatic eggs of the Australian frog *Crinia georgiana*. *Physiol Zool*, 648:206–222.
- Shepherd, T., Costain, K., and Litvak, M. K. (2000). The effect of development rate on swimming behaviour and escape response in American plaice (*Hippoglossoides platessoides*) larvae. *Mar Biol*, 137:737–745.
- Shirone, R. C. and Gross, L. (1968). Effect of temperature on early embryological development of the zebra fish, *Brachydanio rerio*. *J Exp Zool*, 169:43–52.
- Simon, O., Floriani, M., Cavalie, I., Camilleri, V., Adam, C., Gilbin, R., and Garnier-Laplace, J. (2011a). Internal distribution of uranium and associated genotoxic damages in the chronically exposed bivalve *Corbicula fluminea*. *J Environ Radioact*, 102:766–773.
- Simon, O. and Garnier-Laplace, J. (2004). Kinetic analysis of uranium accumulation in the bivalve *Corbicula fluminea*: effect of pH and direct exposure levels. *Aquat Toxicol*, 68:95–108.
- Simon, O., Mottin, E., Geffroy, B., and Hinton, T. (2011b). Effects of dietary uranium on reproductive endpoints - fecundity, survival, reproductive success - of the fish *Danio rerio*. *Envir Toxicol Chem*, 30(1):220–225.
- Smith, M. and Roberts, J. (2003). No sexual size dimorphism in the frog *Crinia georgiana* (Anura: Myobatrachidae): an examination of pre- and post-maturational growth. *J Herpetol*, 37:132–137.
- Sousa, T., Domingos, T., and Kooijman, S. A. L. (2008). From empirical patterns to theory: A formal metabolic theory of life. *Philos Trans R Soc B*, 363:2453–2464.
- Sousa, T., Domingos, T., Poggiale, J. C., and Kooijman, S. A. L. (2010). Dynamic energy budget restores coherence in biology. *Philos Trans R Soc B*, 365:3413–3428.
- Spence, R., Gerlach, G., Lawrence, C., and Smith, C. (2008). The behaviour and ecology of the zebrafish, *Danio rerio*. *Biol Rev*, 83(1):13–34.
- Spence, R. and Smith, C. (2006). Mating preference of female zebrafish, *Danio rerio*, in relation to male dominance. *Behav Ecol*, 17:779–783.
- Spicer, J. I. and Burggren, W. W. (2003). Development of physiological regulatory systems: altering the timing of crucial events. *Zoology*, 106:91–99.
- Swain, S., Wren, J. F., Strzenbaum, S. R., Kille, P., Morgan, A. J., Jager, T., Jonker, M. J., Hankard, P. K., Svendsen, C., Owen, J., Hedley, B. A., Blaxter, M., and Spurgeon, D. J. (2010). Linking toxicant physiological mode of action with induced gene expression changes in *caenorhabditis elegans*. *BMC Systems Biology*, 4:32.
- Thomas, P. G. and Ikeda, T. (1987). Sexual regression, shrinkage, re-maturation and growth of spent female *Euphausia superba* in the laboratory. *Mar Biol*, 95:357–363.
- Thompson, M. and Russell, K. (1999). Embryonic energetics in eggs of two species of Australian skink, *Morethia boulengeri* and *Morethia adelaidensis*. *J Herpetol*, 33:291–297.
- Tsai, S. B., Tucci, V., Uchiyama, J., Fabian, N. J., Lin, M. C., Bayliss, P. E., Neuberg, S., Zhanova, I. V., and Kishi, S. (2007). Differential effects of genotoxic stress on both concurrent body growth and gradual senescence in the adult zebrafish. *Aging Cell*, 6:209–224.

- Tyler, M. (1962). On the preservation of anuran tadpoles. *Aust J Sci*, 25:222.
- Uralbekov, B. M., Smodis, B., and Burkitbayev, M. (2011). Uranium in natural waters sampled within former uranium mining sites in Kazakhstan and Kyrgyzstan. *J Radioanal Nucl Chem*, 289:805–810.
- Uusi-Heikkilä, S., Wolter, C., Meinelt, T., and Arlinghaus, R. (2010). Size-dependent reproductive success of wild zebrafish *Danio rerio* in the laboratory. *J Fish Biol*, 77:552–569.
- van der Veer, H., Kooijman, S. A. L. M., and van der Meer, J. (2010). Intra- and interspecies comparison of energy flow in the North Atlantic flatfish species by means of dynamic energy budgets. *J Sea Res*, 45:303–320.
- van Haren, R. J. F., Schepers, H. E., and Kooijman, S. A. L. M. (1994). Dynamic energy budgets affect kinetics of xenobiotics of the marine mussel *Mytilus edulis*. *Chemosphere*, 29(2):163–189.
- van Leeuwen, I. M. M., Vera, J., and Wolkenhauer, O. (2010). Dynamic energy budget approaches for modelling organismal ageing. *Philos Trans R Soc B*, 365:3443–3454.
- Villa, M., Manjón, G., Hurtado, S., and García-Tenorio, R. (2011). Uranium pollution in an estuary affected by pyrite acid mine drainage and releases of naturally occurring radioactive materials. *Mar Poll Bull*, 62:1521–1529.
- Vleck, C. and Hoyt, D. (1991). Metabolism and energetics of reptilian and avian embryos. In Deeming, D. and Ferguson, M., editors, *Egg Incubation: Its Effect on Embryonic Development in Birds and Reptiles*, pages 285–306. Cambridge University Press, Cambridge.
- Vleck, C. and Vleck, D. (1987). Metabolism and energetics of avian embryos. *Am Zool Suppl*, 1:111–125.
- Vleck, C., Vleck, D., and Hoyt, D. (1980). Patterns of metabolism and growth in avian embryos. *Am Zool*, 20:405–416.
- Wallace, K. N., Akhter, S., Smith, E. M., Lorent, K., and Pack, M. (2005). Intestinal growth and differentiation in zebrafish. *Mech Develop*, 122(2):157 – 173.
- White, C. R., Kearney, M. R., Matthews, P. G. D., Kooijman, S. A. L. M., and Marshall, D. J. (2011). A manipulative test of competing theories for metabolic scaling in animals. *Am Nat*, 178:746–754.
- Whitehead, P. and Seymour, R. (1990). Patterns of metabolic rate in embryonic crocodilians *Crocodylus johnstoni* and *Crocodylus porosus*. *Physiol Zool*, 63:334–352.
- WHO (2001). Depleted uranium: sources, exposure and health effects. Technical report, World Health Organization.
- Woodruff, D. (1976). Courtship, reproductive rates, and mating system in three Australian *Pseudophryne* (Amphibia, Anura, Leptodactylidae). *J Herpetol*, 10:313–318.
- Wren, J. F., Kille, P., Spurgeon, D. J., Swain, S., Sturzenbaum, S. R., and Jager, T. (2011). Application of physiologically based modelling and transcriptomics to probe the systems toxicology of aldicarb for *Caenorhabditis elegans* (Maupas 1900). *Ecotoxicology*, 20:397–408.
- Yin, M. C. and Blaxter, J. H. S. (1986). Morphological changes during growth and starvation of larval cod (*Gadus morhua* L.) and flounder (*Platichthys flesus* L.). *J Exp Mar Biol Ecol*, 104:215–228.

- Zeman, F., Gilbin, R., Alonzo, F., Lecomte-Pradines, C., Garnier-Laplace, J., and Aliaume, C. (2008). Effects of waterborne uranium on survival, growth, reproduction and physiological processes of the freshwater cladoceran *Daphnia magna*. *Aquatic Toxicology*, 86(3):370–378.
- Zhang, R., Yang, J., and Xu, X. (2009). Depletion of zebrafish Tcap leads to muscular dystrophy via disrupting sarcomere-membrane interaction, not sarcomere assembly. *Hum Mol Genet*, 18(21):4130–4140.
- Zimmer, E. I., Jager, T., Ducrot, V., and Kooijman, S. A. L. M. (2012). Juvenile food limitation in standard tests- ecotoxicologists, be warned! *Ecotoxicology*. To appear.
- Zonneveld, C. and Kooijman, S. A. L. M. (1993). Comparative kinetics of embryo development. *Bull Math Biol*, 3:609–635.

Appendix A

Standard DEB model with V1-morphic extension

Graphs were digitalized using PlotReader[®]1.40.0.0 (<http://www.xs4all.nl/~jornbr/plotreader/>) and then imported into the estimation procedure coded in Matlab[®] (version 7.9.0.529). In addition to 1-variate data (e.g. length against time) we have added a number of 0-variate data (e.g. length at birth, egg size and dry weight).

For practical purposes DEBtool routines take compound parameters (simple function of primary parameters) and scaled variables as input. Computations for 0-variate and 1-variate data from the literature all assume constant food and temperature.

A.1 Growth at constant food density

The following equations are used to compute growth at constant food density. Table A.3 gives all quantities used below.

V1-morphic early juvenile stage: $a_b \leq a < a_j$:

$$L(a) = L_b \exp\left(\frac{\dot{r}_{V1}}{3} (a - a_b)\right) \quad (\text{A.1})$$

$$a(L) = a_b + \frac{3}{\dot{r}_{V1}} \ln \frac{L(a)}{L_b} \quad (\text{A.2})$$

and $\dot{r}_{V1} = \frac{\dot{v}}{e+g} \left(\frac{e}{L_b} - \frac{1}{L_m} \right)$ Juvenile and adult stage, $a \geq a_j$:

$$L(a) = L_\infty - (L_\infty - L_j) \exp(-\dot{r}_B (a - a_j)) \quad (\text{A.3})$$

$$a(L) = a_j + \frac{1}{\dot{r}_B} \ln \frac{L_\infty - L_j}{L_\infty - L(a)} \quad (\text{A.4})$$

Table A.1: Compound parameters (functions of primary energetic parameters) followed by parameters which link energies and lengths to (dry) mass. The latter are important in auxiliary theory.

Sym- bol	Unit	Formulation	Value	Biological significance
<i>Compound parameters (functions of primary parameters)</i>				
L_m	cm	$\kappa \frac{\{\dot{p}_{Am}\}}{[\dot{p}_m]}$	0.21	Maximum structural length
$[E_m]$	J cm ⁻³	$\frac{\{\dot{p}_{Am}\}}{\dot{v}}$	8 860	Maximum reserve density
g	-	$\frac{[E_G] \dot{v}}{\kappa \{\dot{p}_{Am}\}}$	1.20	Energy Investment Ratio
\dot{k}_M	d ⁻¹	$\frac{[\dot{p}_m]}{[E_G]}$	0.12	Somatic maintenance rate coefficient
k	-	$\frac{\dot{k}_J}{\dot{k}_M}$	0.15	Maintenance ratio
<i>Auxilliary parameters</i>				
w_E	g mol ⁻¹	Lika et al. (2011a)	23.9	Molar weight of Reserve, E
w_V	g mol ⁻¹	Lika et al. (2011a)	23.9	Molar weight of Structure, V
d_{Ed}	g cm ⁻³	Craig and Fletcher (1984)	0.15	Density of E
d_{Vd}	g cm ⁻³	Craig and Fletcher (1984)	0.15	Density of V
$\bar{\mu}_E$	J mol ⁻¹	Lika et al. (2011a)	550 000	Chemical potential of V
$\bar{\mu}_V$	J mol ⁻¹	Lika et al. (2011a)	500 000	Chemical potential of E

and $\dot{r}_B = \frac{\dot{k}_M/3}{1+e/g}$.

We work with the assumption that $d_{Vd} = d_{Ed}$ and consider that $d_V = 1$ g (wet mass) cm^{-3} and then derive d_{Vd} from observations in [Craig and Fletcher \(1984\)](#) using the following relationship: $d_{Vd} = \frac{AFDW}{W_w} d_V$, with AFDW the ash free dry weight and W_w the wet weight.

Table A.2: Scaled variables of the DEB model used for computational purposes.

Variable	Unit	Name
e	-	scaled reserve density $\frac{E}{[E_m]}$
l	-	scaled structural length $\frac{L}{L_m}$
U_H	$\text{cm}^2 \text{ day}$	scaled maturity level $\frac{E_H}{\{p_{Am}\}}$
N	#	cumulative number of eggs

A.2 Dynamic formulation of the model

Dynamic formulation of the scaled DEB model:

$$\frac{d}{dt}e = \frac{\dot{v}\mathcal{M}(L)}{L} (f - e) \quad (\text{A.5})$$

$$\frac{d}{dt}L = \frac{L}{3} \frac{\dot{v}}{e + g} \left(\frac{e\mathcal{M}(L)}{L} - \frac{1}{L_m} \right) \quad (\text{A.6})$$

$$\frac{d}{dt}U_H = (1 - \kappa) \frac{L^3}{1 + g/e} \left(\frac{g\mathcal{M}(L)}{L} + \frac{1}{L_m} \right) - \dot{k}_J U_H \quad (\text{A.7})$$

$$\text{if } U_H < U_H^P \text{ else } \frac{d}{dt}U_H = 0$$

$$\frac{d}{dt}N = \frac{\kappa_R}{U_E^0} \left((1 - \kappa) \frac{L^3}{1 + g/e} \left(\frac{g}{L} \frac{L_j}{L_b} + \frac{1}{L_m} \right) - \dot{k}_J U_H^P \right) \quad (\text{A.8})$$

$$\text{if } U_H = U_H^P \text{ else } \frac{d}{dt}N = 0$$

U_E^0 is the scaled initial energy in an egg given by $U_E^0 = E_0/\{p_{Am}\}$ and $\mathcal{M}(L) = \max(L_b, \min(L, L_j))/L_b$ and $f = 0$ if $U_H < U_H^b$.

A.3 Survival probability

The ageing module supposes short growth periods relative to life span, constant food density and negligible effects of ageing during the embryo stage (see [Kooijman, 2010](#), pp.218):

$$\dot{h}_W^3 = \frac{\ddot{h}_a \dot{v}}{6 L_m} \quad \text{and} \quad \dot{h}_G = \frac{s_G f^3 \dot{v}}{L_m} \quad (\text{A.9})$$

with \dot{h}_W^3 the Weibull ageing rate, and \dot{h}_G the Gombertz ageing rate. Survival probability is then expressed as:

$$Pr\{a\} = \exp\left(\frac{6\dot{h}_W^3}{\dot{h}_G^3} \left(1 - \exp(\dot{h}_G t) + \dot{h}_G t + \frac{\dot{h}_G^2 t^2}{2}\right)\right) \quad (\text{A.10})$$

Table A.3: How all 0-variate data are computed in predict_Danio_rerio.

Quantity	Sym- bol	Unit	DEBtool routine or formula
<i>Quantities calculated with DEBtool routines</i>			
Age at birth	a_b	day	get_tb
Length at birth	L_b	cm	get_tb
Length at metamorphosis	L_j	cm	get_lj
Length at puberty	L_p	cm	get_lj
Mean life span	a_m	day	get_tm.s
Initial reserve	E_0	J	initial_scaled_reserve
Maximum reproduction rate	\dot{R}_m	#eggs day ⁻¹	reprod_rate_metam
<i>Quantities which can be calculated analytically</i>			
Age at metamorphosis	a_j	day	$a_b + 3/\dot{k}_M \frac{f/g+1}{f L_m/L_b-1} \ln(L_j/L_b)$
Ultimate length	L_∞	cm	$f L_m L_j / L_b$
Von Bert. growth rate	\dot{r}_B	day ⁻¹	$\frac{\dot{k}_M/3}{1+f/g}$
Age at puberty	a_p	day	$a_j + \dot{r}_B^{-1} \ln \frac{L_\infty - L_j}{L_\infty - L_p}$
<i>Quantities which use auxilliary parameters</i>			
Maximum dry mass	W_{dm}	g	$d_V L_\infty^3 \left(1 + (f + e_R) \frac{[E_m] w_E}{d_V \bar{\mu}_E}\right)$
Egg dry mass	W_d^{egg}	g	$E_0 \frac{w_E}{\bar{\mu}_E}$
Egg Volume	V_{egg}	cm ³	$E_0 \frac{w_E}{\bar{\mu}_E d_E}$
Egg diameter	\emptyset_{egg}	cm	$(6 V_{egg} / \pi)^{\frac{1}{3}}$
Growth conversion efficiency	κ_G	-	$\frac{\bar{\mu}_V d_V}{[E_G] w_V}$

Appendix B

Experimental design for observing zebrafish growth and reproduction under controlled feeding conditions

A specific experimental system was custom designed to carry out this experiment (fig B.1). The realisation of the aquariums was carried out by Sud Matière Plastique, Manosque. Each condition consists of a holding tank ($120 \times 25 \times 65$ cm L \times W \times H) containing 5 aquariums (fig B.1A). Each aquarium is $30 \times 28 \times 20$ cm L \times W \times H and is permeable to the surrounding water (presence of fine slits along two opposite sides), fig B.1B1. Each aquarium is further equipped with four removable mesh partitions separating the aquarium into four individual chambers (fig B.1E). A hollow cylinder (5 cm ϕ) occupies the center of the aquarium and provides support for the removable partitions. A water distributor slides into the cylinder (fig B.1B1,C). Aquarium hosing is used for water renewal.

Water is kept in 300L reservoirs and drawn with an immersible pump (Hydor). Hose connectors (Eheim) are used to link the hosing to the pumps and to each of the the water distributors. A removable screen perforated by 1 mm wide slits (fig B.1B2,D) can be placed over the floor of an individual chamber during reproduction trials. The screen is put in place before the couple is formed to prevent egg predation. The system is made of plexiglass. Air stones linked to air pumps and immersed thermostat resistances maintain temperature and oxygen levels. About a quarter of the water is renewed each day.

The motivation behind this system was to (1) simultaneously observe the

growth and reproduction of individual fish without removing the individuals during reproduction trials and (2) control the ingestion ration for each individual. After egg collection couples are separated by delicate insertion of the partition. This eliminates inter-individual ingestion competition. The partition is lifted in the evening, the perforated screen put over the floor on one side, fish are gently guided over the screen and then the partition is put back in place. The following morning the partition is lifted, fish swim to the other side, the partition is put back in place, the perforated screen is lifted, eggs are collected by gentle aspiration and finally fish are separated again during the day by replacing the partition. The reason the partitions were made of mesh was to maintain visual contact between the fish. Zebrafish are social animals and we feared they may lose appetite if kept in total isolation for long periods of time.

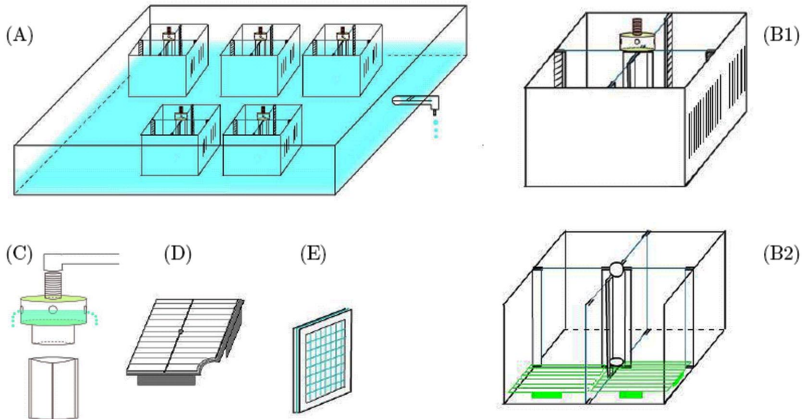


Figure B.1: Experimental design of the caloric restriction experiment. Drawings are not to scale. (A) Holding tank (119 l) with 5 aquariums (each one is 13.4 l) who are permeable to the surrounding water. 4 fish are maintained individually in each aquarium and put together as couples only in the evening. There are 3 experimental conditions so three of such holding tanks. (B1) Aquarium with four partitions, slits on the sides and water distributor. (B2) Transparent view of an aquarium with removable screens resting above the bottom of the aquarium which inhibit egg predation. (C) Close up of water distributor. (D) The removable screen used for reproduction trials. The screen is maintained some 5 cm from the bottom of the aquarium by a support system. Slits are 1 mm wide and allow eggs to pass through. (E) Close up of the removable mesh partition.

Appendix C

Mineral fluxes

Computations of fluxes of dioxygen (\dot{J}_O), carbon dioxide (\dot{J}_C), water (\dot{J}_H) and ammonia (\dot{J}_N) comes with the specification of the stoichiometry of elements (matrix $n_{\mathcal{M}}$ of chemical indices) and the ratios of C, H, O, N to C in the generalized molecule which makes up the four organic compartments: X (food), V (structure), E (reserve) and P (faeces) which are collected in matrix $n_{\mathcal{O}}$.

Chemical indices $n_{\mathcal{O}}$ and $n_{\mathcal{M}}$ (see [Lika et al., 2011a](#), this special issue) are as follows:

$$n_{\mathcal{O}} = \begin{pmatrix} 1.00 & 1.00 & 1.00 & 1.00 \\ 1.80 & 1.80 & 1.80 & 1.80 \\ 0.50 & 0.50 & 0.50 & 0.50 \\ 0.10 & 0.10 & 0.10 & 0.10 \end{pmatrix} \quad n_{\mathcal{M}} = \begin{pmatrix} 1 & 0 & 0 & 0 \\ 0 & 2 & 0 & 3 \\ 2 & 1 & 2 & 0 \\ 0 & 0 & 0 & 1 \end{pmatrix}$$

Organic fluxes are a weighted sum of the three basic powers in DEB theory: assimilation \dot{p}_A , dissipation \dot{p}_D and growth \dot{p}_G . Assimilation (\dot{p}_A) and growth (\dot{p}_G) powers are defined in [subsection 3.2.1](#). Somatic maintenance, maturity maintenance and maturation all contribute to the dissipation power \dot{p}_D such that $\dot{p}_D = [\dot{p}_M] L^3 + (1 - \kappa)\dot{p}_C$. Mineral fluxes are a weighted sum of the organic fluxes. Faeces production is linked only to assimilation so is zero for embryos.

The four organic fluxes, \dot{J}_X flux of food (C-mol X day⁻¹), \dot{J}_V structure flux (C-mol V day⁻¹), \dot{J}_E reserve flux (C-mol E day⁻¹), and \dot{J}_P feces flux (C-mol P day⁻¹) are specified as follows :

$$\begin{aligned} \dot{J}_X &= -\frac{y_{XE}}{\bar{\mu}_E} f \{ \dot{p}_{Am} \} L^2 \\ \dot{J}_V &= \frac{[M_V]}{[E_G]} (\kappa \dot{p}_C - [\dot{p}_M] L^3) \\ \dot{J}_E &= \frac{1}{\bar{\mu}_E} (f \{ \dot{p}_{Am} \} L^2 - \dot{p}_C) \\ \dot{J}_P &= -y_{PX} \dot{J}_X \end{aligned}$$

$[M_V] = d_V/w_E$ and $f = 0$ for embryos. Mineral fluxes ($\dot{J}_{\mathcal{M}}$): \dot{J}_C (mol CO₂ day⁻¹), \dot{J}_H (mol H₂O day⁻¹), \dot{J}_O (mol O₂ day⁻¹), and \dot{J}_N (mol NH₃ day⁻¹),

are a weighted sum of organic fluxes (see Eqn.4.37 Kooijman, 2010, pp.139):

$$\dot{J}_{\mathcal{M}} = -n_{\mathcal{M}}^{-1} n_{\mathcal{O}} \dot{J}_{\mathcal{O}}$$

with:

$$\dot{J}_{\mathcal{M}} = \begin{pmatrix} \dot{J}_C \\ \dot{J}_H \\ \dot{J}_O \\ \dot{J}_N \end{pmatrix} \quad \text{and} \quad \dot{J}_{\mathcal{O}} = \begin{pmatrix} \dot{J}_X \\ \dot{J}_V \\ \dot{J}_E \\ \dot{J}_P \end{pmatrix}$$

Appendix D

Parameter Estimation for *C. georgiana* and *P. bibronii*

The dynamics of the four state variables (fig. 2.1 and table D.1) are fully specified by the following system of ordinary differential equations:

$$\frac{dE}{dt} = \dot{p}_A - \dot{p}_C \quad (\text{D.1})$$

$$\frac{dL}{dt} = \frac{\dot{r}}{3} L \quad (\text{D.2})$$

$$\frac{dE_H}{dt} = (1 - \kappa) \dot{p}_C - \dot{k}_J E_H \quad \text{if } E_H < E_H^p \quad \text{else } \frac{dE_H}{dt} = 0 \quad (\text{D.3})$$

$$\frac{dE_R}{dt} = (1 - \kappa) \dot{p}_C - \dot{k}_J E_H^p \quad \text{if } E_H = E_H^p \quad \text{else } \frac{dE_R}{dt} = 0 \quad (\text{D.4})$$

κ remains constant for *P. bibronii* but decreases linearly from $\kappa_1 = 0.86$ to $\kappa_2 = 0.61$ (table 4.2) as a function of maturity between E_H^{22} and E_H^{27} in *C. georgiana*:

$$\kappa(E_H) = \kappa_2 + (\kappa_1 - \kappa_2) \frac{E_H^{27} - E_H}{E_H^{27} - E_H^{22}} \quad \text{for } E_H \in [E_H^{22}; E_H^{27}]$$

In light of adult life history traits (see full text for discussion) we assumed that κ switches back to its original value κ_1 at metamorphosis.

The mobilization flux \dot{p}_C (J d⁻¹) and the specific growth rate \dot{r} (d⁻¹) are

Table D.1: State variables of the DEB model and additional parameters. Rates are expressed at reference temperature ($T = 20^\circ\text{C}$). See table 4.2 for parameters not specified here.

Symbol	Unit	Name
Forcing variable		
f	-	scaled functional response
DEB model variables		
E	J	energy fixed in reserve
L	cm	volumetric structural length $V^{1/3}$
E_H	J	cumulated energy invested in maturity
E_R	J	cumulated energy invested in reproduction
Simple functions of parameters		
$[M_V]$	mol cm^{-3}	specific structural mass d_V/w_V
κ_G	-	growth efficiency $\frac{[M_V]\bar{\mu}_V}{[E_G]}$
y_{VE}	mol mol^{-1}	yield of reserve on structure $\frac{\bar{\mu}_E [M_V]}{[E_G]}$
m_{Em}	mol mol^{-1}	maximum molar reserve density $\frac{\{\bar{p}_{Am}\}}{y_{VE} [E_G] \bar{v}}$

Table D.2: Additional DEB model parameters and conversion parameters (see text). Rates are expressed at reference temperature ($T = 20^\circ\text{C}$). The estimated values of the additions DEB model parameters (empty fields) can be found in legends of tables E.1 and E.2 and fig. E.1 and E.2.

Symbol	Unit	value	Name
Additional DEB model parameters			
δ_M	-		shape coefficient
T_A	K		Arrhenius temperature
E_H^p	J		maturity threshold at puberty
κ_R	-		reproduction efficiency
\dot{h}_a	d^{-2}		Weibull ageing acceleration
Conversion parameters			
w_*	g mol^{-1}	23.4	molecular weights of organics * $\in [X, V, E, P]$
$\bar{\mu}_E$	J mol^{-1}	577.5	chemical potential of reserve
$\bar{\mu}_V$	J mol^{-1}	500.0	chemical potential of structure
d_V	g cm^{-3}	0.2	specific density of structure
y_{XE}	mol mol^{-1}	1.25	yield of food on reserve
y_{PX}	mol mol^{-1}	0.1	yield of faeces on food

given by Kooijman (Eqn. 2.12 and 2.13 2010, pp.37):

$$\begin{aligned}\dot{p}_C &= E (\dot{v}/L - \dot{r}) \\ \dot{r} &= \frac{E \dot{v}/L^4 - [\dot{p}_M]/\kappa}{E/L^3 + [E_G]/\kappa}\end{aligned}$$

The three powers assimilation \dot{p}_A , growth \dot{p}_G and dissipation \dot{p}_D (J d⁻¹) are:

$$\dot{p}_A = f \{ \dot{p}_{Am} \} L^2 \quad (\text{D.5})$$

$$\dot{p}_G = \kappa \dot{p}_C - [\dot{p}_M] L^3 \quad (\text{D.6})$$

$$\dot{p}_D = \dot{p}_M + \dot{p}_J + \dot{p}_R \quad (\text{D.7})$$

The dissipation power has contributions from somatic maintenance \dot{p}_M , maturity maintenance \dot{p}_J and maturation (or reproduction for adults) \dot{p}_R which are specified as follows:

$$\dot{p}_M = [\dot{p}_M] L^3 \quad (\text{D.8})$$

$$\dot{p}_J = \dot{k}_J E_H \quad \text{if } E_H < E_H^p \quad \text{else } \dot{p}_J = \dot{k}_J E_H^p \quad (\text{D.9})$$

$$\dot{p}_R = (1 - \kappa) \dot{p}_C - \dot{k}_J E_H \quad \text{if } E_H < E_H^p \quad \text{else } \quad (\text{D.10})$$

$$\dot{p}_R = \kappa_R \left((1 - \kappa) \dot{p}_C - \dot{k}_J E_H^p \right)$$

\dot{J}_* denotes flux of compound * (mol * day⁻¹). By convention, fluxes of compounds that disappear in a transformation have a negative sign and fluxes of compounds that appear in a transformation have a positive sign.

Organic fluxes (\dot{J}_O): \dot{J}_X flux of food (c-mol X day⁻¹), \dot{J}_V flux of structure (c-mol V day⁻¹), \dot{J}_E flux of reserve (c-mol E day⁻¹), and \dot{J}_P flux of faeces (c-mol P day⁻¹), see figure 2.1, are given by:

$$\dot{J}_O = \begin{pmatrix} \dot{J}_X \\ \dot{J}_V \\ \dot{J}_E \\ \dot{J}_P \end{pmatrix} = \begin{pmatrix} -y_{XE} \bar{\mu}_E^{-1} & 0 & 0 \\ 0 & 0 & [M_V][E_G]^{-1} \\ \bar{\mu}_E^{-1} & -\bar{\mu}_E^{-1} & -\bar{\mu}_E^{-1} \\ y_{PX} y_{XE} \bar{\mu}_E^{-1} & 0 & 0 \end{pmatrix} \begin{pmatrix} \dot{p}_A \\ \dot{p}_D \\ \dot{p}_G \end{pmatrix} \quad (\text{D.11})$$

So:

$$\begin{aligned}\dot{J}_X &= -\frac{y_{XE}}{\bar{\mu}_E} \dot{p}_A \\ \dot{J}_V &= \frac{[M_V]}{[E_G]} \dot{p}_G \\ \dot{J}_E &= \frac{1}{\bar{\mu}_E} (\dot{p}_A - \dot{p}_D - \dot{p}_G) \\ \dot{J}_P &= -y_{PX} \dot{J}_X\end{aligned}$$

In order to compute mineral fluxes we need to specify the chemical indices n_O and n_M (Kooijman, 2010; Lika et al., 2011a):

$$n_O = \begin{pmatrix} 1.00 & 1.00 & 1.00 & 1.00 \\ 1.80 & 1.80 & 1.80 & 1.80 \\ 0.50 & 0.50 & 0.50 & 0.50 \\ 0.15 & 0.15 & 0.15 & 0.15 \end{pmatrix} \quad \text{and} \quad n_M = \begin{pmatrix} 1 & 0 & 0 & 0 \\ 0 & 2 & 0 & 3 \\ 2 & 1 & 2 & 0 \\ 0 & 0 & 0 & 1 \end{pmatrix}$$

The molecular weights of organics w_* , $* \in [X, V, E, P]$ (table D.1) are:

$$(w_X w_V w_E w_P) = (12 \ 1 \ 16 \ 14) n_O$$

Mineral fluxes (\dot{J}_M): \dot{J}_C (mol CO₂ day⁻¹), \dot{J}_H (mol H₂O day⁻¹), \dot{J}_O (mol O₂ day⁻¹), and \dot{J}_N (mol NH₃ day⁻¹), are a weighted sum of organic fluxes (see Eqn.4.37 Kooijman, 2010, pp.139) such that: $\dot{\mathbf{J}}_M = -\mathbf{n}_M^{-1} \mathbf{n}_O \dot{\mathbf{J}}_O$. Therefore we can write $\dot{\mathbf{J}}_M = \mathbf{y}_{MO} \dot{\mathbf{J}}_O$ with

$$\mathbf{y}_{MO} = -\mathbf{n}_M^{-1} \mathbf{n}_O = \begin{pmatrix} y_{CX} & y_{CV} & y_{CE} & y_{CP} \\ y_{HX} & y_{HV} & y_{HE} & y_{HP} \\ y_{OX} & y_{OV} & y_{OE} & y_{OP} \\ y_{NX} & y_{NV} & y_{NE} & y_{NP} \end{pmatrix}$$

this gives:

$$\dot{\mathbf{J}}_M = \begin{pmatrix} \dot{J}_C \\ \dot{J}_H \\ \dot{J}_O \\ \dot{J}_N \end{pmatrix} = \begin{pmatrix} y_{CX} & y_{CV} & y_{CE} & y_{CP} \\ y_{HX} & y_{HV} & y_{HE} & y_{HP} \\ y_{OX} & y_{OV} & y_{OE} & y_{OP} \\ y_{NX} & y_{NV} & y_{NE} & y_{NP} \end{pmatrix} \begin{pmatrix} \dot{J}_X \\ \dot{J}_V \\ \dot{J}_E \\ \dot{J}_P \end{pmatrix} \quad (\text{D.12})$$

Total dioxygen consumption is expressed as: $\dot{J}_O = y_{OX} \dot{J}_X + y_{OV} \dot{J}_V + y_{OE} \dot{J}_E + y_{OP} \dot{J}_P$

Assimilation, growth, somatic maintenance and maturation plus maturity maintenance each contribute to total dioxygen consumption in the following manner:

$$\begin{aligned} \text{assimilation: } \dot{J}_{OA} &= -\frac{1}{\mu_E} (y_{OP} y_{XE} y_{PX} - y_{OE} + y_{XE} y_{OX}) \dot{p}_A \\ \text{growth: } \dot{J}_{OG} &= \frac{1}{\mu_E} (y_{VE} y_{OV} - y_{OE}) \dot{p}_G \\ \text{somatic maintenance: } \dot{J}_{OS} &= -\frac{1}{\mu_E} y_{OE} \dot{p}_M \\ \text{maturation + maturity maintenance: } \dot{J}_{OJ} &= -\frac{1}{\mu_E} y_{OE} (\dot{p}_R + \dot{p}_J) \end{aligned}$$

Appendix E

Additional model predictions for *C. georgiana* and *P. bibronii*

Parameter estimation follows methodology fully described in [Kooijman et al. \(2008\)](#); [Kooijman \(2010\)](#); [Lika et al. \(2011a\)](#). We use freely downloadable software DEBtool (<http://www.bio.vu.nl/thb/deb/deblab>). We used weighted sum of least squares regression routines (nmregr.m and nrregr.m) with Nelder-Mead simplex method generally followed by a Newton Raphson optimization criterion. Real and pseudo-data were incorporated into the parameter estimation routine.

Real data include mostly data collected in this study. Model prediction against observations for respiration and total dry mass are presented in the main text. The rest of the 0-variate data we used are summed up in tables [E.1](#) and [E.2](#).

We refer to some 0-variate data as being the result of a guesstimate. This means that for age at puberty, ultimate length and ultimate reproduction rate we used values taken from <http://www.frogsaustralia.net.au/frogs/>. We could not find values of ultimate dry mass. The dry mass to wet mass ratio of adults is 0.2 (pers. obs.) and for several frog species we noticed that the cubed length (cm^3) over wet mass (g) for an adult was often around 12. On the basis of the assumption that all frogs have similar shapes and a specific density of wet mass of 1 g cm^{-3} , we derived guesstimates for the ultimate dry mass of both species. This data point is important for the parameter estimation ([Lika et al., 2011a](#)). We used field knowledge on the life span of similar sized frogs to guesstimate mean life span. We also used some additional uni-variate data collected in this study (not shown in the main text): see figures [E.1](#) and [E.2](#).

Auxiliary theory ([Kooijman et al., 2008](#)) relates observable measurable quantities to state variables, see table [D.1](#). Some key points of auxiliary theory

Table E.1: 0-variate data points at ($T=12^\circ\text{C}$) for the standard DEB model of *Pseudophryne bibronii*. Model predictions use $f = 0.8$ unless specified otherwise. $T_A = 12000 \text{ K}$; $\delta_M = 0.35$; $E_H^p = 2103 \text{ J}$; $\dot{h}_a = 3.949 \cdot 10^{-7} \text{ d}^{-2}$; $\kappa_R = 0.95$.

Name	Unit	Observed	Predicted	Reference
age at birth	day	39	39.17	this study
age at metamorphosis	day	185	185.4	this study
age at puberty	day	≤ 420	380.7	guestimate
length at birth	cm	0.44	0.41	this study
length at metamorphosis	cm	1.1	1.0	this study
length at puberty	cm	2.2	1.6	guestimate
maximum length ($f = 1$)	cm	≤ 3	2.3	guestimate
initial dry mass of egg	mg	2.68	2.69	this study
total dry mass at birth	mg	2.40	2.0	this study
total dry mass at metamorphosis	mg	24.369	30.98	this study
total dry mass at puberty ($f = 1$)	mg	150	149.8	guestimate
maximum dry mass excluding reproduction buffer ($f = 1$)	mg	400	398.3	guestimate
total energy at birth	J	52.8	47.0	this study
total energy content at metamorphosis	J	464	718.4	this study
maximum reproduction rate ($f = 1$)	# day $^{-1}$	0.55	0.49	guestimate
mean life span ($f = 1$)	day	1825	1848	guestimate

applied in this study are as follows. We assume that structural length L is proportional to snout to vent length L_f such that $L_f = L/\delta_M$. According to DEB theory biomass is partitioned into structure and reserve. Total dry mass W_d (g) is given by $Wd = E \frac{w_E}{\mu_E} + d_V V$ and maximum reproduction rate (# eggs d^{-1}) is \dot{p}_R/E_0 if $E_H = E_H^p$ else it is zero and E_0 (J) is the mean caloric content of the egg observed in this study. Egg size varies in reality and this should be taken into account when interpreting the predicted value. Predictions for dry mass of structure and reserve do not map directly onto observed yolk-free embryo dry mass (see main text for discussion).

We assume that yolk is depleted at birth. The embryo is made up of newly synthesized structured and reorganized yolk and at birth has a scaled reserve density of $e_b = \frac{E\dot{v}}{L^3 \{\dot{p}_{Am}\}}$. Yolk dry mass is quantified as:

$$W_Y(t) = E(t) \frac{w_E}{\mu_E} - e_b m_{Em} w_E [M_V] V(t) \quad (\text{E.1})$$

and embryo dry mass is

$$W_{\text{emb}}(t) = (w_V + e_b m_{Em} w_E) [M_V] V(t) \quad (\text{E.2})$$

with m_{Em} the maximum molar reserve density (table D.1). Mean life span is calculated with DEBtool routine `get.tm.s` with the assumption that the period where growth occurs is short relative to the entire life span.

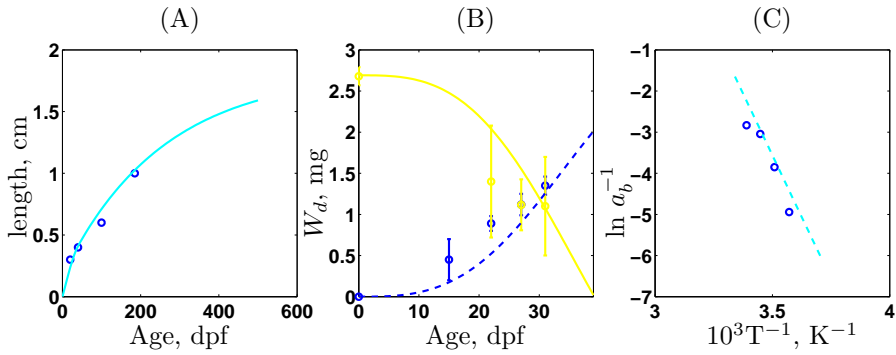


Figure E.1: Model predictions (lines) against observations (circles) for *Pseudophryne bibronii*; $T=12^\circ\text{C}$; $f = 0.8$; $\delta_M = 0.35$. (A) Snout to vent length against age (days post fertilization dpf); (B) yolk free embryo dry mass W_d (blue) and yolk dry mass (yellow); (C) Arrhenius plot: inverse log age at birth (a_b) against inverse of temperature (K).

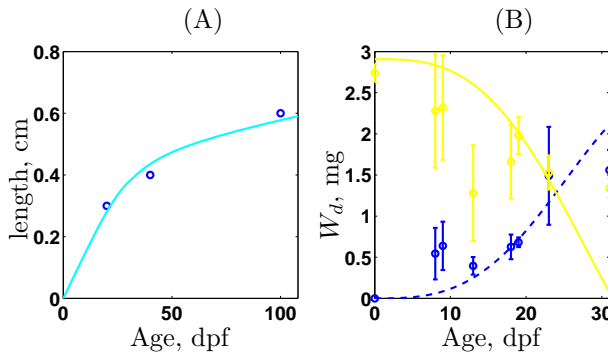


Figure E.2: Model predictions (lines) against observations (circles) for *Crinia georgiana*; $T=12^\circ\text{C}$; $f = 0.8$; $\delta_M = 0.35$. (A) Snout to vent length against age (days post fertilization dpf); (B) yolk free embryo dry mass W_d (blue) and yolk dry mass (yellow).

Pseudo data are composed of parameter values which are supposed to be highly conserved amongst all the taxa (so serve as a kind of a priori knowledge of the organism): $\dot{v} = 0.02 \text{cm d}^{-1}$, $\kappa = 0.8$, $\kappa_R = 0.95$, $[\dot{p}_M] \text{ J d}^{-1} \text{ cm}^{-3}$, $k_J = 0.002 \text{d}^{-1}$, $\kappa_G = 0.8$. Little weight is given to the pseudo-data (relative to real data) allowing these values to deviate in response to the data in this study.

The effect of temperature on all biological rates is captured by the Arrhenius relationship (Kooijman, 2010, Chap.2), quantified by the Arrhenius temperature T_A such that

$$p(T) = \exp\left(\frac{T_A}{T_1} - \frac{T_A}{T}\right) p(T_1) \quad (\text{E.3})$$

where T is the absolute temperature (K), T_1 is the reference temperature (K), T_A is the Arrhenius temperature (K) and p is a physiological rate. We computed predictions for all the data assuming that $T = 285 \text{ K}$ (12°C) and that $T_1 = 293 \text{ K}$ (20°C). The Arrhenius relationship for the log of observed age at birth against inverse temperature is linear for *P. bibronii* (fig. E.1C). The estimated Arrhenius temperature T_A of 12 000 K (which corresponds graphically to the regression slope) is coherent with observations. We assumed that the Arrhenius temperature was the same for both *P. bibronii* and *C. georgiana* in the absence of more detailed data on the thermal performance of *C. georgiana*. We estimated Arrhenius temperatures of 10800 K and 8000 K for *Crinia nimbus* and *Geocrinia vitellina* respectively.

The scaled functional response, f , which relates ingestion as a function of food availability was set at 0.3 for *C. georgiana* and 0.8 for *P. bibronii* based upon length, mass, development and respiration data. The lower for *C. georgiana* reflects the reduced feeding of the juveniles during the experiments.

We included the maturity level at hatching (if different from birth), birth and metamorphosis explicitly into the parameter estimation routine. After a suitable parameter set was established we computed maturity level against age in order to compute maturity level for each developmental stage.

Following Lika et al. (2011a) goodness of fit marks (on a 0 to 10 scale) for all four species are: 7.8 for *P. bibronii*, 7.4 for *C. georgiana*, 6.4 for *G. vitellina* and 4.8 for *C. nimbus*.

Table E.2: 0 variate data points at ($T=12^{\circ}\text{C}$) for the standard DEB model of *Crinia georgiana*. Computations for $f = 0.3$ and $T_A = 12000 \text{ K}$; $\delta_M = 0.4$; $E_H^p = 1686 \text{ J}$; $\dot{h}_a = 3.9 \cdot 10^{-7} \text{ d}^{-2}$; $\kappa_R = 0.95$.

Name	Unit	Observed	Predicted	Reference
age at hatching	day	19	19.16	this study
age at birth	day	31	31.45	this study
age at metamorphosis	day	108	108.1	this study
age at puberty	day	≤ 420	416	guestimate
length at hatching	cm	0.35	0.27	this study
length at birth	cm	0.4	0.4	this study
length at metamorphosis	cm	0.6	0.6	this study
length at puberty ($f = 1$)	cm	2.2	2.0	guestimate
maximum length ($f = 1$)	cm	4.3	3.2	guestimate
initial dry mass of egg	mg	2.74	2.91	this study
total dry mass at hatching	mg	2.66	2.73	this study
total dry mass at birth	mg	2.90	2.2	this study
total dry mass at metamorphosis	mg	2.65	4.25	this study
total dry mass at puberty ($f = 1$)	g	0.2	0.3	guestimate
maximum dry mass excluding reproduction buffer ($f = 1$)	g	1.2	1.3	guestimate
total energy at hatching	J	65.53	65.15	this study
total energy content at metamorphosis	J	43.02	94.15	this study
maximum reproduction rate ($f = 1$)	$\# \text{ day}^{-1}$	0.55	0.52	guestimate
mean life span ($f = 1$)	day	1825	1992	guestimate

Appendix F

Physical and chemical composition of exposure media for uranium toxicity experiments

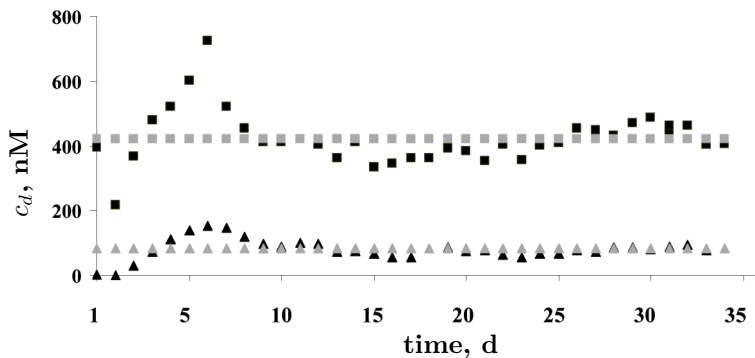


Figure F.1: Concentration of U in exposure media during 37 d accumulation and reproduction experiment. Black squares: ACP-AES measurements of U concentration, c_d nM, in 420 nM condition; grey squares: nominal concentration of 420 nM condition. Black triangles: ACP-AES measurements of c_d in 84 nM condition; grey triangles: nominal concentration in 84 nM condition.

Table F.1: Physical and chemical parameters of all the studies analysed using the DEB model. pH, temperature (T) and uranium (U) correspond to nominal experiment values; see text for mean value \pm standard deviation for pH and T and fig. F.1 for measured U concentration (ACP-AES) for this study.

	adult	(Barillet et al., 2005)	(Barillet et al., 2011)	(Bourrachot et al., 2008)	(Bourrachot, 2009)
life stage	adult	adult	adult	embryo + early juvenile	adult
exposure duration (d)	37	20	20	9	20
deuration duration (d)	no	no	no	no	15
feeding	Tetramin™ granules <i>Ad libitum</i> 2-3 x d	standard fish pellets, 1% body mass per day	standard fish pellets, 1% body mass per day	no feeding	tetramin™ flakes 2 x d
individually fed	yes	no	no	no	no
K ⁺ (mM)	0.15	0.16	0.16	0.15	0.15
Na ⁺ (mM)	0.32	0.50	0.50	0.32	0.32
Mg ²⁺ (mM)	0.20	0.20	0.20	0.19	0.19
Ca ²⁺ (mM)	0.29	0.29	0.29	0.29	0.29
Cl ⁻ (mM)	0.92	0.91	0.91	0.92	0.92
NO ₃ ⁻ (mM)	0.31	0.50	0.50	0.32	0.32
SO ₄ ²⁻ (mM)	0.10	0.10	0.10	0.10	0.10
pH	6.5	6.5	6.5	6.5	6.5
T(°C)	26	25	24	25	25
U (nM)	0, 84, 420	0, 84, 420, 2100	0, 420	0, 84, 1054	0, 84, 1054

Appendix G

Equations for modelling uranium toxicity experiments

The core DEB model equations are specified in table G.1. Additional terms are specified below. \dot{r} is the specific growth rate:

$$\dot{r}_1 = \frac{E\dot{v}\mathcal{M}(L)/L - [\dot{p}_M]L^3/\kappa}{E + [E_G]L^3/\kappa} \quad (\text{G.1})$$

$$\dot{r}_2 = \frac{E\dot{v}\mathcal{M}(L)/L - [\dot{p}_M]L^3/\kappa}{E + \kappa_G[E_G]L^3/\kappa} \quad (\text{G.2})$$

\dot{p}_C is the mobilization flux:

$$\dot{p}_C = E(\dot{v}\mathcal{M}(L)/L - \dot{r}) \quad (\text{G.3})$$

\dot{p}_{Cm} is the mobilization flux assuming $f = 1$ for an individual of structural length L :

$$\dot{p}_{Cm} = [E_m] \frac{[E_G]\dot{v}\mathcal{M}(L)L^2 + [\dot{p}_M]L^3}{\kappa[E_m] + [E_G]} \quad (\text{G.4})$$

$\mathcal{M}(L)$ is the shape correction function:

$$\mathcal{M}(L) = \max(L_b, \min(L, L_j))/L_b \quad (\text{G.5})$$

with L_b and L_j structural length at birth ($E_H = E_H^b$) and metamorphosis ($E_H = E_H^j$) respectively.

Table G.1: Standard DEB model with V1-morphic juvenile I growth (as in [Augustine et al., 2011a](#)) further extended with reproduction buffer handling rules (as in [Pecquerie et al., 2009](#)), a toxico-kinetic module (as in [Kooijman and van Haren, 1990](#)) and degradation of structure to handle starvation (as in [Augustine et al., 2011b](#)). See text for addition specification of terms. The logical boolean, e.g. $(x < y)$, is enclosed in parentheses and has value 1 if true and value 0 if false.

For embryo and juveniles ($E_H < E_H^p$):
if $\kappa\dot{p}_C \geq [\dot{p}_M]L^3$ $\dot{r} = \dot{r}_1$ else $\dot{r} = \dot{r}_2$

For adults ($E_H = E_H^p$):
if $\kappa\dot{p}_C \geq [\dot{p}_M]L^3$
 $\frac{d}{dt}E_R^1 = (E_R^0 > 0) (t > t_b) \left(\kappa_R \left((1 - \kappa) \dot{p}_{Cm} - \dot{k}_J E_H^p \right) \right)$
 $\frac{d}{dt}E_R^0 = \left(\max \left(0, (1 - \kappa) \dot{p}_C - \dot{k}_J E_H^p \right) - \frac{d}{dt}E_R^1 \right) (E_H = E_H^p)$
 $\dot{r} = \dot{r}_1$
else if $\kappa\dot{p}_C < [\dot{p}_M]L^3$
 $\frac{d}{dt}E_R^1 = 0$
 $\frac{d}{dt}E_R^0 = \left(\max \left(0, (1 - \kappa) \dot{p}_C - \dot{k}_J E_H^p \right) - ([\dot{p}_M]L^3 - \kappa\dot{p}_C) (E_R^0 > 0) \right) (E_H = E_H^p)$
 $\dot{r} = 0$ if $E_R^0 > 0$ and $\dot{r} = \dot{r}_2$ if $E_R^0 = 0$

Dynamics of state variables:
 $\frac{d}{dt}E = \dot{p}_A - \dot{p}_C$
 $\frac{d}{dt}L = \frac{\dot{r}}{3}L$
 $\frac{d}{dt}E_H = \max \left(0, \left((1 - \kappa) \dot{p}_C - \dot{k}_J E_H \right) \right) (E_H < E_H^p)$
 $\frac{d}{dt}E_R = \frac{d}{dt}E_R^0 + \frac{d}{dt}E_R^1$
 $\frac{d}{dt}[M_Q] = \frac{\dot{k}_e}{l} (P_{Vdc_d} - [M_Q]P_{Vw}) - [M_Q]\dot{r}$

Appendix H

Additional model simulations for evaluating toxic mode of action on zebrafish metabolism

H.1 Control model fit to U-84 female reproductive data

Table H.1: The control model is fit to toxicity data. Parameters for buffer handling rules for each individual female exposed to 84 nmol l^{-1} in the 37d reproduction trial. At time 0 fish are 0.94 their final length, and have $f[E_m]L^3$ joules in their reserve. We consider that batch preparation is already initiated at the onset of the trial. We also assume that $E_R(0)$ comprises only unripe batch material.

Replicate	f	$[E_B]$ (J cm^{-3})	$E_R(0)$ (J)
1	0.598	1500	737
2	0.863	1500	728
3	0.861	1756	690
4	0.595	1677	712
5	0.830	3000	0
6	0.830	3000	400
7	0.830	2000	600
8	0.550	2000	300
9	0.830	2000	300
10	0.821	2022	311

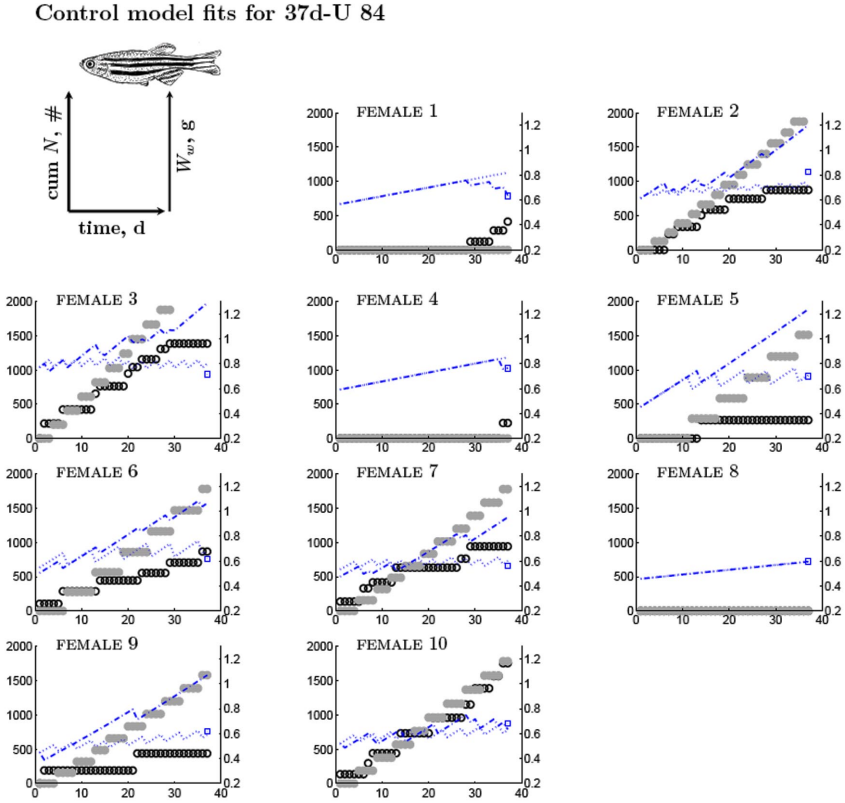


Figure H.1: Control model fits to individual females exposed to 84 nmol l^{-1} . Left y-axis: empty circles (black) represent observed cumulated (cum) number of eggs spawned ($\#$) and full circles (grey) represent model predictions. Right y-axis: dotted line represents predicted wet mass using buffer handling rules, mg. Dot-dashed line represents predicted wet mass without buffer handling rules, g. Physiological parameters for each female are in table H.1. The wet mass of the real number of eggs spawned are subtracted from the total predicted wet mass on each spawning day. See text for computations. The square represents final observed wet mass for that individual.

H.2 Initial amount of reserve in two females

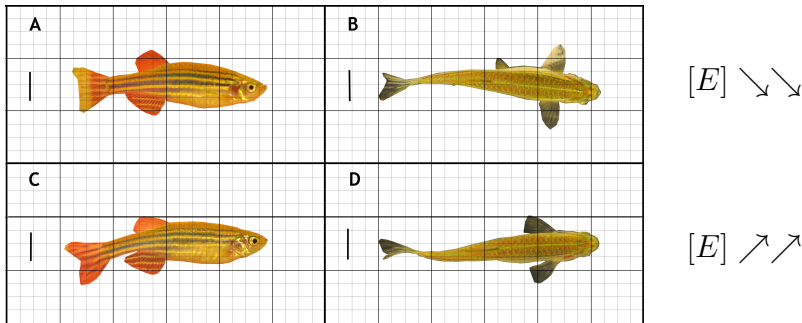


Figure H.2: Portraits taken during the third day of exposure to $420 \text{ nmol U l}^{-1}$. Lateral (A) and dorsal (B) portraits of Female 8. Lateral (C) and dorsal (D) portraits of female 10. Both females had quasi-identical final wet mass and length and both did not reproduce during the 37d exposure (fig. 5.2 and 5.7). The difference between both females is that females 10 spawned 570 eggs ($\approx 280\text{mg}$ wet mass) the day prior to exposure, i.e. 4 days before this photo was taken. Female 8 did not spawn at all during the 35 days acclimation. We suppose that while both female seem almost identical, female 10 must have started the experiment with a higher reserve density than female 8. Scalebar: 6mm.

H.3 Simulating an increase in costs for synthesizing structure

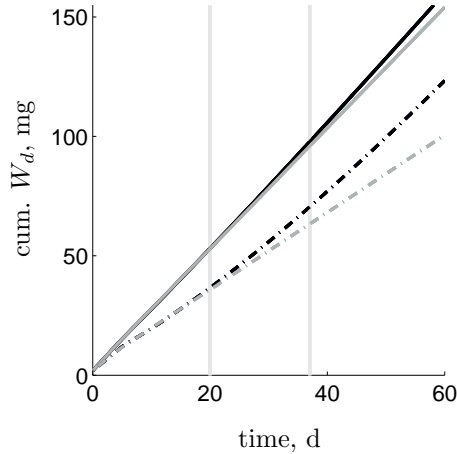


Figure H.3: DEB model simulation studies of mode of action (G) on adult reproduction. $T = 25^\circ\text{C}$, $f = 0.75$. First horizontal light grey line: 20 d; second horizontal light grey line: 37 d. Cumulated (cum.) dry mass W_d invested in reproduction, expressed as mg dry mass of reproduction buffer material, against time. Black: control; darker grey: 84 nM U in the water. The simulations use the same $[M_{Q0}^G]$ and $[M_{QT}^G]$ as that used for modelling embryo and early juvenile data sets (table 5.4). Solid lines: individual of 3.7 cm total length (about the average total length of individuals in the 37d reproduction trial); dot-dashed line: individual of 3.3 cm total length (about the average total length of individuals in the 15d reproduction trial).

Appendix I

**Model fits for individual
females in the 15 day
reproduction trial by
Bourrachot 2009**

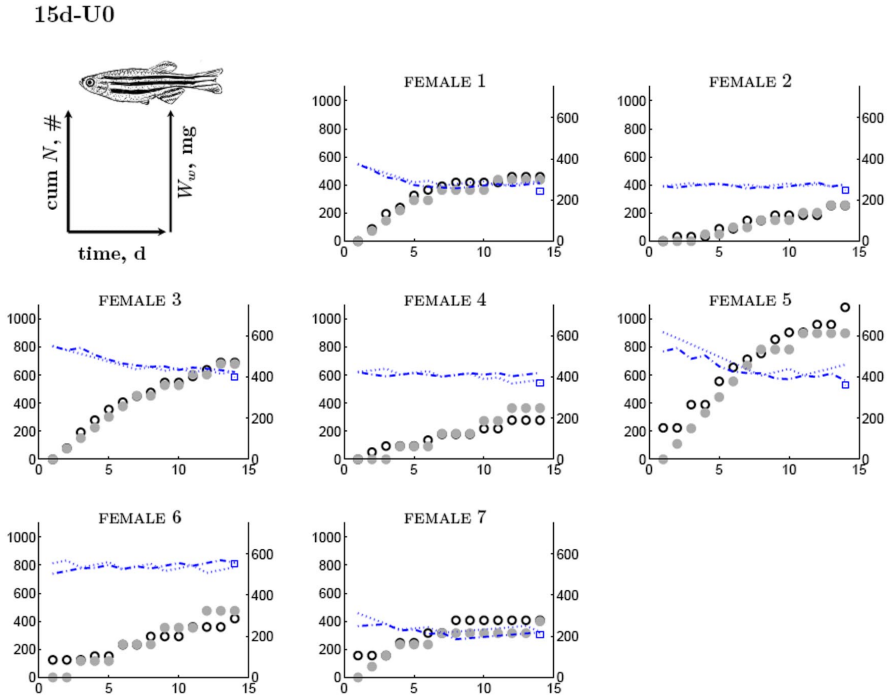


Figure I.1: DEB model fit to individual control females. Data kindly provided by S. Bourrachot from her thesis (Bourrachot, 2009). Parameters can be found in tables 5.4 and 5.3. Left y-axis: empty circles (black) represent observed cumulated (cum) number N of eggs spawned ($\#$) and full circles (grey) represent model predictions. Right y-axis: dotted line represents predicted wet mass using buffer handling rules, mg (eq. 5.8). Dot-dashed line represents predicted wet mass without buffer handling rules, mg (eq. 5.9). The square represents final observed wet mass for that individual.

15d-U84

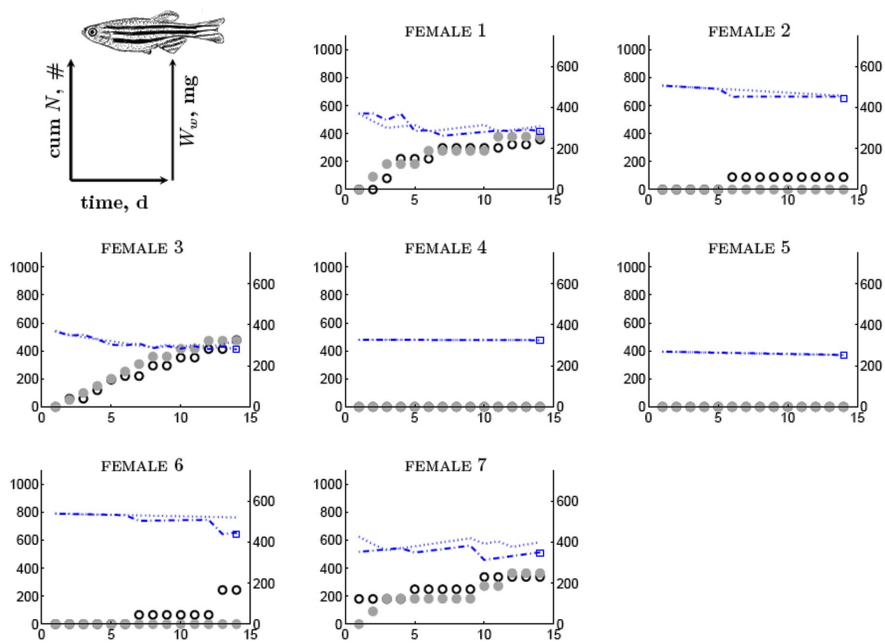


Figure I.2: DEB model fit to individual females exposed to 84 nmol U l^{-1} for 20d prior to the reproduction trial. Data kindly provided by S. Bourrachot from her thesis (Bourrachot, 2009). The model assumes U increases volume-linked somatic maintenance. Parameters can be found in tables 5.4 and 5.3. Left y-axis: empty circles (black) represent observed cumulated (cum) number N of eggs spawned (#) and full circles (grey) represent model predictions. Right y-axis: dotted line represents predicted wet mass using buffer handling rules, mg (eq. 5.8). Dot-dashed line represents predicted wet mass without buffer handling rules, mg (eq. 5.9). The square represents final observed wet mass for that individual.

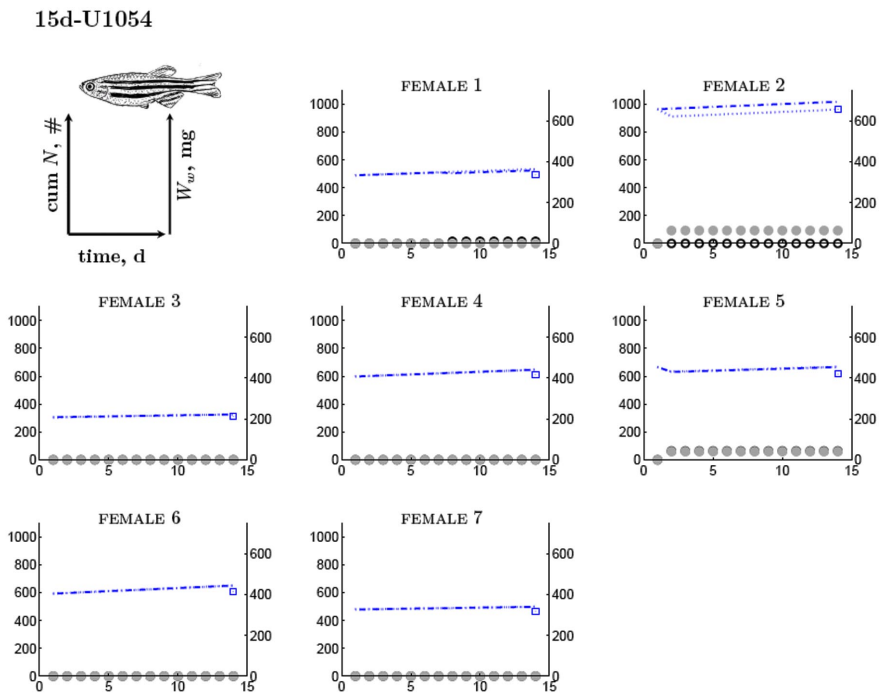


Figure I.3: DEB model fit to individual females exposed to 1054 nmol U l⁻¹ for 20d prior to the reproduction trial. Data kindly provided by S. Bourrachot from her thesis (Bourrachot, 2009). The model assumes U increases volume-linked somatic maintenance. Parameters can be found in tables 5.4 and 5.3. Left y-axis: empty circles (black) represent observed cumulated (cum) number N of eggs spawned (#) and full circles (grey) represent model predictions. Right y-axis: dotted line represents predicted wet mass using buffer handling rules, mg (eq. 5.8). Dot-dashed line represents predicted wet mass without buffer handling rules, mg (eq. 5.9). The square represents final observed wet mass for that individual.

Summary

The aim of this dissertation is to characterize the toxicity of uranium on the metabolism of zebrafish, *Danio rerio*. Because effects of uranium manifest themselves as deviations from the non-stressed situation, the first question this raises is: What do we know about zebrafish metabolism under non-stressed conditions? And the answer is that very little is known, despite the large amount of work on developmental aspects of the zebrafish. This is why the first three chapters of this manuscript are dedicated to characterizing the blank metabolism of zebrafish. I used the Dynamic Energy Budget (DEB) theory for this characterisation; it is presently the only theory that covers the full life cycle of the organism and quantifies feeding, assimilation, growth, reproduction, maturation, maintenance and ageing. Any metabolic effect of uranium should appear as effects on one or more of these fundamental processes. Since the life span of zebrafish is some four and a half years, and larger individuals respond slower to chemical stress, the focus was on the early life stages (embryo, juvenile, and reproductive behaviour of the adult). This focus is of importance not only for practical reasons, but the early life stages also seem to be more sensitive and show particular effects (such as on growth) more clearly.

Considerable breakthroughs in the quantification of zebrafish development, growth and reproduction have been made. It turned out the zebrafish accelerates its metabolism after birth (when feeding starts) till metamorphosis, when acceleration ceases. This process is seen in some, but not all, species of fish. Another striking conclusion was that somatic maintenance was much higher than is typical for fish. We don't yet have an explanation for this finding. Further it turned out that the details of reproduction matter: allocation to reproduction (in adults) accumulates in a reproduction buffer and this buffer is used to prepare batches of eggs. We needed to detail this preparation process to understand how zebrafish can eliminate uranium via eggs.

DEB theory specifies that a particular developmental stage (birth, metamorphosis, puberty) is reached at specified levels of maturity. For different temperatures and food levels, that can occur at different ages and body sizes. We extended this idea to include all the described morphologically defined developmental stages of the zebrafish in the literature; the observed variations in ages and body sizes can now be explained by DEB theory.

To test if DEB theory can also explain perturbations of maturation, we stud-

ied developmental patterns in two types of taxonomically related frog species of similar body size. One type shows a typical developmental pattern as embryo, feeding tadpole and juvenile frog. The other type shows, after hatching, but before birth (= start of feeding) a significant acceleration of maturation, which is visible as an increased respiration and retarded growth, with big effects on size at a given developmental stage. This acceleration is reduced after metamorphosis (when the tiny froglets leave their drying pool), but compared to the standard type of frog, it takes considerable time to catch up in growth. All these changes could be captured accurately with DEB theory by a temporary change in a single parameter: the fraction of mobilised reserve that is allocated to somatic maintenance plus growth, as opposed to maturity maintenance plus maturation. The conclusion is that the observed perturbations of maturation and the age and size variations at various developmental stages provide strong support for how DEB theory incorporates maturation.

We not only required detail on maturation but also on starvation, especially in the early juvenile stages. The problem is that, according to DEB theory, maintenance is paid from mobilised reserve, but when food is scarce or absent, reserve becomes depleted and maintenance can no longer be paid from mobilised reserve. We included more detail on what happens exactly under such conditions. More specifically we modelled the processes of rejuvenation and shrinking (of structure) and their consequence for hazard rate. We managed to capture observed size and survival trajectories of fish fry under controlled starving conditions. These processes are not only important to capture effects of uranium on feeding, but have a much wider ecological significance in field situations. Many species of fish lay over a million eggs per spawn, yet, in stable populations, each individual fish just replaces itself. The survival process of the early life stages is still the most difficult problem in fish population dynamics.

As a result of my work, there is now a formal basis for understanding (and predicting) how the physiological performance of zebrafish relates to food intake. The model was used to detect uranium induced eco-physiological deviations from the blank. For this purpose we developed a dynamic model for the accumulation-elimination behaviour of uranium in a feeding, growing and reproducing fish. We expected that uranium might affect the immune system and other defence systems. In DEB theory, resource allocation to maturation comprises a (fixed) fraction of mobilised reserve minus what is required for maturity maintenance. The idea was that uranium might increase the cost of maturity maintenance, because defence is paid from this flux, and so delay maturation. I, therefore, paid due attention to maturation rates.

Uranium was shown to alter the histology of the gut wall (major player in nutrient assimilation) and may even modify homeostasis of host-microbe interaction (major players in assimilation and innate immunity). We further found that uranium most likely increases cost for structure, decreases assimilation and, possibly, increases somatic maintenance costs. Surprisingly, we could not detect obvious effects on maturation at very low concentrations, as we had expected. Since maturation interacts with growth, reproduction and mainte-

nance, I don't see our work on maturation as lost effort; moreover the topic is of interest in its own right. The toxicity of uranium is such that effects on the costs of structure and somatic maintenance start close to 0 nM uranium in the water.

An important result of my research was that the conditions of the fish (structure, maturity level, reserve, reproduction buffer, stage of batch preparation) at the start of the experiment is very much individual specific and conditions the response of that individual to toxic stress during the experiment. The problem is severe for adults where the contribution of reproduction buffer to total mass can differ considerably between individuals. This not only affects weight trajectories, but also the concentration of toxicant inside the body, since reproduction represents an important elimination route for uranium. The amount of total reserve material (reserve + reproduction buffer) determines the severity of the toxic effect and contributes in an important way to the scatter in the data. By accounting for differences in initial conditions, I was able to explain the seemingly contradictory results that have been reported in the literature and explain my own results for effects of uranium. The take-home message is: observations on individuals should not be averaged for groups of individuals.

Resumé

L'objectif de ces travaux de thèse était de caractériser la toxicité de l'uranium sur le métabolisme du poisson zèbre, *Danio rerio*. Puisque les effets de l'uranium se traduisent par des modifications de la performance du métabolisme, la question suivante se pose : que savons-nous du métabolisme du poisson zèbre témoin? Très peu de chose. En effet, nos connaissances à ce sujet sont assez limitées en dépit d'un grand nombre de travaux sur le développement de ce poisson. C'est pourquoi les trois premiers chapitres de ce manuscrit sont dédiés à la caractérisation du métabolisme témoin du Danio. J'ai utilisé la théorie des bilans d'énergie dynamique (DEB) pour procéder à cette caractérisation ; à l'heure actuelle c'est la seule théorie qui quantifie l'ingestion, l'assimilation, la croissance, la reproduction, la maturation, la maintenance et le vieillissement pendant le cycle de vie entier d'un organisme. L'effet de l'uranium sur l'organisme implique un effet sur au moins une des processus cités ci-avant. Etant donné que la longévité du poisson zèbre est d'environ quatre ans et demi, et que l'intensité des effets liés à un stress chimique est inversement proportionnel à la taille, nous avons centré nos efforts sur les stades de vie précoces (embryon, juvénile et reproduction adulte). De surcroît, les stades de vies précoces semblent plus sensibles aux effets de l'uranium surtout au niveau des effets sur la croissance.

D'importants progrès ont été réalisés dans le domaine de la quantification du développement, de la croissance et de la reproduction du poisson zèbre. Il s'est avéré que le poisson zèbre accélère son développement après la naissance (c'est-à-dire l'instant où l'individu commence à se nourrir), jusqu'à la métamorphose, où l'accélération cesse. Ce processus a été constaté chez d'autres espèces de poissons, mais pas toutes. Une autre conclusion surprenante était que la maintenance somatique est beaucoup plus élevée que la valeur typique d'un poisson. Nous n'arrivons pas encore à expliquer pourquoi. De plus nous avons découvert que les détails sur la physiologie reproductive sont importants pour caractériser les effets de l'uranium : chez l'adulte les ressources allouées à la reproduction sont stockées dans un compartiment où siègent les processus de préparation de "batch" d'œufs (=buffer de reproduction). Il est donc important de comprendre ce processus pour comprendre comment le poisson zèbre élimine l'uranium via les œufs.

La théorie DEB spécifie que l'individu atteint un stade de développement

à un niveau de maturité donné. Selon la température et/ou la nourriture, ce niveau de maturité peut être atteint à des tailles ou des âges différents. Nous avons élargi le concept pour inclure tous les stades de développement (définis sur la base de critères morphologiques) publiés dans les atlas de développement. Ce travail nous a permis d'expliquer par la théorie DEB la variabilité en termes de taille et d'âge.

Dans le but de tester si la théorie DEB peut expliquer des perturbations au niveau de la maturation, nous avons étudié le développement de deux espèces de grenouilles taxonomiquement proches et de taille similaires. Une des espèces possède un développement typique comprenant un stade embryonnaire, un stade têtard qui se nourrit et puis un stade juvénile avec la morphologie typique d'une grenouille. Par contre la deuxième espèce témoigne d'une accélération du développement après l'éclosion mais avant la naissance - qui correspond au stade de développement où l'individu commence à se nourrir. Cette accélération est trahie par une augmentation de la respiration et un retard de la croissance avec au final une diminution de la taille à chaque stade de développement par rapport à la première espèce. Cette accélération s'estompe après la métamorphose (le moment où les jeunes grenouilles quittent l'eau). Toutes les différences entre les deux types de développement ont été expliquées par la théorie DEB en considérant qu'un seul paramètre changeait temporairement de valeur : la fraction de la réserve mobilisée vers la croissance et la maintenance somatique. La conclusion est que les perturbations observées au niveau de la maturation et de la variabilité de l'âge et la taille entre les différents stades de développement soutiennent empiriquement la façon que la théorie DEB incorpore la maturation.

Non seulement notre étude requérait une quantification détaillée de la maturation, mais elle requérait aussi la prise en compte de périodes (prolongées) de jeune, et ce plus particulièrement pour les stades précoces. Selon la théorie DEB la maintenance est alimentée avec l'énergie mobilisée de la réserve. Dès lors que la nourriture devient rare ou disparaît cette dernière ne suffit plus pour alimenter la maintenance somatique. Nous avons détaillé ce cas de figure en modélisant le lien entre les processus de rajeunissement et d'amaigrissement extrême et la probabilité de survie. Les prédictions du modèle sont en accord avec les trajectoires de survie de larves obtenues en conditions de laboratoire. Certaines poissons libèrent plus d'un million d'œufs par événement de ponte et pourtant, si la dynamique de la population est stable, à chaque génération chaque poisson n'est remplacé que par un seul individu. Le processus de survie des larves représente une grande énigme irrésolue dans le domaine de la dynamique de populations de poisson.

Par le biais de ces travaux de doctorat, nous disposons à présent d'un outil permettant de comprendre, et de prédire, la manière dont la performance physiologique du poisson zèbre dépend de son niveau de nutrition. Le modèle a été utilisé pour détecter les modifications induites par l'uranium sur la performance physiologique d'un individu exposé par rapport à celle du témoin. A cette fin, nous avons développé un modèle dynamique qui spécifie la manière

dont l'uranium s'accumule et s'élimine chez un individu qui se nourrit, grandit et se reproduit. Nous avons imaginé que l'uranium pourrait affecter le système immunitaire ainsi que d'autres mécanismes de défense cellulaire (e.g. système antioxydant). Selon la théorie DEB, l'allocation des ressources à la maturation comprend une fraction fixe de la réserve mobilisée auquel est soustrait le coût de maintenance de la maturité. Notre idée est que les coûts du système immunitaire et de défense cellulaire contribuent à la maintenance de la maturité. Si l'uranium augmentait les coûts de ce dernier alors la maturation ralentirait, ainsi j'ai porté une attention soutenue aux taux de maturation.

Nous avons montré que l'uranium altère l'histologie de la paroi intestinale (acteur majeure dans l'assimilation des nutriments) et pourrait potentiellement modifier l'homéostasie des interactions hôte-bactérienne (acteur majeur dans l'assimilation et l'immunité innée). De plus nos travaux suggèrent que l'uranium augmenterait les coûts de synthèse de la structure et diminuerait l'assimilation et/ou augmenterait le coût de la maintenance somatique. Chose étonnante, malgré ce que nous pensions, nous n'avons pas pu détecter d'effets notables sur la maturation à ces faibles concentrations. Puisque la maturation interagit avec la croissance, la reproduction et la maintenance, je considère néanmoins que les travaux que j'ai pu mener sur la maturation sont pertinents. La toxicité de l'uranium est telle que les effets sur le coût de la synthèse de la structure et de la maintenance somatique sont estimés proches de 0 nM d'uranium dans l'eau.

Un résultat très important se dégageant de ces travaux est que la condition des poissons (structure, maturité, réserve, buffer de reproduction, stade de préparation des "batch") au début de l'expérience dépend de l'individu et conditionne la réponse de celui-ci au stress pendant (toute) l'expérience. Ce problème s'aggrave lorsque nous travaillons avec des poissons zèbres adultes car la contribution de la masse du buffer de reproduction par rapport à la masse totale diffère de manière importante entre chaque individu. Ceci affecte alors non seulement les trajectoires de masse dans le temps, mais aussi la concentration interne, car la reproduction représente une voie importante d'élimination de l'uranium. La quantité totale de réserve (à savoir : réserve + buffer de reproduction) conditionne la sévérité de l'effet toxique contribuant ainsi à la variabilité dans les données. En prenant en compte les différences entre les conditions initiales de chaque individu, j'ai pu expliquer les résultats contradictoires publiés dans la littérature ainsi qu'expliquer mes propres résultats sur les effets de l'uranium. La leçon à retenir est que des données acquises sur des individus ne devraient pas être moyennées sur des groupes d'individus.

Samenvatting

Het doel van deze dissertatie is om de toxiciteit van uranium voor het metabolisme van de zebravis *Danio rerio* te karakteriseren. Aangezien effecten van uranium zichtbaar worden als afwijkingen van de niet-gestressede situaties, is de eerste vraag die opkomt: Wat weten we eigenlijk van dit metabolisme onder niet-gestressede situaties? Het eerlijke antwoord is: bitter weinig, ondanks de enorme hoeveelheid werk dat gedaan is aan de ontwikkeling van de zebravis. Dit is de reden waarom de eerste drie hoofdstukken over de kwantitatieve aspecten van het metabolisme van de zebravis gaan. Ik heb de Dynamische Energie Budget (DEB) theorie gebruikt voor deze karakterisering; het is op dit moment de enige theorie die gaat over de complete levenscyclus en de processen van eten, assimilatie, groei, reproductie, maturatie en veroudering kwantificeert. Enig metabool effect van uranium zou zichtbaar moeten worden als een effect op een of meer van deze fundamentele processen. Aangezien de levensverwachting van de zebravis zo'n 4.5 jaar is en grotere individuen, om meerdere redenen, langzamer reageren op toxische stress ligt de focus vooral op de vroege levensstadia (embryo, juveniel en het reproductief gedrag van de adult). Dit is niet alleen om praktische redenen van belang, maar vroege levensstadia lijken ook meer gevoelig en laten bepaalde effecten (zoals op groei) duidelijker zien. Mijn onderzoek heeft belangrijke doorbraken kunnen boeken op het terrein van kwantificeren van ontwikkeling, groei and reproductie. Bij de start van het onderzoek verwachtten wij dat uranium het immuun en andere afweer systemen zou kunnen beïnvloeden. In DEB theory vindt allocatie van voedingsstoffen naar ontwikkeling plaats door een vast fractie van gemobiliseerde reserve te nemen en daar het maturatie onderhoud van af te trekken. Het idee was dat uranium de maturatie onderhoud zou kunnen vergroten, zodat het ontwikkelingsproces vertraagd zou worden. Om deze reden heb ik nauwkeurig naar ontwikkelingsnelheden gekeken.

Het bleek dat zebravissen hun metabolisme na geboorte (wanneer het eetproces wordt gestart) versnellen tot metamorphose plaats vindt en de versnelling stopt. Dit proces wordt ook in sommige andere vissoorten waargenomen, maar niet in alle. Een ander opvallende waarneming is dat het somatisch onderhoud veel hoger is dan voor veel ander vissoorten. Op dit moment is daar nog geen verklaring voor te geven. Verder bleken details van het reproductie-proces van belang te zijn. Allocatie van voedingsstoffen naar

reproductie hoopt zich op in een reproductie-buffer en deze buffer wordt gebruikt om legsels van eieren voor te bereiden. We hebben deze details van het legsel proces nodig om te begrijpen hoe uranium via eieren geëlimineerd kan worden.

DEB theorie specificceert dat een bepaald ontwikkelingsstadium (geboorte, metamorphose, puberteit) wordt bereikt bij een bepaald maturatie niveau. Voor verschillende temperaturen en voedsel niveaus kan dit gebeuren bij verschillende leeftijden en groottes. We hebben dit idee uitgebreid voor alle, morfologisch bepaalde, stadia van de zebravis, zoals die in de literatuur beschreven staan. De waargenomen variaties in leeftijden en groottes konden op deze manier verklaard worden.

Om te testen of DEB theorie ook verstoringen van het ontwikkelings proces kon verklaren hebben we gekeken naar twee type verwante soorten kikkers van dezelfde lichaamsgrootte. Eén type volgt het standaard patroon van een eetend kikkervisje en een juveniele kikker. Het andere type laat, na het uitkomen van het ei, een metabole versnelling zien tot de geboorte (wanneer voedsel-opname begint), wat gepaard gaat met een substantiële verhoging van de respiratie en een vertraging van de groei, met aanzienlijk consequenties voor de grootte bij de verschillende ontwikkelingsstadia. Deze versnelling verdwijnt na metamorphose (wanneer de kleine kikkertjes hun opdrogende waterpoel verlaten), maar het duurt nog een hele tijd voordat de groei weer gelijke tred houdt met het standaard type. Al deze veranderingen konden nauwkeurig met DEB theory beschreven worden door een tijdelijke verandering in één parameter: de fractie van gemobiliseerde reserve dat gealloceerd wordt naar somatisch onderhoud en groei, in plaats van maturatie onderhoud plus maturatie. De conclusie is dat we waargenomen afwijkingen van de ontwikkeling en de variatie in leeftijden en grootten bij de verschillende ontwikkelingsstadia een sterke onsteunsteuning leveren voor de wijze waarom maturatie in DEB theorie is geformuleerd.

We hebben niet alleen meer detail in ontwikkeling maar ook in hongering nodig, vooral in de vroeg-juveniele stadia. Het probleem is dat onderhoud uit gemobiliseerde reserve "betaald" wordt, maar wanneer voedsel schaars of afwezig is, raakt de reserve uitgeput en kan dat niet meer. We hebben daarom in meer detail beschreven hoe de processen van verjonging en krimp verlopen, en wat hiervan de gevolgen zijn voor de overlevingskansen. We zijn erin geslaagd om de waargenomen patronen van hongering bij visbroed onder gecontroleerde omstandigheden nauwkeurig te beschrijven. Dit is niet alleen van belang om de effecten van uranium te begrijpen, maar ook, in een veel ruimer ecologisch perspectief, om te snappen hoe een vis die makkelijk een miljoen eitjes per keer legt toch alleen zichzelf vervangt in een stabiele populatie. Dit is nog steeds het meest ingewikkelde probleem in de visserij-biologie.

Als resultaat van mijn onderzoek ligt er nu een formele basis voor het metabolisme van de zebravis die gebruikt kan worden om het te begrijpen en te voorspellen. We gebruikten het vervolgens om de effecten van uranium te bestuderen. Voor dit doel ontwikkelden we een dynamisch model voor de opname en eliminatie van uranium in een etende, groeiende en reproducerende

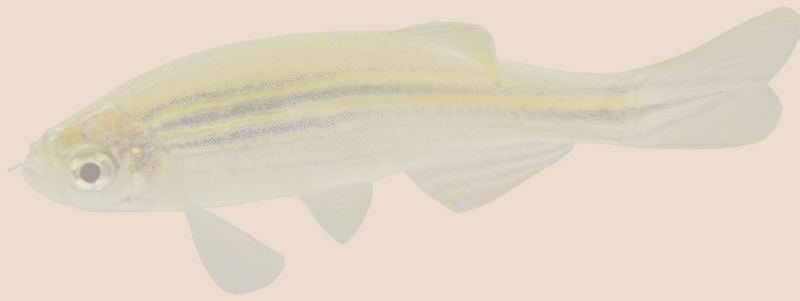
vis. Histologisch onderzoek toonde aan dat uranium ook effect heeft op de darmwand, die van belang is bij de assimilatie; de gastheer-micro-organismen relaties waren verstoord, met gevolgen voor assimilatie en immuniteit. We vonden dat uranium naar alle waarschijnlijkheid de kosten voor structuur en somatisch onderhoud verhoogt en de assimilatie verlaagt. Enigzins tot onze verbazing vonden we geen effecten op ontwikkeling, zoals we verwacht hadden. Toch beschouwen we onze moeite die we aan ontwikkeling besteed hebben niet als verloren. Ontwikkeling beïnvloedt groei, reproductie en onderhoud en is bovendien op zichzelf van groot belang. De effecten op groei en onderhoud vinden al bij zeer lage concentraties plaats, namelijk al bij een orde van 1 nM uranium.

Een belangrijk resultaat van mijn onderzoek is dat de start-condities van individuen, in termen van hoeveelheden structuur, reserve, maturatie, reproductie buffer en voorbereide legsels, van grote invloed op het proef-resultaat bleken te zijn. Door hier goed rekening met te houden kon ik tal van schijnbaar tegenstrijdige resultaten in de literatuur en die van mijn eigen onderzoek mee verklaren. De boodschap is dus: middel geen waargenomen gedrag van verschillende individuen, maar volg ze elk afzonderlijk.

Ce travail de thèse s'est intéressé aux effets de l'uranium appauvri (U) sur le poisson zèbre, *Danio rerio*. L'hypothèse de travail majeure est que les effets de l'U peuvent se traduire par des modifications du métabolisme. Par conséquent nous avons caractérisé la performance physiologique par le biais de la théorie des bilans d'énergie dynamique (DEB) car c'est la seule théorie qui quantifie simultanément l'ingestion, l'assimilation, la croissance, la reproduction, la maturation, la maintenance et le vieillissement au cours du cycle de vie entier à des niveaux de nourriture variable. Un modèle DEB a ainsi été construit et a permis de quantifier et de prédire la manière dont la performance physiologique du poisson zèbre dépend de son niveau de nutrition (et de la température). Nous avons montré que le développement s'accélère après la naissance jusqu'à la métamorphose où l'accélération cesse. De plus les coûts de maintenance somatique sont très élevés.

Un module spécifiant la toxico-cinétique de l'U, chez un individu qui se nourrit, croît et se reproduit, a été incorporé dans le modèle DEB. Le modèle a été appliqué aux données de toxicité (publiés et acquis pendant la thèse) afin de découvrir quel processus est affecté par l'U. Les résultats montrent qu'à partir de 0 nM, l'U augmenterait les coûts de croissance et diminuerait l'assimilation et/ou augmenterait le coût de la maintenance somatique. Nous n'avons pas pu détecter d'effets notables sur la maturation. Une étude histologique révèle que l'U altère l'intégrité de la paroi intestinale et pourrait perturber l'homéostasie des interactions hôte-bactéries. En prenant en compte les différences interindividuelles dans les conditions initiales, certains résultats qui semblaient être contradictoires sont expliqués. La leçon à retenir est que les données acquises sur des individus ne devraient pas être moyennées sur des groupes d'individus.

Mots clés: théorie DEB, effets et cinétique de l'uranium, *Danio rerio*, *Crinia georgiana*, *Pseudophryne bibronii*, métabolisme, maturation, développement, vieillissement, croissance, reproduction



The aim of this dissertation is to characterize the toxicity of depleted uranium (U) on the metabolism of zebrafish, *Danio rerio*. The underlying hypothesis of this work is that effects of U show up as effects on the metabolism of the individual. Consequently, we characterized physiological performance using Dynamic Energy Budget (DEB) theory since it is the only theory which simultaneously specifies ingestion, assimilation, growth, reproduction, maturation, maintenance and ageing over the whole life-cycle at varying food availability. Thus a DEB model was built which quantifies and predicts how the physiological performance of zebrafish relates to food level (and temperature). We showed that development accelerates after birth until metamorphosis after which acceleration ceases. Furthermore, somatic maintenance costs are very high.

A module specifying toxico-kinetics of U in a feeding, growing and reproducing individual was incorporated into the DEB model. The model was then applied to toxicity data (from the literature or acquired during this thesis) in order to determine which processes are affected by U. Our results show that, from 0 nM onwards, U increases costs for growth and either increases somatic maintenance or decreases assimilation. We were unable to detect effects on maturation. A histological study showed that U alters histology of the gut wall and may perturb host-microbe homeostasis. By accounting for differences in initial conditions between individuals we were able to explain a number of seemingly contradictory results. The take home message is: observations on individuals should not be averaged for groups of individuals.

Key words: DEB theory, uranium effects and kinetics, *Danio rerio*, *Crinia georgiana*, *Pseudophryne bibronii*, metabolism, maturation, development, ageing, growth, reproduction